# *A Kinetic and mechanistic Study on the Substitution Behaviour of Mononuclear and Dinuclear Platinum(II) Complexes*

By

**Grace Kinunda**

BSc. Ed(Hons), MSc. (Dar es Salaam, Tanzania)

Submitted in Partial fulfilment of the academic requirements for the degree of

**Doctor of Philosophy**

in the College of Agriculture, Engineering and Science

School of Chemistry and Physics

University of KwaZulu-Natal, Pietermaritzburg

South Africa

## Declaration

This thesis report is based on results from an original work carried out in the School of Chemistry and Physics, University of KwaZulu-Natal, Pietermaritzburg and has not been submitted for the award of a Degree or a Diploma at any University. Where use has been made of work of others, it is duly accredited in the text.

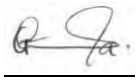

Grace Kinunda

I hereby certify that the statement is true.

……

Professor D. Jaganyi

Supervisor

Pietermaritzburg

December 2013

## Table of Contents

**Acknowledgements**

Apart from my efforts the success of any project depends largely on the encouragement and guidelines of many others. I take this opportunity to express my gratitude to the institutions and people who have been instrumental in the successful completion of my thesis. Firstly, I would like to show my utmost appreciation to my supervisor Prof. D. Jaganyi for his tremendous support and help. Without his encouragement and constant guidance this thesis would not have materialized.

I thank my sponsor, CIBI World Bank Project, University of Dar es Salaam (UDSM) for the financial support. Without their support this study would have not been possible. I also acknowledge my employer, UDSM for granting me study leave.

My grateful thanks are also extended to the following Drs; Allen Mambanda, Desigan Reddy and Peter Ongoma for their valuable and constructive suggestions during the laboratory work and writing of this thesis. Their willingness to give their time so generously has been very much appreciated. I am grateful to all my friends Sophia Wilson, Tshepiso Rose Papo, Claire Ijumba, Anna Kabuje, Elizabeth Diu, Anna Ahmed, Celina Mabula, Victoria Mariam Mgendi, Nozipho Kethukhutula Hadebe and Restituta Mushi for being the surrogate family during the period of my studies and for their continual moral support thereafter.

To my colleagues in the kinetic group who willingly helped me gather the necessary data and information needed for this compilation, I thank you. In particular, I want to give special thanks to Dr Isaac Masika Wekesa who was like my brother in academics

over the years. I appreciate the good working relationship we shared in the lab and compiling this thesis. Mr Muvhango, thank you very much for your yarns during lunch time which ended up invigorating my mind and made me rather active to concentrate on my work than dozing off after lunches. Furthermore, I extend my deepest appreciation to the staffs of school of Chemistry and Physics for all that they meant to me during the crucial times of the completion of this PhD. In a special way I would also like to thank Mr Craig Grimmer for his guidance and assistance regarding NMR spectra.

I am indebted to my beloved parents and siblings who inspired, encouraged and fully supported me in every trial that came my way. I really thank them for giving me moral and spiritual support. No words in this world can express my deepest indebtedness to my beloved husband Bennet Kapinga for the love and care he showed me during the course of my studies. Thank you very much BK for your forbearance and interminable support while I was pursuing this study.

It is difficult to mention all as the list is boundless; however my heartfelt thanks are extended to all those who in one way or another contributed to make the accomplishment of this hard and long work possible. Above all, God the father of all, I am thankful for the wellbeing, strength and guidance that keeps me standing and for the sureness that keeps me believing that this work would be possible. Dear Lord, confidently you are my strength and shield (Psalm 28:7) and through your strength I can do all things (Philippians 4:13). My heart will always trust in you Lord and my mouth will continuously speak your praise!

**Dedication**

This work is dedicated to;

*My wonderful husband Bennet*

*My caring parents Edmund and Bernada*

*My charming sisters Martha and Gloria*

*and*

*My exquisite brother Danford.*

**Abstract**

The electronic and steric effects of the ligand framework on reactivity of a series of Pt(II) complexes has been investigated. For this purpose, three sets of mononuclear Pt(II) complexes and one set of azine bridged dinuclear Pt(II) complexes were synthesized and characterized by various spectroscopic methods. Substitution reactions of the Pt(II) with chloride leaving group were studied in the presence of 10 mM LiCl to prevent spontaneous parallel reaction due to hydrolysis or solvolysis. For the Pt(II) complexes with aqua molecules as leaving groups substitution reactions were studied in acidic aqueous medium. Thiourea nucleophiles of varying steric hindrance were used as the entering group throughout the studied systems. The reactions were studied under *pseudo* first-order conditions as a function of concentration and temperature using Stopped-flow and UV-Visible spectrophotometric techniques. DFT calculations were performed with the Gaussian 09 program suite to account for the observed reactivity of the complexes.

The first set of complexes (**Chapter Three**) deals with the series of mononuclear Pt(II) complexes with N^N^N chelated framework where the π-conjugation of the complexes were varied by either introducing quinoline ligand or imine bond to the well known bis(2-pyridylmethyl)amine ligand. The results showed that increasing electronic communication without increasing π-backbonding has little effect in increasing the reactivity of Pt(II) complex. Introduction of the quinoline moiety within the non-labile chelated framework of Pt(II) complexes results into a more electron-rich metal centre which retards the approach of the nucleophile through repulsion.

In the second series presented in **Chapter Four**, the ligand 2,2'-dipyridylamine chelate was altered by incorporating an alkyl group of variable chain length spacing tertiary nitrogen of the bidentate chelate giving out analogues of cisplatin Pt(II) complexes. The substitution reactions of the coordinated aqua ligands were characterized by two separate steps. The first was assigned to the simultaneous displacement of the diaqua ligands whereas the second step corresponds to dechelation of the dipyridylamine ligand. This was confirmed by the NMR analysis. The trend in rate constant shows that introduction of the alkyl chain on the tertiary nitrogen joining the two pyridine moieties brings in the steric effect which blocks the approach of the nucleophile to the Pt(II) centre. In addition, the σ-donor effect of the pendant alkyl chain towards the tertiary bridging nitrogen is felt in the *cis* pyridine rings resulting into the decrease in their π-acceptor ability. The decrease in reactivity of the Pt(II) complexes with the increase in length of the alkyl chain is also supported by the dipole moments and the calculated electrophilicity indices.

The third set of complexes (**Chapter Five**) comprise of novel azine bridged dinuclear Pt(II) complexes of the type $[\{PtCl(Py)_2\}_2\text{-}\mu\text{-}pzn]\ (ClO_4)_2$ where py = pyridine, pzn = pyrazine linker and its derivatives. It was found that the introduction of pyridine ligands at each metal centre increases the substitution rates of diaqua complexes by a factor of 10 or 23 compared to $[\{cis/trans\text{-}Pt(NH_3)_2(OH_2)\}_2(\mu\text{-}pzn)](ClO4)_4$. This was attributed to the structural geometry which allows π-backbonding to take place where the electrons from the metal centres are accepted to the empty $\pi^*$-orbitals of the pyridine sub units. The effect of the methyl σ-electron-donating groups present on the pyrazine linker and the trend in reactivity of these azine bridged dinuclear

complexes remained the same as those reported for [*{cis/trans*-Pt($NH_3$)$_2$($OH_2$)*}*$_2$(μ-pzn)](ClO4)$_4$.

The last set of complexes (**Chapter Six**) aimed at investigating the role of *trans* effect as well as π-conjugation effects of the ligand on the reactivities of the Pt(II) centre. For this case **N^S^N** and **N^N^N** mononuclear Pt(II) complexes were investigated to account for the strength of π-back bonding versus the *trans* effect. Results have shown that the chloro ligand in **Pt(N^S^N)** complexes is more labile than **Pt(N^N^N)** complexes due to the high *trans* labilizing effect of the S-donor atom. Quinoline based Pt(II) complexes *viz*. [{N-(2-pyridinylmethyl)-8-Quinolinamine} platinum(II) chloride]Cl, (**Pt2**) and [{8-((2-pyridylmethyl)thiol)Quinoline} platinum(II) chloride]Cl, (**Pt4**) were found to react slower than their pyridine counterparts [{bis(2-pyridylmethyl)amine} platinum(II) chloride]$ClO_4$, (**Pt1**) and {di-(2-picolyl) sulfide} platinum(II) chloride ]Cl, (**Pt3**) due to poor π-acceptor ability of quinoline.

The experimental results in all sets of complexes investigated were supported by the DFT calculations performed with the Gaussian 09 program suite. The thermodynamic parameters ($\Delta H^{\neq}$ and $\Delta S^{\neq}$) suggest that the substitution processes are associative in nature.

## List of Abbreviations

| | |
|---|---|
| A | Adenine or Associative |
| AG | Adenine-Guanine |
| B3LYP | functional hybrid exchange of Becke with the functional correlation gradient of Lee and Yang |
| CBCD | *cis*-diammine-1,1-cyclobutanedicarboxylatoplatinum(II) |
| CML | Chronic Myelogenous Leukemia |
| D | Dissociative |
| dpa | 2,2'-Dipyridylamine |
| dpba | 2,2'-Dipyridyl)-1-butylamine |
| dpea | 2,2'-Dipyridyl)ethylamine |
| DFT | density functional theory |
| dpha | 2,2'-Dipyridyl)-1-hexylamine |
| dpma | 2,2'-Dipyridylmethylamine |
| DMSO | dimethylsulfoxide |
| DMTU | 1,3-dimethylthiourea |
| DNA | Deoxyribonucleic acid |
| dppa | 2,2'-Dipyridyl)-1-propylamine |
| dpzm | 4,4'-dipyrazolylmethane |
| EU | European Union |
| $E_N$ | Electrophilic substitution |
| ESP | electrostatic potential |
| Equiv | equivalent |
| G | Guanine |
| GG | Guanine-Guanine |

| | |
|---|---|
| h | hours |
| $\Delta H^{\neq}$ | Enthalpy of activation |
| HMG | High-Mobility Group |
| HOMO | Highly Occupied Molecular Orbitals |
| I | Interchange |
| $I$ | ionic strength |
| $I_a$ | Associative interchange mode of activation |
| $I_d$ | Dissociative interchange mode of activation |
| $k_{-2}$ | rate constant of the solvolytic pathway or rate constant for the first substitution step |
| $k_2$ | rate constant for the direct attack of the entering nucleophile or rate constant for the second substitution step |
| $k_{obs}$ | Observed rate constant |
| LanL2DZ | Los Alamos National Laboratory 2 Double ζ |
| LUMO | Lowest Unoccupied Molecular Orbital |
| M | mole per litre |
| MeOH | methanol |
| MTU | 1-methylthiourea |
| NBO | natural bond order |
| Nu | nucleophile |
| p$K_a$ | acid dissociation constant |
| Ptdpea | (2,2'-Dipyridyl)ethylamine)platinum(II) |
| Ptdpba | (2,2'-Dipyridyl)-1-butylamine)platinum(II) |
| Ptdpha | (2,2'-Dipyridyl)-1-hexylamine)platinum(II) |

| | |
|---|---|
| Ptbpma | (2,2'-Dipyridyl)methylamine)platinum(II) |
| Ptdppa | (2,2'-Dipyridyl)-1-propylamine)platinum(II) |
| s | seconds |
| Solv | solvent |
| $\Delta S^{\neq}$ | Entropy of activation |
| US | United States |
| T | temperature |
| TOF MS $ES^+$ | A time-of-flight mass spectrometer with an electron spray source operated in the positive ion mode |
| TMTU | 1,1,3,3-tetramethylthiourea |
| TU | thiourea |
| UV | ultra violet |

## Publications and Conference Contributions

### Publications

The work presented in **Chapter Three** & **Four** is ready for publication while the manuscripts for **Chapter Five** & **Six** are under preparation.

1. D. Jaganyi and G. Kinunda, *Understanding the Electronic and π-conjugation Roles of Quinoline on Ligand Substitution Reactions of Pt(II) Complexes*, **(submitted to Transition Metal Chemistry)**.
2. D. Jaganyi and G. Kinunda, *Kinetic and Mechanistic Studies of Cisplatin Analogues Bearing 2,2'-Dipyridylalkylamine Ligands*, **(submitted to Dalton Transactions)**.

### Conference Contributions

**Oral Presentation**

**The 2nd Tanzania Chemical Society International Conference, Dar es Salaam, Tanzania** 5th –7th October 2011. *Kinetic and Mechanistic studies of Phenylenediamine Platinum(II) complexes*.

**Posters**

1. **Dalton 2012 Conference, Warwick University (UK)** on 2nd to 5th April 2012. *Influence of Electronic and π-conjugation Effects on Ligand Substitution Reactions of Pt(II) Complexes with Tridentate N-Donor Ligands.*
2. **INORG2013 conference, Southern Sun Elangeni Hotel, Durban South Africa,** from 30th June to 4th July 2013, *Kinetic and Mechanistic Studies of Cisplatin Analogous Bearing 2,2'-Dipyrydylalkylamine Ligands*.

# Table of Contents

**List of Figures**

# Chapter 1

## 1.1 Cancer

Cancer is the most killer disease in which certain cells in our body grow in an uncontrolled way.[1] It is one of the world's most serious disease because some cancer cells penetrate the walls of lymphatic and/or blood vessels and travel through the lymph and blood systems and lodge in other organs where they again repeat the uncontrolled growth cycle forming new tumours. Tumours can grow and interfere with the digestive, nervous, circulatory systems and they can release hormones that alter body function. Genetic changes in the cancer cells can be inherited or more often changes happen because of the environmental factors such as exposure to carcinogens such as tobacco, asbestos, arsenic, radiation gamma and x-rays, sun and compounds in car exhaust fumes that are directly responsible for damaging DNA, promoting or aiding cancer.[2]

Cancer treatment depends on the type of cancer, the stage of the cancer (how much it has spread), age, health status and additional personal characteristics. Advances in surgery, radiation, immunotherapy, hormonal therapy, gene therapy and chemotherapy are needed to improve the curability of cancer. Generally, there is no single treatment for cancer and patients often receive a combination of therapies with the aim of decelerating and stopping the cancer from spreading. Recently, coordination complexes either as drugs or pro-drugs have become very attractive probes as anticancer agents due to their ability to affect the natural processes, such as cell division and gene expression.[3] This follows the earliest reports on the therapeutic use of transition metal complexes in cancer as from the 19$^{th}$ century after the discovery of cis-diamminedichloroplatinum(II), (cisplatin).[4] The use of

cisplatin in treatment of cancer has encouraged investigators to search and develop many other platinum-based drugswhich are inherently more cytotoxic as well as those that exhibit a broader range of activitywithout causing too much damage to the healthy cells.[5] Since the subject of this thesis is ligand substitution reactions of Pt(II) complexes, it is appropriate to have a brief look at the chemistry of platinum.

## 1.2 Chemistry of Platinum

Platinum has six naturally occurring isotopes; $^{190}$Pt, $^{192}$Pt, $^{194}$Pt, $^{195}$Pt, $^{196}$Pt and $^{198}$Pt with $^{195}$Pt being the most abundant comprising 33.83% of all platinum. It has two dominant oxidation states the +2 and +4, designated as Pt(II) and Pt(IV)respectively. $^{195}$Pt can also be found in the +5 and +6 oxidation states. In Pt(II)complexes, the coordination number of platinum is usually four with a preference of square planar geometry. The complexes of Pt(IV) have coordination number of six with an octahedral configuration. Both Pt(II) and Pt(IV) complexes can have *cis* and *trans* configurations.

The chemical, physical and mechanical properties of platinum and its alloys make them uniquely versatile for a variety of medical applications. Platinum and its alloys are characterised by low corrosivity, high biocompatibility and good mechanical resistance appropriate for medical applications.[6] Platinum's biocompatibility makes it superlative for short-term and everlasting implantation in the body, a quality which is exploited in a range of treatments. Its inertness prevents corrosion inside the body minimizing chances of allergic and side reactions. In addition, platinum electrodes are found in pacemaker-like devices which are used to help people at risk of fatal disturbances in the heart's rhythm.[7] In

some cases flexible tubes with platinum marker bands and guide wires are inserted into the body to diagnose or treat heart diseases. Since platinum is radio-optic it becomes clearly visible in X-ray images, enabling doctors to monitor the position of the device during treatment.7

## 1.3 Platinum Based Anticancer Drugs

Platinum substances have been used in cancer treatment for several decades as they trigger cell death upon DNA binding. Pt-based drugs with a variety of ligands around the Pt centre exist today in clinics and in clinical trials.[8] This is because Pt complexes have ligand exchange kinetics which is in the same order of magnitude as the division of cancer cells, making them proper candidates to obstruct their multiplication[9] with cisplatin being the parent compound among tumour active platinum complexes.

### 1.3.1 Cisplatin

The discovery of anticancer activity of cisplatin[10] (**Figure1.1**) constitutes the most impressive contribution to the use of platinum metal in medicine. To date, cisplatin is highly effective in the treatment of testicular and ovarian cancers and also widely employed in treatment of bladder, cervical, head, neck, oesophageal and small cell lung cancers.[11]

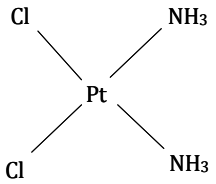


**Figure 1.1:** Structure of cisplatin

The sensitivity of cells towards cisplatin is dependent on DNA platination because DNA is the ultimate drug target.[12] Once administered, cisplatin enters the cell by either passive diffusion or active uptake by the cell (**Figure 1.2**) where hydrolysis of the drug takes place. This hydrolysis process is believed to be the key activation step before the drug reaches its intracellular target DNA. Since inside the cell there is a low concentration of chloride ion compared to that of water, water molecules then attack the Pt(II) centre and sequentially displace the two chlorine atoms.

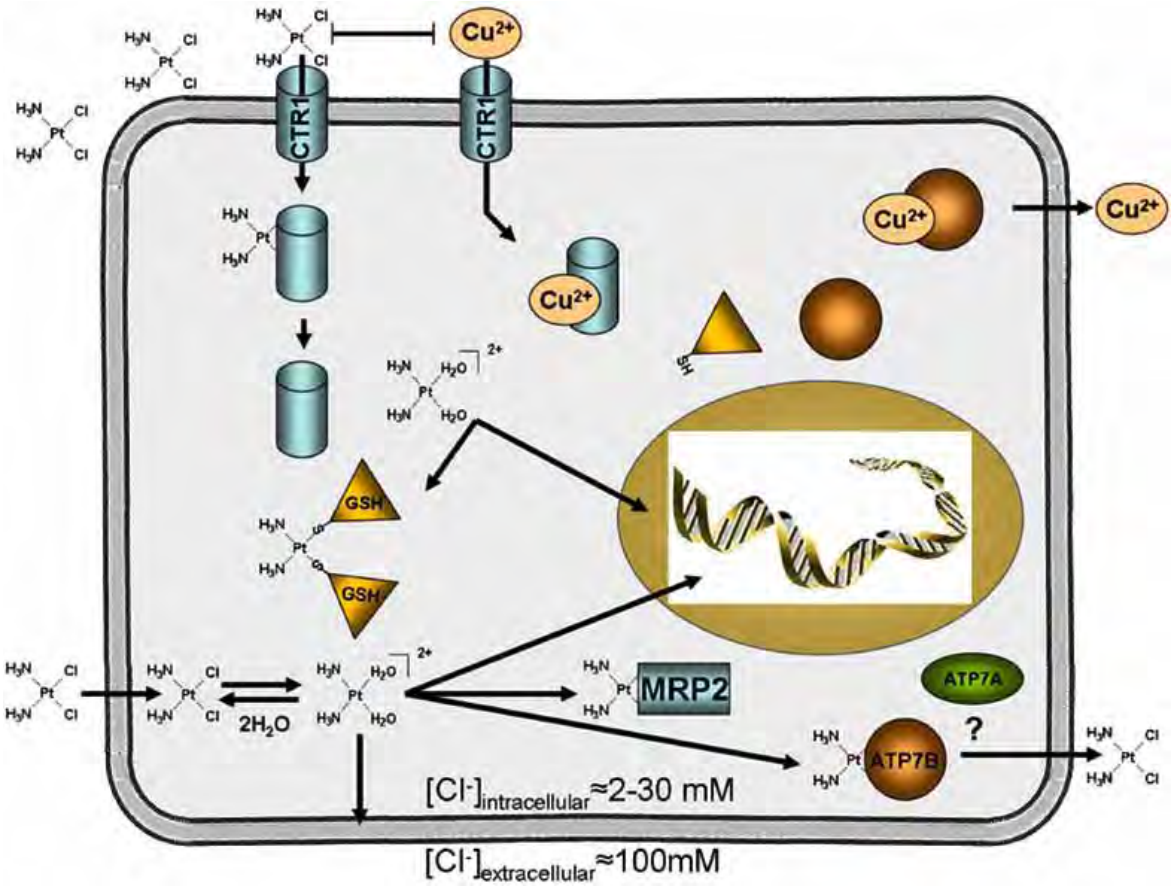


**Figure 1.2:** Schematic diagram of cisplatin uptake and binding to nuclear DNA.[13]

Hydrolysed cisplatin causes platination of DNA, which involves mainly 1,2-intrastrand cross-link 60-65% (**Figure 1.3**) formed usually through the N7 atoms of vicinal guanine.[14]

Formation of cisplatin-DNA adducts causes distortion of the DNA double helix and results in inhibition of DNA replication.1a,[15] Cisplatin-DNA adducts also serve as binding sites for cellular proteins such as repair enzymes, histones, transcription factors and high-mobility group (HMG) domain proteins.[16] The binding of HMG proteins to cisplatin-DNA adducts has been suggested to enhance the anticancer effect of the drug.[16,17]

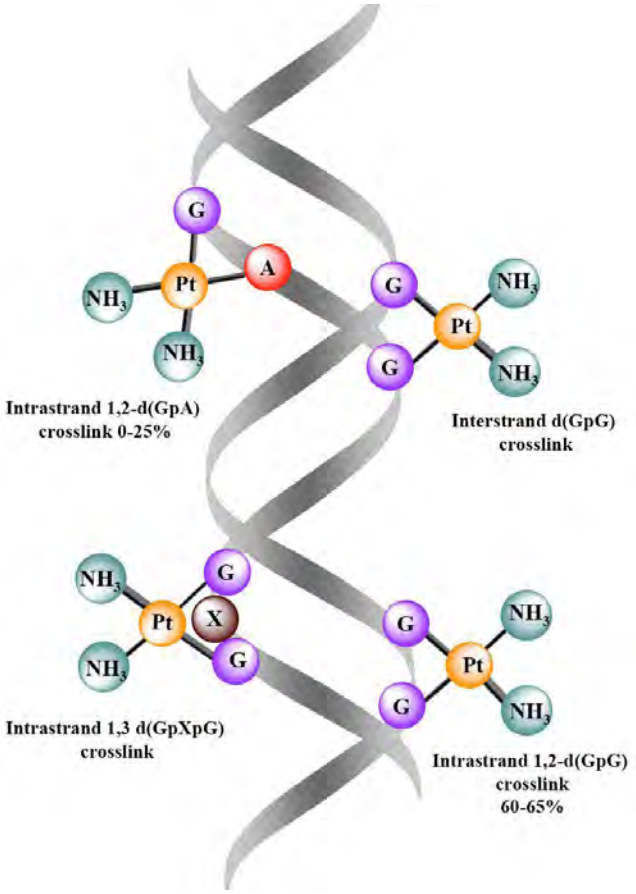


**Figure 1.3:** Formation of DNA adduct with cisplatin.[18]

The efficacy of cisplatin has been greatly hampered by drug resistance and severe side effects.[19] Many tumours display inherent resistance to cisplatin while others develop acquired resistance after initial treatment,[20] and metastasis tumours lack response to this

agent.[21] Acute toxicity is another disadvantage of cisplatin, especially nephrotoxicity, neurotoxicity, ototoxicity, and emetogenesis, which cause patients to suffer from severe side effects.[22] Furthermore, poor water solubility of cisplatin makes its use inconvenient in clinical practice.

### 1.3.2 Cisplatin Analogous

The limitations associated with the clinical use of cisplatin prompted a wide-cast search for more effective and less toxic alternative platinum antitumour agents. These efforts have led to the synthesis of thousands of platinum complexes by changing the nature of the leaving groups and carrier ligands.[23] In the development of platinum compounds which are commonly known as second and third generation platinum drugs, the primary goal was to reduce the toxic side effects and to a lesser extent broaden the spectrum of activity.[24] As such, many cisplatin analogous have been tested in cancer patients but most were found to be unsuitable for further development because of poor aqueous solubility, formulation difficulties and severe toxicity.[23]Those that have achieved routine clinical use and have been approved for clinical administration are analogous of cisplatin which are carboplatin, oxaliplatin, nedaplatin and lobaplatin (**Figure 1.4**).[23a,25]

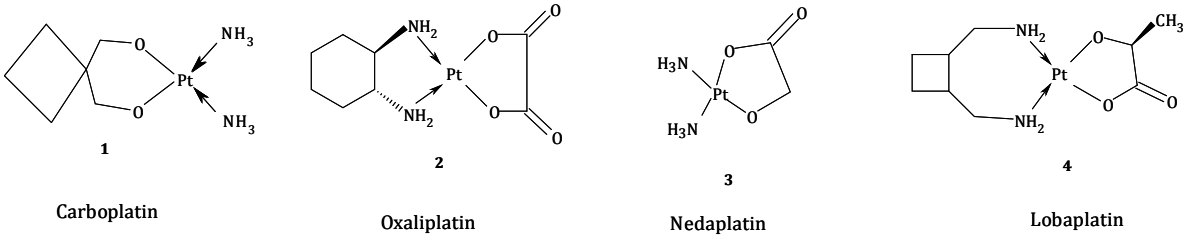


**Figure 1.4:** Structures of cisplatin analogous

*Carboplatin* (*cis*-diammine-1,1-cyclobutanedicarboxylatoplatinum(II)) abbreviated as CBCD (**Figure 1.4**, (**1**)) is used in treating patients with ovarian, non-small cell lung, testicular, stomach, and bladder cancers.[26] Carboplatin kills cancer cells by binding to DNA and interfering with the cell's repair mechanism, which eventually leads to cell death. Chemically Carboplatin differs from cisplatin by being a bigger molecule, with a less labile cyclobutanedicarboxylato ligand. This allows the drug to be retained longer in the body and reduces the rate of formation of toxic by-product. In its use carboplatin exhibits cross-resistance in cisplatin resistant cell lines and it has not demonstrated any substantial advantages over cisplatin.[27]

*Oxaliplatin* differs from cisplatin in that the amine groups of cisplatin are replaced by diaminocyclohexane (DACH) and the chloro groups are swapped by oxalate group. Oxaliplatin was the first Pt(II) drug to be used for the treatment of metastatic colorectal cancer which has recurred or become worse following initial therapy with a combination of other drugs.[28] It has also been used in clinical trials for the treatment of other cancers but has found the most success in gastrointestinal neoplasms including gastric, esophageal and pancreatic cancers.[28c] Compared to cisplatin, oxaliplatin has increased cellular uptake due to the presence of oxalate group which increases the aqueous solubility of the complex and the DACH group which makes the complex less polar.

Inside the cell oxaliplatin rapidly undergoes non-enzymatic transformation into reactive compounds following displacement of the oxalate group. The remaining dichloro(DACH) platinum complex exerts its cytotoxic effect mostly through DNA damage by forming

essentially three types of cross-link adducts; intrastrand, interstand and DNA-protein.[28c,29] The most commonly adduct (**Figure 1.5**) is the intrastrand between the neighbouring purine bases (1,2-GG or AG) at the N7 positions.[30] These adducts were found to be more massive and hydrophobic than that of both cisplatin and carboplatin and subsequently were more effective in inhibiting DNA synthesis than cisplatin adducts. Nevertheless, oxaliplatin shows several limitations such as a reversible peripheral neuropathy characterized by paraesthesia and dysaesthesia in hands, feet and the oral region.[31] The presence of the kinetically less labile carboxylate or oxalate in carboplatin and oxaliplatin, contributes to the reduced side effects observed in patients compared with those treated with cisplatin.[23]

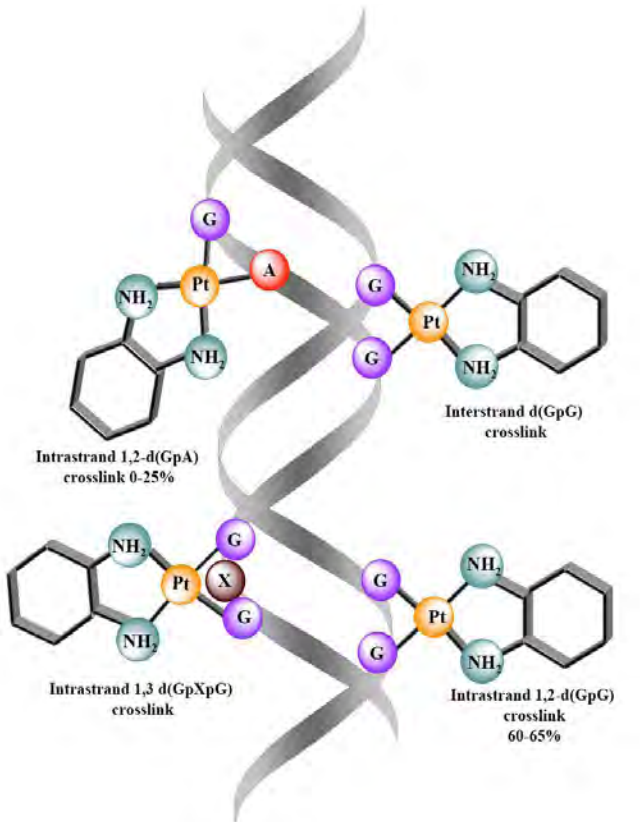


**Figure 1.5:** DNA adducts formed by oxaliplatin.[30]

*Nedaplatin* has a novel structure involving a glycolate ring bound to platinum atom as a bidentate ligand and two ammine ligands like cisplatin and carboplatin. Nedaplatin binds to DNA in a similar way to cisplain and therefore they have identical types of combined bases after reaction with DNA.[32] As for cisplatin, after uptake the hydrolysis of the leaving group takes place where the glycolate portion of nedaplatin is cleaved, forming active species which exists in three different forms and at equilibrium depending on the pH condition (**Figure 1.6**). The active species bind to DNA thereby inhibiting its replication. Phase II studies have shown that nedaplatin has a spectrum of activity similar that of cisplatin but with lower nephrotoxcitiy.[33] Myelosuppression associated with thrombocytopenia is the dose-limiting toxicity of nedaplatin.[23,33]

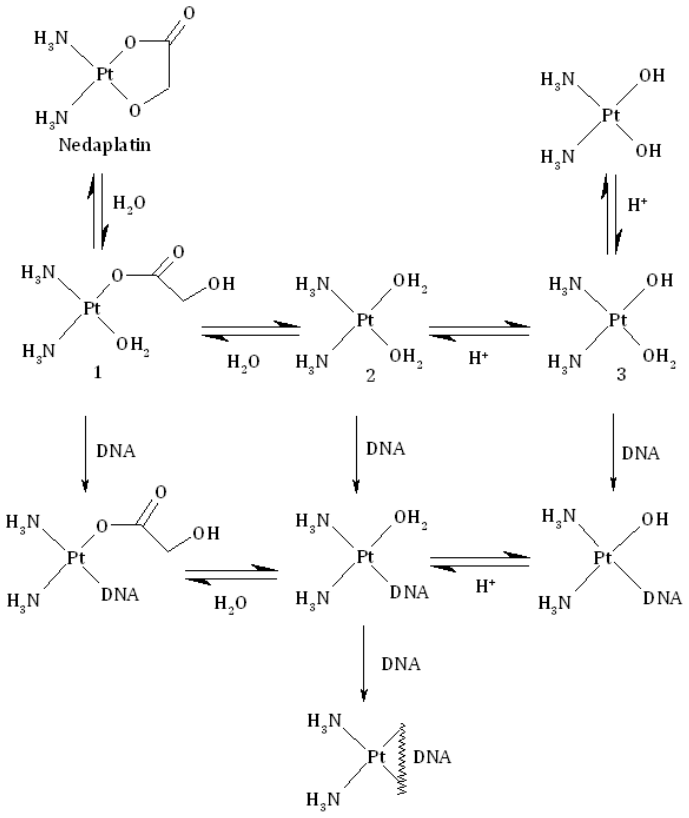


**Figure 1.6:** Hydrolysis and DNA binding of nedaplatin.[32] Charges of the complexes are omitted for clarity.

*Lobaplatin* has completed phase II clinical trials in the US, Australia, EU, Brazil and South Africa for the treatment of various cancers, including breast, esophageal, lung and ovarian cancers as well as Chronic myelogenous leukemia (CML).[18] The antitumour activity of lobaplatin is believed to result from the formation of DNA-adducts, mainly as GG and AG intra-strand cross-links. It also influences the expression of the c-myc gene, which is involved in regulation of cell proliferation, differentiation and eventually death. This has been proposed to contribute to the increased antitumour activity of lobaplatin over cisplatin and carboplatin in a wide range of cancer lines.[34]

### 1.3.3 Non-classical Pt(II) Drugs

Cisplatin analogous generally form comparable adducts with DNA that translate into the same domain of spectral activity. Therefore, there is a need to develop compounds that will have different chemical structures and biological properties that are different from that of cisplatin analogous. Consequently, attention has been turned to the synthesis of 'non-classical' platinum complexes which are capable of forming different DNA adducts that display a different spectrum of anticancer activity compared to cisplatin.[35] Examples of these non-classical platinum complexes include; platinum(IV) complexes, monofunctional complexes like *cis*-$[Pt(NH_3)_2(Am)Cl]^+$ where Am = pyridine, pyrimidine, or purine,[36] *trans* complexes of the general formula *trans*-$[PtCl_2(NH_3)L]$ where L is a planar N donor[37] and multinuclear complexes.[38]

### 1.3.3.1 MonofunctionalPt(II) Complexes

Monofunctional complexes of Pt(II) are complexes with a stable tridentate ligand, while the fourth coordination place is occupied by a labile ligand, mostly a chloride or an aqua ligand. In early studies monofunctional Pt(II) complexes such as [PtCl(dien)]Cl, (dien = diethylenetriamine) and $[PtCl(NH_3)_3]Cl$ were considered to be biologically inactive. The monofunctional binding of such complexes to DNA contributed to their inactivity because DNA conformation and downstream cellular processes were hardly affected.[37,36] Recent investigations show that some monofunctional Pt(II) complexes (**Figure 1.7**) indeed exhibit significant antineoplastic activity.[39] Moreover, the profile of cellular response to these monofunctional complexes is different from those of the classic bifunctional, charged/neutral platinum-based drugs.[39a-c] For example pyriplatin, (**Figure 1.7**(**1)**) is an excellent substrate for organic cation transporters expressed in human colorectal cancers and associated with the uptake of oxaliplatin. Pyriplatin DNA adducts block transcription nearly efficiently as cisplatin.

Phenanthriplatin (**2**) destroys cancer cells with greater efficacy than either cisplatin or oxaliplatin. On another hand, monofunctional Pt(II) complex of 8-aminoquinoline derivatives (**3**) exhibited activity against many cancer cell lines. The higher cytotoxicity of complexes **2** and **3** in **Figure 1.7** originates from their efficient cellular uptake and strong transcription inhibitory properties of their ligands.[39a-c] Platinum-acridinylthiourea (**4**) showed promising biological activity superior to cisplatin in a wide range of solid tumour cell lines at micromolar concentrations, especially in non-small cell lung carcinomas.[39d,e]

Good enough, the complex binds to DNA in a dual manner involving platinum coordination and acridine intercalation.

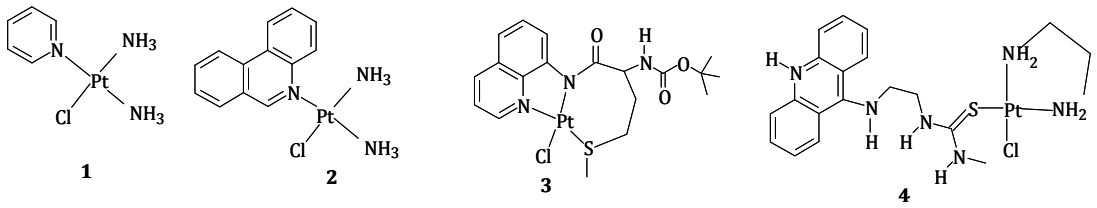

**Figure 1.7:** Examples of monofunctional Pt(II) complexes with antitumour activity.

Generally, toxicity of these new hybrid agents suggests that additional structural modifications of the tridentate ligand are still needed. In order to improve the potency and cellular uptake of monofunctional Pt(II) complexes, the tridentate stable ligand of the complexes has to be varied so that various N/S-heterocyclic ligands can be included. Modifications by the introduction of lipophilic ligands facilitate the uptake of the drug molecules across the cell membrane and affect the activity of the drug. In the same way, bulky ligands maintain the cytotoxicity of the complexes while significantly reducing their rate of deactivation by S-containing molecules (such as cysteine and glutathione) due to their slow ligand exchange reactions. Such modifications of the tridentate/bidentate carrier ligands of monofunctional Pt(II) complexes form part of this research as presented in **Chapter Three**, **Four** and **Six** of this thesis.

### 1.3.3.2 *Trans* Geometry Platinum Compounds

Previously, it has been generally accepted as a standard that a *cis*-configuration of the leaving groups is necessary for antitumour activity of platinum compounds.[40] However, it

has been observed that certain *trans*-platinum complexes have both *in vitro* and *in vivo* antitumour activity through a different mode of binding to DNA. The *trans* analogue of cisplatin, *trans* diaminedichloroplatinum(II), transplatin, is inactive as it is kinetically not stable and therefore susceptible to deactivation. Substitution of one or both ammine ligands in transplatin with more bulky ligands retard ligand substitution reactions of the two chloride ions, thereby decreasing undesired reactions between platinum and cellular constituents and simplifying its interaction with DNA.[41] The spectator ligands in these complexes can be categorized into; planar aromatic amines, alkylamines and iminoethers (**Figure 1.8**). These compounds in general are more active against cisplatin-resistant cell lines than their *cis* analogous.[41] These results are encouraging and have forced the re-examination of the structure-activity relationships for platinum antitumour drugs.

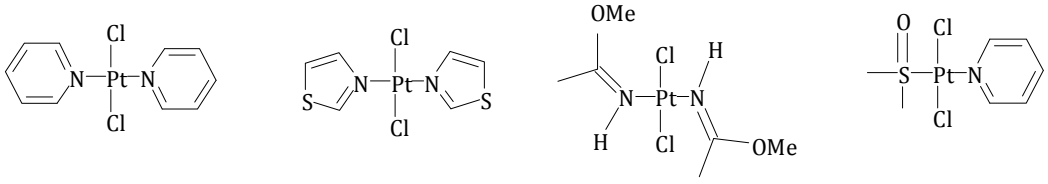


**Figure 1.8:** Examples of *trans*Pt(II) complexes with antitumour activity.

### 1.3.3.3 Multinuclear Platinum Complexes

Multinuclear platinum complexes contain two or more linked platinum centres that can each covalently bind to cellular DNA to form flexible, non-directional DNA adducts as well as long range DNA adducts to induce DNA conformational changes. The difference in the cytotoxic DNA adducts formed and the cell death mechanisms induced by multinuclear Pt drugs may potentially overcome cisplatin drug resistance.[35c,42]

#### 1.3.3.3.1 Bi-Functional Platinum Centres

Initially, the synthesis of multinuclear platinum complexes (**Figure1.9**) was based upon the linking of two cisplatin-like centres.[43] The first complex developed was a simple cisplatin derivative (2,2/c,c), (**1**) with two [$PtCl_2(NH_3)$] centres linked by a flexible diaminechain.[43f,h] This kept with the traditional structure activity rules of a neutral complex consisting of a square planar platinum with two *cis*-chloro ligands and with at least one am(m)ine group. The replacement of the chloro ligands with malonate (**2**), to improve water solubility, resulted in a series of 2,2/c,c complexes with good activity in cisplatin resistant cancer cell lines.[43e]

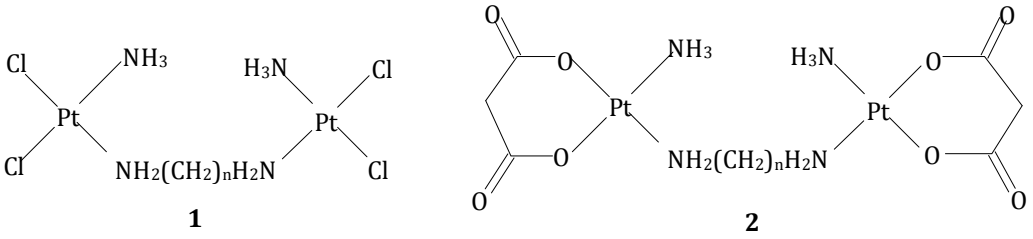


**Figure 1.9:** Dinuclear platinum complexes containing two linked cisplatin centres, where n= 2-6.

While these complexes were capable of binding to DNA in a manner similar to cisplatin, they were also capable of forming longer range intra- and interstrand adducts.[43] Mechanistic studies demonstrated that the 2,2/c,c complexes (**I**) produced a high percentage of interstrand adducts.[41e] A similar approach was also adopted by Broomhead and co-workers (**Figure1.10**), who linked two cisplatin-like centres together using the 4,4'-dipyrazolylmethane (dpzm) ligand.[43a-d] While single bridged complexes exhibited better

cytotoxicity than the double bridged complexes in three cancer cell lines, they were insoluble in water and did not show any significant advantage compared to cisplatin.[43d]

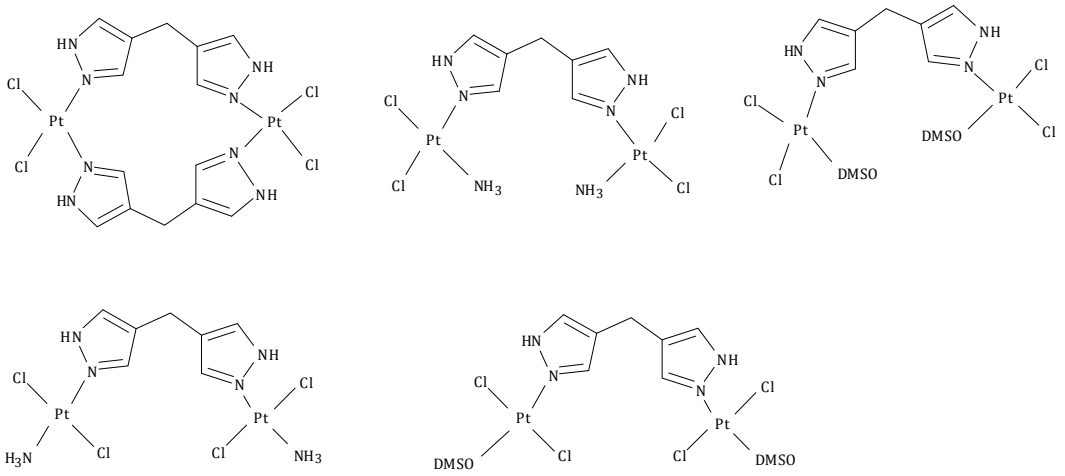

**Figure 1.10:** Double and single bridged, multi-nuclear platinum complexes linked by the 4,4'-dipyrazolylmethane (dpzm) ligand.[43a,b,d]

### 1.3.3.3.2 Mono-Functional Platinum Centres

While the synthesis of dinuclear complexes with two bi-functional platinum centres resulted in complexes that could bind to DNA in a different manner than cisplatin, the more important development was the subsequent synthesis of dinuclear complexes that contained mono-functional platinum centres.[46] The first complexes, called 1,1/t,t and 1,1/c,c, (**Figure 1.11**) represented a truly new class of metal based anticancer compounds, as they were cationic and contained only one chloro leaving group on each platinum centre. These complexes show good water solubility and excellent activity in both cisplatin sensitive and resistant cell lines.

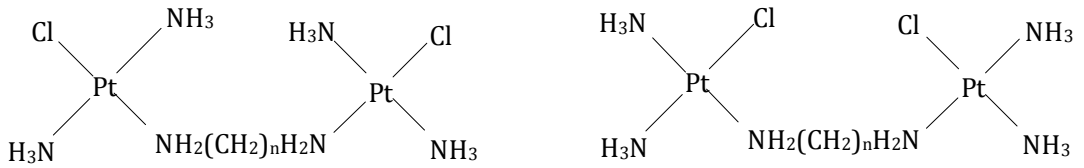


**Figure 1.11:** Dinuclear platinum complexes with charged mono-functional platinum centres.[44,45(a)] Charges of the complexes are omitted for simplicity.

From all the multinuclear complexes tested, the first to enter clinical trials based on *in vitro* and *in vivo* trials was the tri-nuclear complex BBR3464 (**Figure1.12**). BBR3464 was more active than cisplatin in all cancer cell lines tested.[47] For example, in an assay of seven human cancer cell lines the mean $IC_{50}$ of BBR3464 (0.6 μM) was much lower than that observed for cisplatin (27.8 μM).[48] Most importantly, BBR3464 shows activity in several cancer cell lines that have a natural resistance to cisplatin.[49] From clinical trials it appears that BBR3464 is most useful in the treatment of non-small cell lung cancer, gastric cancer, ovarian cancer, small-cell lung cancer and other solid tumours including pancreatic cancer.[49]

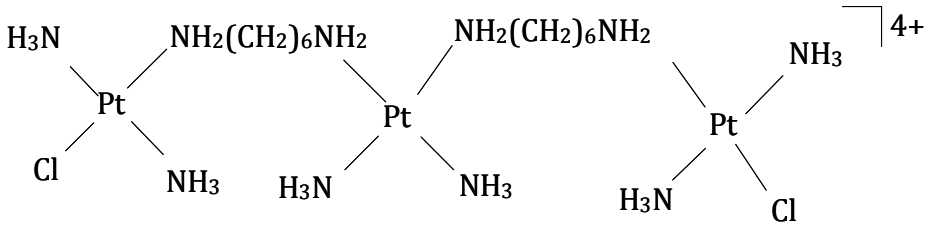


**BBR 3464**

**Figure 1.12:** Structure of the tri-nuclear compound BBR3464.

Data from the studies of the binding of DNA with multinuclear platinum complexes in different cancer cell lines shows some important structure-activity rules.[47] The main factors consistent in designing multinuclear platinum drugs include; chain length and flexibility, hydrogen-bonding capacity and charge of the linking chain and the geometry of the leaving ligand with respect to the linker. For the aliphatic chains the ideal length of the linker appears to be eight atoms (two ammine and six methylene groups). For the polyamine family of multinuclear platinum complexes, it is evident that increasing the charge and the chain length results into high activity.[50] However flexibility also appears to be a major factor. In studies where the dpzm ligand was used as the linker, their complexes were found to be less active than their aliphatic equivalents 1,1/t,t (n=6, 12) and BBR3464.[43(a)] The decrease in activity of the mentioned complexes was therefore attributed to the rigidity of the linker. Interestingly, these complexes were less reactive compared to azole and isomeric azine-bridged Pt(II) complexes due to their steric differences on their DNA adducts. Geometric isomerisation also plays a role for instance complexes with the chloro ligand *trans* to the bridging ligand are generally more active, particularly in cisplatin resistant cell lines.[50] This type of dinuclear Pt(II) complexes form part of the research objectives and are further discussed in **Chapter Five**.

## 1.4 Aims of the Study

Pt(II) complexes have been used for the treatment of many diseases but with little understanding of their mechanism of action in biological systems. A search for new platinum drugs remains a continuous process and knowledge of the interaction of the different platinum complexes with sulfur-bonding bio-molecules therefore deserves much

attention. Pt(II) has high affinity for binding to sulfur donors, especially thiols, compared to nitrogen donor ligands such as DNA bases. Due to high intra-cellular concentrations of sulfhydryl groups (cysteine and glutathione), it has been hypothesised that sulfur containing nucleophiles initially bind to the platinum atom and then convert to thermodynamically more stable products platinum–DNA adducts.[51] To date it is generally accepted that the antitumour activity of platinum drug can be ascribed to interactions between the metal complex and DNA, primarily with the genetic DNA, which is located in the nucleus.

Ligand substitution reactions of Pt(II) complexes contribute to a better understanding of the precise biochemical mechanism of some Pt(II) complexes. The results of the substitution reactions with biologically relevant ligands could help to get more information on the possible interaction modes of Pt(II) complexes with *in vivo* targets and their representative application in the study of their antitumour properties. Moreover, the reactivity of the complexes will be useful in predicting the extent of drug of similar structure which reaches the target sites as well as the degree of side reactions, its circulation lifetime and more importantly the antitumour activity of the drug in the target sites.

Within the aforementioned basic structural frameworks concerning the development of new clinically useful platinum based anticancer agents, it is clear that novel structures unrelated to those agents assigned to cisplatin and its analogous platinum complexes can circumvent cisplatin resistance and enhance their activity. For mononuclear Pt(II)

complexes, the choice of the bidentate or tridentate ligand adds stability to cationic platinum complexes and decreases the possibility of undesired substitution reactions at the chelate. In the development of multinuclear Pt(II) complexes, the nature and size of the linker plays a role in determining the biological activity of the resultant complexes. Therefore, to fulfil the main objective of this study, several complexes such as monofunctional Pt(II) complexes (**Chapter Three** and **Six**), bifunctional-platinum(II) complexes (**Chapter four**) and dinuclear platinum(II) complexes (with rigid linker, **Chapter Five**) have been synthesized and their mechanistic and kinetic investigations using thiourea as the strong sulfur nucleophiles evaluated. Thiourea nucleophiles were selected as entering nucleophile because of their biological relevance and their high nucleophilicity prevents a possible back reaction.[52] The non-labile chelate ligand framework of the complexes was carefully electronically/sterically tuned to enable a systematic study of the reactivity of the complexes towards relevant nucleophile. The specific aims of the study undertaken are:

1. To understand the electronic π-conjugation role of quinoline moiety on ligand substitution reactions of Pt(II) complexes.

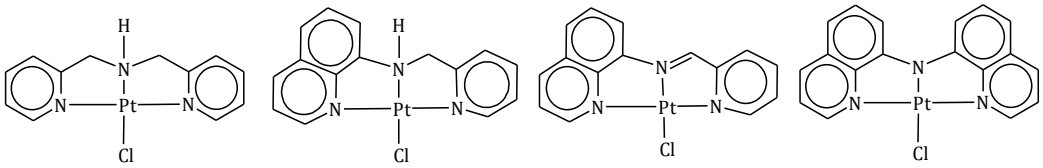

In this study the competing σ-donor effect of quinoline and π-acceptor property of pyridine in the set of complexes is examined.

2. Carry out kinetic and mechanistic studies of cisplatin analogous bearing 2,2'-dipyridylalkylamine ligands.

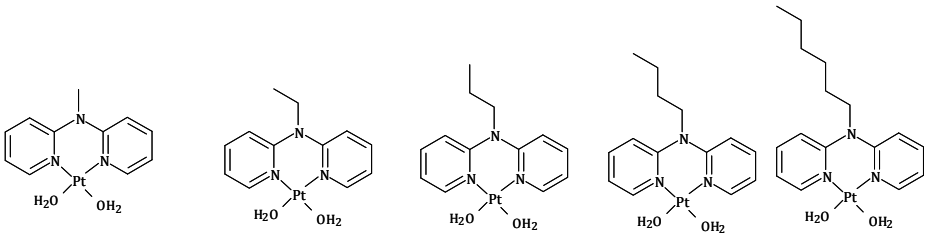

**Ptdpma** **Ptdpea** **Ptdppa** **Ptdpba** **Ptdpha**

The electronic and steric effects of the alkyl group of variable chain length spacing tertiary nitrogen of the bidentate chelate is investigated. Results obtained were compared with those of Pt(bpy) (where bpy = N,N'-bipyridine) which also contains two pyridine rings in the bidentate chelate.

3. To study the kinetics of novel dinuclear Pt(II) complexes containing four non-planar pyridine ligands. Possibility of pyridine rings to enter into electronic communication with the Pt(II) orbitals through π-backbonding is assessed.

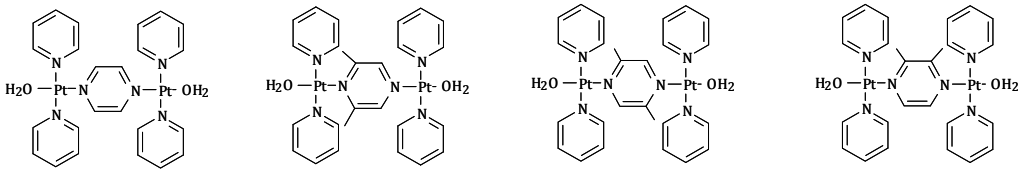

**Pt-PZN** **Pt-2,6 PZN** **Pt-2,5 PZN** **Pt-2,3 PZN**

4. To investigate the role of *trans* and π-conjugation effects on ligand substitution reactions of Pt(II) complexes with tridentate N/S-donor ligands. The chapter examined the competing roles of π-backbonding through the extended chelate and the strong σ-donor *trans* effect of sulfur atom.

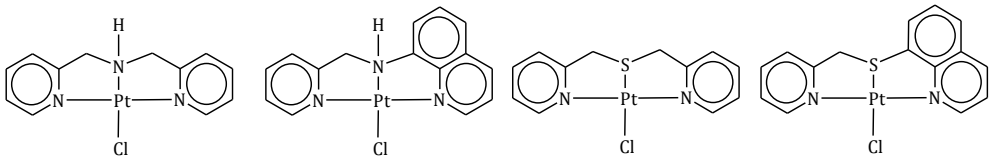

It is worth mentioning that no other participants were involved in the work presented in Chapter 3 to 6.

## 1.5 References


1. (a) Marques, M. P. M., *ISRN Spectroscopy*, **2013**, Article ID 287353, http://dx.doi.org/10.1155/2013/287353; (b) Pan, M. and Ho, C., *Chem. Soc. Rev*., **2008**, *37*, 2558.
2. (a) Parkin, D. M., Boyd, L, Walker, L. C., *Br J Cancer*., **2011**, 105 Suppl 2:S77-81; (b) Parkin, D. M, Mesher, D, Sasieni P., *Br J Cancer*., **2011**, 105 Suppl 2:S66-9; (c) Parkin, D. M., *Br J Cancer*., **2011**, 105 Suppl 2:S6-S13.
3. (a) Prezza, M., Hindo, S., Chen, D., Devenport, A., Schmitt, S., Tomco, D and Dou, Q. P. *Curr. Pharm. Des*., **2010**, *16*(16), 1813; (b) Ott, I., Gust, R., *Arch. Pharm(Weinheim)*., **2007**, *340*(3), 117.
4. Rosenberg, B., Van Camp, L and Krigas, T*., Nature,* **1965**, *205*, 698.
5. (a) Monneret, C. *Ann. Pharm. Fr*., **2011**, *69*(6), 286.
6. (a) Agnew, W. F., Yuen, T. G. H., McCreery, D. B and Bullara, L. A., *Exp. Neurol*., **1986**, *92* (1), 162; (b) Brummer, S. B and Turner, M. J. *IEEE Trans. Biomed. Eng*. **1977**, BME-*24(*5), 440.
7. Cowley, A and Woodward B., *Platinum Metals Rev*., **2011**, *55*(2), 98.
8. Palm-Espling, M. E, Wittung-Stafshede P., *BiochemPharmacol*., **2012**, *83*(7), 874.
9. Koskova, I., *Frontiers in Anti-Cancer Drugs Discovery*., **2010**, *1*, 298.
10. (a) Rosenberg, B. *Plat. Met.Rev.* **1971**, *15,* 42; (b) Guo, Z., Sadler, P., *J.Adv. Inorg. Chem.,* **2000**, *49,* 183.
11. (a) Waxman, E. S., Review article on *Current Treatment Options for Non–Small-Cell Lung Cancer.In*:-*Oncology Nurse Edition*., **2012**, *26*(8 ), 1; (b) Giaccone, G. *Drugs*, **2000**, *59*, U4; (c)Fernandes, D., Louzada, M. L., Souza, C.A., Matzinger, F., *Current*

*Oncology*, **2011**, *18*(2); (d)Oliver, T. G., Mercer, K. L., Sayles, L. C., Burke, J. R., Mendus, D., Lovejoy, K. S., Cheng, M.-H., Subramanian, A., Mu, D., Powers, S., Crowley, D., Bronson, R. T., Whittaker, C. A., Bhutkar, A., Lippard, S. J., Golub, T., Thomale, J., R. T., Jacks, T and Sweet-Cordero,E. A., *Genes & Dev*., **2010**, *24,* 837.

12. Min, Y., Mao, C.-Q., Chen, S., Ma, G., Wang, J., Liu, Y., *Angew. Chem. Int. Ed*., **2012**, *51*, 6742.
13. Cepeda, V., Fuertes, M. A., Castilla, J., Alonso, C., Quevedo, C andPérez, J. M., *Anti-Cancer Agents in Medicinal Chemistry,* **2007, 7**,**3.**
14. (a) Sadler, P. J. and Guo, Z., *Pure &Appl. Chem.,* **1998**, *70*( 4), 863; (b) Kostova, I., *Recent Patents on Anti-Cancer Drug Discovery.*, **2006**, *1*, 1.
15. Lee, K-B, Wang, D., Lippard, S.J., Sharp, P.A. *Proc. Natl. Acad. Sci.* USA, **2002**, *99*, 4239.
16. (a) Gómez-Ruiz, S., Maksimović-Ivanić, D., Mijatović, S., and Kaluđerović, G. N. *Bioinorganic Chemistry and Applications*., **2012**, Article ID 140284, **doi:10.1155/2012/140284**; (b) Louie, A.Y., Meade, T., *J. Chem. Rev*.,**1999**, *99*, 2711; (c) Volkter, W. A., Hoffman, T. J. *Chem. Rev*., **1999**, *99*, 2269; (d) Cohen, S. M., Lippard, S. J. *Prog. Nucleic Acid Res. Mol. Biol.,* **2001**, *67*, 93; (e) Ohndorf, U-M, Rould, M. A, He, Q, Pabo, C. O, Lippard, S. J., *Nature.,* **1999**, *399*(6737), 708.
17. (a) Semi, P and Lippard,S. J., *Biochemistry.*, **2011**, *50*(13), 2567; (b) He, Q., Liang, C. H., Lippard., S. J. *Proc. Natl. Acad. Sci.* USA, **2000**, *97*, 5768; (c) Wong, B., Masse, J. E., Yen, Y.-M., Giannikoupolous, P., Feigon, J., Johnson, R. C. *Biochem*., **2002**, *41*, 5404.
18. Boulikas, T., Pantos, A., Bellis, E and Christofis, P., *Cancer Therapy*., **2007**, *5*, 537.
19. (a) Galluzi, L., Senovila, L., Vitale, I., Michels, J., Martins, I., Kepp, O., Cascedo, M, Kroemer, G., *Oncogene*, **2012**, *31*(15), 1869; (b) Dempke, W., Voigt, W., Grothey, A.,

Hill, B. T and Schmoll, H. J., *Anti-Cancer Drugs*, **2000**, *11*, 225; (c) Michels, J., Vitale, I., Galluzzi, L., Adam, J., Olaussen, K. A., Kepp, O., Senovilla, L., Talhaoui, I., Guegan, J., Enot, D. P., Talbot, M., Robin, A., Girard, P., Orear, C., Lissa, D., Sukkurwala, A. Q., Garcia, P., Behnam-Motlagh, P., Kohno, K., Wu, G. S., Brenner, C., Dessen, P., Saparbaev, M., Soria, J.-C., Castedo, M., Kroemer, G., *Cancer Research.*, **2013**, *73*(7), 2271.

20. (a) Eckstein, N., *Journal of Experimental & Clinical Cancer Research*., **2011**, *30*, 91; (b) Galanski, M., Jakupec, M. A and Keppler, B. K. *Curr. Med. Chem*., **2005**, *12*, 2075; (c) Ott, I and Gust, R. *Pharm. unsererZeit.*, **2006**, *35*, 124.

21. (a) Wang, D and Lippard, S. *J. Nat. Rev. Drug Discovery.*, **2005**, *4*, 307; (b) Cohen, S. M.,Goel, A., Phillips, J., Ennis, R. D., Grossbard, M. L., *Oncologis*t., **2006**, *11*, 630.

22. (a) Xiaoyong, W., *Anti-Cancer Agents in Medicinal Chemistry*., **2010**, *10*( 5), 396; (b) McWhinney, S. R., Goldberg, R. M., and McLeod, H. L., *Mol. Cancer. Ther*., **2009**, *8*, 10; (c) Sun, R. W.-Y., *Mod. Chem. Appl.,* **2013**, *1*(3), 1.

23. (a)Wong, D. Y. Q. and Ang, W. H., *Cosmos*, **2012**, *8*( 1), 121; (b) Abu-Surrah, A. S., and Kettunen, M., *Current Medicinal Chemistry*, **2006**,*13*, 1337; (c) Kelland, L. R. *Critical Reviews in Oncology Hematology*, **1993**, *15*(3), 191;(d) Hay, R. W and Miller, S. *Polyhedron*, **1998**, *17*, 2337.

24. (a)Amptoulach, S. and Tsavaris, N., *Chemotherapy Research and Practice*, **2011**, 1; (b)Kelland, L. R., Barnard, C. F., Evans, I. G., Murrer, B. A., Theobald, B. R., Wyer, S. B., Goddard, P. M., Jones, M., Valenti, M. and Bryant, A. *J. Med. Chem*., **1995**, *38*(16), 3016; (c) Bloemink, M. J. and Reedijk, J., *Metal Ions in Biological Systems.*, **1996**, *32*, 641.

25. (a) Alberto, M. E., Butera, V., and Russo, N., *Inorg.Chem*., **2011**, *50*, 6965; (b) Fuertes, M. A., Alonso, C. and P´erez, J. M, *Chem. Rev*., **2003**, *103*, 645.

26. (a) Katsumata, N., *Annals of Oncology.*, **2011**, *22* (Suppl. 8), 29; (b) Highley, M. S. and. Calvert, A. H, *in*: *Platinum-Based Drugs in Cancer Therapy*, Kelland, L. R. and Farrell, N. P. (Eds), Humana Press Inc., Totowa/NJ, **2000**, 171–194; (c) Bamias, A., Tiliakos, I., Karali, M-D., Dimopoulos,M. A., *Annals of Oncology*., **2006**, *17*, 553; (d) Bournakis, E., Dimopoulos, M. A, Bamias, A., *Expert Rev Anticancer Ther*., **2011**, *11*(6), 931.

27. (a) Stewart, D. J., *Crit Rev Oncol Hematol*., **2007**, *63*(1), 12; (b) Lokich, J., *Cancer Invest*., **2001**, *19*, 756.

28. (a) Brienza, S., Bignound, J., Itzhaki, M., Krikorian, A. *Eur. J. Cancer*., 1**995**, *31*A, S194; (b) Dunn, T. A., Schmoll, H. J., Grunwald, V., Bokemeyer, C., Casper, J., *InVest. New Drugs*, **1997**, *15*, 109; (c) Alcindor, T., Beauger, N., *Curr Oncol*., **2011**, *18*(1), 18.

29. Jamieson, E. R., Lippard, S. J., *Chem. ReV*., **1999**, *99*, 2467.

30. (a) Reedijk, J., *Pure Appl. Chem*.,**1987**, 59, 181; (b) Schmidt, W., Chaney, S. G. *Cancer Res*. **1993**, *53*, 799; (c) Saif, W. M, Reardon, J., *TherClin Risk Manag*., **2005**, 1(4), 249.

31. (a) Weickhardt, A., Wells, K., and Messersmith W., *J. Oncol.*, **2011**, doi:10.1155/2011/201593; (b) Cassidy, J., Misset, J. L.*SeminOncol*.,**2002**, *29*(Suppl 15), 11; (d) Grothey, A., *Clin Colorectal Cancer*., **2005**(Suppl 1), 38; (e) Amptoulach, S., Tsavaris, N., *Chemother Res Pract*., **2011**, doi: 10.1155/2011/843019.

32. Shimada, M., Itamochi, H., Kigawa, J., *Cancer Management and Research*., **2013**, *5*, 67.

33. Akaza, H., Togashi, M., Nishio, Y., Miki, T., Kotake, T., Matsumura, Y., Yoshida, O. and Wong, E., Giandomenico, C. M. *Chem. Rev*., **1999**, *99*, 2451.

34. (a) Welink, J., Boven, E., Vermorken, J. B., Gall, H. E., and van der Vijgh, W. J. F., *Clin. Cancer. Res*., **1999**, *5*, 2349; (b) McKeage, M., *J.Exp. Opin. Invest. Drugs*., **2001**, *10*(1), 119.

35. (a) Momekov, G., Bakalova, A, Karaivanova, M., *Curr. Med. Chem*., **2005**, *12*(19), 2177; (b) Quiroga A. G., *Curr Top Med Chem*., **2011**, *11*(21), 2613; (c) Xiao, H., Stefanick, J. F., Jia, X., Jing, X. Kiziltepe, T., Zhang, Y and Bilgicer, B., *Chem. Commun.,* **2013**, *49*, 4809.

36. (a) Hollis, L. S., Sundquist, W. I., Burstyn, J. N., Heiger-Bernays, W. J., Bellon, S. F., Ahmed, K. J., Amundsen, A. R., Stern, E. W., Lippard, S. J., *Cancer Res*., **1991**, *51*, 1866; (b) Hollis, L. S., Amundsen, A. R., Stern, E. W., *J. Med. Chem*., **1989**, *32*, 128; (c) Reedijk, J., *Chem Commun*., **1996**, 801; (d) Bursova, V., Kasparkova, J., Hofr C., Brabec, V., *Biophys J*., **2005**, *88*, 1207.

37. (a) Hollis, L. S., *Platinum Other and Metal Coordination Compounds in Cancer Chemotherapy,* Plenum, New York, **1991**, 115; (b) Zhang, C. X. and Lippard, S. J., *Current Opinion in Chemical Biology*., **2003**, *7*, 481.

38. Broomhead, J. A, Rendina, L. M., Sterns, M., *Inorg. Chem*., **1991**, *31*, 1880

39. (a) Lovejoy, K. S., Todd, R. C., Zhang, S., McCormick, M. S., D'Aquino, J. A., Reardon, J. T., Sancar, A., Giacomini, K. M., and Lippard, S. J., *PNAS*., **2008**, *105*(26), 8902; (b) Lovejoy, K. S., Serova, M., Bieche, I., Emami, S., D'Incalci, M., Broggini, M., Erba, E., Gespach, C., Cvitkovic, E., Faivre, S., Raymond, E., Lippard, S. J., *Mol Cancer Ther*., **2011**, *10*, 1709; (c) Park, G. Y., Wilson, J. J., Song, Y. and Lippard, S. J., www.pnas.org/cgi/doi/10.1073/pnas.1207670109; (d) Guddneppanavar, R., Bierbach, U., *Anti-Cancer Agents Med. Chem.,* **2007**, *7*, 125-138; (e) Hess, S. M.,

Mounce, A. M., Sequeira, R. C., Augustus, T. M., Ackley, M. C., Bierbach, U., *Cancer Chemother. Pharmacol.,* **2005**, *56*, 337-343.

40. (a) Coluccia, M., Natile, G., *Anti-Cancer Agents in Medicinal Chemistry*, **2007**, *7*, 111; (b) Natile, G, Coluccia, M.,*Coord Chem Rev*., **2001**, 216-217, 383-410; (c) Abu-Surrah, A. S., Kettunen, M., *Current Medicinal Chemistry*., **2006**, *13*, 1337; (d) Montero, E. I., Díaz, S., González-Vadillo, A. M., Peréz, J. M., Alonso, C. and Navarro-Ranninger, C., *J. Med. Chem*., **1999**, *42*, 4264.

41. (a) Kelland, L. R., Farrell, N. P. (Eds.), *Platinum-Based Drugs in Cancer Therapy, Humana Press*, Totowa, **2000**, p 321-338; (b) Van Beusichem, M. and Farrell, N., *Inorg. Chem*., **1992**, *31*, 634.

42. (a) Geierstanger, B. H., Wemmer, D. E. *Annu. ReV. Biophys. Biomol. Struct*. **1995**, *24,*463;(b) Pullman, A., Pullman, B. Q. *Rev. Biophys*., **1981**, 14, 289; (c) Lavery, R., Pullman, B. *J. Biomol. Struct. Dyn*., **1985**, 2, 1021.

43. (a) Broomhead, J. A., Rendina, L. M., Webster, L.K., *J. Inorg. Biochem*., **1993**, *4*, 221; (b) Rendina, L. M., *Ph.D. Thesis*, Australian National University, **1991**; (c) Broomhead, J. A., Lynch, M*., J. Inorg. Chim. Acta.,* **1995**, *240*, 13; (d) Farrell, N., Qu, Y., Feng, L., Van Houten, B., *Biochemistry.*, **1990**, *29*, 9522; (e) Farrell, N., Qu, Y., *Inorg. Chem*., **1989**, *28*, 3416; (f) Qu, Y., Appleton, T. G., Hoeschele, J. D, Farrell, N., *Inorg. Chem*., **1993**, *32*, 2591; (g) Farrell, N., del Ameida, S. G., Skov, K. A. *J. Am. Chem. Soc*., **1988**, *110*, 5018; (h) Qu, Y., Gama, de Almeida, G., Farrell, N., *Inorg. Chim. Acta*, **1992**, *201*, 123; (i) Farrell, N., Qu, Y., Hacker, M. P. *J. Med. Chem*., **1990**, 33, 2179; (j) Qu, Y., Farrell, N. *Inorg. Chem*., **1992**, *31*, 930;

44. Qu, Y., Farrell, N. *J. Am. Chem. Soc*., **1991**, *113*, 4851.

45. (a) Hoeschele, J. D., Kraker, A. J., Qu, Y., Van Houten, B., Farrell, N., *in*: Pullman, B., Jortner, J., (Eds.), *Chemistry, Antitumor Activity and DNA-Binding: Molecular Basis of Specificity in Nucleic Acid-Drug Interactions*, Kluwer Academic, Dordrecht, **1990**, 301; (b) Qu, Y., Rauter, H., Soares Fontes, A. P., Bandarage, R., Kelland, L. R., Farrell, N., *J. Med. Chem*. **2000**, *43*, 3189; (c) Jansen, B. A. J., van der Zwan, J., den Dulk, H., Brouwer, J., Reedijk, J. *J. Med. Chem*., **2001**, *44*, 245; (d) Jansen, B. A. J., Brouwer, J., Reedijk, J. *J. Inorg. Biochem*., **2002**, *89*,197; (e) Qu, Y., Fitzgerald, J. A., Rauter, H., Farrell, N. *Inorg. Chem*., **2001**, *40*, 6324; (f) Zhao, G., Lin, H., Zhu, S., Sun, H., Chen, Y., *Anti-Cancer Drug Des*., **1998**, *13*, 769; (g) Wheate, N. J., Cullinane, C., Webster, L. K., Collins, J. G., *Anti- Cancer Drug Des*., **2001**, *16*, 91.

46. (a) Jansen, B. A. J., van der Zwan, J., Reedijk, J., den Dulk, H., Brouwer, J. *Eur. J. Inorg. Chem.,* **1999**, 1429; (b) Bierbach, U., Roberts, J. D., Farrell, N., *Inorg. Chem*., **1998**, *37*, 717; (c) Komeda, S., Lutz, M., Spek, A. L., Chikuma, M., Reedijk, *J. Inorg. Chem*., **2000**, *39*, 4230; (d) Komeda, S., Lutz, M., Spek, A. L,. Yamanaka, Y., Sato, T., Chikuma, M., Reedijk, J., *J. Am. Chem. Soc*., **2002**, *124*, 4738

47. (a) Banerjee, T, Dubey, P, Mukhopadhyay, R., *Biochimie*., **2012**, *94*(2), 494; (b) Roberts, J. D., Peroutka, J., Farrell, N*., J. Inorg. Biochem.,* **1999**, *77*, 51.

48. Novuspharma, *Product Profiles*: BBR3464, BBR3571, BBR3610, BBR3611, **2002**.

49. (a) Banerjee, T., Dubey, P., Mukhopadhyay, R., *Biochimie.*, **2010**, *9*, 2846; (b) Hegmans, A., Qu, Y., Kelland, L. R., Roberts, J. D., Farrell, N., *Inorg. Chem.*, **2001**, *40* 6108; (c) Wheate, N. J., Collins, J. G., *Coord. Chem. ReV*., **2003**, *241*, 133.

50. Roberts, J. D, Peroutka, J., Beggiolin, G., Manzotti, C., Piazzoni, L, Farrell, N., *J. Inorg. Biochem.*, **1999**, 77, 47

51. Soldatović, T., Bugarčić, Ž. D., *J. Inorg. Biochem.*, **2005**, *99*(7), 1472.

52. Schiessl, W. C., Summa, N. K., Weber, C. F., Gubo, S., Dücker-Benfer, C., Puchta, R., van Eikema Hommes, N. J. R., van Eldik, R., *Z. Anorg. Allg. Chem.,* **2005**, *631*, 2812.

**Table of Contents**

**List of Figures**

**List of Tables**

# Chapter 2

## Substitution Reaction at Square-Planar Complexes

### 2.1 General Introduction

Square planar complexes are formed by the $d^8$ systems of Pt(II), Pd(II), Ni(II), Au(III), Rh(I) and Ir(I). Ligand substitution reactions of these metal ions play a fundamental role in many chemical processes, for instance, in the treatment of tumours and in homogeneous catalysis.[1] In anticancer therapy, drugs such as cisplatin are designed to inhibit tumour growth by substituting the chloride ligand with guanosine base of DNA.[2] To date, most of the work done on substitution reactions of square-planar complexes involves the inert and stable platinum(II) complexes because their rate are conveniently slow. Other low-spin $d^8$ (nickel(II), palladium(II), gold(III) and rhodium(I)) systems have been studied and all appear to have the same general behaviour.[3] Informative reviews[4] have been written on the subject and only a brief summary will be given here along with some recent observations.

### 2.2 Mechanism of Ligand Substitution Reactions at Square-Planar

A simple ligand substitution reaction involves transfer of a lone pair of electron from a donor called nucleophile to an acceptor also called electrophile. In coordination chemistry, the central metal atom is an electrophilic reagent and the ligands are nucleophilic reagents.[5,6] The mechanism of substitution reactions can be described as either associative, dissociative or interchange.[7,8]

### 2.2.1 Associative, (A)

This is the most common mechanism for coordinatively unsaturated metal complexes and square-planar complexes of which Pt(II) are prototypical examples.[7,8] The mechanism proceeds mostly via a five coordinate transition state with an intermediate with a trigonal bipyramidal structure (**Equation 2.1** and **Figure 2.1**). In this mechanism, if the concentration of the electrophilic reagent is maintained constant, then a kinetic effect proportional to the concentration of the nucleophilic reagent can be identified as the nucleophilic reagent is involved in the formation of transition state. Furthermore, the stereochemical specificity of such reactions can be accommodated readily in terms of the five-coordinated associated intermediate.

$$ML_3X + Y \rightarrow \underset{\downarrow}{ML_3XY} \rightarrow ML_3Y + X \qquad (2.1)$$

*Intermediate*

where M = central metal atom, L = carrier ligand, X = leaving group and Y = incoming nucleophile

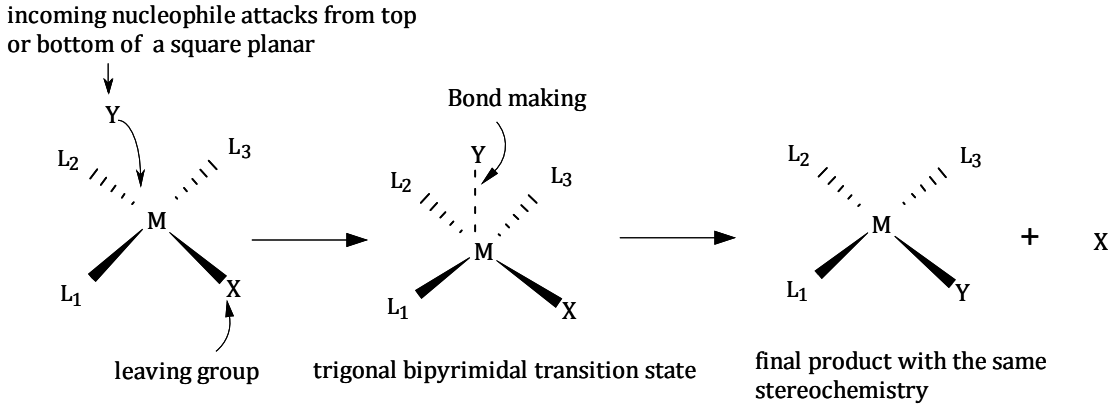


**Figure 2.1**: Reaction pathway for the associative substitution reaction showing direct Substitution of leaving group X by incoming group Y.

### 2.2.2 Dissociative, (D)

Dissociative mechanism of substitution is common in octahedral metal complexes of the first transition metal series because they have reached their maximum stable coordination number of six. In this mechanism, the leaving ligand is lost in the first step, producing an intermediate of reduced coordination number (**Equation 2.2**). A dissociative mechanism is expected to result in the formation of a mixture of two geometric isomers with different types of kinetic behaviour. For square planar complexes, a dissociative mechanism will only prevail in the presence of very bulky ligands, good leaving groups and strongly coordinating solvent.[9] Bulky ligands clearly obstruct the nucleophile from reaching the metal centre. On the other hand, if the bond breaking between the metal centre and the leaving group dominates upon the approach of the nucleophile, dissociative mechanism will be favoured. The same will occur in the presence of strongly coordinating solvent. Because the solvent is usually provided in excess, it can easily knock out the leaving group enhancing the formation of the intermediate of reduced coordination number.

$$ML_3X \rightarrow \underset{\underset{\textit{intermediate}}{\downarrow}}{ML_3} + X \rightarrow ML_3 + Y \rightarrow ML_3Y \qquad (2.2)$$

### 2.2.3 Interchange, (I)

In this instance, the leaving group and entering group are both involved in the formation of the activated complex (**Equation 2.3**). If the bond formation between the entering ligands and the metal centre dominates over its bond breaking with the leaving group, and shows sensitivity to the nature and concentration of the incoming ligand, then the mode of

activation becomes associatively-activated interchange mechanism ($\mathbf{I_A}$). On the other hand if the rate of reaction is affected by the leaving group and bond breaking dominates over bond formation the mode of activation turn out to be dissociatively-activated interchange mechanism, $\mathbf{I_D}$. The defining characteristic of interchange is the absence of an intermediate (**Figure 2.2**) in which the primary coordination number of the metal is modified.

$$XML_3 + Y \rightarrow X\text{--}ML_3\text{--}Y \rightarrow ML_3Y + X \qquad (2.3)$$

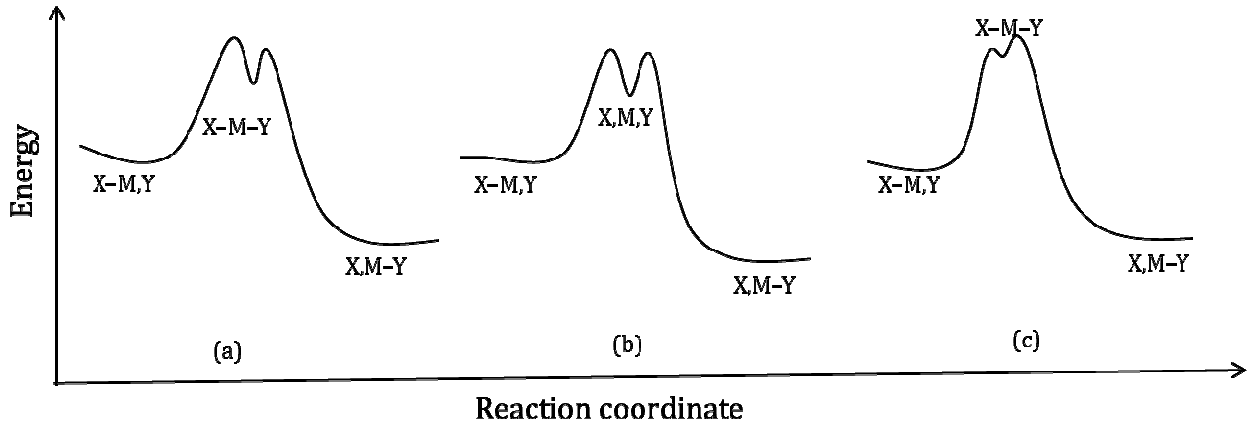


**Figure 2.2**: Reaction profile[10] for (a) associative, (b) dissociative and (c) interchange mechanisms. A true intermediate exists in (a) and (b) but not in (c).

## 2.3 Kinetics Parameters

### 2.3.1 Determination of Rate Constants

Experimentally, the rate of a reaction is found to depend principally on the concentration of the reactants. To determine the reaction rate and hence the rate constant one need to monitor the concentration of one of the reactants as a function of time. This may be achieved by measuring the time dependence of a variable that is proportional to the concentration, such as absorbance. Kinetic measurements of ligand substitution reactions

of Pt(II) complexes are often done by following the change in absorbance at suitable wavelengths as a function of time. These substitution reactions mainly do not go to completion but rather towards equilibrium and can be written as;

$$A + B \underset{k_{-2}}{\overset{k_2}{\rightleftharpoons}} C \qquad (2.4)$$

or

$$ML_3X + Y \underset{k_{-2}}{\overset{k_2}{\rightleftharpoons}} ML_3Y + X$$

where A = Metal centre ($ML_3X$), B = Incoming nucleophile Y, X = leaving group, $k_2$.= second-order rate constant for the direct attack of the entering nucleophile and $k_{-2}$ = second-order rate constant of the reverse reaction.

The forward reaction is second-order while that of the reverse reaction is first-order. The overall reaction exhibits the mixed-order behaviour which complicates the study. Ligand substitution reactions for the forward reaction is therefore simplified by employing *pseudo* first-order conditions[11] where concentration of the incoming nucleophile is at least ten fold excess of that of the metal complex ($[B]_0 >>> [A]_0$) and the rate of formation of product C can be expressed as,

$$-\frac{d[A]}{dt} = -\frac{d[B]}{dt} = \frac{d[C]}{dt} = k_2[A]_t[B]_t - k_{-2}[C]_t \qquad (2.5)$$

Applying the mass balance at any time t,

$$[A]_t = [A]_0 - [C]_t \text{ and } [B]_t = [B]_0 - [C]_t \qquad (2.6)$$

and at equilibrium,

$$[A]_e = [A]_0 - [C]_e \quad \text{and} \quad [B]_e = [B]_0 - [C]_e \tag{2.7}$$

Knowing that at equilibrium the rate of forward and backward reactions are equal, then,

$$-\frac{d[A]}{dt} = k_2[A]_e[B]_e - k_{-2}[C]_e = 0 \tag{2.8}$$

This follows that,

$$k_2[A]_e[B]_e = k_{-2}[C]_e \tag{2.9}$$

Since $[C]_t = [A]_0 - [A]_t$ and at equilibrium $[C]_e = [A]_0 - [A]_e$, substituting this in **Equation 2.9** provides

$$k_2[A]_e[B]_e = k_{-2}([A]_0 - [A]_e) \tag{2.10}$$

and then,

$$k_{-2}[A]_0 = k_2[A]_e[B]_e + k_{-2}[A]_e \tag{2.11}$$

Taking **Equation 2.5** and substituting for $[C]_t = [A]_0 - [A]_t$ and then introducing it in **Equation 2.11** gives

$$-\frac{d[A]}{dt} = k_2[A]_t[B]_t - k_2[A]_e[B]_e - k_{-2}[A]_e + k_{-2}[A]_t \tag{2.12}$$

Under *pseudo* first-order conditions where $[B]_0 >>> [A]_0$, **Equation 2.12** becomes

$$-\frac{d[A]}{dt} = k_2[A]_t[B]_0 - k_2[A]_e[B]_0 - k_{-2}[A]_e + k_{-2}[A]_t \tag{2.13}$$

$$= (k_2[B]_0 + k_{-2})([A]_t - [A]_e) \tag{2.14}$$

Separation of the variables and integration gives

$$\int_{[A]_0}^{[A]_t} \frac{d[A]}{([A]_t - [A]_e)} = -(k_2[B]_0 + k_{-2})\int_0^t dt \tag{2.15}$$

which results in

$$\ln\left(\frac{[A]_t - [A]_e}{[A]_0 - [A]_e}\right) = -(k_2[B]_0 + k_{-2})t = -k_{obs}t \qquad (2.16)$$

where $k_{obs} = k_2[B]_0 + k_{-2}$, $[B]_0$ = initial concentration of the incoming nucleophile

In ligand substitution reactions, second-order rate constants are determined by measuring the dependence of observed *pseudo* first-order rate constant, $k_{obs}$ on the initial concentration of the nucleophile, [Nu] using **Equation 2.17**.

$$k_{obs} = k_2[Nu] + k_{-2} \qquad (2.17)$$

A plot of $k_{obs}$ versus $[Nu]$ gives a straight line with the slope of $k_2$ and an intercept of $k_{-2}$. Plots of this type are common for the substitution reactions of square planar Pt(II) complexes, an example of which is shown in **Figure 2.3**.

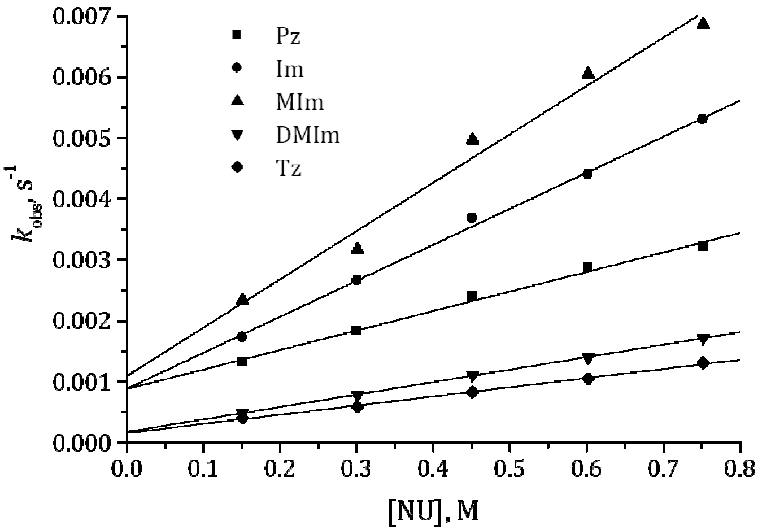


**Figure 2.3:** Typical plots of $k_{obs}$ versus the concentration of the incoming azole nucleophiles for the substitution reaction of a mononuclear Pt(II) complex in methanol solution.[12]

The magnitude of the second-order rate constant ($k_2$) calculated is a direct measure of the reactivity of the complex towards the nucleophile. A plot which passes through zero implies that the forward reaction is irreversible and directly goes to completion, whereas a non-zero y-intercept signifies that the nucleophile Y is being substituted from the metal centre by the solvolysis process or there is a back reaction taking place.[13,14] The two-term rate law (**Equation 2.17**) represents two-path reaction mechanisms as summarized in **Figure 2.4**.

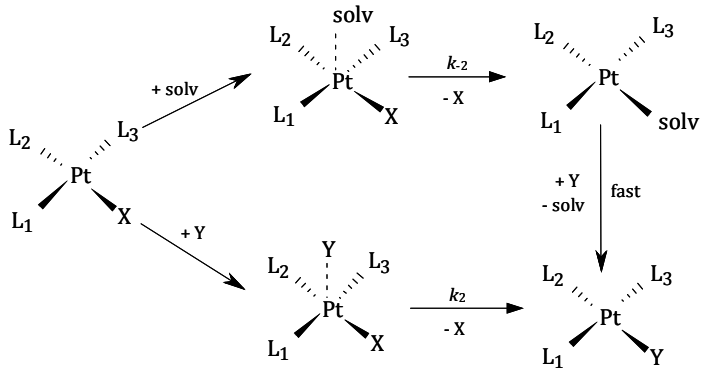


**Figure 2.4:** A proposed dual reaction pathway for an associative substitution mechanism at the Pt(II) centre[11] where solv = solvent.

In the presence of coordinating solvents (e.g. water or methanol) and good leaving group, the $k_{-2}$ term may be attributed to the solvolysis pathway. In such cases, the $k_{-2}$ pathway involves two sequential associative steps, *viz.* the rate-determining step in which a solvent-metal complex is formed followed by rapid substitution of the co-ordinated solvent molecule by the entering nucleophile (**Figure 2.4**). This solvolysis pathway follows first-order kinetics and is therefore independent of the concentration of the incoming

nucleophile. The second path involves direct nucleophilic attack by the entering ligand, Y and so the $k_2$ is sensitive to the nature of the entering nucleophile.

$$k_{obs} = k_2[\mathrm{Nu}] \qquad (2.18)$$

It is worth noting that in all substitution reactions reported in this thesis the $k_{-2}$ term is very small thus, under *pseudo* first-order conditions the values of $k_2$ can be calculated directly from **Equation 2.18**. Typical plots of **Equation 2.18** are found in **Figures 3.2**, **4.5**, **5.4** and **6.3** in **chapter three**, **four**, **five** and **six** respectively.

### 2.3.2 Activation Parameters

In inorganic substitution reactions, apart from rate law, the magnitude of the activation parameters helps to elucidate the mechanism of the chemical reaction. These parameters can be determined by measurement of reaction rates and rate constants as a function of many chemical and physical variables among which includes temperature and pressure dependence.[15]

#### 2.3.2.1 Determination of Enthalpy of Activation ($\Delta H^{\neq}$) and Entropy of Activation, ($\Delta S^{\neq}$).

The temperature dependence of the rate constant is very useful in determining the enthalpy of activation, $\Delta H^{\neq}$ and entropy of activation, $\Delta S^{\neq}$. The value of $\Delta H^{\neq}$ is a good estimate of the energy barrier necessary to activate reactants to the transition state. The entropy, $\Delta S^{\neq}$ reveals information on the degree of order at transition state which in turn is controlled by the degree of bond formation or bond breakage on going to the transition state. Both

$\Delta H^{\neq}$ and $\Delta S^{\neq}$ of the reactions are normally derived from the temperature dependence of their rate constants based on the transition state theory.[16,17] The theory works on the assumption that many reactions between A (metal centre) and B (incoming nucleophile) proceed via a pre-equilibrium mechanism between the reactants and the transition-state species (activated complex, AB#) before it is converted to the product C.[18] The mechanism can be represented by **Equation 2.19**.

$$A + B \underset{k_{-1}}{\overset{k_1}{\rightleftharpoons}} AB^{\#} \xrightarrow{k_2} C \qquad (2.19)$$

The rate of the reaction can be written as,

$$-\frac{d[A]}{dt} = k_2[AB]^{\#} \qquad (2.20)$$

At equilibrium,

$$K^{\neq} = \frac{[AB]_{eq}^{\#}}{[A]_{eq}[B]_{eq}} \qquad (2.21)$$

where $K^{\neq}$ = equilibrium constant of the activated complex

Implying that, $[AB]_{eq}^{\#} = K^{\neq}[A]_{eq}[B]_{eq}$ (2.22)

Substituting **Equation 2.22** into **Equation 2.20** results into,

$$-\frac{d[A]}{dt} = \frac{k_b T}{h} K^{\neq}[A]_{eq}[B]_{eq} \qquad (2.23)$$

where $k_b$ = Boltzmann's constant (1.38 x $10^{-23}$ J/K) and $h$ = the Planck's constant (6.626 x $10^{-34}$ J s).[19]

but, $-\frac{d[A]}{dt} = k_2[A]_t[B]_t$ (2.24)

Therefore, comparing **Equation 2.23** and **2.24** gives

$$k_2 = \frac{k_b T}{h} K^{\neq} \tag{2.25}$$

To further describe the pre-equilibrium constant in thermodynamics, we have;

$$\Delta G^{\neq} = -RT \ln K^{\neq} \tag{2.26}$$

where $\Delta G^{\neq}$ is the Gibbs activation energy which consists of the entropy of activation $\Delta S^{\neq}$ and the enthalpy activation term, $\Delta H^{\neq}$ [20] as shown in **Equation 2.27**.

$$\Delta G^{\neq} = \Delta H^{\neq} - T\Delta S^{\neq} \tag{2.27}$$

Combining **Equations 2.26** and **2.27** to solve for $\ln K^{\neq}$ results into,

$$\ln K^{\neq} = \frac{\Delta H^{\neq}}{RT} + \frac{\Delta S^{\neq}}{R} \tag{2.28}$$

The Eyring equation is finally obtained by substituting **Equation 2.28** into **Equation 2.25**

$$k_2 = \frac{k_b T}{h} e^{\frac{-\Delta H^{\neq}}{RT}} e^{\frac{\Delta S^{\neq}}{R}} \tag{2.29}$$

Taking natural logarithm of both sides gives,

$$\ln\left(\frac{k_2}{T}\right) = \frac{-\Delta H^{\neq}}{R} . \frac{1}{T} + \left(\ln\frac{k_b}{h} + \frac{\Delta S^{\neq}}{R}\right) \tag{2.30}$$

The values for $\Delta H^{\neq}$ and $\Delta S^{\neq}$ can be determined from kinetic data obtained from a plot of $\ln {k_2}/{T}$ versus ${1}/{T}$. This plot is known as the Eyring plot and it provides a straight line with negative slope, $\frac{-\Delta H^{\neq}}{R}$ and an intercept of $\left(\frac{\Delta S^{\neq}}{R} + \ln\frac{k_b}{h}\right)$ from which the enthalpy of activation ($\Delta H^{\neq}$) and the entropy of activation ($\Delta S^{\neq}$) can be calculated, respectively. Typical example of the Eyring plots is shown in **Figure 2.5**. The magnitudes of $\Delta H^{\neq}$ and $\Delta S^{\neq}$ provide

information about how the enthalpy and entropy of the transition state differ from those of the reactants. Large and negative values of $\Delta S^{\neq}$ indicate that the transition state is highly ordered and more compact than either the reactant or product species. On the other hand low values of $\Delta H^{\neq}$ show the ease with which the new bond can form due to the electrophilicity of the metal centre. In an associatively-activated substitution reaction, the relative magnitude of the $\Delta H^{\neq}$ values tend to be small while their values of $\Delta S^{\neq}$ are usually negative when compared to those for dissociatively activated reactions whose values of $\Delta H^{\neq}$ and $\Delta S^{\neq}$ are usually large and positive.

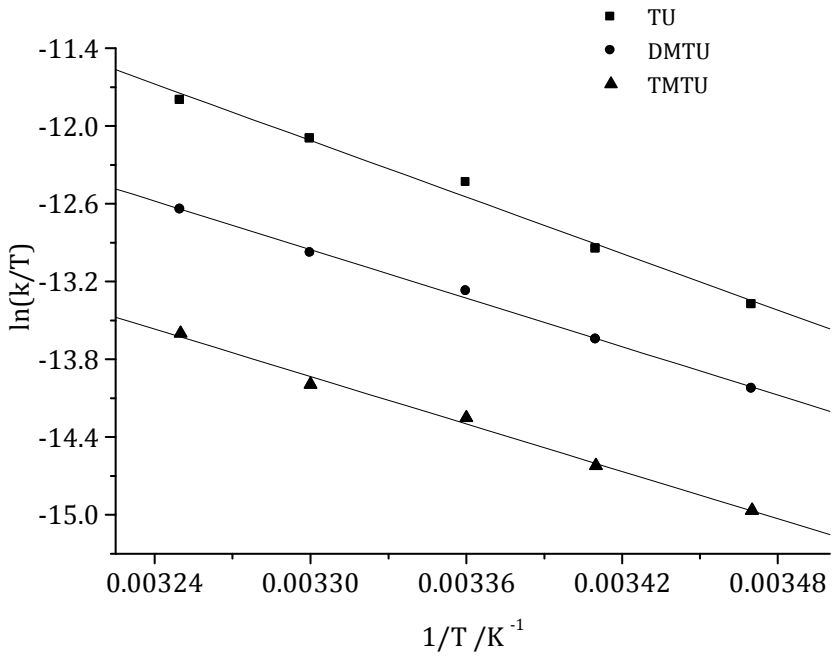


**Figure 2.5:** Eyring plots for the reaction of Pt(II) complex with a series of neutral nucleophiles at various temperatures in a range 15 to 35 ˚C.

### 2.3.2.2 Determination of Activation Volume ($\Delta V^{\#}$)

Experimental determination of the entropy of activation is associated by lack of exactness and is subjected to large relative errors since the data are calculated from values extracted to infinite temperatures on the y-intercept. The more precise parameter is volume of activation, $\Delta V^{\#}$. This can be determined from a series of experiments in which one measures the observed rate constants, $k_{obs}$, as the pressure which is applied on a reaction mixture is varied. Measurement of activation volume is therefore useful in studies of ligand substitution reactions as it allows a precise assignment of the underlying substitution mechanism.[21] However, for better diagnosis, it is still significant to include the values of the $\Delta V^{\neq}$ and $\Delta S^{\neq}$ for the purposes of making conclusive mechanism assignment.[22] Pressure dependence of the rate constant results in the volume of activation as outlined below;

From the thermodynamic equation **Equation 2.31**,

$$\Delta V = \left(\frac{\delta \Delta G}{\delta P}\right)_T \qquad (2.31)$$

Since $\Delta G = RT \ln K$, therefore,

$$\left(\frac{\delta \ln K}{\delta P}\right)_T = -\frac{\Delta V}{RT} \qquad (2.32)$$

where $\Delta V$ = the difference between the partial molar volume of products and partial molar volume of reactants, $K$ = equilibrium constant.

Taking into account the formation of the transition state, it is possible to write,

$$\left(\frac{\delta \ln K^{\neq}}{\delta P}\right)_T = -\frac{\Delta V^{\neq}}{RT} \qquad (2.33)$$

where $\Delta V^{\neq}$ = volume of activation and is equal to the difference in the partial molar volumes between the transition state and the reactants.

Comparing **Equation 2.25** and **2.33** we get,

$$\delta\left(\frac{\ln k_2}{\delta P}\right)_T = -\frac{\Delta V^{\neq}}{RT} \tag{2.34}$$

According to **Equation 2.34**, clearly if rate constant, $k_2$ increases with increasing pressure, $\Delta V^{\neq}$ is negative. On the other hand a positive $\Delta V^{\neq}$ denotes a decrease in $k_2$ with increasing pressure.

Integrating **Equation 2.34** from $P = 0$ to $P = P$ gives,

$$\ln k_2 = -\frac{\Delta V^{\neq}}{RT} P + \ln(k_2)_0 \tag{2.35}$$

where $(k_2)_0$ = rate constant at zero pressure.

Values of $\Delta V^{\neq}$ can be determined from experimental measurements of rate constants at different pressures by plotting of $\ln k_2$ versus $P$. The slope of such a plot is equal to $-\frac{\Delta V^{\neq}}{RT}$.

Volume of activations, $\Delta V^{\neq}$ are usually considered to be the combination of an intrinsic contribution, $\Delta V^{\neq}_{\text{int}}$ resulting from changes in internuclear distances within the reactants during the formation of the transition state, and from an electrostrictive contribution, $\Delta V^{\neq}_{\text{elec}}$. For substitution reactions involving charged species, the observed $\Delta V^{\neq}$ is dominated by $\Delta V^{\neq}_{\text{elec}}$, whereas for solvent exchange reactions due to the absence of electrostrictive changes $\Delta V^{\neq} \approx \Delta V^{\neq}_{\text{int}}$.

In ligand substitution reactions of Pt(II) square planar complexes $\Delta V^{\neq} < 0$ for associative mechanism as it involves a volume collapse on going to the transition state. For dissociative mechanism the process towards transition state encompasses expansion in volume therefore, $\Delta V^{\neq} > 0$ .[23]

## 2.4 Techniques of Studying Reaction Kinetics

Experimental techniques have been developed to monitor reactions over timescales varying from hours or days all the way down to fractions of seconds. While it is somewhat simple to monitor the kinetics of a slow reaction occurring over minutes to hours or longer, highly specialized techniques are required in order to study fast reactions. Whatever the details of the experimental arrangement, any kinetics experiment essentially consists of mixing the reactants and initiating reaction on a timescale that is negligible relative to that of the reaction, and then monitoring the concentration(s) of one or more reactants and/or products as a function of time. Because rate constants vary with temperature, it is also important to determine and control accurately the temperature at which the reaction occurs.

Various techniques can be used to study reaction kinetics. The list includes flow methods (e.g. stopped-flow or continuous flow), UV-Visible spectrophotometry, Nuclear Magnetic Resonance (NMR) spectrophotometry, conductivity measurements and gas chromatography.[24] The choice of the technique to be used for the particular reaction depends on the nature and rate of the reaction. Since Pt(II) substitution reactions are either

fast or slow, flow and UV-Visible techniques are mainly used and so will be discussed here in detail.

### 2.4.1 UV-Visible Spectrophotometry

UV-Visible spectrophotometry is a sensitive technique which can detect samples of low concentrations in the range of $10^{-4}$ to $10^{-6}$ M.[25] The method is useful for detecting electronic transitions originating from highest occupied molecular orbital (HOMO) to the lowest unoccupied molecular orbital (LUMO) of the compounds upon absorption of light in the ultraviolet and visible regions. In addition, it is used to track reactions in which the reactants and products have different absorption spectra. **Figure 2.6** depicts that the instrument comprises of two sources of radiation spanning from the Visible and ultra-violet, sample cubicles, monochromator, detector, output-readout system and an internal or external temperature control unit. For acquisition of the kinetic data special transparent tandem cuvettes made up of quartz or fused silica are used for initiating the reaction. These cuvettes have two sections that allow one to pre-equilibrate the reactants at the required temperature before manually mixing them to initiate the reaction.

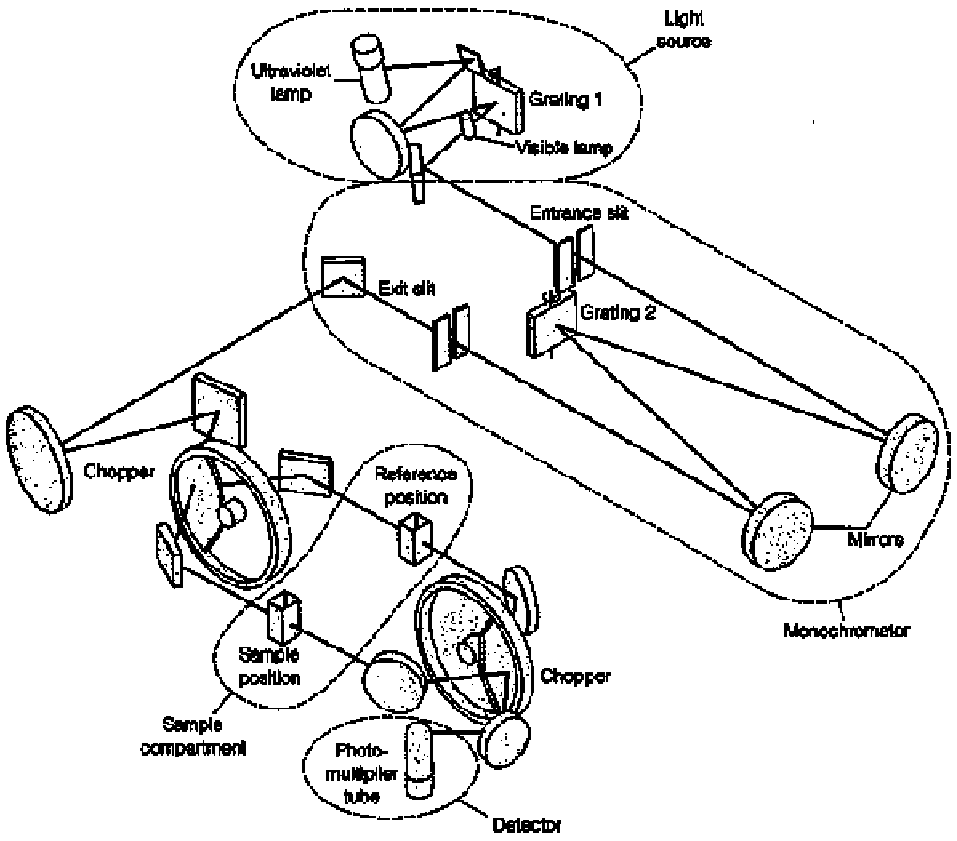


**Figure 2.6**: Schematic diagram of a UV-Visible spectrophotometer.[26]

The degree of interaction of the sample with radiation (transmittance or absorbance) is determined by measuring both the intensity of the incident radiation, $I_0$ (without the sample) and the transmitted intensity, $I$ (with the sample). The light transmitted from the sample is defined as follows:

$$T = \frac{I_0}{I} \tag{2.36}$$

where $I_0$ = the intensity of the incident light obtained from the solvent reference cell, $I$ = the intensity of the transmitted light from the power source after passing through the sample cell.

Absorbance is defined as follows,

$$A = -\log T \tag{2.37}$$

In ligand substitution reactions, absorbance values are used since the relationship between absorbance and both concentration of the reacting species and path length normally is linear and obeys Beer's law (**Equation 2.38**).

$$A = \varepsilon c l \tag{2.38}$$

where, $A$ = absorbance, ε = molar absorptivity (L $mol^{-1}$ $cm^{-1}$), $c$ = concentration (mol $dm^{-3}$), $l$ = path length (cm).

For the first-order reaction,

$$X \xrightarrow{k_1} Y \tag{2.39}$$

at any time *t,* the absorption is given by;

$$A_t = \varepsilon_X[X] + \varepsilon_Y[Y] \tag{2.40}$$

where, $A_t$ = the absorbance at any time, $t$, $\varepsilon_X$ and $\varepsilon_Y$ = molar absorptivity of X and Y respectively

When the reaction goes to completion, the absorption is given by

$$A_\infty = \varepsilon_X[X]_0 + \varepsilon_Y[Y]_0 \tag{2.41}$$

where $A_\infty$ = absorbance upon completion of reaction, $[X]_0$ and $[Y]_0$ = initial concentration of X and Y respectively.

The kinetic analysis relating the concentration or optical absorbance (**Equation 2.38**) can therefore be obtained from the integrated rate-law given on **Equation 2.42**. The

absorbance-time resolved data in kinetic reactions are used directly to evaluate the observed rate constants using this equation.

$$\ln\frac{[X]_o}{[X]_t} = \ln\left(\frac{A_0 - A_\infty}{A_t - A_\infty}\right) = k_{obs}t \qquad (2.42)$$

In this study slow substitution reactions were carried out on a Cary 100 Bio UV-Visible spectrophotometer with a cell compartment thermostated by a Varian Peltier temperature controller having an accuracy of ± 0.05 °C. UV-Visible scans were recorded at set time intervals over the wavelength range of 200 to 800 nm immediately after mixing the reactants. The obtained kinetic data were graphically analysed using the software package, Origin 7.5®[27] to give the kinetic trace with the time taken for the reaction to go to completion. The time obtained from the kinetic trace gave the observed first-order rate constant, $k_{obs}$. A typical set of scans and its kinetic trace is shown in **Figure 2.7**.

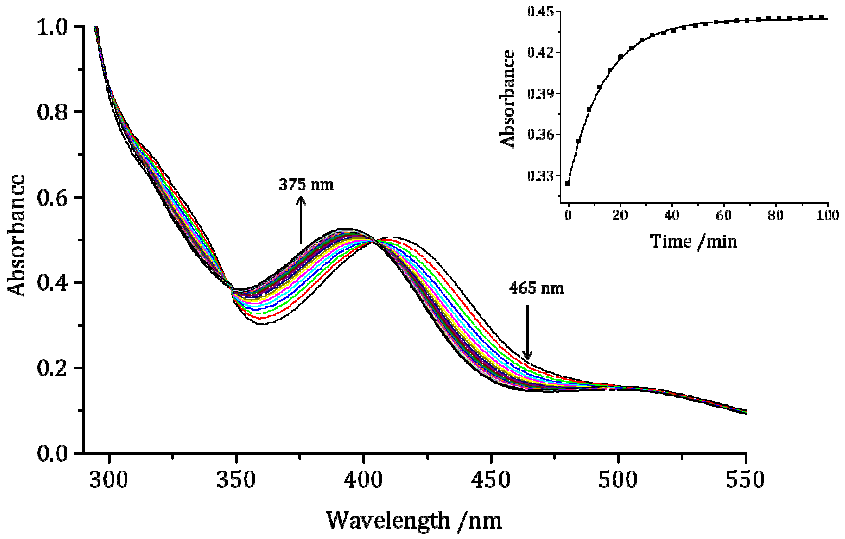


**Figure 2.7**: UV-Vis scans for the substitution reaction of **Pt2** (studied in Chapter 3) with thiourea in MeOH recorded at 25 °C. *Inset* is the kinetics trace obtained at 375 nm.

It is important mentioning that the UV-Visible absorption spectroscopy is also used to perform spectrophotometric titrations, especially in p*K*a determinations. The p*K*a values of the coordinated aqua ligand are important thermodynamic set of data used as indicator of the electrophilicity of the metal centre.[28]

### 2.4.2 Flow Techniques

Flow techniques are typically used to study reactions occurring on timescales of seconds to milliseconds. These can be either **continuous flow** or **stopped flow** techniques. The design of the flow instrument is usually associated with monitoring of reaction progress by UV-Vis spectrophotometry techniques where **Equation 2.42** is used to evaluate the observed rate constants.

#### 2.4.2.1 Continuous Flow Techniques

In the simplest continuous flow method, shown schematically on **Figure 2.8** (a), reactants are mixed at one end of a flow tube, and the composition of the reaction mixture is monitored at one or more positions further along the tube. If the flow velocity along the tube is known, then measurements at different positions provide information on concentrations at different times after initiation of reaction. In a variation on this method, shown on **Figure 2.8** (b), the detector may be in a fixed position, but a moveable injector may be used to inject one of the reactants into the flow tube at different positions relative to the detector in order to study the time dependence of the reaction mixture composition.

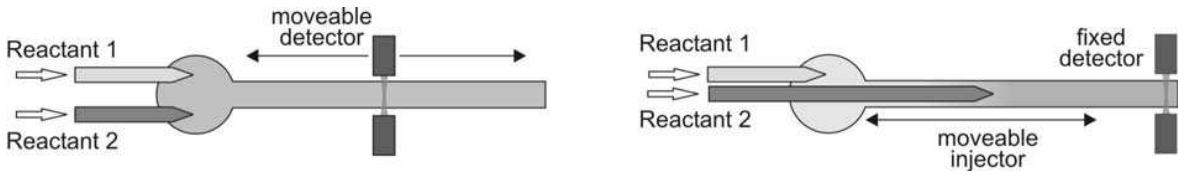


(a) (b)

**Figure 2.8**: Schematic diagram of continuous flow kinetic system.[29]

Continuous flow methods have the disadvantages that relatively large quantities of reactants are needed, and very high flow velocities are required in order to study fast reactions. These problems may be avoided by using a **stopped flow techniques**.[30]

### 2.4.2.2 Stopped Flow Techniques

Stopped flow methods (**Figure 2.9**) constitute commonly used tools for investigation of mechanisms of molecular kinetic processes in the time range from milliseconds to hundreds of seconds.[31] In this study an Applied Photophysics SX 20 stopped-flow reaction analyser coupled to an online data acquisition system was used to study the fast reactions. The temperature of this instrument was controlled to within ± 0.1 °C.

In the stopped flow experiments, small volumes of solutions are rapidly driven from syringes by a compressed gas-driven piston (800 kPa) into a high efficiency mixer to initiate a fast reaction at a specific temperature. The fresh reaction mixture is rapidly transferred into an observation cell while the previous contents of the cell are flushed out. The volume injected is limited by the stop syringe which provides the "stopped-flow". The composition of the reaction mixture is then monitored spectrophotometrically at specified wavelength

where by the amount of light transmitted through the mixed solution undergo changes as the reaction proceeds in the static mixed solution. A photomultiplier unit converts the transmitted light into an electric current and a signal is fed to the computer over an appropriate time interval. The kinetic traces acquired under *pseudo* first-order conditions are then fitted to exponential functions to evaluate the *pseudo* first-order rate constant. Examples of the stopped flow kinetic traces are shown in **Figures 4.3**, **5.3** and **6.1** in **Chapters Four**, **Five** and **Six** respectively.

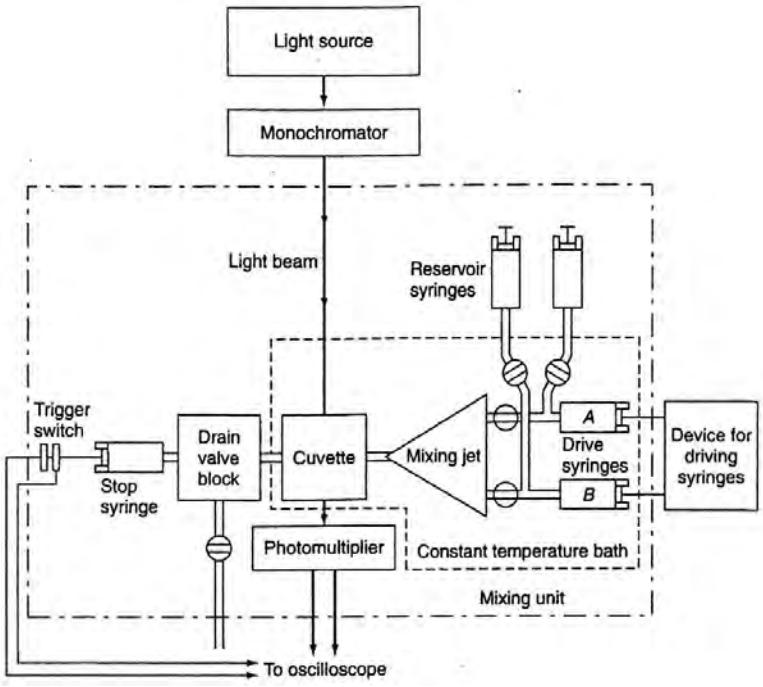


**Figure 2.9:** Schematic diagram of a stopped-flow reaction analyzer.[32]

## 2.5 Factors Affecting the Rate of Substitution

### 2.5.1 The Role of Incoming Ligand

Numerous investigations have established that associative mechanism of ligand substitution reactions in Pt(II) complexes depends on the nucleophilicity of different entering groups.[33-38] The concept of nucleophilicity gives the quantitative measure of the ability of a Lewis base to act as the entering group and to influence the reaction rate in a nucleophilic substitution reaction. A scale of nucleophilicity is established by determining the relative rate of the reaction of a range of nucleophiles with a standard substrate. In inorganic chemistry the substitution reactions of *trans*-$[Pt(py)_2Cl_2]$ in methanol solution is used as the standard and the nucleophilicity factor is usually expressed, as far as Pt(II) complexes are concerned, in terms of $n_{Pt}$ index given by **Equation 2.43**.[39]

$$n_{Pt} = \log \frac{k_2}{k_{-2}} \tag{2.43}$$

where $k_2$ = the rate constant for the reaction of the entering nucleophile, $k_{-2}$ = the rate constant for attack of the solvent (methanol).

Studies done on the Pt(II) complexes showed that the nucleophilic reactivity order is;[40,41]

$R_3P > Tu > I^- > SCN^- > N_3^- > NO_2^- > Br^- > py > aniline \sim NH_3 \sim Cl^- > H_2O > OH^-$.

The $n_{Pt}$ index can be applied to other Pt(II) complexes according to the expression given in **Equation 2.44**.[5,34,42]

$$\log k_2 = S(n_{Pt}) + \log k_{-2} \tag{2.44}$$

**Equation 2.44** shows that for a specific substrate except for complexes with π-acceptor ligands,[34] there is linear free energy relationship between $\log k_2$ for a particular

nucleophile and nucleophilicity index, $n_{Pt}$ value (**Figure 2.10**). This is because π-acceptor ligands are capable of forming metal-ligand π-bonding at the transitional state and then lowering the energy of the transition state. This also depends on the π-donor ability of the metal complex which makes some reagents more reactive towards some better π-donor metal complexes or less reactive to certain complexes.[34] The slope $S$ of the plots in **Figure 2.10**, is the nucleophillic discrimination factor and the intercept $\log k_{-2}$, is the intrinsic factor. The former is dependent on the nature of the complex and is a relative measure of its ability to discriminate between the various entering nucleophiles.

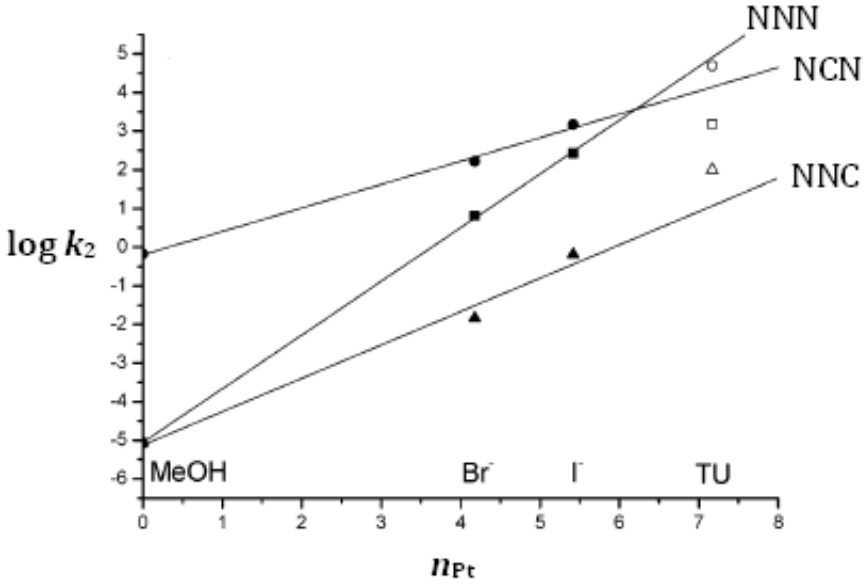


**Figure 2.10:** Plots of $\log k_2$ *versus* $n_{Pt}$ for the determination of the nucleophilic discrimination factor, $S$ of Pt(II) complexes[43]

A large value of $S$ means that the complex is very sensitive to changes in the nature of the nucleophillic reagent. The magnitude of $k_{-2}$ is a measure of the "intrinsic" reactivity of the

platinum complex with the poorest nucleophillic reagent whose effect can be measured in any solution.[42] Having such a poor nucleophile, the greatest burden is put on the complex to reach the activated complex of the reaction. If the value of $k_{-2}$ is small, the tendency of the complex to react is minor and will rely more on the nucleophile.

It is important to recall that nucleophilicity is a kinetic term which is most heavily correlated with the polarizability of the entering ligand, basicity and the nature of the substituent on the ligand.

#### 2.5.1.1 Polarizability of the Nucleophile

It is known that polarizable molecules and ions such as thiourea, iodide ion and unsaturated systems are more nucleophilic than their basicities would warrant.[44] In the case of uncharged nucleophiles, size dictates the nucleophilicity. This is because larger elements have bigger, more diffuse and more polarizable electron density. This density facilitates the formation of a more effective orbital overlap in the transition state of bimolecular nucleophilic substitution reactions, resulting in a transition state that is lower in energy and a nucleophilic substitution that occurs at a faster rate. This is also supported by the hard and soft acid-base theory. “Hard” nucleophiles prefers “hard” metal centres and “soft” nucleophiles prefers “soft” substrates or metal centres.[45,46]

The term soft nucleophiles as used here refer to the relatively polarizable nucleophiles and hard refers to relatively non polarizable. Like soft bases, soft nucleophiles have high HOMO

energy making them efficient nucleophile.[47] In solution, polarizable nucleophiles are better than non-polarizable nucleophiles because they can respond better to demand for charge reorganization. For ionic nucleophiles the polarizability of the nucleophilicity follows the order $I^- > Br^- > Cl^- > F^-$. This polarizability order explains the trend in reactivities of the ionic nucleophiles reported by a number of studies.[33b,d,43,48]

#### 2.5.1.2 Basicity of the Nucleophile

Basicity have an important role in determining the nucleophilic reactivity toward Pt(II) complexes.[12,33e,44,49] As already observed in the cases of Pd(II) complexes,[50] the reactivity of Pt(II) complexes is linearly related to the basicity of the entering nucleophiles.[51] Pitteri *et al*[52] found that for the reversible substitution reaction, there is a relatively large dependence of reactivity upon the basicity of the nucleophile in the reverse as compared to the forward reactions. The observation suggests that the formation of the transition state involves a structure containing a well formed Pt–X and a weak Pt–Nu where X and Nu are leaving group and the incoming nucleophile, respectively. Generally, the relationship between basicity of the nucleophiles and the rate constant of a given substitution reaction can be described by **Equation 2.44.**

$$\log k_2 = \alpha(\mathrm{p}K_\mathrm{a}) + \text{constant} \qquad (2.44)$$

A plot of $\log k_2$ versus $\mathrm{p}K_\mathrm{a}$ is the straight line with the slope of α which indicates the ability of the platinum(II) centre to discriminate the incoming ligands of different basicity.[42] The positive slopes indicate the increase of the electron density around the reactive metal

centre which is typical of associative mode of substitution behaviour. The negative slope is an indication of the solvolytic reverse reaction.[14]

#### 2.5.1.3 Substituents on the Nucleophiles

In an associative mechanism for ligand substitution reactions, the transition state is more crowded than the ground state as there are a total of five groups around the electrophilic centre. As a result, the steric bulk and the size of the entering nucleophile play a dominant role in determining the rate of the substitution reaction. Steric hindrance merely slows down the associative attack of a bulky nucleophile, but does not alter the nature of the substitution mechanism suggesting that steric effects are more important than electronic effects.[8,33] Extensive studies have rationalized the steric effect of the entering group.[33,53] Basically, larger entering group will hinder the approach of the entering group and will slow the formation of the five-coordinate activated complex leading to slow substitution reaction.

### 2.5.2 The Nature of Non-participating Groups in the Complex

#### 2.5.2.1 *Trans* Effect

The concept of the *trans* effect was introduced by Chernyaev in 1926 to explain the empirical observation that the rate of substitution of a ligand in a square planar or octahedral metal complex is dependent on the group *trans* to it much more so than groups in *cis* positions.[54] Since then, the kinetics of many other systems has been explained by the *trans* effect.[54,55,56] The *trans* effect is best defined as the effect of a coordinated ligand upon

the rate of substitution of ligands opposite to it. The ligand *trans* to the leaving group can influence the reaction rate by several orders of magnitude ($10^5$-$10^6$).[57]

In general, the rate of substitution of the leaving group by the incoming group is faster if the *trans* ligand is a strong σ donor or a good π-acceptor.[58] However, relatively hard pure σ-donors like $NH_3$, $H_2O$ and $OH^-$ have a weak *trans*-directing effect. This apparent contradiction seems to indicate that there is another factor responsible to *trans* directing of substitution and it is the *trans* influence.

*Trans* influence is the extent to which a ligand weakens the bond that is *trans* to itself. This is a purely thermodynamic effect and manifests itself as changes in bond lengths, force constants and vibrational frequencies.[59] For example, for a series of *trans*-metal complexes if a *trans* ligand $T$ is changed, the $M-X$ bond length is very sensitive to the electronegativity of $T$ (where T, M and X stands for *trans* ligand, metal centre and leaving group respectively). If the electronegativity decreases, the distance $M-X$ increases.[59] This increase in length is as a result of a weakened bond in the ground state and leads to the increase in the reactivity of the association process. In general, the structural *trans* influence follows the order:[59]

$$H^- > PR_3 > SCN^- > I^- > CH_3^- \sim \text{olefin} \sim CO \sim CN^- > Br^- > Cl^- > NH_3 > OH^-$$

#### 2.5.2.1.1 σ-donation *Trans* Effect

Polarization theory considers the *trans* effect to be principally electrostatic in origin and transmitted through σ-bonds (σ-*trans* effect).[60] In a square-planar complex and in the ground state strong σ-donor ligands donate electrons very effectively to the metal via σ-bonds. The effective donation is attributed by their good overlap with the metal orbital resulting into interaction which goes down low in energy (**Figure 2.11**). If the *trans* ligand is a strong σ-donor, the metal *p*-orbital bonds more favourably with it than the ligand *trans* to it. This results into elongation and weakening of the $M-X$ bond while strengthening the $M-T$ bond (**Figure 2.12**). In substitution reactions the weak bond will break easily leading to the increase in the rate of substitution.

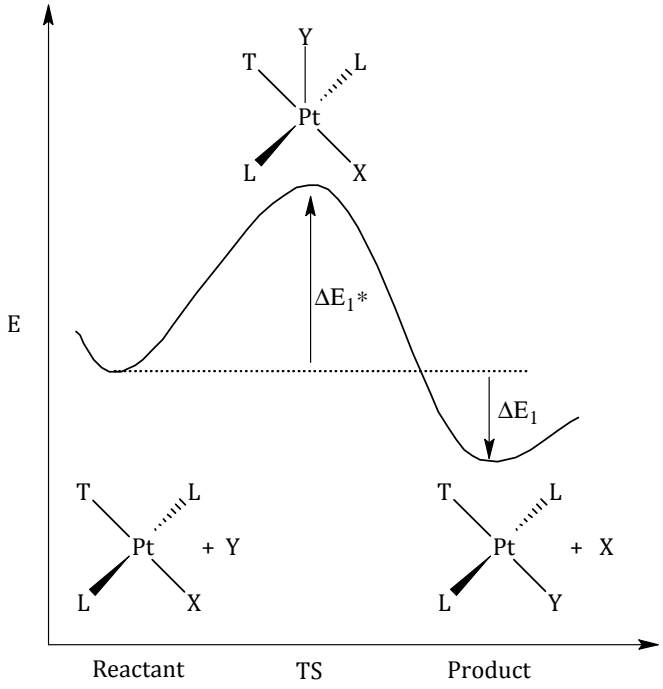


**Figure 2.11:** Sketch diagram showing the effect of σ-donor *trans* ligand on energies of ground state and transition state of a square-planar Pt(II) complex. TS = transition state.[61]

The σ-*trans* effect order which is approximately the order of decreasing polarizability of the ligands is;[7] $H^- > PR_3 > SCN^- > I^- > CH_3^- > CO > CN^- > Br^- > Cl^- > NH_3 > OH^-$.

Since the polarizability of the metal ion is important, this theory readily accounts for the observation that the *trans* effect is greatest in the most polarizable or softest platinum(II) than palladium(II) complexes.

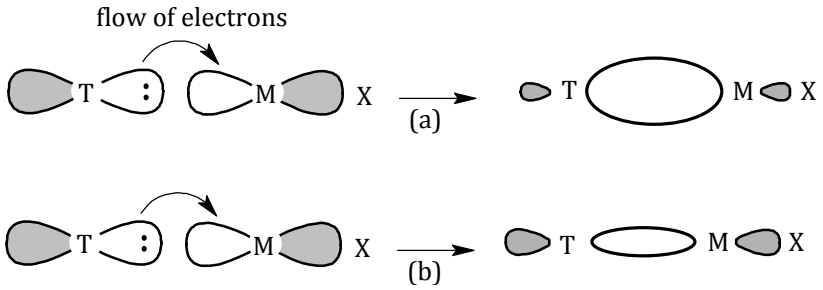


**Figure 2.12**: *σ*-bonding effect.[60] (a) Strong σ-donor ligand T, the σ-bond strength of M – T is much greater than that of M – X, (b) weak σ-donor *trans* ligand gets poorer overlap with the metal orbital.

It is worth noting that as electrons are donated from the filled ligand orbital to the vacant metal orbital, this kind of interaction will diminish the total (positive) natural bonding order (NBO charge) of the Pt(II) centre due to an increase of electron density in the *xy* plane as shown by the complexes studied in **Chapter six** of this thesis. Increase in the rate of substitution reaction in Pt(II) complexes as a result of *trans* σ-donation effect has been reported by a number of studies.[33d,56]

#### 2.5.2.1.2 π-back-donation *Trans* Effect

In the π-*trans* effect theory for square-planar complexes,[62,63] the trigonal bipyramidal intermediate can be stabilized by removal of electron density from π-orbitals of the entering group Y (via metal *d* orbitals) to π-acceptor orbitals of the *trans* ligand T (**Figure 2.13**).[64] This electronic communication through π-bonding is only possible if the three ligands and the metal centre all lie in the same plane at transition state facilitating the effective delocalization of the extra charge from the metal. π-back bonding also favours low energy of the transition state which results into a low activation energy for the substitution reaction (**Figure 2.14**).[7,65] Calculation of the overlap of the valence orbitals of several ligands with the platinum $6p_\pi$ orbital suggests a π-*trans* effect order;[7] $C_2H_4 \approx CO > CN^- > NO_2^- > SCN^- > I^- > Br^- > Cl^- > NH_3 > OH^-$. The overall *trans* effect trend is therefore the combination of the σ- and π-*trans* effects as follows;[7]

$$C_2H_4 \approx CO > CN^- > PR_3 \approx H^- > CH_3 \approx SCN_2H_4 > NO_2^- \approx SCN^- \approx I^- > Br^- > Cl^- > py,\ NH_3 > OH^- > H_2O$$

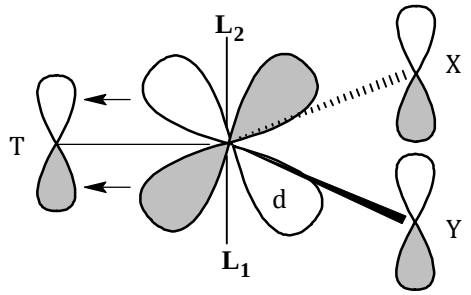


**Figure 2.13**: Schematic diagram of the π-bonding mechanism for the *trans*-effect.[66]

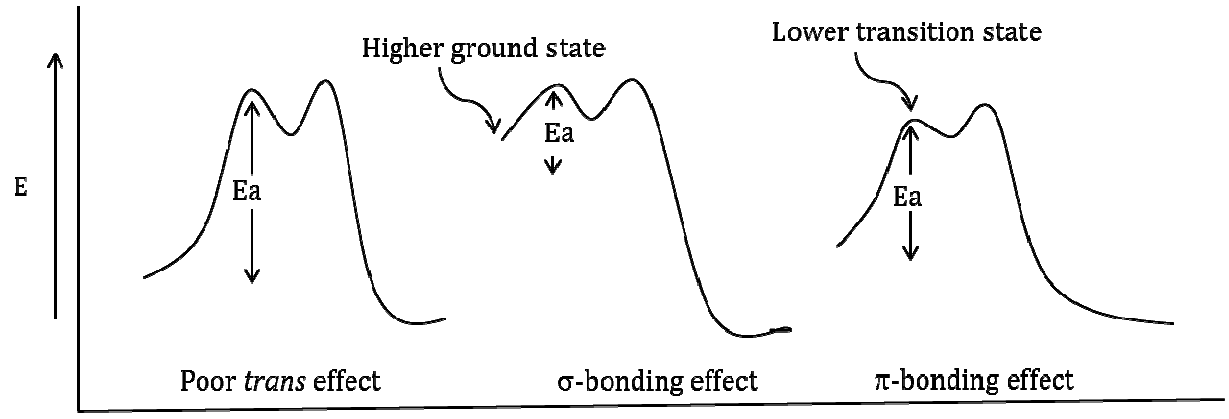


**Figure 2.14:** Activation energy and the *trans* effect.[8a]

Unlike σ-donor groups, π-acceptor groups increases the total (positive) NBO charge of the Pt(II) atom by a decrease of electron density in the *xz* plane through π-back-donation. It also facilitates a nucleophilic attack in the *xz* plane and stabilizes corresponding pentacoordinated transition state.[67] Systematic alteration of the position of π-acceptor groups (*cis*/*trans*) affects the electronic communication in the system hence affecting the reactivity of the Pt(II) centre with *cis* π-back bonding found to be stronger than *trans* π-back bonding.[68] Hitherto, it has been generally acknowledged that increase in π-surface and hence π-acceptor properties in the system accelerates the nucleophilic substitution process of Pt(II) complexes.[33] However, a recent study[33b] has found that increased π-surface of isoquinoline does not enhance the rate of substitution reactions but rather it slows the reactivity by a magnitude of three due to the fact that isoquinoline is a net σ-donor. A detail kinetic study on the effects of π-acceptor ligands and *trans* effect is presented in **Chapter Three** and **Six** of this thesis.

#### 2.5.2.2 The-*cis* Effect

The ligands *cis* to the leaving group exert only a small electronic effect and is observed for poor nucleophiles only. The *cis* effect becomes important if the *cis* ligands are bulky as they block the open axial sites for the incoming group[33f,34,69] and in some cases may cause a mechanistic change from an associative to a dissociative mechanism. This is because, in associative ligand substitution reactions, a trigonal-bipyramidal transition state is greatly strained by *cis* blocking but not nearly so crowded by *trans* blocking. A survey in literature shows that *cis* blocking causes the relative drop in the rate of reaction by a factor of thousands compared to *trans* blocking.[5] Apart from *cis* steric hindrance, electronically, *cis* σ-donor effect also increases the electron density at the metal centre and slows down the reactivity of the Pt(II) complex[43,70] with *cis* π-effect having an opposite influence.

### 2.5.3 Role of the Leaving Group

It is difficult to generalize the effect of the leaving group on the rate of substitution reaction because it is dependent on the nature of the reaction centre, nature of incoming nucleophiles and the nature of the *trans* ligand.[71] For systems in which marked leaving group effects occur, it is suggested that bond breakage of the five-coordinate intermediate produced during an associative substitution process may contribute significantly toward the observed kinetic parameters and may even be the rate-determining step under extreme conditions like strongly bonded leaving groups.[59] One of the most extensive series of reactions used to study the leaving group effect has been the reaction given in **Equation 2.45**.[34]

$$[Pt(dien)X]^{(2-n)+} + Nu^{x-1} \rightarrow [Pt(dien)(Nu)]^{(2-x)+} + X^{n-1} \quad (2.45)$$

In this case the three other coordination positions are rendered inert by using the strongly complexing dien ligand, and the entering ligand (Nu) was always pyridine (py). The rates in aqueous solution obtained from reaction **Equation 2.45** are given in **Table 2.1** and the rate constant for the displacement of $X$ decreases in the order;[7,34]

$$NO_3^- > H_2O > Cl^- > Br^- > I^- > N_3^- > SCN^- > NO_2^- > CN^-$$

A substantial difference in the relative rates of different leaving groups observed indicates that a considerable perturbation of the $Pt-X$ bond at the transition state does not lead to a dissociation process but merely requires that $Pt-X$ bond breaking make a contribution comparable to that of $Pt-py$ bond forming. It is worth stating that the leaving groups high in the *trans*-effect series are substituted more slowly. This is consistent with the combined σ- and π-*trans*-effect theory which suggests that good *trans*-effect groups will be strongly bonded to the metal. The reverse that a poor *trans* activator/labilizer is readily replaced need not be true. For example $OH^-$ is a very poor *trans* labilizer but is very difficult to substitute. Another poor *trans* labilizer that is an inert leaving group is $NH_3$.[7] Generally, groups which best stabilize a negative charge are the best leaving groups, as for example the weakest bases are most stable anions and are the best leaving groups.

**Table 2.1:** Effect of the leaving group on rates of reaction of Pt(II) complexes in water at 25 °C.[7,34]

| Leaving group, X | $k_{obs}$, $s^{-1}$ |
|---|---|
| $NO_3^-$ | very fast |
| $H_2O$ | 1900 |
| $Cl^-$ | 35 |
| $Br^-$ | 23 |
| $I^-$ | 10 |
| $N_3^-$ | 0.83 |
| $SCN^-$ | 0.3 |
| $NO_2^-$ | 0.05 |
| $CN^-$ | 0.017 |

### 2.5.4 Effect of the Metal Centre

In general, the square-planar complexes of Pd(II) and Ni(II) are much more labile than analogous Pt(II) complexes.[72] This order of reactivity is ascribed to the tendency of forming 5-coordinate intermediate complexes. The more readily the formation of a 5-coordinate intermediate complex, the greater the stabilization of the transition state and so the greater the rate enhancement of the associative substitution.

### 2.5.5 Effect of the Solvent

The solvent dependence of the reaction rates of Pt(II) complexes provides another test of the suggestion of associative activation involving solvent for the $k_{-2}$ term in the rate law **Equation 2.17**. van Eldik and Weber studied the influence of solvent on ligand substitution reactions of Pt(II) complexes as function of the π-acceptor properties of the spectator

chelate.[73] It was found that in the case of alcoholic solvents, there was an increase in the second-order rate constant with increasing length of the carbon chain of the alcohol and ascribed it to a possible role of van der Waals forces in stabilizing the transition state of the substitution process. An increase in rate constant was also observed in going from methanol to water, which is in line with the expected trend in terms of the polarity of the solvent, *viz*. a more polar solvent will stabilize the polar transition state formed through the associative attack of the neutral nucleophile.

The $k_{-2}$ term is important in solvents that are capable of coordinating with Pt(II) (**Table 2.2**) as the rate of reaction is found to be independent of the concentration of the incoming group but dependence on the nucleophilicity of the solvent. From **Table 2.2** it can be seen that pyridine and dimethylsulfoxide (DMSO) are top in the series and therefore are better nucleophiles towards Pt(II) centre.[69b] In solvents that are poor entering groups such as chloroform and dichloromethane, the $k_2$ term for reaction is more important.

**Table 2.2**: Coordinating ability index, $a^{TM}$ for solvents relative to transition metals[74].

| **Solvent** | $\boldsymbol{a^{TM}}$ |
|---|---|
| Pyridine | 1.4 |
| Dimethylsulfoxide | 0.3 |
| Hexamethylphosphoramide | 0.2 |
| Triethylamine | 0.1 |
| n-Propanol | 0.0 |
| Water | -0.1 |
| Dimethoxyethane | -0.2 |
| Dimethylformamide | -0.2 |
| Ethylene glycol | -0.2 |
| Acetonitrile | -0.2 |
| i-Propanol | -0.3 |
| Acetic acid | -0.3 |
| Tetrahydrofuran | -0.3 |
| n-Butanol | -0.4 |
| Methanol | -0.4 |
| t-Butanol | -0.4 |
| Dimethylacetamide | -0.5 |
| Ethanol | -0.5 |
| Ethyl acetate | -0.8 |
| Acetone | -1.0 |
| Cyclohexane | -1.0 |
| Toluene | -1.2 |
| Nitromethane | -1.4 |
| Diethyl ether | -1.4 |
| Dichloromethane | -1.7 |
| Chloroform | -2.2 |

Generally, to have a complete understanding of the factors governing reactivity of Pt(II) complexes towards ligand substitution reactions, one has to perform a systematic study in which all other structural features within the series of complexes under study are kept constant while the feature of interest is varied. In this thesis the electronic and steric effects of the ligand framework on reactivity of a series of mononuclear and dinuclear Pt(II) complexes has been investigated. The leaving group was varied from chloride to water depending on the solubility of the complexes whereas the entering group in all systems investigated was thiourea nucleophiles of different steric demand. The details of the result for the substitution reactions of the complexes and the aforesaid nucleophiles as specified in objectives **Chapter One** will be discussed in **Chapter three** to **six** of this thesis.

## 2.6 References


1. (a) B. Lippert, *Cisplatin. Chemistry and Biochemistry of a Leading Anticancer Drug*, Wiley-VCH, Weinheim, **1999**; (b) U, Fekl, K. I. Goldberg, *Adv. Inorg. Chem*., **2003**, *54*, 260.
2. I. Bertini, H. B, Gray, E. I, Stiefel, J. S, Valentine, *Biological Inorganic Chemistry Structure and Reactivity*, **2007**, pg 100-103.
3. R. G. Wilkins, *Kinetics and Mechanisms of Reactions of Transition Metal Complexes*, 2nd Ed., VCH, Weinheim, **1991**, pg. 199-201; 232-237.
4. (a) D. T. Richens, *Chem. Rev*., **2005**, *105*, 1961; (b) R. J. Cross, *Chem. Soc. Rev*. **1985**, *14*, 197; (c) F. Basolo, *Advances in Chemistry*, **1965**,*49*, 81; (d) A. Mambanda, *PhD Thesis*, University of KwaZulu-Natal, Republic of South Africa, **2009**; (e) P. Ongoma, *PhD Thesis*, University of KwaZulu-Natal, Republic of South Africa, 2012.
5. C. K Ingold, *Structure and mechanism in organic chemistry*, Cornell University press, Ithanca, **1953**, chapters 5 and 7.
6. F. Basolo and R. G. Pearson, *Mechanisms of Inorganic Reactions*, 2nd Ed., Wiley, New York, **1967**, pg. 193-195; 351-356, 369-400; 453
7. C. H. Langford, H. B. Gray, *Ligand Substitution Processes*, New York, Amsterdam, **1965**, pg 1-14;33, 40
8. (a) G. L. Miessler and D. A. Tarr, *Inorganic Chemistry*, Pearson Education Internatioal, Singapore, **2004**, pg. 397; 415-426; (b) R. B. Jordan, *Reaction mechanisms of Inorganic and Organometallic Systems*, New York, Oxford, **1991**, pg 30

9. (a) M. Rashidi, S. M. Nabavizadeh, A. Zare, S. Jamali and R. J. Puddephatt, *Inorg.Chem*., **2010**, *49*, 8435; (b) S. C. L., Kamerlin, J. Florián and A. Warshel, *ChemPhysChem.,* 2008, 9, 1767; (c) S. Choi, L. Vastag, C.-H. Leung, A. M. Beard, D. E. Knowles, and J. A. Larrabee, *Inorg. Chem.*, **2006**, *45*(25), 10108; (d) R. Van Eldik, D. A. Palmer, H. Kelm, *Inorg. Chem.*, **1979**, *18*(3), 572

10. http://www.ilpi.com/organomet/substitution.html **accessed on 12/03/2013**

11. K. Helmut and R. van Eldik, *J. Chem. Soc., Chem. Commun*., **I990**, *4*, 330.

12. Jaganyi, D. and Shaira, A., Dalton Trans, 2013, Accepted manuscript

13 A. Hofmann, L. Dahlenburg, and R. van Eldik, *Inorg. Chem*., **2003**, *42*, 6528-6538.

14. D. Jaganyi and P. Ongoma, *Dalton Trans*., **2013**, *42*, 2724.

15. R. Van Eldik, *High Pressure Molecular Science*, **1999**, 358, pg 267-289

16 J. D. Atwood, *Inorganic and Organic Reaction Mechanisms*, 2nd Ed., Wiley-VCH Inc., New York, **1997**, pg. 1-32.

17 R. B. Jordan, *Reaction mechanisms of Inorganic and Organometalic Systems*, Oxford University Press Inc, New York, **1991**, pg. 1-17.

18. P. W. Atkins, *Physical Chemistry*, 6th ed., Oxford University Press, Oxford, **1998**, pg. 761, 830.

19 R. Chang, *Physical chemistry for Biosciences*, USA, University Science Books, **2005**, pg. 338-342.

20 (a) J. Krupčík, J. Mydlová, P. Májek, P. Šimon, D. W. Armstrong, *J. Chromatogr. A*, **2008**, *1186*, 144; (b) J. J. Rooney, *J. Mol. Catal. A*, **1998**, *129*, 131.

21. (a) G. Jenner, *J. Phys. Org. Chem.* **2002**, *15*, 1; (b) A. E. Merbach, *Pure &AppI. Chem*., **1987**, *59*(2), 161.

22. (a) A. Mambanda, D. Jaganyi, S. Hochreuther and R. van Eldik, *Dalton Trans.*, **2010**, *39*, 3595; (b) S. Hochreuther, R. Puchta, and R. van Eldik, *Inorg. Chem*. **2011**, *50*, 12747; (c) B. Petrović, Ž. D. Bugarčić, A. Dees, I. Ivanović-Burmazović, F. Heinemann, R. Puchta, F. W. Heinemann, S. N. Steinmann, C. Corminboeuf, R. van Eldik, *Inorg. Chem*., **2012** *51*, 1516; (d) S. Hochreuther, S. T. Nandibewoor, R. Puchta and R. van Eldik, *Dalton Trans.*, **2012**, *41*, 512.

23. A. Brausm, R. van Eldik, *Advances in Inorganic Chemistry; Inorganic/Bioinorganic Reaction Mechanisms*, Academic Press Publication, **2012**, 1st Edition, vol. 64, pg 114 (ebook).

24. (a) J. Krupčík, J. Mydlová, P. Májek, P. Šimon, D. W. Armstrong, *J. Chromatogr. A*, **2008**, *1186*, 144; (b) J. J. Rooney, *J. Mol. Catal. A*, **1998**, *129*, 131.

25 D. Katakis, G. Gordon, *Mechanisms of lnorganic Reactions,* John Wiley & Sons, New York, **1987**, pg. 99.

26. D. C. Harris, *Quantitative Chemical Analysis*, 4th Ed., W. H. Freeman and Company, New York, **1995**, pg. 480.

27. Origin7.5TM SRO, v7.5714 (B5714),Origin Lab Corporation, Northampton, One, Northampton, MA, 01060, USA, **2003**.

28. (a) J. Bogojeski, Ź. D. Bugarčić, R. Puchta and R. van Eldik, *Eur. J. Inorg. Chem.,* **2010**, 5439; (b) S. Jovanović, B. Petrović, D. Čanović and Ž. D. Bugarčić, *Int. J. Chem. Kinet*., **2011**, *43*,99; (c) N. Summa, W. Schiessl, R. Puchta, N. van Eikema Hommes and R. van

Eldik, *Inorg. Chem*., **2006**, *45*, 2948; (d) T. Soldatoví, Ž. D. Bugarčić and R. van Eldik, *Dalton Trans*., **2009**, 4526.

29. http://vallance.chem.ox.ac.uk/pdfs/KineticsLectureNotes.pdf accessed on **24th March**, **2013.**

30. (a) P. Atkins, J. de Paula, *Atkins' Physical Chemistry*, 8th Ed., Oxford University Press, **2006**, pg. 793; (b) K.A. cannors, *Chemical Kinetics*; *The Study of Reaction Rates in Solution*, VCH Publishers, Ney York, **1990**, pg. 179.

31. R-Y. Wang, *Application of Physical methods in Inorganic and Bioinorganic Chemistry*, Edited by R. A. Scott and C. M. Lukehart, **2007**, John Wiley & Sons, Ltd. ISBN978-0-470-032176.

K. J. Laidler, J. H Meiser, and B. C. Sanctuary, *Physical Chemistry*, 4th Ed., Houghton Mifflin Company, New York, **2003**, pg. 374-379; 390-393.

33. (a) J. Bogojeski, Ž. D. Bugarčić, R. Puchta and R. van Eldik, *Eur. J. Inorg. Chem*., **2010**, 5439; (b) D. Jaganyi, P. Ongoma., *Dalton Trans.*, **2012**, *41*, 10724; (c) T. Soldatović, S. Jovanović, Ž. D. Bugarčić and R. van Eldik, *Dalton Trans.*, **2012**,*41*, 876; (d) A. Mambanda, D. Jaganyi, S. Hochreuther and R. van Eldik, *Dalton Trans.*, **2010**, *39*, 3595; (e) D. Reddy, K. J. Akerman, M. P. Akerman, D. Jaganyi, *Transition Met Chem*, **2011**, *36*,593; (f) A. Mijatović, J., Bogojeski, B., Petrović, Ž. D. Bugarčić, *Inorg. Chim. Acta* **2012**, *383*, 300.

34. M. L. Tobe and J. Burgess, *Inorganic Reaction Mechanisms*, Addision Wesley, London, **1999**, pg. 30-39; 73-94; 103-106.

35. J. D. Atwood, *Inorganic and Organic Reaction Mechanisms*, 2nd Ed., Wiley- VCH Inc., New York, **1997**, pg. 32-34; 43-61.

36. F. Basolo, W. R. Matoush, and R. G. Pearson, *J. Am. Chem. Soc*., **1956**, *78*, 4883.

37. J. W. Palmer and F. Basolo*, J. Inorg. Nucl. Chem.,* **1960**, *15*, 279.

38. T. J. Swift and R. E. Connick, J. *Chem. Phys.,***1962**, *37*, 307

39. R. G. Pearson, H. R. Sobel and J. Songstad. *J. Amer. Chem. Soc.,* **1968***, 90*(2), 319.

40. D. Banerjea, F. Basolo and R. G. Pearson, *J. Amer. Chem. Soc.,* **1957**, *79*, 4055.

41. H. B. Gray, *J. Am. Chem. Soc.,* **1962**, *84*, 1548.

42. U. Belluco, *Organometalic Coordination Chemistry of Platinum*, Academic Press, London, **1974**, pg. 40-53; 138-160; 220-221.

43. A. Hofmann, L. Dahlenburg and R. van Eldik, *Inorg. Chem*., **2003**, *42*, 6528.

44. J. O. Edwards, R. G. Pearson. *J. Am. Chem. Soc.*, **1962**, *84*(1), 16.

45. Ašperger, *Chemical Kinetics and Inorganic Reaction Mechanisms*, 2nd Ed., Kluwer Academic/Plenum Publisher, New York, **2003**, pg. 38-39; 105-106; 140-153.

46. R. G. Pearson, *J. Am. Chem. Soc.,* **1963**, *85*, 3533.

47. A. Jacob, *Undestanding Organic reaction mechanisms*, Cambridge University Press, United Kingdom, **1997**, pg. 45

48. D. Jaganyi, F. Tiba, O. Q. Munro, B. Petrović and Z. D. Bugarčić, *Dalton Trans*., **2006**, 2943.

49. A. Shaira., *Msc thesis*, University of KwaZulu-Natal, Republic of South Africa, **2010**.

50. Ž. D. Bugarčić, B. Petrović and E. Zangrando, *Inorg. Chim. Acta*, **2004**, *357*, 2650.

51. (a) Ž. D. Bugarčić, S. T. Nandibewoor, M. S. A. Hamza, F. Heinemann and R. van Eldik *Dalton Trans.*, **2006**, 2984; (b) L. Cattalini , A. Orio , M. L. Tobe., *J. Am. Chem. Soc.*, **1967**, *89*(13), 3130.

52. (a) M. Bellicini, L. Cattalini, G. Marangoni and B. Pitteri, *J. Chem. Soc. Dalton Trans.,* **1994**, 1805; (b) M. Bellicini, L. Cattalini, G. Marangoni and B. Pitteri, *J. Chem. Soc. Dalton Trans.,* **1994**, 3539.

53. (a) Ž. D. Bugarčić, G. Liehr and R. van Eldik., *J. Chem. Soc*., *Dalton Trans*., **2002**, 2825; (b) S. Jovanović, B. Petrović, D. Čanović, and Ž. D. Bugarčić., *Int. J. Chem. Kinet*., **2011**, *43*, 99; (c) Ž. D. Bugarčić, J. Rosić, B. Petrović, N. Summa, R. Puchta, R. van Eldik., *J Biol Inorg Chem*., **2007**, *12*, 1141.

54. (a) I. I. Chernyaev,. *Ann. Inst. Platine USSR*, **1926,** *4,* 261; (b) F. Basolo, R.G. Pearson, *Prog. Inorg. Chem*., **1962**, *4*, 381.

55. I. I, Chernyaev,. *Ann. Inst. Platine* (USSR) **1926**, *4*, 423.

56. (a) A. S. Fleischhacker., R. G. Matthews,. *Biochem.,* **2007**, *46*, 12382; (b) A. C. Albeniz., P. Espinet., B. Martin-Ruiz,. *Dalton Trans*, **2007**, *33*, 3710; (c) D. B. Berezin., O. V. Toldina., B. D. Berezin., *Russ. J. Inorg. Chem., **2006**, 51*, 1728; (d) H. Chermette., K. Rachedi., F. Volatron., *J. Mol .Struct .(Theochem).*, **2006**, *762*, 109; (e), L. Randaccio., S. Geremia., G. Nardin., J. Wuerges., *Coord. Chem. Rev.,* **2006,** *250*, 1332; (f) V. S. Sergienko., *Crystallogr. Rep.,* **2004**, *49*, 907; (g) A. Mambanda and D. Jaganyi., *Dalton Trans.*, **2011**, *40*, 79; (h) S. Hochreuther., R. Puchta., and R. van Eldik., *Inorg. Chem.*, **2011**, *50*(24), 12747.

57. J. R. Gispert., *Coordination chemistry*, Wiley,VCH Verlag GmbH and Co. KGaA. Weinheim, **2008**, pg. 225-228.

58. L. E., Orgel., *J. Inorg. Nucl. Chem*., **1956**, *2*, 137.

59. P. N. Kapoor, R. Kakkar., *J. Mol. Str.* (*Theochem*), **2004**, *679*, 149.

60. (a) http://employees.csbsju.edu/cschaller/Reactivity/MLnSub/lstranseffect.htm, **Accessed on 23rd May 2013**; (b) A. A. Grinberg, *Acta Physicochim. (U.S.S.R.),* **1935**, 3, 573 *(Chem. Abs.,* **1936**, *30*, 4074).

61. D. V. Khoroshun, D. G. Musaev, K. Morokuma, *J. Comput. Chem*., **2006**, *28*(1), 423.

62. J. Chatt, L. A. Duncanson, and L. M. Venanzi, *J. Chem. Soc.,* **1955**,4456.

63. L. E. Orgel, *J. Inorg. Nuclear Chem.,* **1956**, *2*, 137.

64. N. Kuznik and O. F. Wendt, *J. Chem. Soc., Dalton Trans.*, **2002**, 3074.

65. (a) L. G. Vanquickenborne, J. Vranckx, and C. Gorller-Walrand, J.Am. Chem.Soc. **1974**, *96*(13), 4121;(b) L. Oleari, L. Di Sipio, and *G.* De Michelis, *Ricercu sci., Rend. Sez. A,* **1965**, *8*, 413 *(Chem. Abs.,* **l966**, *64*, 4567d).

66. http://cheminnerweb.ukzn.ac.za/Files/5 Reaction mechanisms.pdf, accessed on **25th May 2013**.

67. Z. Chval, M. Sip, J. V. Burda., *J. Comput*. *Chem*., **2008**, *29*(14), 2370

68. A. Hofmann, D. Jaganyi, O. Q. Munro, G. Liehr, and R. van Eldik., *Inorg. Chem.* **2003**, *42*, 1688.

69. (a) J. Bogojeski, R. Jelić, D. Petrović, E. Herdtweck, P. G. Jones, M. Tamm and. Ž. D. Bugarčić., *Dalton Trans.*, **2011**, *40*, 6515; (b) M., Đurovic´, J., Bogojeski, B., Petrovic´, D., Petrovic´, F. W., Heinemann, Ž. D., Bugarčić, *Polyhedron.*, **2012**, *41*, 70.

70. D. Jaganyi, D. Reddy, J. A. Gertenbach, A. Hofmann and R. van Eldik, *Dalton Trans.*, **2004**, 299.

71. M. Kotowski., R. Van Eldik,. *Inorganic Chemistry.*, **1986**, *25*(22), 3896.

72. B. Petrović., Ž. D. Bugarčić, A. Dees, I. Ivanović-Burmazović, F. Heinemann, R. Puchta, R. van Eldik., *Inorg. Chem*., **2011**, *51*, 1516.

73. C. F. Weber, and R. van Eldik, *Eur*. *J*. *Inorg*. *Chem.*, **2005**, 4755.

74. R. Díaz-Torres and S. Alvarez, *Dalton Trans*., **2011**, *40*, 10742.

## Table of Contents

**List of Tables**

**List of Figures**

# Chapter 3

## Understanding the Electronic and π-conjugation Roles of Quinoline on Ligand Substitution Reactions of Pt(II) Complexes.


### Abstract

A kinetic and mechanistic study of chloro substitution by thiourea nucleophiles *viz*. thiourea (TU), *N*-methylthiourea (MTU), *N*,*N*-dimethylthiourea (DMTU) and *N*,*N*,*N*',*N*'-tetramethylthiourea (TMTU) in the complexes bis-(2-pyridylmethyl)amine platinum(II) chloride (**Pt1**), *N*-(2-pyridinylmethyl)-8-quinolinamine platinum(II) chloride (**Pt2**), *N*-(2-pyridinylmethylene)-8-quinolinamine platinum(II) chloride (**Pt3**) and bis(8-quinolinyl)amine platinum(II) chloride (**Pt4**) was undertaken under *pseudo* first-order conditions using UV-Visible spectrophotometry. The study showed that lability of the chloro leaving group is dependent on the strength of π-interactions between the filled *d*π-orbitals of the metal with the empty π*-orbitals of the chelating ligand in the following manner; **Pt1 > Pt3 > Pt2 > Pt4**. Introduction of the quinoline moiety within the non-labile chelated framework of the Pt(II) complexes results into a more electron-rich metal centre which retards the approach of the nucleophile through repulsion. Moreover, the net σ-effect of the ligand moiety plays a significant role on controlling the reactivity of the complexes. The experimental results are interpreted with aid of computational data obtained by DFT (B3LYP(CPCM)/LANL2DZp//B3LYP/-LANL2DZp) calculations. The mode of substitution remains associative as supported by negative entropies and the dependence of the second-order rate constants on the concentration of entering nucleophiles.

## 3.1 Introduction

The rate of substitution on square-planar Pt(II) tridentate chelates of the type $[Pt(NNN)X]^+$ where X= chloride or aqua ligand can be varied by tuning structural, steric and electronic properties of the non-labile ligands.[1] Most of the studies have involved monofunctional tridentate Pt(II) complexes; $[Pt(dien)Cl]^+$,[2] $[Pt(bpma)Cl]^+$,[3] $[Pt(terpy)Cl]^+$,[3,4] and $[Pt(tpdm)Cl]^+$.[5,] (where dien = diethylentriamine, bpma = bis-(2-pyridylmethyl)amine, terpy = 2,2′:6′,2″-terpyridine and tpdm = terpyridinedimathane). These complexes are highly stable even under acidic conditions due to the chelate effect and synergistic combination of σ-donor and π-acceptor N-heterocyclics that incorporate five-membered rings.[6]

van Eldik and co-workers[3c,7,8] have reported that reactivity of Pt(terpy), Pt(bpma) and Pt(dien) increased in the order of Pt(terpy) >> Pt(bpma) >Pt(dien) by introduction of π-backbonding by systematically displacing amine ligands by pyridine donor groups. The higher reactivity of approximately 3-5 orders of magnitudes reported for Pt(terpy) compared to Pt(bpma) and Pt(dien) was attributed to effective communication through π-backbonding of the in-plane pyridine moieties in the terpy ligand. This was shown to increase the electrophilicity of the metal centre and stabilize the five-coordinate transition state relative to the ground state during an associative substitution process. In a related study, it was found that *cis*-π backbonding is stronger than *trans*-π backbonding.[9] On the other hand, *cis*-σ-donor effect has been reported to slow down the lability of the leaving group in Pt(II) complexes[1a, 6,9] through the accumulation of electron on the Pt centre while

the *trans*-σ-donor effect accelerates the rate of substitution reaction by the well-known *trans* labilization effect.[10] In recent studies by our group, it was shown that if one of the outer pyridine rings in the terpy system is substituted by isoquinoline ligand in the *cis*-position, a net *cis*-σ-donor effect is experienced by the complex, slowing down the lability of the leaving group.[11] When the pyridine group is replaced by a pyrazine moiety the lability of the leaving group is enhanced due to stronger π-acceptor properties of pyrazine as a ligand.[12] Thus, in principle, such tuning of the lability of the leaving group in Pt(II) complexes plays an important role in the development of new antitumour agents. This is evident by the number of platinum-based complexes that have been synthesized and investigated for their anticancer efficacy since the discovery of [*cis*-diamminedichloridoplatinum(II)], (cisplatin) in 1969,[13] which is greatly hampered by severe side effects and drug resistance.[14]

To extend my understanding of the role played by σ-donation of quinoline moiety and the π-conjugation system on ligand substitution reactions in tridentate monofunctional Pt(II) complexes, a series of ligands with quinoline ring systems coordinated to Pt(II) via amine/imine bond was undertaken. Based on data available in the literature the expectation was that by increasing the electronic communication through π-conjugation the reactivity of the Pt(II) centre towards substitution would be enhanced, but this will be in competition with quinoline's σ-donation. Therefore, Pt(II) compounds; bis-(2-pyridylmethyl)amine platinum(II) chloride, (**Pt1**), *N*-(2-pyridinylmethyl)-8-quinolinamine platinum(II) chloride, (**Pt2**), *N*-(2-pyridinylmethylene)-8-quinolinamine platinum(II)

chloride, (**Pt3**) and bis(8-quinolinyl)amine platinum(II) chloride, (**Pt4**) were synthesized and their kinetics investigated using sulfur donor nucleophiles; thiourea (TU), 1-methyl thiourea (MTU), 1,3-dimethyl-2-thiourea (DMTU), and 1,1,3,3,-tetramethyl-2-thiourea (TMTU). Thiourea nucleophiles were chosen due to their good nucleophilicity, high solubility and can act as good model compound for thiolate and thioether present in the cell. The structures of the complexes studied are summarized in **Figure 3.1**. DFT calculations were performed to provide the insight and understanding of the experimental results.

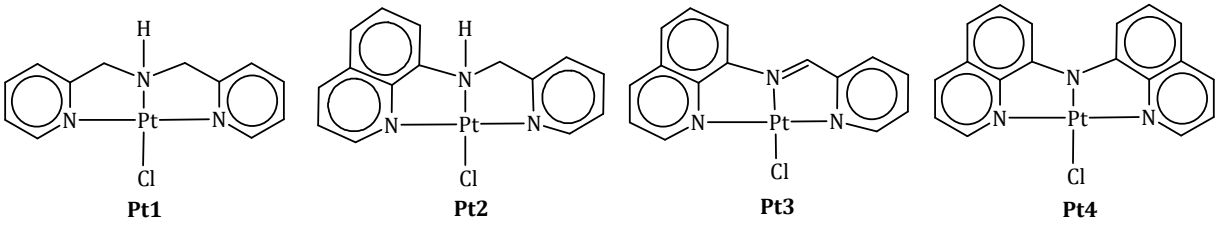


**Figure 3.1:** Structures of investigated Pt(II) complexes (charges are omitted for clarity).

## 3.2 Experimental

### 3.2.1 Materials

All synthetic work was performed under an inert atmosphere of nitrogen. Solvents used for synthesis and kinetic measurements were dried by standard methods[15] and distilled prior to use. Tris(dibenzylideneacetone)dipalladium(0) (97%), *rac*-2,2'-bis(diphenylphosphino)-1,1'-binaphthyl (97%), 8-bromoquinoline (98%), 8-aminoquinoline (98%), NaO$^t$Bu (97%), pyridine-2-carboxyaldehyde (99%), 2-picolylchloride hydrochloride (98%), lithium perchlorate (98%), sodium borohydride (98%), 2-picolylamine, BPMA (99%) and thiourea nucleophiles were obtained from Aldrich. Potassium tetrachloroplatinate, ($K_2PtCl_4$ 99.99%)

was obtained from Strem. All other chemicals were of analytical grade and were used as supplied.

### 3.2.2 Synthesis of the Ligands

**Bis(8-quinolinyl)amine**, (**BQA**): Into a two necked flask (100 mL) was filled with tris(dibenzylideneacetone)dipalladium(0) (22 mg, 0.024 mmol), *rac*-2,2'-bis(diphenylphosphino)-1,1'-binaphthyl (29.87 mg, 0.048 mmol) and dry toluene (10 mL) under an inert atmosphere of nitrogen. The resulting solution was stirred for 5 min and 8-bromoquinoline (0.16 mL, 1.201 mmol), 8-aminoquinoline (0.1737 g, 1.205 mmol), and additional dry toluene (20 mL) were added. The subsequent addition of $NaO^tBu$ (0.1387 g, 1.437 mmol) resulted in a red solution that was left stirring vigorously for 3 days at 110 ˚C. The solution was then allowed to cool and filtered through a silica plug and extracted with dichloromethane to ensure complete removal of the desired product. Concentration of the collected extracts and removal of solvent yielded a crude red solid. Purification by flash chromatography on silica gel (4:1 toluene:ethyl acetate) yielded an orange solid as a spectroscopically pure compound. Character identification data for BQA compared favourably with that previously reported data.[16] Yield: 24.7 mg, Orange solid (76%). $^1$H NMR ($CDCl_3$, 400 MHz,): δ/ppm = 10.64 (s, 1H), 8.92 (dd, 2H), 8.15 (dd, 2H), 7.90 (d, 2H), 7.53-7.44 (m, 4H), 7.33 (d, 2H). $^{13}$C NMR ($CDCl_3$, 400 MHz,): δ/ppm = 148.1, 140.0, 138.8, 136.2, 129.0, 127.1, 121.6, 117.9 and 110.1. *Anal. Calcd*. for $C_{18}H_{13}N_3$: C 79.70, H 4.80, N 15.50. *Found* C 79.63, H 5.01, N 15.24. TOF MS ES$^+$: $m/z$, $[M+Na]^+$ = 294.10.

***N*-(2-pyridinylmethyl)-8-quinolinamine**, **Qui-py**: Published method[17] was followed with minor modifications. To a suspension of anhydrous $MgSO_4$ (20 mmol) in $CH_2Cl_2$ (30 mL) was added 2-pyridinecarboxaldehyde (5 mmol) followed by 8-aminoquinoline (5 mmol). After the mixture had been stirred for 3 h at room temperature, the suspension was filtered, washed with $CH_2Cl_2$ and the solvent removed under vacuum. The yellow oil which resulted was dissolved in 20 mL $CH_3CN$ and cooled to -5 ˚C followed by addition of glacial acetic acid (0.3 mL, 5 mmol). The resulting imine compound was reduced by careful addition of suspension of sodium borohydride (0.3783 g, 10 mmol) in absolute ethanol (10 mL) over a period of 1 h at -5 ˚C. A white precipitation was formed. The colour of the solution changed from yellow to red by the end of addition. After stirring for 18 h at room temperature, the reaction mixture was quenched with 5 M HCl (30 mL) and finally heated at 60 ˚C for 2 h until no more hydrogen was evolved. The resultant white precipitate was filtered off and the filtrate concentrated in *vacuo* and then redissolved in water (20 mL). The resulting yellow aqueous solution was basified by adding NaOH under ice-water temperature. The obtained oil was extracted with ether and dried over $MgSO_4$. Evaporation of the solvent yielded brown oil. Yield: 686.7 mg, (63%). $^1$H NMR ($CDCl_3$, 400 MHz,) δ/ppm =9.82( s,1H), 8.76(td, 1H), 8.62 (d, 1H), 8.05(ddd, 1H), 7.60 (td, 1H), 7.42-7.29 (m, 2H), 7.14 (dd, 1H), 7.09(dd, 1H), 6.92(dd, 1H), 6.61 (d, 1H), 4.47 (s, 2H). $^{13}$C NMR ($CDCl_3$, 400 MHz,): δ/ppm = 159.3, 149.3, 147.6, 136.7, 136.3, 127.7, 127.4, 122.0, 121.4, 121.3, 116.3, 114.5, 110.2, 105.6, 49.3. TOF MS ES$^+$: $m/z$, $[M+Na]^+$ = 258.10.

### 3.2.3 Synthesis of Platinum(II) Complexes

The preparations of platinum precursors; $Pt(COD)Cl_2$,[18] and *cis*/*trans*-$PtCl_2(SMe_2)_2$ [19] were carried out following literature procedures and their purity was confirmed by NMR, microanalysis and mass spectra.

**Pt1**: The complex was synthesized according to the literature procedure[20] with minor modifications. To a solution of $K_2PtCl_4$ (0.2 g, 0.48 mmol) dissolved in 0.005 m HCl (100 mL) was added bis(2-pyridylmethyl)amine (0.1 mL). The solution was stirred under reflux for 3 days and then cooled to room temperature. The colourless solution was filtered and concentrated to about 10 mL. Addition of saturated $NaClO_4$ solution (2–3 mL) produced the precipitate of the desired complex. The title compound was collected by filtration and sequentially washed with small amounts of water, ethanol and ether, and dried under vacuum. Yield: 242.3 mg, yellow powder (95 %). $^1$H NMR (DMSO-$d_6$, 400 MHz,): δ/ppm = 8.82(dd, 2H), 8.60 (br s, 1H), 8.23(ddd, 2H), 7.76 (d, 2H), 7.63 (t, 2H), 4.92(m, 2H), 4.51 (dd, 2H). $^{13}$C NMR (DMSO-$d_6$, 400 MHz): δ/ppm = 167.4, 149.4, 141.4, 125.7, 123.4, 59.4. $^{195}$Pt NMR (DMSO-$d_6$) δ/ppm: -2344.8. *Anal. Calcd*. for $C_{12}H_{13}N_3PtCl_2O_4$: C 27.22, H 2.46, N 7.94. *Found* C 26.72, H 2.45, N 7.62. TOF MS ES$^+$: *m*/*z*, $[M + H]^+$ = 430.05.

**Pt2**: The solution of *N*-(2-pyridylmethyl)-8-quinolinamine (0.1177 g, 0.47 mmol) dissolved in MeOH (5 mL) was added to a refluxing solution of *cis*/*trans*-$[PtCl_2(SMe_2)_2]$ (0.1821 g, 0.47 mmol) in MeOH (15 mL). The solution was allowed to reflux for 12 h to give the olive green residue that was collected by filtration, washed with methanol, ethanol and diethyl

ether and dried under reduced pressure. Yield: 15.1 mg, (57 %). $^{1}$H NMR (DMSO-$d_6$, 400 MHz,): δ/ppm =8.91 (d, 1H), 8.78(dd, 1H), 8.64 (dd, 1H), 8.54 (dd, 1H), 8.40 (td, 1H), 8.29 (ddd, 1H), 8.17-8.09 (m, 1H), 7.93 (m, 1H), 7.76 (m, 2H), 7.64 (m, 1H), 7.57 (s, 2H). $^{13}$C NMR (DMSO-$d_6$, 400 MHz,): δ/ppm = 159.8, 148.7, 147.6, 135.7, 135.3, 128.7, 128.4, 125.0, 122.4, 121.7, 115.3, 113.5, 109.2, 106.6, 51.1. $^{195}$Pt NMR (DMSO-$d_6$) δ/ppm: -2514.8. *Anal. Calcd*. for $C_{15}H_{13}N_3PtCl_2$: C 35.93, H 2.59, N 8.38. *Found* C 35.44, H 2.39, N 7.91. TOF MS ES$^+$: *m*/*z*, $[M+H]^+$ = 466.04.

**Pt3**: The complex was synthesized following metal-assisted condensation of pyridine-2-carboxaldehyde and 8-aminoquinoline as proposed by Bortoluzzi *et al*.[21] whereby a suspension of *cis*/*trans*-$PtCl_2(SMe_2)_2$ (0.22 g, 0.57 mmol) in 20 mL of methanol was heated to 50 ˚C until the complete dissolution of the complex. A solution containing 8-aminoquinoline (0.082 g, 0.57 mmol) and pyridine-2-carboxyaldehyde (0.05 mL, 0.57 mmol) in 10 mL of methanol was added dropwise. The resulting solution was stirred at room temperature for 3 h. Subsequently, excess of lithium perchlorate (0.35 g, 2.85 mmol) was added. A brown solid started to precipitate slowly. After maintaining the reaction mixture at -25 ˚C overnight, the product was filtered, washed with methanol, ethanol and diethyl ether. Yield: 218.2 mg, (68 %). $^{1}$H NMR (DMSO-$d_6$, 400 MHz,): δ/ppm = 9.88(s, 1H), 8.86 (dd, 1H), 8.54(d, 1H), 8.50 (dd, 1H), 8.32 (d, 1H), 8.30 (td, 1H), 8.19 (dd, 1H), 7.99 (d, 1H), 7.62 (ddd, 1H), 7.50 (t, 1H), 7.42 (d, 1H). $^{13}$C NMR (DMSO-$d_6$, 400 MHz): δ/ppm = 166.9, 156.9, 149.0, 150.8, 149.6, 148.8, 147.5, 144.5, 141.4, 140.1, 129.6, 129.1, 126.8,

122.9, 122.1, 120.3. $^{195}$Pt NMR (DMSO-$d_6$) δ/ppm: -2536.3 *Anal. Calcd.* for $C_{15}H_{11}N_3PtCl_2O_4$: C 31.97, H 1.95, N 7.46. *Found* C 31.48, H1.92, N 7.91. TOF MS ES$^+$: *m/z*, $[M + H]^+$ = 464.03.

**Pt4**: To a reaction vessel containing BQAH (132.1 mg, 0.487 mmol) and (COD)$PtCl_2$ (182 mg, 0.487 mmol) dissolved in THF (10 mL), triethylamine (88 $\mu$L, 0.63 mmol) was added. The vessel was sealed and stirred at 95 ˚C for 48 h under nitrogen atmosphere. The resulting purple solution was cooled and dried in vacuo, extracted with $CH_2Cl_2$ (30 mL), and filtered through celite on a sintered-glass frit. The solvent was removed under reduced pressure, and the precipitate washed with methanol (3 x 30 mL), hexane (2 x 10 mL) and diethyl ether (2 x 10 mL) and then dried in vacuo to give the desired product with spectral data consistent with those reported in previous study.[16] Yield: 158 mg, purple powder, (65%). $^1$H NMR ($CDCl_3$, 400 MHz,): δ/ppm = 9.17 (d, 2H), 8.24 (d, 2H), 7.64 (d, 2H), 7.45 (t, 2H), 7.38 (m, 2H), 7.04 (d, 2H). $^{13}$C NMR (CDCl3, 400 MHz,): δ/ppm = 148.9, 148.7, 148.4, 138.8, 131.4, 129.3, 121.2, 115.7, 113.4. $^{195}$Pt NMR (DMSO-$d_6$) δ/ppm: -2556.1 *Anal. Calcd.* for $C_{18}H_{12}N_3PtCl$: C 43.16, H 2.40, N 8.39. *Found* C 42.86, H 1.98, N 7.91. TOF MS ES$^+$: *m/z,* $[M]^+$ = 500.04.

### 3.2.4 Preparation of Complex and Nucleophile Solutions for Kinetic Analysis

Platinum(II) complexes of known concentration were prepared by dissolving a specified amount in 2 % DMF to enhance the solubility and topped up with 98 % of methanolic solvent system of 0.1 M ionic strength ($NaClO_4$/LiCl). Solutions of the nucleophiles were prepared shortly before use by dissolving in a 0.1 M $NaClO_4$ solution in methanol whose ionic strength had been adjusted by addition of 10 mM LiCl to prevent any solvolysis of the

complexes. The ionic strength of the solution was maintained using sodium perchlorate monohydrate ($NaClO_4.H_2O$) because the perchlorate ion, ($ClO_4^-$), does not coordinate to Pt(II).[22,23] The stock solution of each nucleophile of concentration approximately 50-fold in excess of the complex was then diluted with the 0.1 M ionic strength solution to afford serial concentrations which were 40; 30; 20 and 10-fold in excess over that of the metal complex. These concentrations of the nucleophiles were chosen to maintain *pseudo* first-order conditions and to push the reactions to completion.

### 3.2.5 Instrumentation and Measurements

$^{1}H$, $^{13}C$ and $^{195}Pt$ NMR spectra were recorded on a Bruker Avance III 500 or Bruker Avance III 400 at frequencies of 500 MHz or 400 MHz and 125 MHz/100 MHz using either a 5 mm BBOZ probe or a 5 mm TBIZ probe. All proton and carbon chemical shifts are quoted relative to the relevant solvent signal. All data were recorded at 30°C unless stated otherwise. The mass spectrometric data of the ligands and complexes were acquired on a Waters Micromass LCT Premier spectrometer. Selected NMR and mass spectra are represented as supporting information in **Figures SI 3.1-3.15**. Elemental compositions of the ligands and complexes were performed on Carlo Erba Elemental Analyzer 1106. A Varian Cary 100 Bio UV-Visible spectrophotometer thermostated to within ± 0.05 °C was used for the kinetic measurements.

### 3.2.6 Kinetic Measurements

Spectral changes resulting from mixing of the Pt(II) complex and nucleophile solutions were recorded over the wavelength range 200 to 650 nm to establish a suitable wavelength for kinetic measurements. The identified wavelengths are summarized in Supporting information, (SI) **Table S1 3.1**. All kinetics reactions were studied as a function of concentration and temperature under *pseudo* first-order conditions. The kinetic data obtained were graphically analysed using the software package, Origin 7.5®.[24] All reported rate constants represent an average value of at least three independent kinetic runs for each experimental measurement. The temperature dependence of the rate constants were studied over a range of 15-35 °C at a 5 °C intervals with the nucleophile concentration being held constant at 30 times the concentration of the metal complex.

### 3.2.7 Computational Modelling

Density functional theoretical (DFT) calculations were performed with the Gaussian 09 program suite[25] using the B3LYP method,[26] a three parameter hybrid functional method, utilizing the LANL2DZ (Los Alamos National Laboratory 2 Double ζ)[27] basis set. The influence of the bulk solvent was evaluated via single-point computations using the CPCM[28] formalism, i.e., B3LYP(CPCM)/LANL2DZp//B3LYP/-LANL2DZp and methanol as solvent. The complexes were each modelled at +1 or 0 with respect to their total charges.

## 3.3 Results

### 3.3.1 Computational Analysis

In an effort to understand the interplay of structural and electronic properties of the Pt(II) complexes, Density Functional Theoretical (DFT) calculations were undertaken. As mentioned earlier computational calculations for all the chloro platinum(II) complexes were modelled as cations except for **Pt4** complex which was gauged as a neutral complex.[16,29] The geometry optimized structures and the mapping of the frontier molecular orbitals of the complexes are shown in **Table 3.1**. The key geometric data from DFT calculations are presented in **Table 3.2**. The HOMO-LUMO gap increases in the order of 2.890 < 3.357 < 3.511 < 3.571 for **Pt4**, **Pt3**, **Pt2** and **Pt1** respectively. One would expect the increase in π-conjugation would result in increase in the electrophilicity at the metal centre through π-backbonding however; for example in **Pt2** complex the direction of the HOMO map is on the $d_z^2$-orbital of the metal centre signalling lack of or minimum chance of π-backbonding between the metal centre and the ligand. The LUMO in all complexes is mostly centred on the aromatic rings of the ligands with only a small contribution from the *d*-orbital on the Pt atom. The electrophilicity index (ω) (**Table 3.2**) as the measure of energy lowering due to maximal electron flow between donor and acceptor for **Pt4** is found to be very small compared to other complexes indicating that it is a poor electrophile and expected to be the least reactive complex in the series. It is evident from the optimized structures that the planarity of the complexes increases with the increase in π-conjugation.

**Table 3.1**: DFT-calculated (B3LYP (CPCM)/LANL2DZp//B3LYP/-LANL2DZp) HOMOs, LUMOs and planarity of the investigated complexes.

| Complex Structure | HOMO | LUMO | Planarity |
|---|---|---|---|
|  **Pt1** |  | 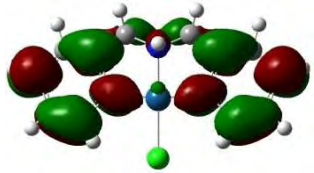 |  |
| 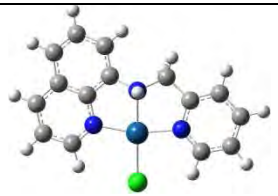 **Pt2** | 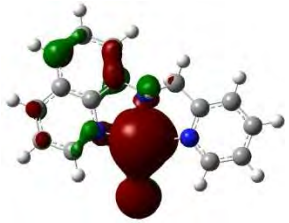 |  |  |
|  **Pt3** |  |  |  |
|  **Pt4** | 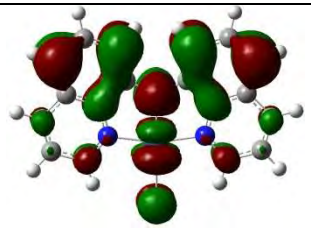 | 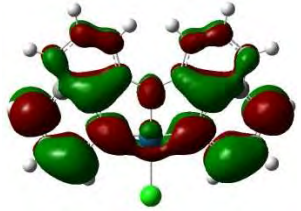 |  |

**Table 3.2:** Summary of DFT calculated parameters for complexes studied

| 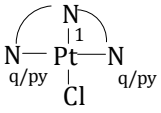 | **Pt1** | **Pt2** | **Pt3** | **Pt4** |
|---|---|---|---|---|
| **HOMO-LUMO energy** | | | | |
| LUMO /eV | -3.396 | -2.860 | -3.595 | -2.284 |
| HOMO/ eV | -6.967 | -6.371 | -6.952 | -5.174 |
| ΔE/eV | 3.571 | 3.511 | 3.357 | 2.890 |
| **NBO Charge** | | | | |
| Pt | 0.540 | 0.550 | 0.598 | 0.508 |
| $N_1$ | -0.637 | -0.651 | -0.445 | -0.580 |
| $N_{q/py}$ | -0.510 | -0.495 | -0.494 | -0.493 |
| $N_{q/py}$ | -0.510 | -0.509 | -0.491 | -0.493 |
| Cl | -0.497 | -0490 | -0.488 | -0.542 |
| **Electrophilicity index** (ω) | 7.518 | 6.067 | 8.284 | 4.811 |
| **Bond Length** (Å) | | | | |
| Pt–$N_1$ | 2.051 | 2.062 | 1.989 | 2.002 |
| Pt–$N_{q/py}$ | 2.040 | 2.037 | 2.037 | 2.029 |
| Pt–$N_{q/py}$ | 2.040 | 2.040 | 2.047 | 2.029 |
| Pt–Cl | 2.440 | 2.437 | 2.434 | 2.475 |
| **Bond Angles** (°) | | | | |
| $N_1$–Pt–Cl | 179.43 | 178.35 | 179.41 | 179.91 |
| **Dipole moment** (Debye) | 14.005 | 12.071 | 13.271 | 7.026 |

Hint: $N_q$ and $N_{py}$ stands for quinoline and pyridine respectively.

### 3.3.2 Kinetic Measurements

Substitution of labile chloride from each of the Pt(II) complexes (**Figure 3.1**) by neutral sulfur containing nucleophiles, *viz.* thiourea (TU), 1-methylthiourea (MTU), 1,3-dimethyl-2-thiourea (DMTU), and 1,1,3,3-tetramethyl-2-thiourea (TMTU) was investigated under *pseudo* first-order conditions and followed on a UV-Visible spectrophotometer. Spectral changes resulting from mixing the complex and nucleophile (TU, MTU, DMTU and TMTU) were recorded over the 200-650 nm wavelength range and typical representative spectra with the corresponding kinetic trace as an inset are shown in **Figure 3.2**. The presence of certain isosbestic points in the spectra (at 405 nm) indicates the conversion of the reactants to the product(s).[30]

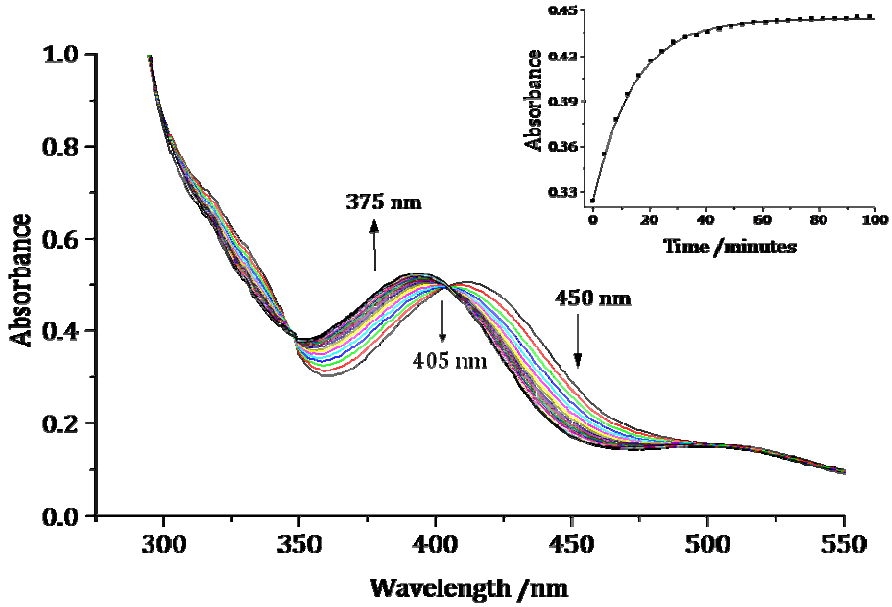


**Figure 3.2:** UV-Visible spectra recorded as a function of time for the reaction between **Pt2** (0.2 mM) and TU (6 mM) at 25°C in MeOH, $I$ = 0.1 M $NaClO_4$/LiCl. *Inset*: Kinetic trace obtained at 375 nm.

All the kinetic traces for the substitution reactions gave an excellent fit to first-order exponential decay to generate observed *pseudo* first-order rate constants, ($k_{obs}$). These $k_{obs}$ were plotted against the concentration of the entering nucleophile to generate the second-order rate constants, $k_2$ from the slopes. The plots gave straight-line fits with zero intercepts as shown in the representative plots in **Figure 3.3** (also **Figures SI 3.16-3.19**) for each of nucleophiles suggesting the absence of solvolytic or parallel reactions.[22] Therefore, the rate law can be described by **Equation 3.1**. The values of the $k_2$ representing the direct attack of the nucleophiles on the Pt(II) metal complexes are summarized in **Table 3.3**.

$$k_{obs} = k_2[\mathrm{Nu}] \qquad (3.1)$$

where Nu= TU, MTU, DMTU and TMTU.

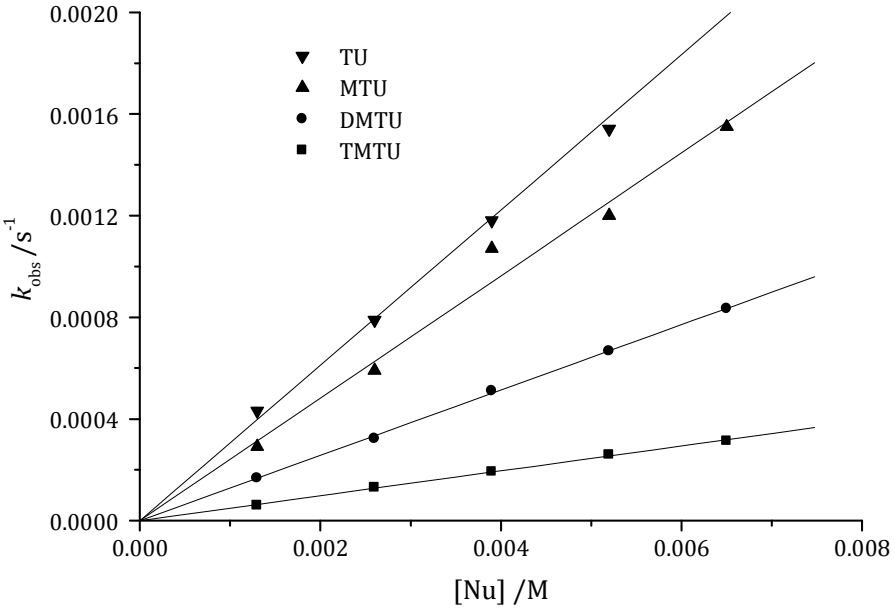


**Figure 3.3:** Dependence of $k_{obs}$ on the concentration of entering nucleophile for chloride substitution on **Pt2** (0.20 mM) in methanol, *I* = 0.1 M (NaClO4/LiCl), T = 25 °C.

Kinetic measurements were also carried out at different temperatures to obtain different $k_2$ values for calculating entropy of activation ($\Delta S^{\neq}$) and enthalpy of activation ($\Delta H^{\neq}$). These were obtained from the Eyring plots (**Figure 3.4** also **Figure SI 3.20-3.23**) by treating the data with **Equation 3.2**[31] where $R$ and T represent the gas constant and temperature respectively.

$$\ln\left(\frac{k_2}{\mathrm{T}}\right) = \frac{-\Delta H^{\#}}{R\mathrm{T}} + \left(23.8 + \frac{\Delta S^{\#}}{R}\right) \qquad (3.2)$$

The activation data from the plots are summarized in **Table 3.3**.

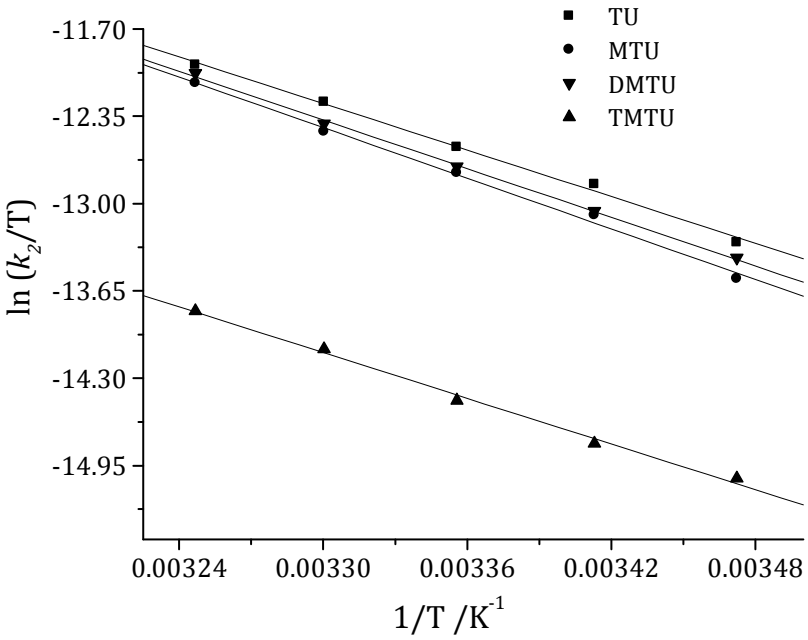


**Figure 3.4:** Eyring plots for the reaction of **Pt3** with a series of neutral nucleophiles at various temperatures in range of 15-35 °C.

**Table 3.3**: Summary of $k_2$ values and activation parameters, $\Delta H^{\neq}$ and $\Delta S^{\neq}$.

| Complex | Nu | $k_2$ ***10$^{-2}$** /M$^{-1}$ s$^{-1}$ | ($\Delta H^{\neq}$) /kJ mol$^{-1}$ | ($\Delta S^{\neq}$) /J K$^{-1}$ mol$^{-1}$ |
|---|---|---|---|---|
| 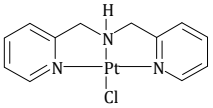 **Pt1** | TU | 50.0 ± 0.7 | 50 ± 2 | -130 ± 6 |
| | MTU | 43.3 ± 0.7 | 62 ± 4 | -91 ± 15 |
| | DMTU | 16.2 ± 0.4 | 75 ± 3 | -58 ± 10 |
| | TMTU | 3.4 ± 0.04 | 77 ± 1 | -109 ± 4 |
| 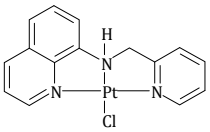 **Pt2** | TU | 28.6 ± 0.3 | 59 ± 3 | -104 ± 10 |
| | MTU | 24.0 ± 1.0 | 50 ± 2 | -135 ± 6 |
| | DMTU | 12.8 ± 0.1 | 51 ± 1 | -138 ± 3 |
| | TMTU | 4.9 ± 0.1 | 50 ± 2 | -150 ± 5 |
| 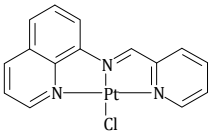 **Pt3** | TU | 30.6 ± 0.8 | 48 ± 2 | -141 ± 6 |
| | MTU | 28.8 ± 0.4 | 50 ± 1 | -136 ± 4 |
| | DMTU | 14.3 ± 0.3 | 52 ± 2 | -129 ± 7 |
| | TMTU | 5.5 ± 0.1 | 47 ± 2 | -143 ± 7 |
| 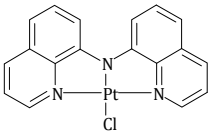 **Pt4** | TU | 8.9 ± 0.2 | 53 ± 1 | -129 ± 2 |
| | MTU | 8.1 ± 0.1 | 49 ± 1 | -144 ± 5 |
| | DMTU | 4.8 ± 0.1 | 51 ± 1 | -143 ± 3 |
| | TMTU | 2.8 ± 0.1 | 40 ± 2 | -181 ± 7 |

## 3.4 Discussion

The current study focuses on understanding the competing effect of increasing π-conjugation through fusing the aromatic rings around the Pt(II) metal centre and the net σ-donor effect of quinoline moiety which has both π-acceptor/donor phenyl as well as electron deficient pyridine ring.[32]

Using the substitution rate constant for coordinated chloro with TU in **Pt1**, as a reference, the reactivity trend follows **Pt1 > Pt2 ≃ Pt3 > Pt4** with **Pt1** reacting five times faster than

**Pt4**. A similar trend in reactivity is observed for the other nucleophiles as indicated in **Table 3.3**. The observed reactivity of the investigated complexes can be accounted for in terms of the electronic effects.

The π-conjugation of the complexes in this study was varied by introducing quinoline ligand and the imine bond. The role of extended π-conjugation on reactivity of Pt(II) complexes has been reported in literature.[1-5,8,11,12] The study showed that the reactivity of the associative substitution reaction on Pt(II) metal complexes could be increased stepwise by increasing the π-conjugation around the metal starting from Pt(dien) to Pt(terpy).[8] Jaganyi *et al* have reported that extending π-conjugation beyond the first pyridine ring surrounding the Pt(II) metal centre results in increased substitution reaction in the case of 2'-pyridyl-1,10-phenanthroline moiety but reduction in case of isoquinoline ligand moiety.[11] The increase in reactivity due to increase in conjugation as reported in literature[1,8,11,12] is contrary to the reactivity of the complexes investigated in this study, where **Pt4** which is highly conjugated is the least reactive complex in the series. This anomaly can be explained by looking at the electronic properties of quinoline ligand which is more basic compared to pyridine as more resonance structures can be drawn to delocalize the positive charge on the conjugate acid.[33] The basicity nature of the quinoline ligands means an increase in σ-inductive effect to the complex which diminishes the π-acceptability of the ligand which is in agreement with the fact that quinoline forms a number of charge transfer complexes by acting as a σ-donor.[34] The net effect of this is destabilization of the 18-electron five coordinate transition state resulting in reduced reactivity.

In addition, according to Betley *et al.*[35] bis(8-quinolinyl)amine (BQA) ligand is a typical monoanionic when coordinated to a metal centre making the resulting complexes appreciably more electron-rich than the Pt(terpy). Therefore, the weak substitution behaviour of **Pt4** is due to the electron rich environment around the metal centre and the poor π-acceptor ability of the quinoline ligand.[34,36] This is supported by the DFT calculation which shows the electrophilicity index of the complexes as a whole decreases from **Pt1** to **Pt4** with exception of **Pt3**. This is because the introduction of the imine bond in **Pt3** changes the nature of the *trans* effect and accounts for its DFT values falling out of the line with that of the other complexes. DFT calculation also show that the Pt–$N_q$ bond length is shorter in **Pt4** compared to the other complexes an indication of stronger σ-interaction between the Pt metal and the *cis* nitrogen atoms. This is supported by NBO charge which shows **Pt4** to be less positive than the rest.

The increase in π-conjugation is reflected in the HOMO-LUMO energy gap which decreases from **Pt1** to **Pt4** indicating that complexes becomes softer and as such should be more reactive.[37] This is counteracted by the electrophilicity and the dipole moment of the complexes which are in agreement with the reactivity trend. It can therefore be concluded that the electron-rich environment around the ligand moiety is responsible for decreasing the electrophilicity of the complexes as observed. This in turn retards the entry of the incoming nucleophiles through repulsion, slowing the rate of substitution of the chloride. It is clear that π-backbonding in these systems is weaker than the dominant σ-donation from the quinoline moiety.

From the DFT calculations, the π*-orbitals of **BQA** ligand are of appropriate symmetry to mix with a filled metal *d*π-orbital, however, the LUMO energies in **Pt4**(2.284 eV) is very high (**Table 3.2**) in relation to **Pt1**(-3.396 eV), **Pt2**(-2.860 eV) and **Pt3**(-3.595 eV). The rise in the LUMO energy describes **Pt4** as a poor electrophile[37a] and is expected to result in dampening the general reactivity. The increase in the LUMO energy levels with expansion of the π-system observed for **Pt4** and **Pt2** is attributed to either increase in total antibonding character or an increased localization of the π*-orbital on the complexes.[38, 39,40]

What is observed is that by introducing an imine bond in **Pt3** results in a slight increase in the reactivity of **Pt3** compared to **Pt2**. This is mostly due to the increase in π-communication which increases the π-backbonding of Pt(II) metal centre and the change in the *trans* effect.[5,41,42] The fact that the reactivity does not almost change moving from **Pt2** to **Pt3** is in support that the net σ-effect around the ligand moiety is stronger and controls the reactivity of these complexes. What is also noted from the DFT calculation is that the introduction of quinoline increases the planarity of the complexes from **Pt1** to **Pt4**. However, even though this has significant effect on the π-backbonding, it had little or no effect in influencing the reactivity trend of the complexes investigated. In all Pt(II) complexes investigated, the trend in dipole moment is in accord to the reactivity of the complexes given that the parameter correlate to the π-withdrawing character of the complex.[43] **Pt1** contain two π-acceptor pyridine rings in *cis* position relative to the leaving ligand. The π-acceptor ligands withdraw electron density from the Pt(II) centre, making it more electrophilic for a nucleophilic attack and stabilization of the electron-rich five-

coordinate transition state. This result in a reduction of the activation barrier and an acceleration of the reaction observed for **Pt1**.

The reactivity of the nucleophiles follows the trend **TU > MTU > DMTU > TMTU** for all complexes and is in agreement with the steric hindrance and their sizes. The large negative values of entropy, $\Delta S^{\neq}$ and positive enthalpy, $\Delta H^{\neq}$ of activation support an associative mechanism that is typical of Pt(II) square planar complexes.[44,45]

## 3.5 Conclusion

This study has shown that tuning electronic communication at platinum(II) metal centre towards ligand substitution reactions using quinoline-based ligand has an opposite effect to that reported for pyridine ligand. It is evident that increasing electronic communication without increasing π-backbonding has little effect in increasing the reactivity of Pt(II) complex. In **Pt4**, the electronic communication based on the number of aromatic rings jointed together is greater than for the Pt-terpy system but the difference in reactivity is $10^5$ slower. This is because of the σ-inductive effect of the quinoline ligands towards the metal centre which weakens the π-backbonding effect of the aromatic system. This effect is very dominant and controls the reactivity of the metal complex which remains associative in nature.

## 3.6 References


1. (a) Jaganyi, D., Reddy, D., Gertenbach, J. A., Hoffman, A. and van Eldik, R., *J. Chem*. *Soc., Dalton Trans.,* **2004**, 299; (b) Ertürk, H., Puchta, R. and van Eldik, R., *Eur. J. Inorg. Chem*., **2009**, 1331.

2. (a) Deubel, V., *J. Am. Chem. Soc*., **2002**, *124*, 5834; (b) Lemma, K., Elm Roth, S. K. C. and Elding, L. I., *J. Chem. Soc., Dalton Trans*., **2002**, 1288; (c) Teuben, J., Rodriguez ,M., Zubiri, I. and Reedijk, J., *J. Chem. Soc., Dalton Trans*., **2000**, 369.

3. (a) Jaganyi D. and Tiba F., *Transition Met. Chem.*, 2003, **28**, 803; (b) Jaganyi, D., Tiba, F., Munro, O. Q., Petrovi´c, B. and Bugarčic´, Z. D., *J. Chem. Soc., Dalton Trans.*, **2006**, 2943; (c) Bugařcíc,, Z. D., Liehr G. and van Eldik, R. *J. Chem. Soc., Dalton Trans.*, **2002**, 951; (d) Pitteri, B., Annibale, G., Marangoni, G., Cattalini, L., Visentin, F., Bertilasi, V. and Gilli, P., *Polyhedron.*, **2001**, *20*, 869; (e) Annibale, G., Brandolisio, M. and Pitteri, B., *Polyhedron.*, **1995**, *14*, 451; (f) Bogojeski, J and Bugařcíc Z. D., *Transition Met Chem*., **2011**, *36*, 73.

4. (a) Annibale, G., Brandolisio, M., Bugařcíc Z. D and Cattalini, L., *Transition Met*. *Chem*., **1998**, *23*, 715; (b) Pitteri, B., Marangoni, G., Cattalini, L., Viseulim F. V. and Bobbo, T., *Polyhedron.*, **1998**, *17*, 475; (c) Petrovi´c, B. V., Djuran M. I. and Bugařcíc, Z. D., *Met.-Based Drugs*, **1999**, *6*, 355; (d) Pitteri, B., Annibale, G., Marangoni, G., Bertilasi V. and Ferretti, V., *Polyhedron.*, **2002**, *21*, 2283; (e) Bugařcíc, Z. D., Heinmann F. W. and van Eldik, R., *J. Chem. Soc., Dalton Trans*., **2004**, 279; (f) Reddy ,D. and Jaganyi, D., *Dalton Trans*., **2008**, 6724; (g) Jaganyi, D., de Boer, K., Gertenbach, J. and Perils, J., *Int. J. Chem. Kinetics.*, **2008**, 809.

5. (a) Petrović, B., Bugarčić, Ž. D., Dees, A., Ivanović-Burmazović, I., Heinemann, F., Puchta, R., Heinemann, F. W., Steinmann, S. N., Corminboeuf, C., van Eldik, R., *Inorg. Chem*., **2012** *51*, 1516; (b) Đurović, M., Bogojeski, J., Petrović, B., Petrović, D., Heinemann, F. W. Bugarčić, Ž. D., Polyhedron., **2012**, *41*, 70; (c)

6. Williams, J. A. G., *Chem. Soc. Rev*., **2009**, *38*, 1783.

7. (a) Burdett, J. K., *Inorg. Chem.* **1975**, *14*, 931; (b) Burdett, J. K., *Inorg. Chem*., **1977**, *16*, 3013.

8. (a) Jaganyi, D., Hofmann, A., and van Eldik R., *Angew. Chem. Int. Ed.,* **2001**, *40*, 1680; (b) Weber, C. F. and van Eldik, R. *Eur. J. Inorg. Chem.,* **2005**, 4755; (

9. Hofmann, A and van Eldik, R., *Dalton Trans.,* **2003**, 2979.

10. Mambanda, A., Jaganyi, D., *Dalton Trans*., **2011**, *40*, 79

11. Ongoma, P and Jaganyi, D., *Dalton Trans.*, **2012**, *41*, 10724.

12. Reddy, D., Akerman, K. J., Akerman, M. P., Jaganyi, D., *Transition Met Chem.*, **2011**, *36*, 593.

13. Rosenberg, B.; Van Champ, L.; Trosko, J. E.; Mansour, V. H. *Nature.*, **1969**, *22*, 385.

14. (a) Florea, A.-M. and Büsselberg, D., *Cancers.,* **2011**, *3*, 1351; (b) Dempke, W., Voigt, W., Grothey, A., Hill, B. T and Schmoll, H. J. *Anti-Cancer Drugs.*, **2000**, *11*, 225; (c) Wang, J., Wang, X., Song, Y., Zhu, C., Wang, J., Wang, K. and Guo, Z., *Chem. Commun.,* **2013**, *49*, 2786; (d) Pabla, N. and Dong, Z., *Oncotarget*., **2012**, *3*(1), 107.

15. Carlsen, L., Egsgaard, H., Anderson, J.R., *Anal Chem.*, **1979**, *51*, 1593.

16. Peters, J. C., Harkins, S. B., Brown, S. D., Day, M. W. *Inorg. Chem.,* **2001**, *40,* 5083.

17. Incarvito, C., Lam, M., Rhatigan, B., Rheingold, A. L., Qin, C.J., Gavrilova, A.L., Bosnich, B., *J. Chem. Soc., Dalton Trans*., **2001**, 3478.

18. Clark, H. C., Manzer, L. E., *J. Organomet. Chem.,* **1973,** *59*, 411.

19. Darensbourg, M.Y., Hill, G. S., Irwin, M. J., Levy, C. J., Rendina, L. M., Puddephatt, R. J., Andersen, R. A., Mclean, L., *Inorganic Syntheses.*, **2007,** *32*, 149.

20. Weber, C.F and van Eldik, R., *Eur*. *J*. *Inorg*. *Chem.*, **2005**, 4755.

21. Bortoluzzi, M., Paolucci, G., Pitteri, B., Zennaro, P., Bertolasi, V., *J. Organomet. Chem.*, **2011**, *696*, 2565.

22. Hofmann, A., Dahlenburg, L., and van Eldik, R., *Inorg. Chem*., **2003**, *42*, 6528.

23. Appleton, T. G., Hall, J. R., Ralph, S. F. and Thompson, C. S M., *Inorg. Chem*., **1984**, *41*, 3521.

24. Origin7.5TM SRO, v7.5714 (B5714),Origin Lab Corporation, Northampton, One, Northampton, MA, 01060, USA, **2003**.

25. Frisch, M. J., Trucks, G. W., Schlegel, H. B., Scuseria, G. E., Robb, M. A., Cheeseman, J. R., Scalmani, G., Barone, V., Mennucci, B., Petersson, G. A., Nakatsuji, H., Caricato, M., Li, X., Hratchian, H. P., Izmaylov, A. F., Bloino, J., Zheng, G., Sonnenberg, J. L., Hada, M., Ehara, M., Toyota, K., Fukuda, R., Hasegawa, J., Ishida, M., Nakajima, T., Honda, Y., Kitao, O., Nakai, H., Vreven, T., Montgomery, J. A., Peralta, J. E., Ogliaro, F., Bearpark, M., Heyd, J. J., Brothers, E., Kudin, K. N., Staroverov, V. N., Kobayashi, R., Normand, J., Raghavachari, K., Rendell, A., Burant, J. C., Iyengar, S. S., Tomasi, J., Cossi, M., Rega, N., Millam, J. M., Klene, M., Knox, J. E., Cross, J. B., Bakken, V., Adamo, C., Jaramillo, J., Gomperts, R., Stratmann, R. E., Yazyev, O., Austin, A. J., Cammi, R., Pomelli, C.,

Ochterski, J. W., Martin, R. L., Morokuma, K., Zakrzewski, V. G., Voth, G. A., Salvador, P., Dannenberg, J. J., Dapprich, S., Daniels, A. D., Farkas, O., Foresman, J. B., Ortiz, J. V., Cioslowski, J., and Fox, D. J., *Gaussian 09, Revision A.1*, Gaussian, Inc., Wallingford CT, **2009**.

26. (a) Becke, A.D., *J. Chem .Phys.*, **1993**,*98*, 5648; (b) Lee, C. T.,Parr, R. G., *Phys. Rev. B.* **1988**, *37*, 785.

27. Hay, P, J, Wadt, W.R., *J. Chem .Phys.,* **1985**, *82*, 299.

28. (a) Barone, V.; Cossi, M. *J. Phys. Chem., A.,* **1998**, *102*, 1995; (b) Cossi, M.; Scalmani, G.; Rega, N.; Barone, V. J. *Comput. Chem*., **2003**, *24*, 669.

29. Harkins, S. B. and Peters, J. C., *Organometallics.*, **2002,** *21,* 1753.

30. Ray, M., Bhattacharya S. and Banerjee, P., *Polyhedron.,* **1999**, *18*, 1569.

31. Eyring, H., *J. Chem. Phys*., **1935**, *3*, 107.

32. (a)http://myweb.unomaha.edu/~dstack/2250/Overheads/EWG_EDG.PDF, accessed on 15th March **2013**; (b) Bruice, P. Y., *Organic Chemistry*, Prentice-Hall, Inc., New Jersey, 2nd edn, **1998**.

33. Hosmane, R. S. Liebman, J.F., *Struct. Chem*., **2009**, *20*, 693.

34. Gurnos, J. *The Chemistry of heterocyclic compounds*; I*n Quinolines*, John Wiley and Sons, London. New York. Sydney. Toronto, **2009**, vol 32, pg 9.

35. Betley, T. A., Qian, B. A., and Peters, J. C., *Inorg. Chem.,* **2008**, *47*, 11570.

36. Suzuki, T., Kuchiyama, T., Kishi, S., Kaizaki, S., Takagi, H. D and Kato, M., *Inorg*. *Chem*., **2003**, *42*(3), 785.

37. (a) Singh, R. K., Verma, S. K. and Sharma, P. D., *Int. J. Chem.Tech Res.*, **2011**, *3*(3), 1571; (b) Chattaraj, P. K., and Maiti, B., *J. Am. Chem. Soc*., **2003**, *125*, 2705;

38. Adachi, M. and Nagao, Y., *Chem. Mater.,* **2001**, *13*, 662.

39. Adachi, M. and Murata, Y., *J. Phys. Chem. A.,* **1998**, *102*, 841.

40. Juris, A., Barigelletti, F., Balzani, V., Belser, P., von Zelewsky, A., *Inorg. Chem.,* **1985**, *24*, 202.

41. Đurovic´, M., Bogojeski, J., Petrovic´, B., Petrovic´, D., Heinemann, F. W., Bugarčić, Ž. D., *Polyhedron.*, **2012**, *41*, 70.

42. Romeo,R., Plutino, M. R., Scolaro, L. M., Stoccoro, S., and Minghetti, G., *Inorg Chem*., **2000**, *39*, 4749.

43. Rillema, D. P., Cruz, A. J., Moore, C., Siam, K., Jehan, A., Base, D., Nguyen, T., and Huang, W., *Inorg. Chem*., **2013**, *52*, 596.

44. (a) Basolo, F. and Pearson, R.G., *Mechanisms of Inorganic Reactions*, 2nd *Ed.*, Wiley, New York **1967**, pg. 80-115; (b) Purcell, K. F., Kotz, I., *Inorganic Chemistry*, Holt-Saunders, **1977**, pg. 694-755; (c) Tobe, M. L. and Burgess, J., *Inorganic Reaction Mechanisms*, Addison Wisey, Longman, Ltd., Essex, **1999**, pg. 30-33; 70-112.

45. Atwood, J.D., *Inorganic and organometallic reaction mechanisms*, 2nd Edition. Wiley-VCH Inc, New York, **1997**, pg 43–61.

## 3.7 Supporting Information (SI)

The available SI at the end of this chapter includes a number of NMR and mass spectra, wavelengths for kinetic measurements, concentration dependence and Eyring plots for determination of second order rate constant and activation parameters, planarity and electrostatic potential map of the investigated complexes

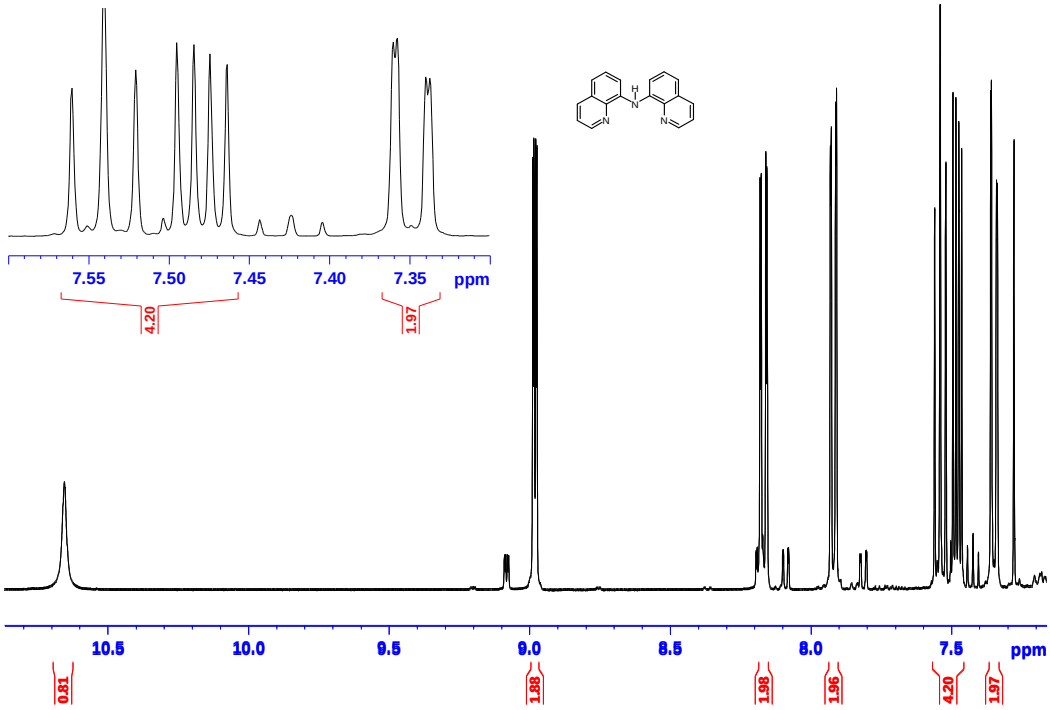


**Figure SI 3.1**: $^{1}$H NMR spectrum of BQAH

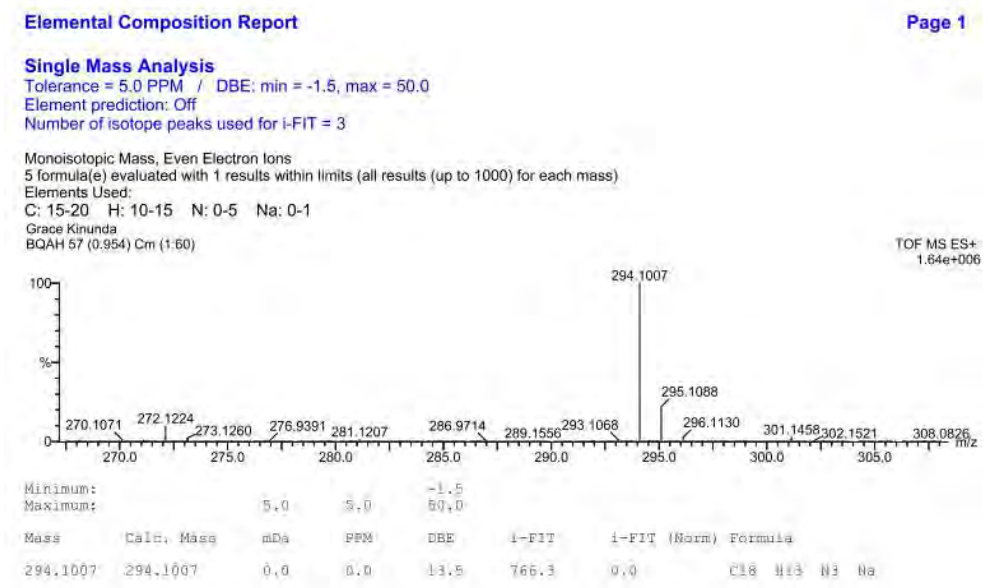


**Figure SI 3.2**: Mass spectrum of **BQAH**

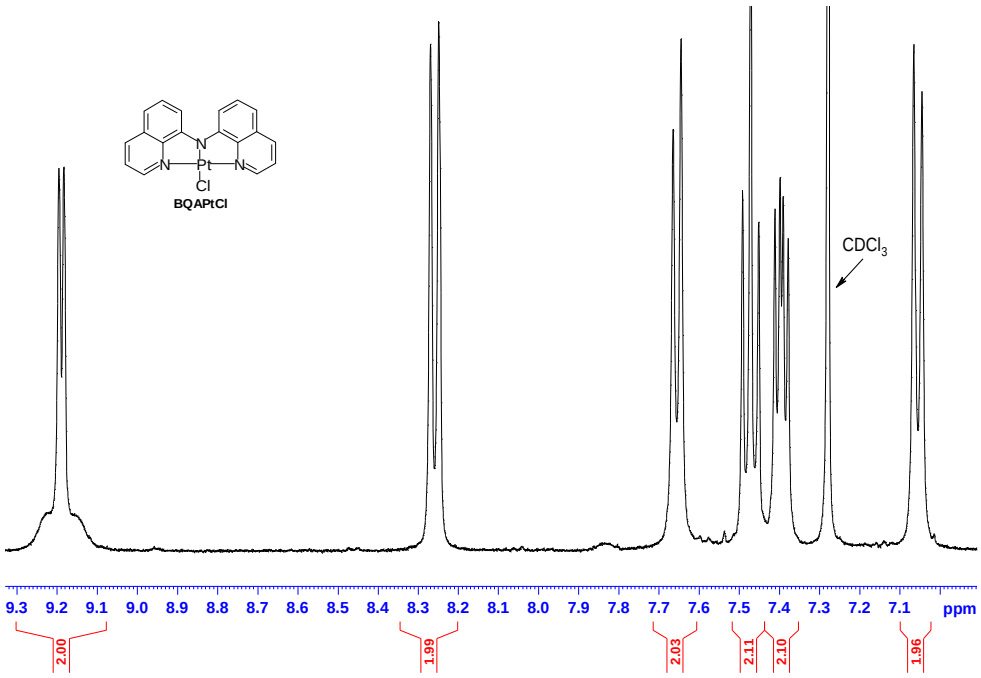


**Figure SI 3.3**: $^{1}$H NMR spectrum of **Pt4**

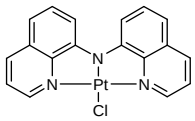


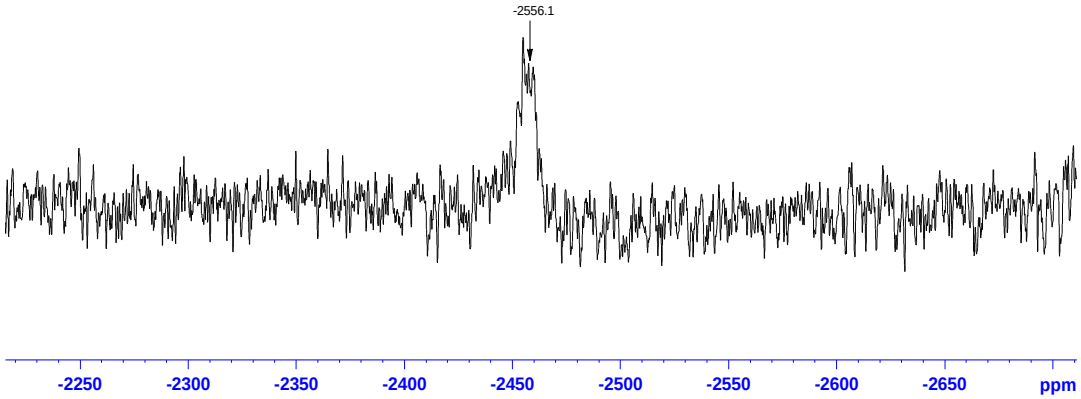


**Figure SI 3.4**: $^{195}$Pt NMR spectrum of **Pt4**

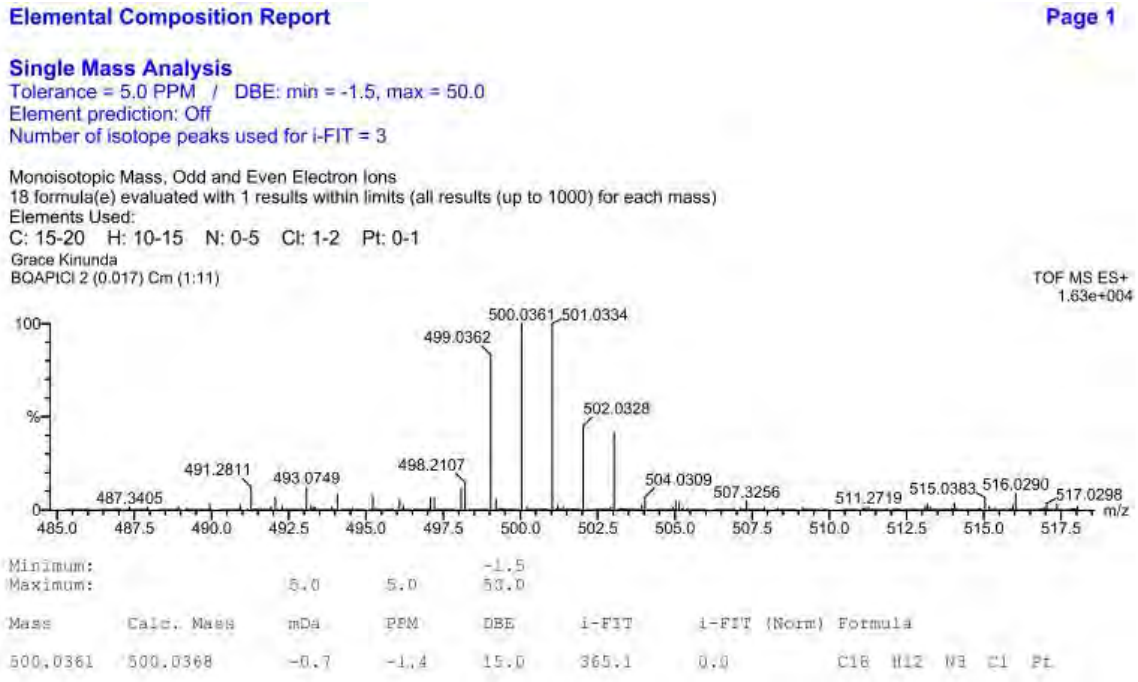


**Figure SI 3.5**: Mass spectrum of **Pt4**

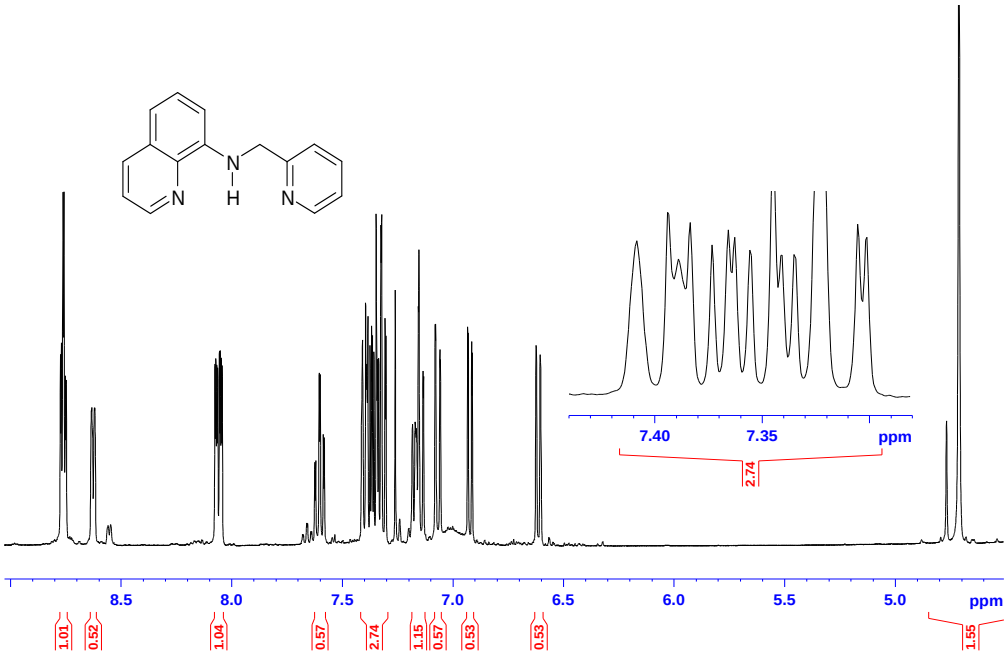


**Figure SI 3.6**: $^{1}$H NMR spectrum of **Qui-py**

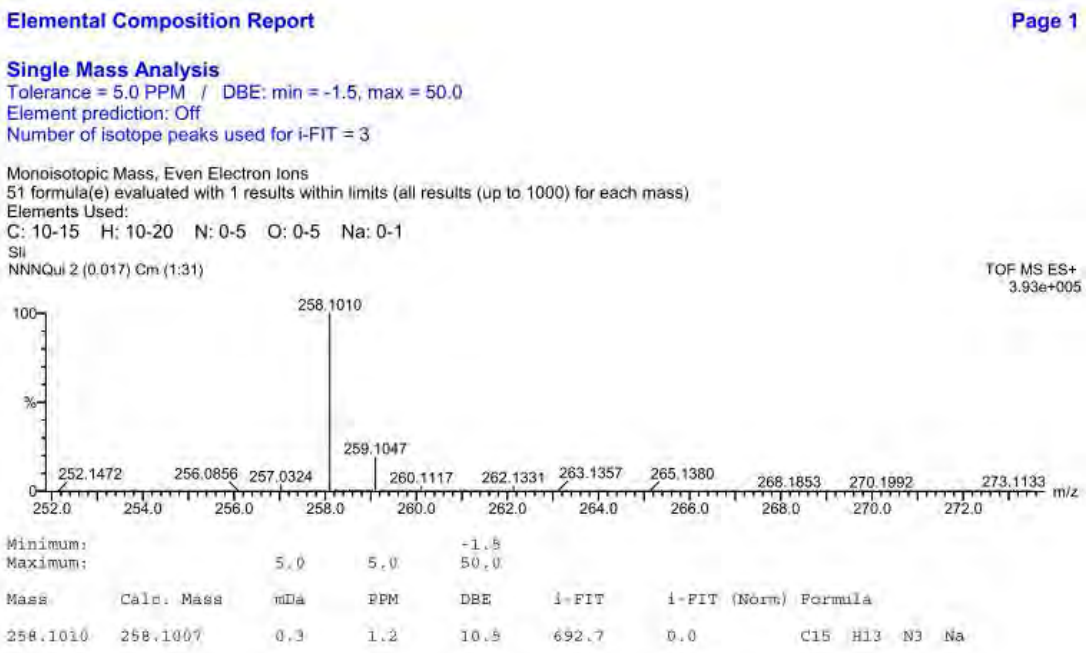


**Figure SI 3.7**: Mass spectrum of **Qui-py**

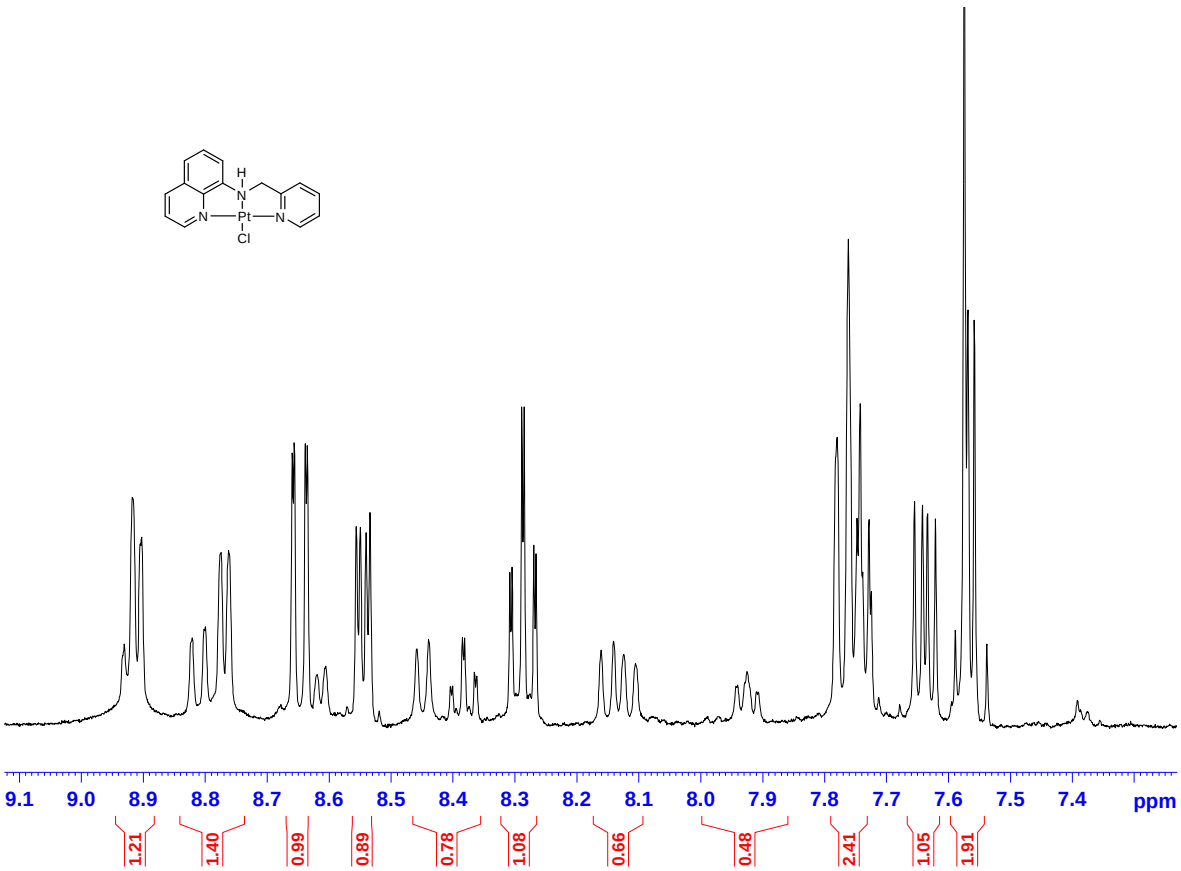


**Figure SI 3.8**: $^{1}$H NMR spectrum of **Pt2**

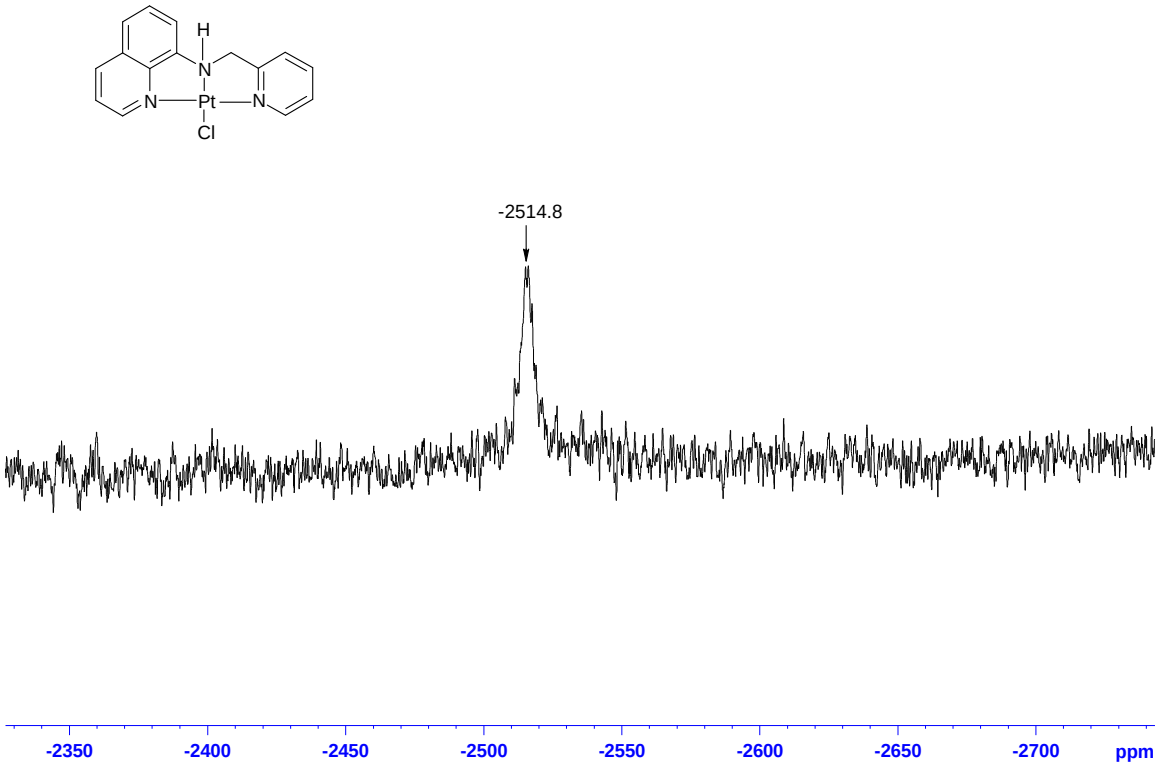


**Figure SI 3.9**: $^{195}$Pt NMR spectrum of **Pt2**

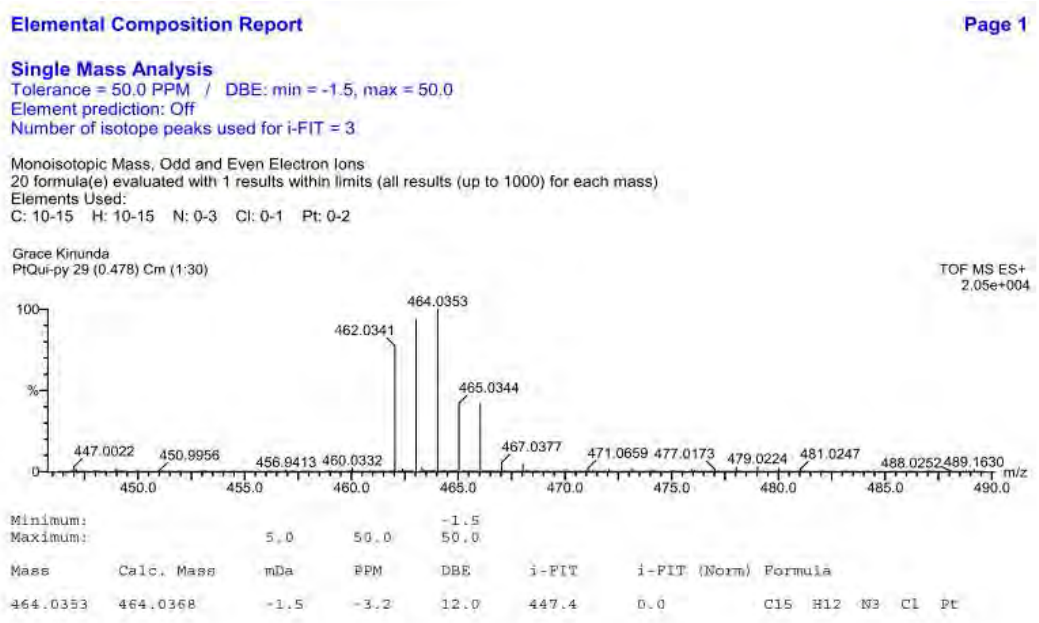


**Figure SI 3.10**: Mass spectrum of **Pt2**

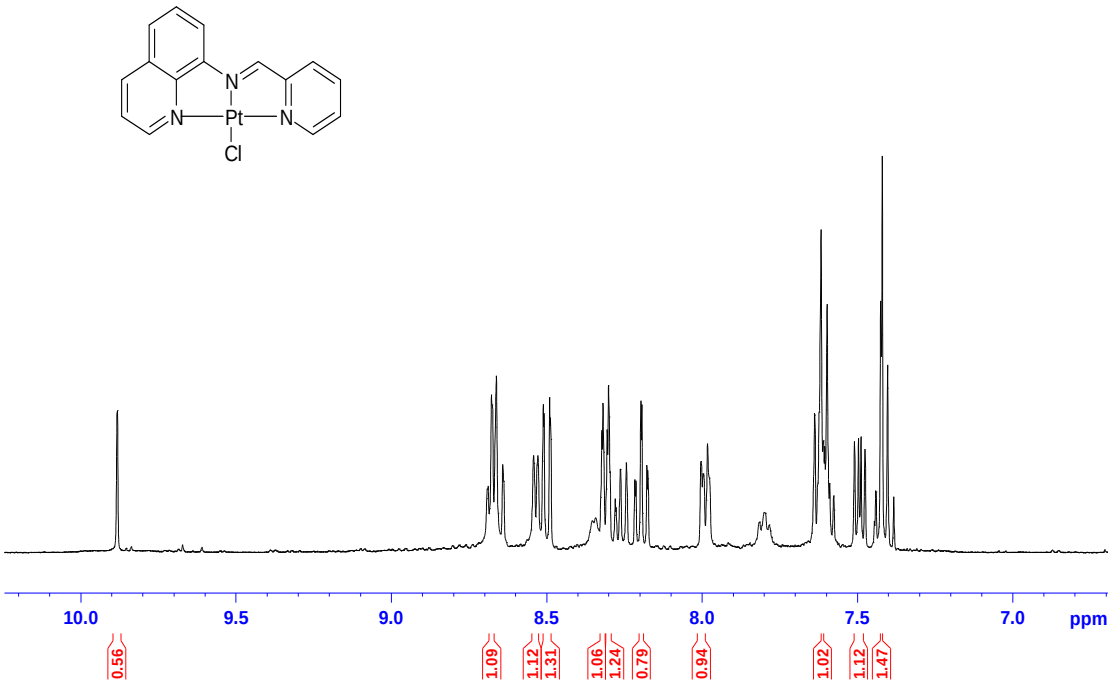


**Figure SI 3.11**: $^{1}$H NMR spectrum of **Pt3**

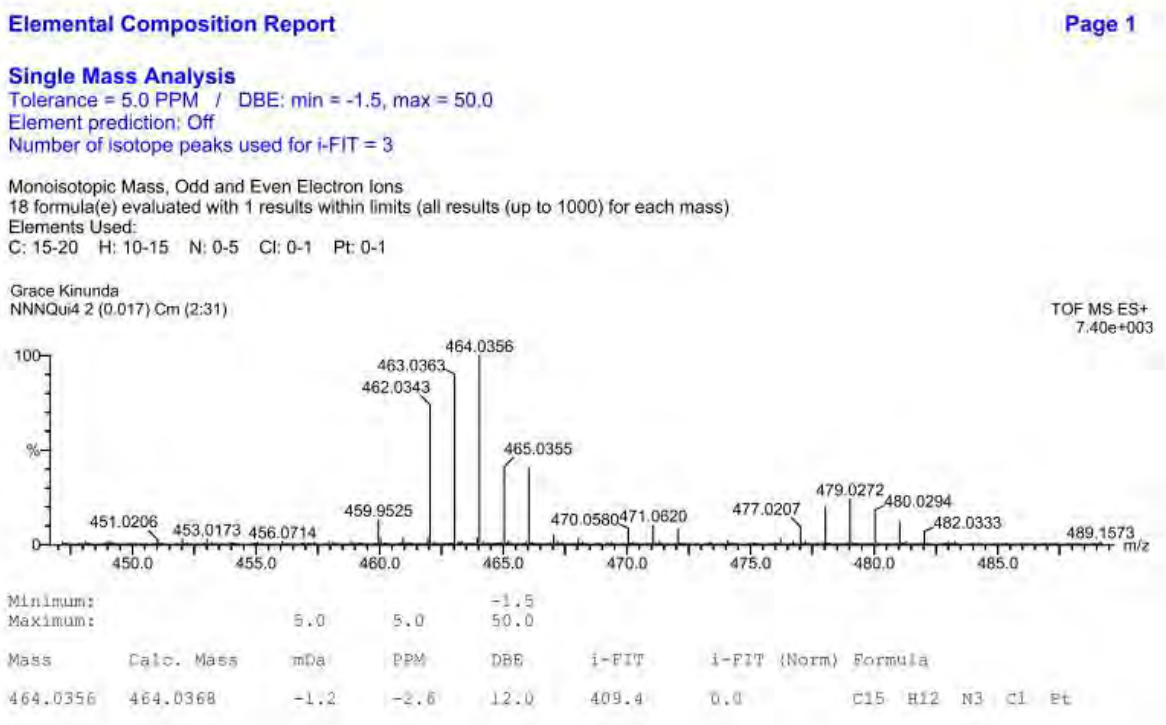


**Figure SI 3.12**: Mass spectrum of **Pt3**

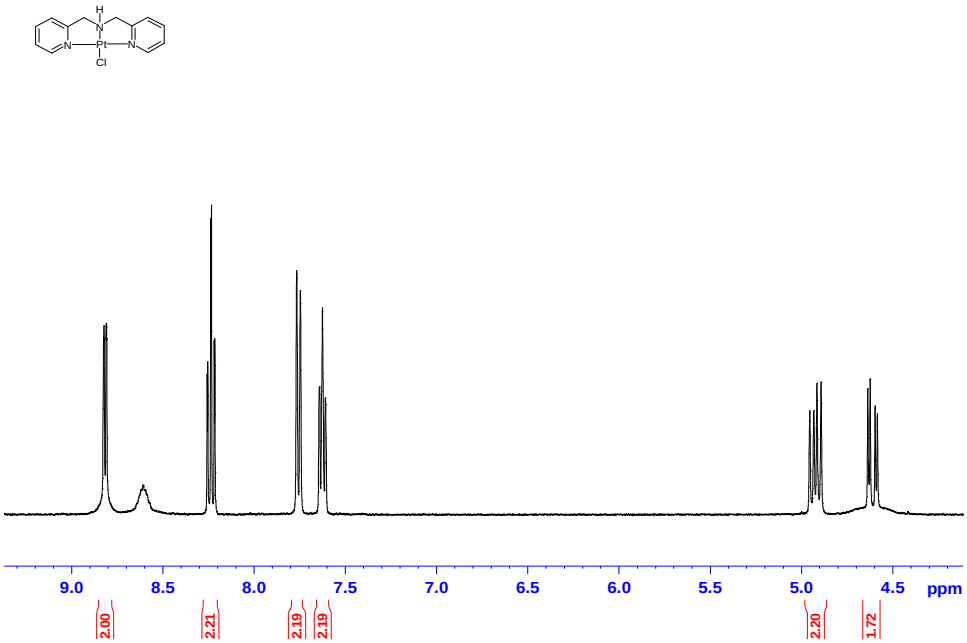


**Figure SI 3.13**: $^{1}$H NMR spectrum of **Pt1**

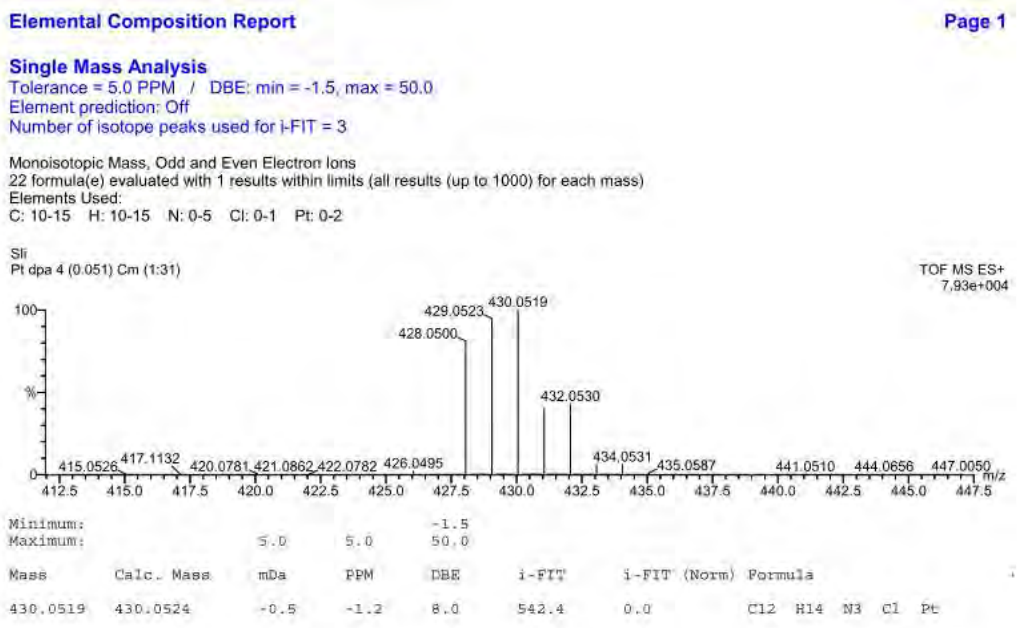


**Figure SI 3.14**: Mass spectrum of **Pt1**

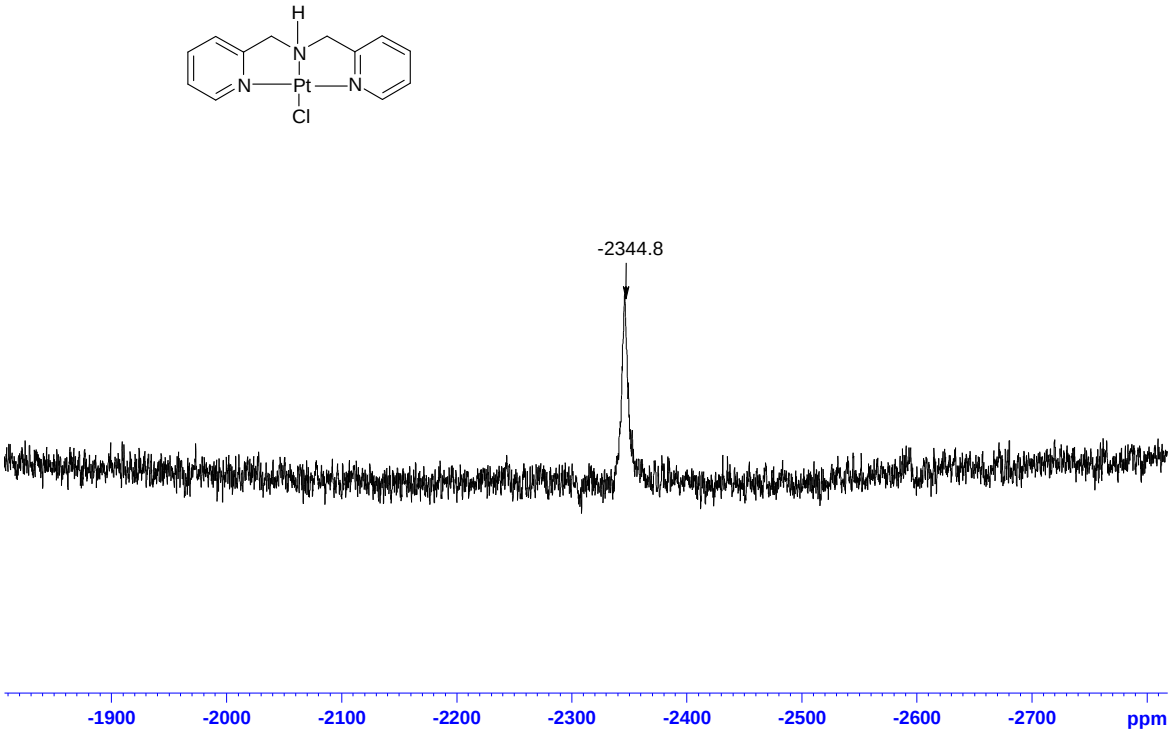


**Figure SI 3.15**: $^{195}$Pt NMR spectrum of **Pt1**

**Table S1 3.1:** Summary of the wavelengths (nm) used for monitoring the kinetic reactions between a series of Pt(II) complexes with tridentate ligands and thiourea nucleophiles.

| Complex | Nucleophiles | Wavelength, λ (nm) |
|---|---|---|
| **Pt1** | TU | 302 |
| | MTU | 300 |
| | DMTU | 300 |
| | TMTU | 363 |
| **Pt2** | TU | 375 |
| | MTU | 368 |
| | DMTU | 368 |
| | TMTU | 363 |
| **Pt3** | TU | 375 |
| | MTU | 450 |
| | DMTU | 445 |
| | TMTU | 443 |
| **Pt4** | TU | 305 |
| | MTU | 288 |
| | DMTU | 300 |
| | TMTU | 317 |

**Table SI 3.2:** Average observed rate constants, $k_{obs}$, $s^{-1}$**,** for the displacement of the chloro ligand in **Pt4**, **Pt2, Pt3** and **Pt1** by thiourea, (TU) nucleophile, T = 298 K, $I$ = 0.1 M $NaClO_4$/LiCl (0.09 M $NaClO_4$ + 0.01 LiCl).

| **Pt4** | | **Pt2** | | **Pt3** | | **Pt1** | |
|---|---|---|---|---|---|---|---|
| [TU] /M | $k_{obs}$ /$s^{-1}$ | [TU] /M | $k_{obs}$ /$s^{-1}$ | [TU] /M | $k_{obs}$ /$s^{-1}$ | [TU] /M | $k_{obs}$ /$s^{-1}$ |
| 0.002 | 1.93E-4 | 0.0013 | 4.31E-4 | 0.001 | 2.89E-4 | 0.001 | 5.80E-4 |
| 0.004 | 4.08E-4 | 0.0026 | 7.88E-4 | 0.002 | 6.31E-4 | 0.002 | 0.0010 |
| 0.006 | 5.44E-4 | 0.0039 | 0.0012 | 0.003 | 0.0010 | 0.003 | 0.0015 |
| 0.008 | 7.38E-4 | 0.0052 | 0.0015 | 0.004 | 0.0012 | 0.004 | 0.0020 |
| 0.01 | 8.44E-4 | 0.0065 | 0.0020 | 0.005 | 0.0015 | 0.005 | 0.0025 |

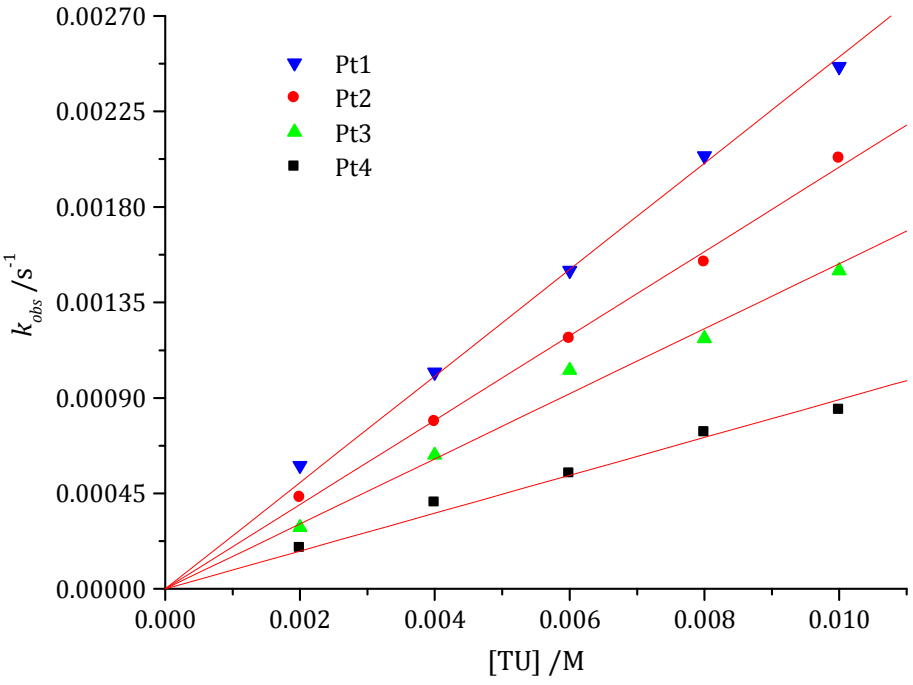


**Figure SI 3.16**: Dependence of the *pseudo* first-order rate constants ($k_{obs}$) on the entering TU nucleophile concentration for chloride substitution on **Pt4**, **Pt2**, **Pt3** and **Pt1** in methanol, $I$ = 0.1 M (NaClO4/LiCl), T = 25 °C.

**Table SI 3.3**: Average observed rate constants, $k_{obs}$ , $s^{-1}$, for the displacement of the chloro ligand in **Pt4**, **Pt2**, **Pt3**and **Pt1** by 1-methyl thiourea (MTU) nucleophiles, T = 298 K, $I$ = 0.1 M $NaClO_4$/LiCl (0.09 M $NaClO_4$ + 0.01 LiCl).

| **Pt4** | | **Pt2** | | **Pt3** | | **Pt1** | |
|---|---|---|---|---|---|---|---|
| [MTU]/M | $k_{obs}$ /$s^{-1}$ | [MTU]/M | $k_{obs}$ /$s^{-1}$ | [MTU]/M | $k_{obs}$ /$s^{-1}$ | [MTU]/M | $k_{obs}$ /$s^{-1}$ |
| 0.002 | 1.63E-4 | 0.0013 | 2.910E-4 | 0.001 | 2.920E-4 | 0.001 | 4.028E-4 |
| 0.004 | 3.12E-4 | 0.0026 | 5.907E-4 | 0.002 | 5.486E-4 | 0.002 | 8.125E-4 |
| 0.006 | 4.82E-4 | 0.0039 | 0.0011 | 0.003 | 8.468E-4 | 0.003 | 0.00124 |
| 0.008 | 6.50E-4 | 0.0052 | 0.0012 | 0.004 | 0.00113 | 0.004 | 0.0018 |
| 0.01 | 8.079E-4 | 0.0065 | 0.00155 | 0.005 | 0.00148 | 0.005 | 0.00218 |

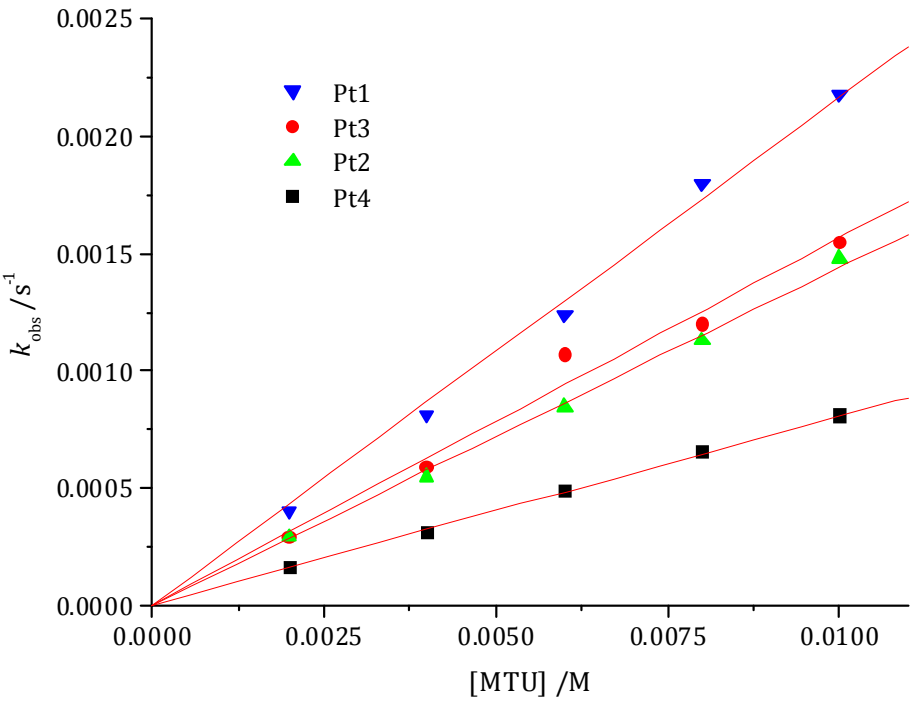


**Figure SI 3.17**: Dependence of the *pseudo* first-order rate constants ($k_{obs}$) on the entering MTU nucleophile concentration for chloride substitution on **Pt4**, **Pt2**, **Pt3** and **Pt1** in methanol, $I$ = 0.1 M (NaClO4/LiCl), T = 25 ℃.

**Table SI 3.4:** Average observed rate constants, $k_{obs}$, $s^{-1}$, for the displacement of the chloro ligand in **Pt4, Pt2, Pt3** and **Pt1** by 1,3-dimethyl-2-thiourea (DMTU) nucleophile, T = 298 K, $I$ = 0.1 M $NaClO_4$/LiCl (0.09 M $NaClO_4$ + 0.01 LiCl).

| **Pt4** | | **Pt2** | | **Pt3** | | **Pt1** | |
|---|---|---|---|---|---|---|---|
| [DMTU]/M | $k_{obs}$ /$s^{-1}$ | [DMTU]/M | $k_{obs}$ /$s^{-1}$ | [DMTU]/M | $k_{obs}$ /$s^{-1}$ | [DMTU]/M | $k_{obs}$ /$s^{-1}$ |
| 0.002 | 1.075E-4 | 0.0013 | 1.668E-4 | 0.001 | 1.916E-4 | 0.001 | 3.083E-4 |
| 0.004 | 2.170E-4 | 0.0026 | 3.227E-4 | 0.002 | 3.558E-4 | 0.002 | 6.171E-4 |
| 0.006 | 2.939E-4 | 0.0039 | 5.107E-4 | 0.003 | 5.020E-4 | 0.003 | 8.852E-4 |
| 0.008 | 3.900E-4 | 0.0052 | 6.672E-4 | 0.004 | 6.223E-4 | 0.004 | 0.00118 |
| 0.01 | 4.625E-4 | 0.0065 | 8.343E-4 | 0.005 | 7.984E-4 | 0.005 | 0.00137 |

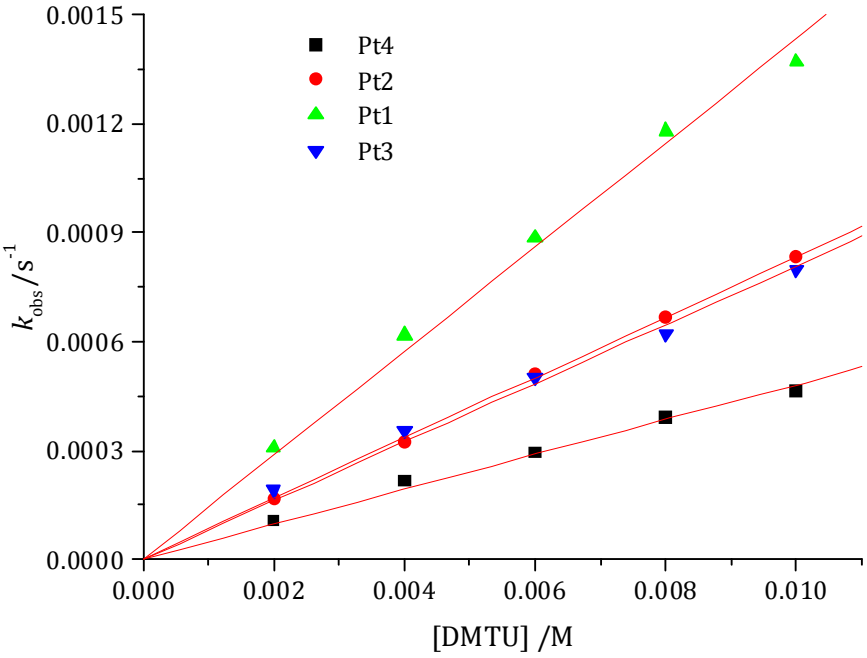


**Figure SI 3.18**: Dependence of the *pseudo* first-order rate constants, $k_{obs}$ on the entering DMTU nucleophile concentration for chloride substitution on **Pt4**, **Pt2**, **Pt3** and **Pt1** in methanol, $I$ = 0.1 M (NaClO4/LiCl), T = 25 °C.

**Table SI 3.5:** Average observed rate constants, $k_{obs}$, $s^{-1}$, for the displacement of the chloro ligand in **Pt4**, **Pt2**, **Pt3** and **Pt1** by 1,1,3,3-tetramethyl-2-thiourea (TMTU) nucleophile, T = 298 K, $I$ = 0.1 M $NaClO_4$/LiCl (0.09 M $NaClO_4$ + 0.01 LiCl).

| **Pt4** | | **Pt2** | | **Pt3** | | **Pt1** | |
|---|---|---|---|---|---|---|---|
| [TMTU]/M | $k_{obs}$ /$s^{-1}$ | [TMTU]/M | $k_{obs}$ /$s^{-1}$ | [TMTU] /M | $k_{obs}$ /$s^{-1}$ | [TMTU] /M | $k_{obs}$ /$s^{-1}$ |
| 0.002 | 3.790E-5 | 0.0013 | 5.853E-5 | 0.001 | 6.319E-5 | 0.001 | 6.038E-5 |
| 0.004 | 7.238E-5 | 0.0026 | 1.131E-4 | 0.002 | 1.356E-4 | 0.002 | 1.306E-4 |
| 0.006 | 1.038E-4 | 0.0039 | 1.557E-4 | 0.003 | 1.761E-4 | 0.003 | 1.924E-4 |
| 0.008 | 1.355E-4 | 0.0052 | 2.126E-4 | 0.004 | 2.166E-4 | 0.004 | 2.589E-4 |
| 0.01 | 1.719E-4 | 0.0065 | 2.807E-4 | 0.005 | 2.728E-4 | 0.005 | 3.135E-4 |

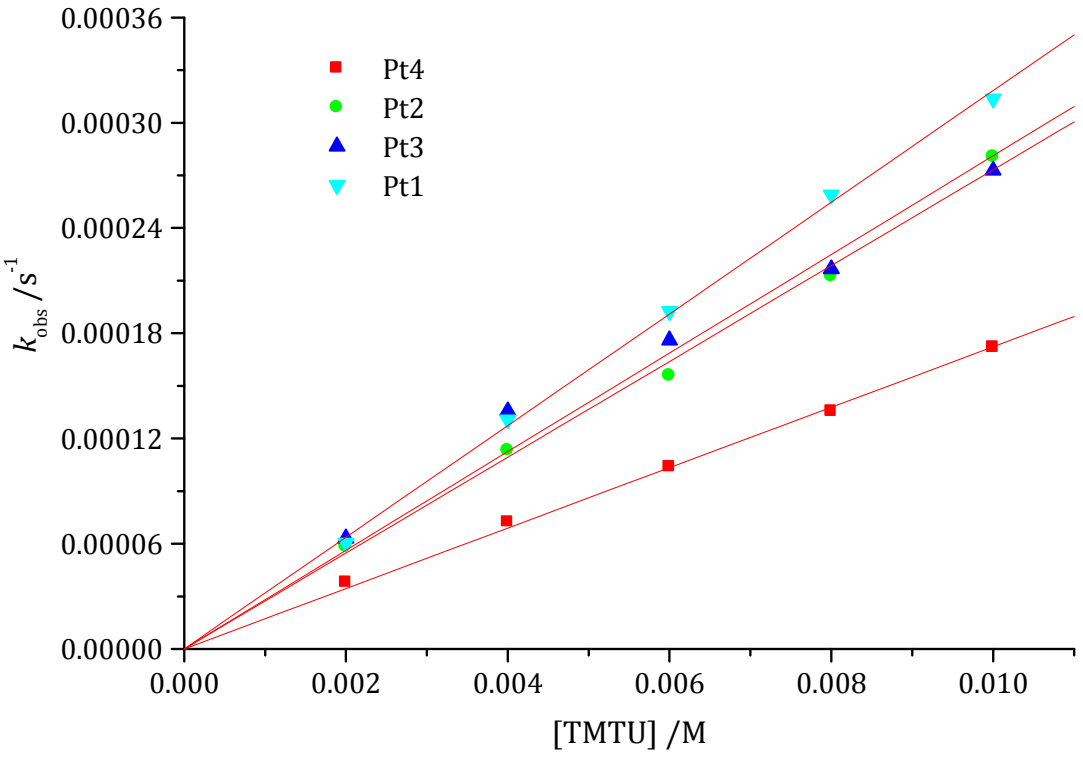


**Figure SI 3.19**: Dependence of the *pseudo* first-order rate constants, $k_{obs}$ on the entering TMTU nucleophile concentration for chloride substitution on **Pt4**, **Pt2**, **Pt3** and **Pt1** in methanol, $I$ = 0.1 M ($NaClO_4$/LiCl), T = 25 °C.

**Table SI 3.6:** Temperature dependence of $k_2$ / $M^{-1}$ $s^{-1}$ for the displacement of chloro ligands in **Pt4**, **Pt2**, **Pt3** and **Pt1** by thiourea (TU) nucleophile at 30-fold excess over [Pt], $I$ = 0.1 M $NaClO_4$/LiCl (0.09 M $NaClO_4$ + 0.01 LiCl).

| **Pt4** | | **Pt2** | | **Pt3** | | **Pt1** | |
|---|---|---|---|---|---|---|---|
| $1/T$ /$K^{-1}$ | $\ln(k_2/T)$ | $1/T$ /$K^{-1}$ | $\ln(k_2/T)$ | $1/T$ /$K^{-1}$ | $\ln(k_2/T)$ | $1/T$ /$K^{-1}$ | $\ln(k_2/T)$ |
| 0.00347 | -13.9430 | 0.00347 | -13.3801 | 0.00347 | -13.2893 | 0.00347 | -12.836 |
| 0.00341 | -13.5717 | 0.00341 | -12.9495 | 0.00341 | -12.85559 | 0.00341 | -12.5203 |
| 0.00336 | -13.2137 | 0.00336 | -12.4375 | 0.00336 | -12.57993 | 0.00336 | -12.2018 |
| 0.0033 | -12.8647 | 0.0033 | -12.1018 | 0.0033 | -12.2425 | 0.0033 | -11.7880 |
| 0.00325 | -12.4904 | 0.00325 | -11.8035 | 0.00325 | -11.96922 | 0.00325 | -11.4989 |

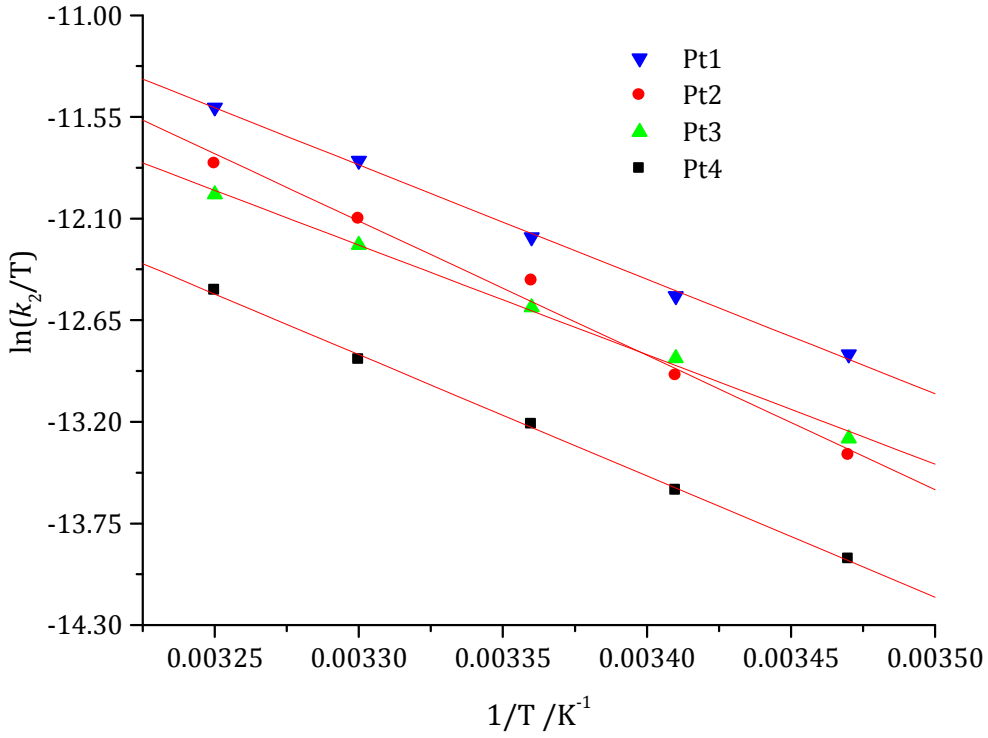


**Figure SI 3.20**: Eyring plots for the reaction of **Pt4**, **Pt2**, **Pt3** and **Pt1** with TU nucleophile at various temperatures in the range of 15-35 °C.

**Table SI 3.7:** Temperature dependence of $k_2$ / $M^{-1}$ $s^{-1}$ for the displacement of chloro ligands in **Pt4**, **Pt2**, **Pt3** and **Pt1** by 1-methylthiourea (MTU) nucleophile at 30-fold excess over [Pt], $I$ = 0.1 M $NaClO_4$/LiCl.

| **Pt4** | | **Pt2** | | **Pt3** | | **Pt1** | |
|---|---|---|---|---|---|---|---|
| $1/T$ /$K^{-1}$ | $\ln(k_2/T)$ | $1/T$ /$K^{-1}$ | $\ln(k_2/T)$ | $1/T$ /$K^{-1}$ | $\ln(k_2/T)$ | $1/T$ /$K^{-1}$ | $\ln(k_2/T)$ |
| 0.00347 | -14.0057 | 0.00347 | -13.3892 | 0.00347 | -13.5594 | 0.00347 | -13.1930 |
| 0.00341 | -13.6849 | 0.00341 | -12.9740 | 0.00341 | -13.0862 | 0.00341 | -12.8487 |
| 0.00336 | -13.3337 | 0.00336 | -12.6178 | 0.00336 | -12.7712 | 0.00336 | -12.3895 |
| 0.0033 | -12.9568 | 0.0033 | -12.3641 | 0.0033 | -12.4632 | 0.0033 | -12.0729 |
| 0.00325 | -12.7086 | 0.00325 | -11.9928 | 0.00325 | -12.1030 | 0.00325 | -11.4582 |

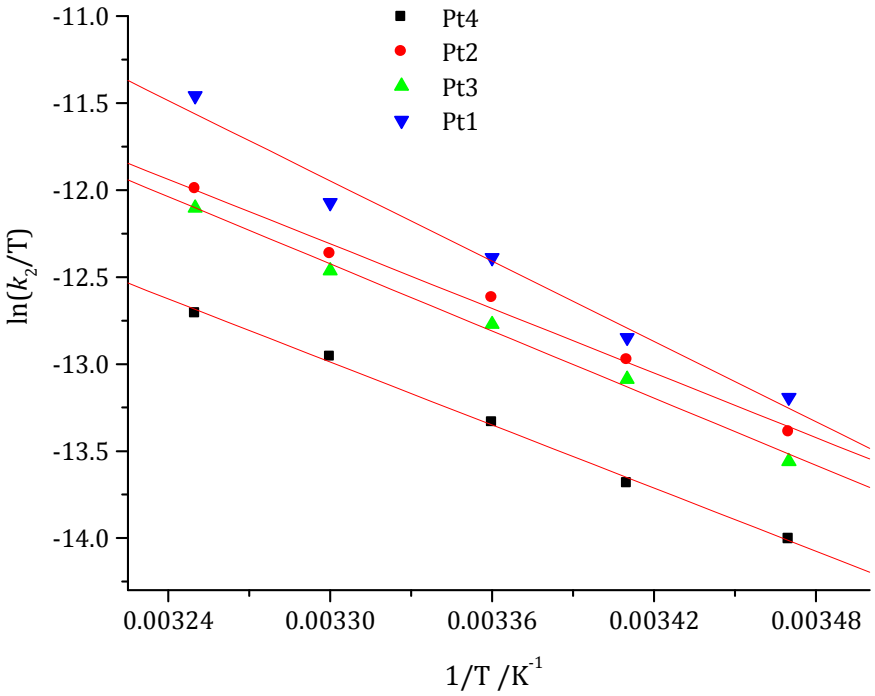


**Figure SI 3.21**: Plots of $\ln \frac{1}{T}$ *versus* $\frac{1}{T}$ for the reaction of **Pt4**, **Pt2**, **Pt3** and **Pt1**with MTU nucleophile at various temperatures in the range of 15-35 ℃.

**Table SI 3.8:** Temperature dependence of $k_2$ / $M^{-1}$ $s^{-1}$ for the displacement of chloro ligands in **Pt4**, **Pt2**, **Pt3** and **Pt1** by 1,3-dimethyl-2-thiourea (DMTU) nucleophile at 30-fold excess over [Pt], $I$ = 0.1 M $NaClO_4$/LiCl

| **Pt4** | | **Pt2** | | **Pt3** | | **Pt1** | |
|---|---|---|---|---|---|---|---|
| $1/T$ /$K^{-1}$ | $\ln(k_2/T)$ | $1/T$ /$K^{-1}$ | $\ln(k_2/T)$ | $1/T$ /$K^{-1}$ | $\ln(k_2/T)$ | $1/T$ /$K^{-1}$ | $\ln(k_2/T)$ |
| 0.00347 | -14.5714 | 0.00347 | -14.0292 | 0.00347 | -13.4055 | 0.00347 | -14.4637 |
| 0.00341 | -14.1699 | 0.00341 | -13.6484 | 0.00341 | -13.0581 | 0.00341 | -13.8058 |
| 0.00336 | -13.8292 | 0.00336 | -13.2767 | 0.00336 | -12.72683 | 0.00336 | -13.2939 |
| 0.0033 | -13.5078 | 0.0033 | -12.9819 | 0.0033 | -12.4068 | 0.0033 | -12.8767 |
| 0.00325 | -13.1861 | 0.00325 | -12.6458 | 0.00325 | -12.0293 | 0.00325 | -12.4028 |

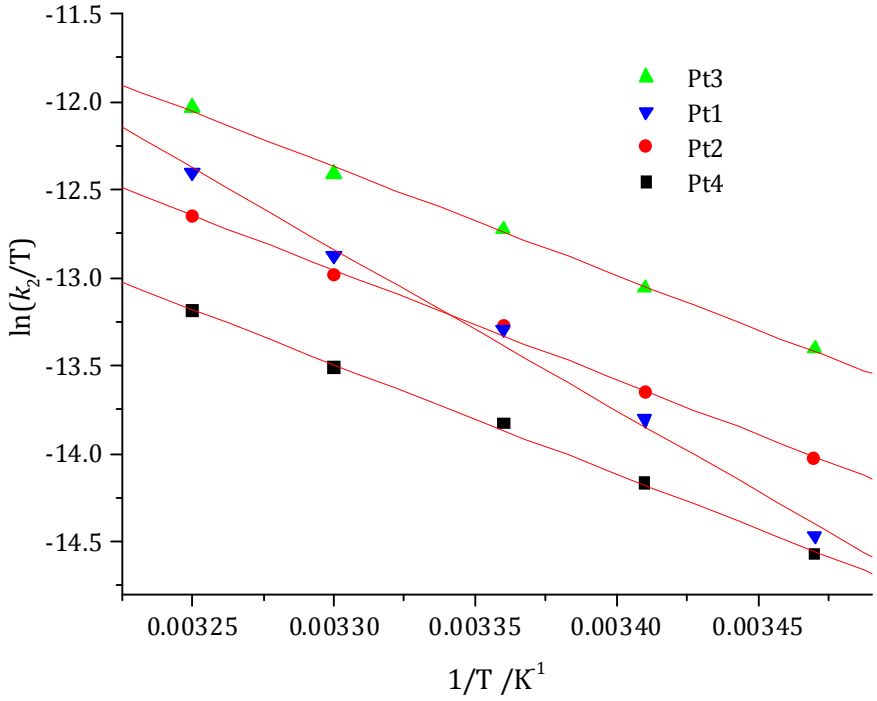


**Figure SI 3.22**: Plots of $\ln {}^{1}/_{T}$ *versus* ${}^{1}/_{T}$ for the reaction of **Pt4**, **Pt2**, **Pt3** and **Pt1** with DMTU nucleophile at various temperatures in the range of 15-35℃.

**Table SI 3.9:** Temperature dependence of $k_2$ / $M^{-1}$ $s^{-1}$ for the displacement of chloro ligands in **Pt4**, **Pt2**, **Pt3** and **Pt1** by 1,1,3,3-tetramethyl-2-thiourea (TMTU) nucleophile at 30-fold excess over [Pt], $I$ = 0.1 M $NaClO_4$/LiCl.

| **Pt4** | | **Pt2** | | **Pt3** | | **Pt1** | |
|---|---|---|---|---|---|---|---|
| $1/T$ /$K^{-1}$ | $\ln(k_2/T)$ | $1/T$ /$K^{-1}$ | $\ln(k_2/T)$ | $1/T$ /$K^{-1}$ | $\ln(k_2/T)$ | $1/T$ /$K^{-1}$ | $\ln(k_2/T)$ |
| 0.00347 | -14.8638 | 0.00347 | -14.9683 | 0.00347 | -15.0448 | 0.00347 | -15.2822 |
| 0.00341 | -14.6817 | 0.00341 | -14.6214 | 0.00341 | -14.7858 | 0.00341 | -15.0834 |
| 0.00336 | -14.3414 | 0.00336 | -14.253 | 0.00336 | -14.4649 | 0.00336 | -14.8701 |
| 0.0033 | -14.0483 | 0.0033 | -13.9947 | 0.0033 | -14.0829 | 0.0033 | -14.7227 |
| 0.00325 | -13.810 | 0.00325 | -13.6007 | 0.00325 | -13.7990 | 0.00325 | - |

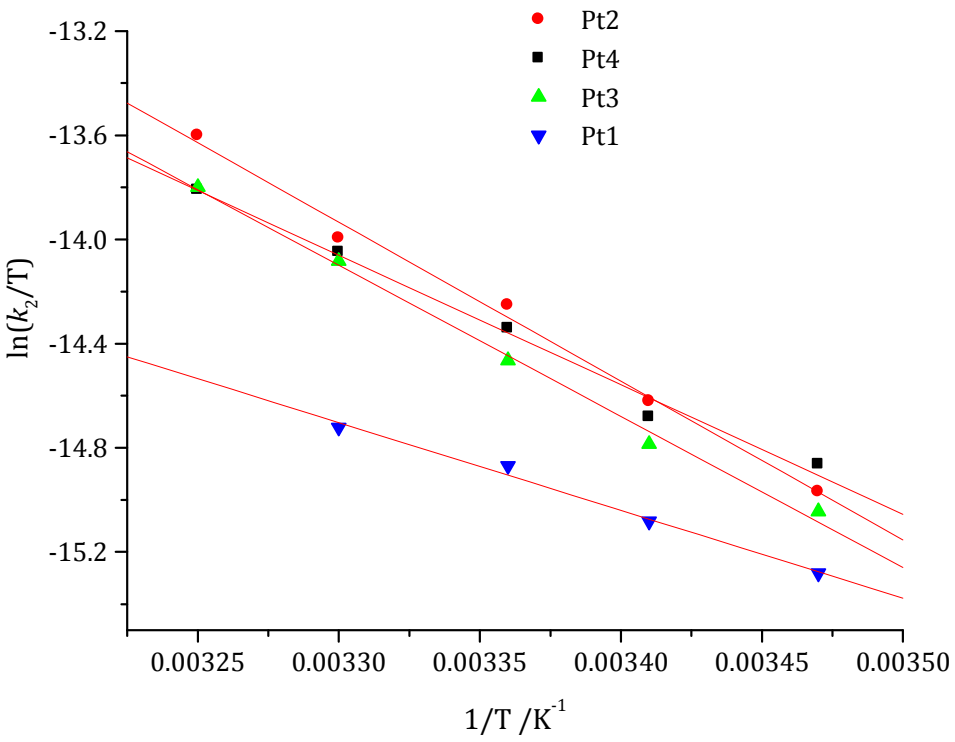


**Figure SI 3.23**: Eyring plots for the reaction of **Pt4**, **Pt2**, **Pt3** and **Pt1** with TMTU nucleophile at various temperatures in the range of 15-35℃

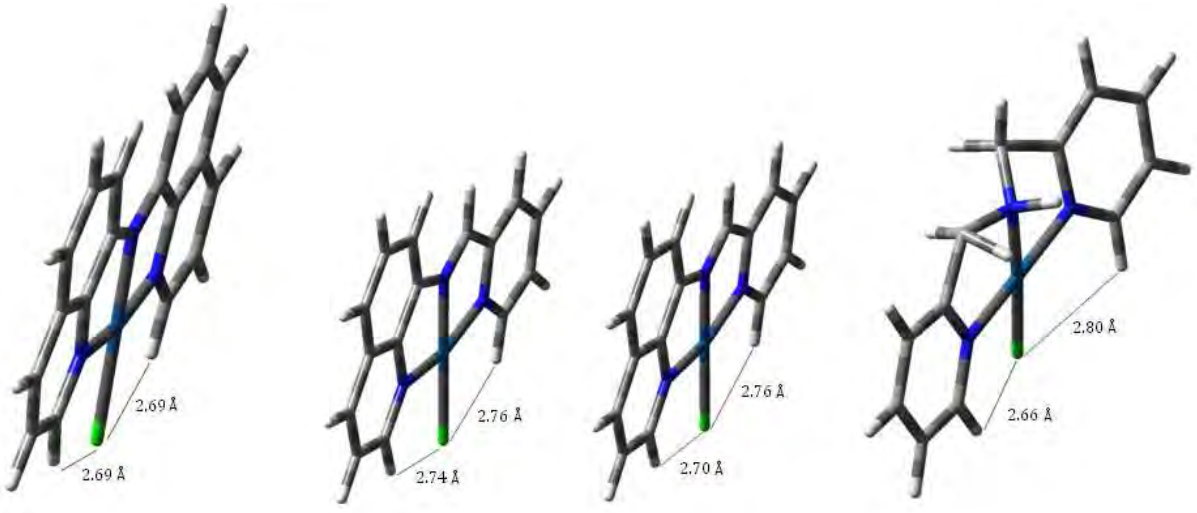


**Figure SI 3.24**: Planarity of the investigated complexes showing nearby H–Cl bond length (Å).

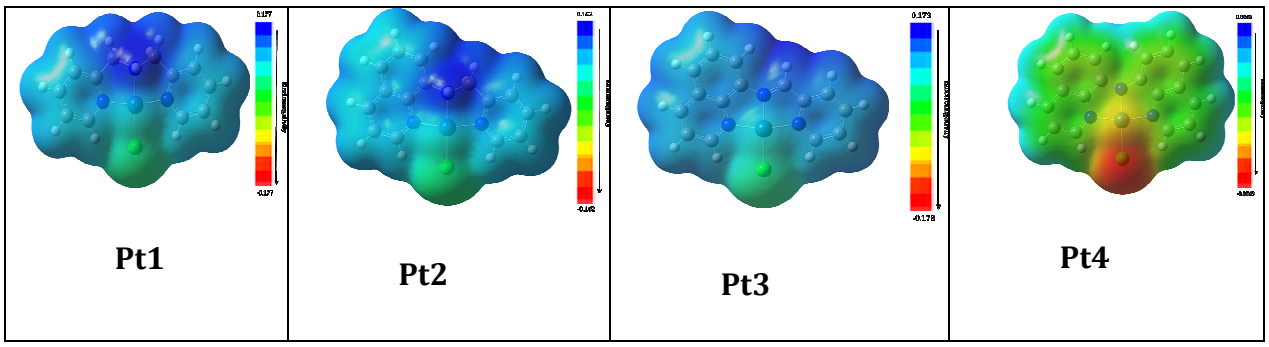


**Figure SI 3.25:** Electron density surface painted according to the value of the electrostatic potential (ESP) of the investigated complexes. The colours used in rendering a mapped surface are based on a uniform scaling between minimum and maximum ESP values (in Hartrees) as specified in the text box to the bottom and top of each spectrum respectively.

# Table of Contents

**List of Schemes**



**List of Tables**

**List of Figures**

# Chapter 4

## Kinetic and Mechanistic Studies of Cisplatin Analogues Bearing 2,2'-Dipyridylalkylamine Ligands.


### Abstract

A series of mononuclear Pt(II) complexes of the type diaqua(2,2'-dipyridylalkylamine)platinum(II) (where the alkyl group = methyl, ethyl, propyl, butyl and hexyl) were synthesized to investigate their substitution behaviour and the influence the alkyl chain bonded to the tertiary nitrogen atom joining the two pyridine rings will have on the reactivity of the chosen complexes. The trend in rate constant shows that introduction of the σ-donating alkyl chain on the tertiary nitrogen joining the two pyridine moieties reduces the π-acceptability of the *cis* coordinated pyridine rings resulting into a less reactive Pt(II) centre which cause a decrease in the reaction rate. This is well supported by data from DFT calculations. It is also evident that the alkyl chain also brings in the steric effect which blocks the approach of the nucleophile to the Pt(II) centre. The boat like structure of the six-membered chelate ring also contributes to the steric effect. The study has also shown that two substitution processes going through an associative mode of activation are observed. The first being the simultaneous substitution of the two aqua molecules and the second is due to the dechelation of the ligand an indication of possible disintegration of the complex if used as a drug.

## 4.1 Introduction

The kinetic study on the interaction of various platinum(II) complexes with nucleophiles often reveals an important chemical behaviour of these compounds in the area of chemotherapy. This work reports the kinetics of Pt(II) complexes featuring 2,2'-dipyridylamine, (dpa). 2,2'-Dipyridylamine is an aromatic amine which behaves as a neutral or monoanionic ligand. The NH group is usually not involved in coordination because of geometrical constraints and the two pyridine rings are flexible in their coordination to metal centres, leading to different coordination modes such as monodentate, chelating bidentate and bridging tridentate.[1,-6] It is well established that upon coordination with the metal centers, dpa forms six-membered chelate ring with the pyridyl rings adopting either nearly co-planar or inclined pyridyl ring planes. This property of dpa and its derivatives affect either the electronic or stereo chemical properties of the systems and have been observed in a number of metal complexes.[7]

To date, platinum(II) complexes of 2,2'-dipyridylamine, (dpa) have received increasing attention and have been investigated due to their potential use as anticancer agents owing to their structural similarity to cisplatin.[8,9] Reactions with model nucleobases and cytotoxicity of mononuclear complexes with a 2,2'-dipyridylamine ligand system, have been extensively studied.[10-11] Results show that 2,2'-dipyridylamine unit provides a favourable structural feature for an unhindered DNA-complex interaction[12] leading to significant cytostatic activity in the range of cisplatin in several tumour cell lines.[13,14]

Substitution reactions on Pt(II) complexes with N-N/N-S bidentate ligands such as ethylenediamine (en), bipyridine (bpy), aminomethylpyridine (amp) and thiomethylpyridine (mtp) have been investigated.[15] Results show that the lability of the leaving groups depends on the electronic and steric effect of the bidentate ligand. For example, substitution reactions of the complexes *cis*-$[Pt(NH_3)_2Cl_2]$, $[Pt(SMC)Cl_2]^-$, $[Pt(en)Cl_2]$, and $[Pt(dach)Cl_2]$, (where SMC =S-methyl-L-cysteine, en = ethylenediamine and dach = 1,2-diaminocyclohexane), follow the trend $[Pt(SMC)Cl_2]^-$ > *cis*-$[Pt(NH_3)_2Cl_2]$ >$[Pt(en)Cl_2]$ > $[Pt(dach)Cl_2]$.[15a] The high reactivity of $[Pt(SMC)Cl_2]^-$ was attributed to the strong *trans*-labilization effect of coordinated sulfur donor, because the strong σ-donating effect of sulfur leads to elongation of the Pt–Cl bond in the *trans* position and therefore making it more labile. Similar results on *trans* labilizing effect of sulfur were also reported by van Eldik *et al*.[15c,e] The reactivity of the complexes *cis*-$[Pt(NH_3)_2Cl_2]$, $[Pt(en)Cl_2]$, $[Pt(dach)Cl_2)$ depends on the steric effects. $[Pt(dach)Cl_2]$ is reported to be the most sterically congested complex because of the cyclohexane ring which also imparts some positive inductive to the metal centre and making it less electrophilic.[15a,b] In a related study where the π-acceptor groups of the bidentate ligand were varied, it was found that the electrophilicity on the Pt(II) centre increased due to the electron-withdrawing properties of the π-acceptor groups, which results in increasing reaction rates for nucleophilic substitution reactions especially when two pyridine rings are adjacent to each other.[15d]

To extend the understanding on the effect of π-acceptors on the thermodynamic and kinetic properties of Pt(II) complexes, a series of five Pt(II) complexes with dpa ligands (**Figure 4.1**) namely; diaqua(2,2'-dipyridylmethylamine)platinum(II), (**Ptdpma**), diaqua(2,2'-

dipyridylethylamine)platinum(II), (**Ptdpea**), diaqua(2,2'-dypyridylpropylamine)platinum(II), (**Ptdppa**), diaqua(2,2'-dipyridylbutylamine) platinum(II), (**Ptdpba**) and diaqua(2,2'-dipyridylhexylamine) platinum(II), (**Ptdpha**) were therefore chosen and their kinetic behaviour undertaken so as to provide an understanding on their interactions with sulfur-donor nucleophiles. The ligand 2,2'-dipyridylamine chelate was altered by incorporating an alkyl group of variable chain length spacing tertiary nitrogen of the bidentate chelate. This endowed surfactant properties to the resulting Pt(II) complexes known to improve diffusion through cell membrane and hence facilitating their entrance into the cell compared to cisplatin.[16] For comparison purposes kinetic data for Pt(bpy) (where bpy = N,N'-bipyridine) which also contains two pyridine rings in the bidentate chelate were included. The two pyridine rings of Pt(dpa) complexes are flexible in the coordination compared to that of Pt(bpy). This is expected to affect the electronic properties of the Pt(II) centre and hence the substitution reactions. The thiourea nucleophiles were chosen because of their good solubility, neutral character, different nucleophilicity, steric hindrance, binding properties, and biological relevance.[17] In addition, thiourea is a very useful nucleophile since it combines the ligand of thiolates (σ-donor) and thioethers (σ-donor and π-acceptor).[18-20]

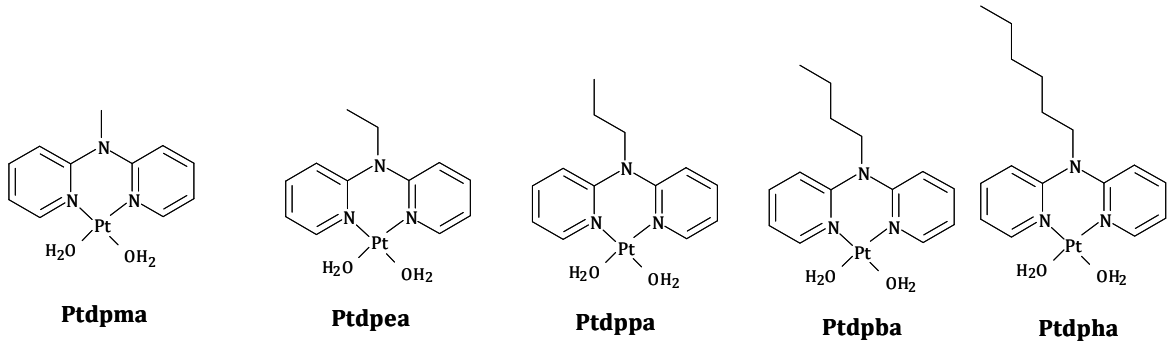


**Figure 4.1:** Structures of the complexes investigated.

## 4.2 Experimental

### 4.2.1 Chemicals

Potassium tetrachloroplatinate, $K_2PtCl_4$, (99%) was purchased from Strem Chemicals. The nucleophiles thiourea (TU, 99%), 1,3-dimethyl-2-thiourea (DMTU, 99%), 1,1,3,3-tetramethyl-2-thiourea (TMTU, 98%) and ligands methyl iodide (99%), 1-bromoethane, (99%), 1-bromopropane (97%), 1-bromobutane (98%), 1-bromohexane and 2,2'-dipyridylamine (97%) were obtained from Aldrich and used without further purification. $AgClO_4$ (99.99%, Aldrich) was stored under nitrogen and used as supplied. Ultrapure water (PureLab Systems) was used in all experiments. All other reagents used were of analytical grade quality and were used without further purification.

### 4.2.2 Synthesis of the Ligands

The ligands namely; (2,2'-Dipyridyl)methylamine, (**dpma**), (2,2'-Dipyridyl)ethylamine, (**dpea**), (2,2'-Dipyridyl)-1-propylamine, (**dppa**), (2,2'-Dipyridyl)-1-butylamine, (**dpba**) and (2,2'-Dipyridyl)-1-hexylamine, (**dpha**) were synthesized using the same procedure[11]

starting from 2,2'-dipyridylamine and their respective bromo alkyl halides. For **dpma**, methyl iodide was used as a precursor.

To a suspension of potassium hydroxide (1.3 g, 0.02 mol) in 15 mL of DMSO, 2,2'-dipyridylamine (0.0855 g, 0.5 mmol) was added. The mixture was stirred at room temperature for 45 min after which respective alkyl halide (0.5 mmol) was added. After stirring at room temperature for a further period of 60 minutes, 20 mL of water was added. The solution was extracted with diethyl ether (30 mL) and the organic extracts dried over $MgSO_4$. The solvent was removed *in vacuo* to yield the desired ligand. All ligands were characterized by NMR spectroscopy and LC-MS and used for complex-formation without further purification.

**dpma**, Brown oil, yield 49.3 mg (53.3 %). $^1$H NMR ($CDCl_3$, 400 MHz): δ = 8.23 (ddd, 2H), 7.44 (ddd, 2H), 7.06 (td, 2H), 6.76 (dd, 2H), 3.53 (s, 3H). $^{13}$C NMR ($CDCl_3$, 400 MHz): 157.6, 148.1, 137.1, 116.9, 114.4 and 36.1. TOF MS ES$^+$: $m/z$ $[M+H]^+$ = 186.01.

**dpea**, Yellow oil, yield 55.4 mg (55.7 %). $^1$H NMR ($CDCl_3$, 400 MHz): δ = 8.10 (dd, 2H), 7.31 (dddd, 2H), 6.86 (brd, 2H), 6.64 (dddd, 2H), 4.00 (t, 2H), 1.03(t,3H). $^{13}$C NMR ($CDCl_3$, 400 MHz): 157.0, 148.1, 137.0, 116.8, 114.6, 39.2 and 13.3. TOF MS ES$^+$: $m/z$ $[M+H]^+$ = 200.12.

**dppa**, Brown oil, yield 54.5 mg (51.2 %). $^1$H NMR ($CDCl_3$, 400 MHz): δ = 8.15 (dddd, 2H), 7.36 (dddd, 2H), 6.91 (dddd, 2H), 6.68 (dddd, 2H), 3.96 (t, 2H), 1.55 (m, 2H), 0.76 (t, 3H). $^{13}$C

NMR ($CDCl_3$, 400 MHz): 157.4, 148.1, 137.0, 116.7, 114.6, 49.81, 21.3 and 36.1. TOF MS $ES^+$: $m/z$ $[M+H]^+$ = 214.13.

**dpba**, Brown oil, yield 60.5 mg (53.3 %). $^1H$ NMR ($CDCl_3$, 400 MHz): δ = 7.93 (dddd, 2H), 7.15 (dddd, 2H), 6.70 (dddd, 2H), 6.48 (dddd, 2H), 3.78 (t, 2H), 1.28 (m, 2H), 0.98 (m, 2H), 0.53 (t, 3H). $^{13}C$ NMR ($CDCl_3$, 400 MHz): 147.8, 136.9, 115.9, 114.7, 47.7, 30.0, 19.9 and 13.7. TOF MS $ES^+$: $m/z$ $[M+H]^+$ = 228.15.

**dpha**, Brown oil, yield 69.6 mg (54.6 %). $^1H$ NMR ($CDCl_3$, 400 MHz): δ = 7.84 (dddd, 2H), 7.07 (dddd, 2H), 6.62 (brd, 2H), 6.39 (dddd, 2H), 3.68 (t, 2H), 1.20 (m, 2H), 0.83 (m, 6H), 0.40 (t, 3H). $^{13}C$ NMR ($CDCl_3$, 400 MHz): 157.0, 147.8, 136.8, 115.7, 114.5, 47.8, 30.5, 27.8, 25.9, 22.2 and 13.7. TOF MS $ES^+$: $m/z$ $[M+H]^+$ = 256.18.

### 4.2.3 Synthesis of the Complexes

The complexes **Ptdpma**, **Ptdpea**, **Ptdppa**, **Ptdpba** and **Ptdpha** were synthesized from their respective ligands according to a literature method.[9b] To a stirred red solution of 0.2075 g (0.5 mmol) $K_2PtCl_4$ dissolved in 25 mL of water, the corresponding ligand (0.5 mmol) dissolved in a small amount of water was added. The reaction mixture was stirred overnight at 50 °C. The resulting yellow precipitate was collected, washed with water, ethanol, methanol and diethyl ether and dried in vacuum. The purity of the complexes was confirmed by NMR, LC-MS and elemental analysis.

**Ptdpma**, Yield 132.3 mg, (52.3 %). $^{1}$H NMR (DMSO-$d_6$, 400 MHz) δ = 8.84 (ddd, 2H), 8.11 (ddd, 2H), 7.50 (td, 2H), 7.28 (dd, 2H), 3.66 (s, 3H). $^{13}$C NMR (DMSO-$d_6$, 400 MHz): 153.5, 151.6, 141.5, 121.2, 115.3 and 40.9. *Anal. % calcd*. for $C_{11}H_{11}Cl_2N_3Pt$: C 29.27, H 2.44, N 9.31. *Found*: C 28.85, H 2.50, N 8.87. TOF MS ES$^+$: $m/z$ $[M+Na]^+$ = 473.99.

**Ptdpea**, Yield 94.4 mg, (40.6 %). $^{1}$H NMR (DMSO-$d_6$, 400 MHz): δ = 8.10 (dd, 2H), 7.31 (dddd, 2H), 6.86 (brd, 2H), 6.64 (dddd, 2H), 4.00 (t, 2H), 1.03(t,3H). $^{13}$C NMR (DMSO-$d_6$, 400 MHz): 153.3, 151.8, 141.5, 121.6, 116.9, 45.1 and 13.7*. Anal. % calcd*. for $C_{12}H_{13}Cl_2N_3Pt$: C 30.97, H2.79, N 9.03. *Found*: C 30.71, H 2.82, N 8.74. TOF MS ES$^+$: $m/z$ $[M+Na]^+$ = 488.00

**Ptdppa**, Yield 136.7 mg, (57.1 %). $^{1}$H NMR (DMSO-$d_6$, 400 MHz): δ = 8.81 (dd, 2H), 8.09 (dddd, 2H), 7.54 (dddd, 2H), 7.29 (dddd, 2H), 4.09 (t, 2H), 1.67 (m, 2H), 1.09 (t, 3H). $^{13}$C NMR (DMSO-$d_6$, 400 MHz): 153.3, 151.7, 141.4, 121.6, 117.0, 51.9, 20.8 and 11.6. *Anal. % calcd*. for $C_{13}H_{15}Cl_2N_3Pt$: C 32.56, H 3.13, N 8.76. *Found*: C32.67, H 3.15, N 8.40. TOF MS ES$^+$: $m/z$ $[M+Na]^+$ = 502.02.

**Ptdpba**, Yield 256.3 mg, (57.4 %). $^{1}$H NMR (DMSO-$d_6$, 400 MHz): δ = 8.81 (dd, 2H), 8.09 (dddd, 2H), 7.55 (d, 2H), 7.28 (dddd, 2H), 4.11 (t, 2H), 1.64 (m, 4H), 0.90 (t, 3H). $^{13}$C NMR (DMSO-$d_6$, 400 MHz): 153.3, 151.7, 151.4, 121.6, 116.9, 50.3, 29.6, 19.7 and 14.0. *Anal. % calcd*. for $C_{14}H_{17}Cl_2N_3Pt$: C 34.07, H 3.45, N 8.52. *Found*: C 34.37, H 3.47, N 8.51. TOF MS ES$^+$: $m/z$ $[M+Na]^+$ = 516.03.

**ptdpha**, Yield 108.6 mg, (41.7 %). $^{1}$H NMR (DMSO-$d_6$, 400 MHz): δ = 7.84 (dddd, 2H), 7.07 (dddd, 2H), 6.62 (brd, 2H), 6.39 (dddd, 2H), 3.68 (t, 2H), 1.20 (m, 2H), 0.83 (m, 6H), 0.40 (t,

3H). $^{13}$C NMR (DMSO-$d_6$, 400 MHz): 153.3, 151.7, 141.4, 121.6, 116.9, 50.3, 31.1, 27.3, 26.5, 26.2 and 26.0. *Anal. % calcd*. for $C_{16}H_{21}Cl_2N_3Pt$: C 36.85, H 4.03, N 8.06. *Found*: C 37.14, H 4.03, N 7.59. TOF MS ES$^+$: $m/z$ $[M+Na]^+$ = 544.06.

### 4.2.4 Preparation of diaqua Pt(II) complexes

Solutions of the aqua complexes were prepared by suspending an accurately weighed amount of the chloro complex in 0.1 M $HClO_4$ and adding a stoichiometric amount of $AgClO_4$ (1.98 equiv) with respect to chloro complex. The mixture was then stirred in the dark at 50 ˚C for 24 h. The white precipitate of silver chloride which formed was filtrated through a 0.45-μm nylon membrane filter using a Millipore filtration unit. The clear, colourless filtrate was then made to the required concentration in a volumetric flask using a solution of 0.1 M $HClO_4$. The use of the acidic solution at pH 1 was necessary to ensure that only the aqua complex, and not a mixture of the aqua and hydroxo complexes, was present in solution once the metathesis reaction was complete, and also, to ensure a constant ionic strength of 0.1 M. This solution was used in the titration with NaOH solution to determine the p$K_a$ of the complexes whilst for kinetic investigations; the pH of the solution was maintained at 2 based on the p$K_a$ study and the ionic strength was maintained at 0.1 M using $NaClO_4$.

### 4.2.5 Instrumentation and Measurements

$^1$H, $^{13}$C and $^{195}$Pt spectra were recorded on a Bruker Avance III 500 or Bruker Avance III 400 at frequencies of 500 MHz or 400 MHz (1H) and 125 MHz/100 MHz using either a 5 mm BBOZ probe or a 5 mm TBIZ probe. All proton and carbon chemical shifts are reported

relative to the relevant solvent signals at 30 °C unless stated otherwise. Elemental compositions of the ligands and complexes were performed on a Thermo Scientific Flash 2000. The pH of the aqueous solutions of the complexes were measured using a Jenway 4330 Conductivity/pH meter equipped with a 4.5 μm diameter glass electrode. The electrode was calibrated at 25 ˚C using standard buffer solutions of pH 4.0, 7.0 and 10.0 (Merck). The electrolyte of pH electrode was replaced with 3.0 M NaCl to prevent the precipitation of $KClO_4$ during pH measurement. The mass spectral data of the ligands and complexes were acquired on a Waters Micromass LCT Premier spectrometer. Kinetic studies for fast reactions were monitored using an Applied Photophysics SX 20 stopped-flow spectrophotometer coupled to an online data acquisition system. Slow reactions were monitored using a Varian UV-Visible Cary 100 spectrophotometer. The temperature of these instruments was controlled throughout all kinetic experiments to ± 0.02 ˚C. p$K_a$ and kinetic traces were graphically analysed using the software package, Origin 7.5®.[21]

### 4.2.6 p$K_a$ Determination

In order to avoid formation of hydroxo species during kinetic studies it was important to determine the pH range within which the complexes exist in their aqua form. The measured p$K_a$ data are helpful in explaining the substitution lability of the aqua ligands in the metal complex as the p*K*a values of coordinated water serve as an experimental indicator for the electron density around the metal centre. A low p$K_a$ value is associated with the most electrophilic and reactive Pt(II) centre and vice versa.[15]

To determine p$K_a$ values, the solution of the complex of known concentration was spectrophotometrically titrated with NaOH within the pH range of 1-10 at 25 ˚C. To avoid dilution effects due to the addition of the titrant, a large volume (150 mL) of the complex was used for the titration. To circumvent adding a large volume of NaOH to effect the change in pH within the pH range of 1-3, small granules of crushed NaOH pellets were added to the solution. Between a pH range of 4-10, various concentrations of NaOH solutions were used making sure that there was an even distribution of the UV-Vis spectra. To avoid contamination of the complex solution by chloride ions leaching from the pH electrode, it was necessary to take 0.6 mL aliquots from the complex solution, which was then transferred into narrow vials for the pH measurements. These were then discarded after each measurement. The reversibility of the titration was also tested using aqueous solutions of perchloric acid.

### 4.2.7 Kinetic Measurements

All kinetic measurements were performed under *pseudo* first-order conditions by making sure that the concentration of the nucleophile was at least 20-fold in excess to the concentration of Pt(II) complexes. This was to ensure that the reaction goes to completion. All the substitution reactions involving aqua complexes were studied at pH 2. Concentration dependence study of the complexes was performed at 25 °C. Reported rate constants in **Table 4.4** represent an average value of at least three to five independent kinetic runs for each set of experimental conditions on UV-Visible and Stopped flow spectrophotometers respectively. The activation parameters, $\Delta H^{\#}$ and $\Delta S^{\#}$, were obtained by studying the temperature dependence of the rate constant in the temperature range of 15-35 °C at an

interval of 5 °C with the nucleophile concentration held constant at 80 times the concentration of the metal complex.

### 4.2.8 Computational Analysis

Density functional theoretical (DFT) calculations were performed with the Gaussian 09 programme suite.[22] Geometrical optimizations were carried at B3LYP/LanL2DZ level of theory. B3LYP refers to a three parameter functional hybrid exchange of Becke[23] with functional correlation gradient of Lee, Yang and Parr,[24,25] whereas LanL2DZ refers to Los Alamos National Laboratory 2 Double ζ [26] basis set. The singlet states were used due to low electronic spin of Pt(II) complexes. The aqua complexes were each modelled at +2 with respect to their total charges.

## 4.3 Results

### 4.3.1 Acidity of the Aqua Complexes

The acidities of the coordinated diaqua ligands on the Pt(II) complexes were determined through spectrophotometric titration. A typical plot of the UV-Visible spectra obtained during the course of the titration of the complex **Ptdpba** with NaOH is shown in **Figure 4.2**. Inset to the figure is the plot of absorbance versus pH at 290 nm for the **Ptdpba**. When the data points of the plot of absorbance versus pH were fitted on standard sigmoid equation using Origin 7.5®[21] it revealed that two dissociation steps were involved. This was observed for each of the investigated complexes. The overall process can therefore be presented by the equilibrium reaction given in **Scheme 4.1**. The p$K_a$ values obtained are summarized in

**Table 4.1** and as stated before for comparison purposes included in the table is the p$K_a$ value of **Pt(bpy)**. The results show that by changing the length of the alkyl group attached to the spacing tertiary nitrogen of the bidentate chelate has insignificant influence on the deprotonation of the aqua molecules as the p$K_a$ values are similar in magnitude, true for both deprotonation steps.

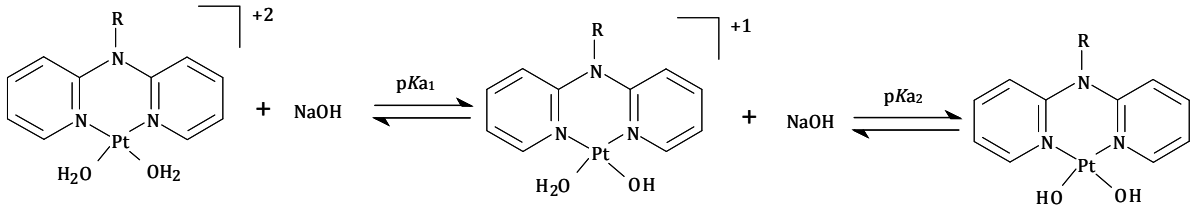


R = methyl, ethyl, propyl, butyl and hexyl

**Scheme 4.1:** Schematic presentation of the acid-dissociation equilibria of the investigated complexes.

**Table 4.1:** Observed p$K_a$ values for the deprotonation of Pt-bound aqua ligands for each of the mononuclear Pt(II) complexes investigated.

| Complex | **Ptdpma** | **Ptdpea** | **Ptdppa** | **Ptdpba** | **Ptdpha** | **Pt(bpy)** |
|---|---|---|---|---|---|---|
| p$K_{a1}$ | 5.24 ± 0.07 | 5.27 ± 0.02 | 5.31 ± 0.03 | 5.36 ± 0.08 | 5.45 ± 0.12 | 4.80* |
| p$K_{a2}$ | 6.19 ± 0.04 | 6.29 ± 0.07 | 6.29 ± 0.02 | 6.31 ± 0.06 | 6.35 ± 0.11 | 6.32* |

***** p$K_a$ values extracted from reference 15d.

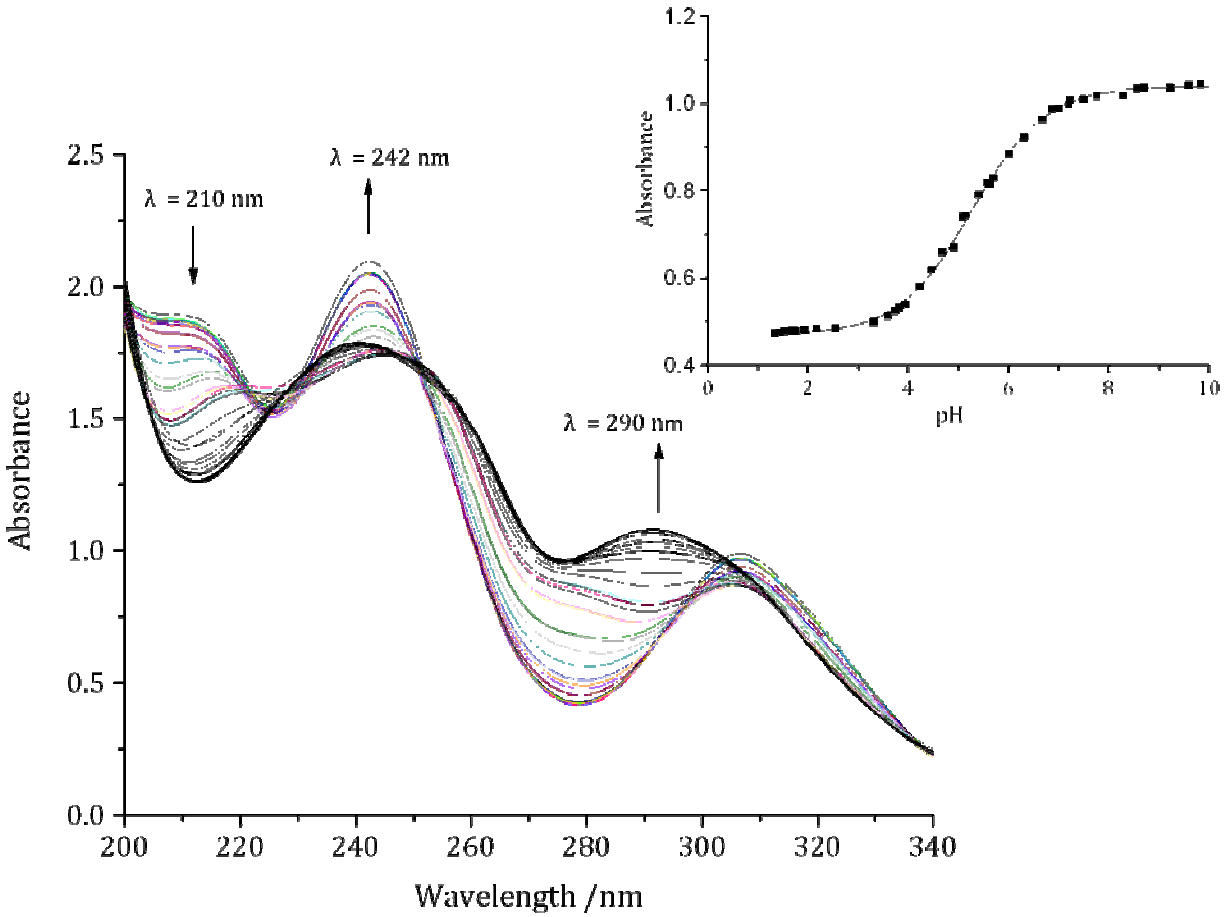


**Figure 4.2** UV-Visible spectra of the titration of **Ptdpba** with NaOH (pH range1-10). *Inset*: Plot of absorbance versus pH at 290 nm for the Ptdpba.

It is also observed that deprotonation of the second coordinated water molecule to the dihydroxo species occurs at higher pH values than in the first step in all the five complexes. This results from a reduction of the overall charge to +1 after deprotonation of one coordinated water molecule. Hence, the Pt(II) centre of the aqua/hydroxo species is less electrophilic compared to that of the diaqua complex,[27-30]leading to higher p$K_{a2}$ values. The lower p$K_a$ values of **Pt(bpy)** is ascribed to the rigid and planar π-acceptor pyridine moieties

*cis* to the aqua ligands which help to stabilize the electron density of the hydroxo ligands formed making the complex more electrophilic and acidic.

### 4.3.2 Computational Studies

The geometry optimized structures and the mapping of frontier molecular orbitals are presented in **Table 4.2**. The bidentate dpa ligand coordinates the metal centres via its two nitrogen donor atoms forming a six-membered chelating ring which exists in a boat conformation due to high flexibility of the nitrogen linker between the coordinative pyridines. Two aqua ligands complete the coordination spheres, resulting in a square-planar geometry around the metal centre. The two heterocyclic rings of dpa form a dihedral angle in a range of 38˚-42˚. The basal angle around the Pt centre of all complexes with respect to *cis* pyridine rings lies between 113-119˚ (**Figure 4.3** and **Figure SI 4.28**). The calculated bond lengths and angles (**Table 4.3**) fit well with the values given in literature for the chloro complexes of Pt(II) and Pd(II).[10d]

Mappings of the frontier orbitals indicate that for all investigated complexes, the HOMOs are localized mainly on the platinum metal with significant contribution from the pyridine rings and the $(CH_2)_n$ units of the alkyl chain. The LUMOs of these complexes are symmetrically delocalised on the Pt atom, pyridine nitrogens and on aqua groups. Because of the location of HOMO and LUMO, an electron-donating effect would be expected to increase electron density on the complex as a whole, raise the HOMO energy, and destabilize the LUMO. The individual energy levels of HOMO and LUMO increase with the

length of the aliphatic chain from **Ptdpma** to **ptdpha**. This trend can be explained by the increase in σ-donicity of the alkyl chain to the pyridyl side arms which increases with an increase in length of the alkyl chain. Literature shows that presence of electron donating groups in a system increases the energy of the molecular orbitals.[31-34]

Included in **Table 4.3** is global chemical reactivity descriptor for electrophilicity indices of the complexes calculated using a literature method.[35] Electrophilicity values of the complexes (**Table 4.3**) follow the trend **Ptdpha** < **Ptdpba** < **Ptdppa** < **Ptdpea** < **Ptdpma**. Among the complexes, **Ptdpha** is the weakest electrophile whilst **Ptdpma** is the strongest electrophile. It is worth noting that the NBO charges of the Pt atom are of the same magnitude so the influence of the σ-donor ability of the alkyl chain to the metal centre is minimal.

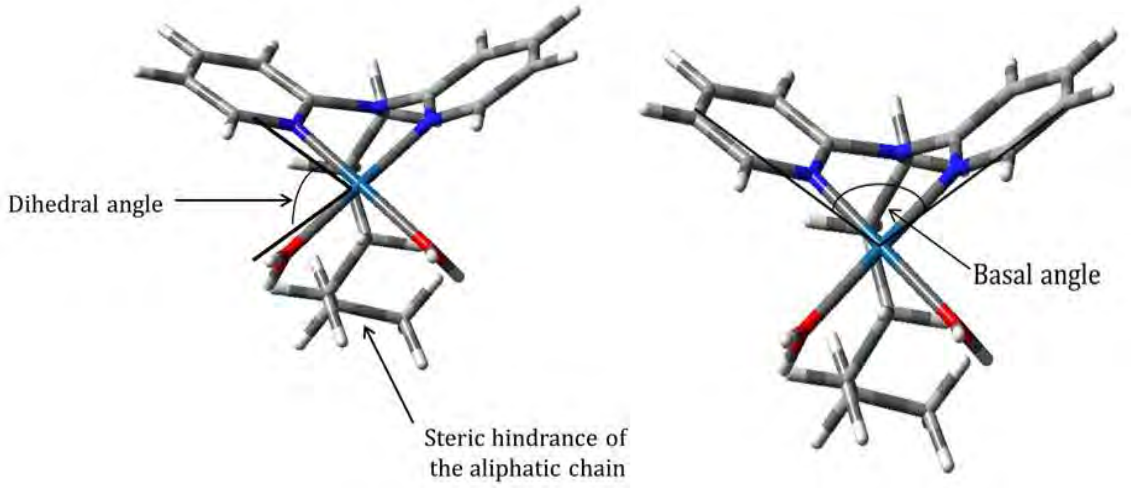


**Figure 4.3**: DFT-Optimized structures of Ptdpha showing dihedral angle, steric hindrance of the aliphatic chain and basal angle of the boat conformed pyridine rings.

**Table 4.2:** Geometry optimized structures and DFT-calculated (B3LYP/LanL2DZ HOMOs and LUMOs for the investigated complexes.

| Complex | HOMO | LUMO | Planarity |
|---|---|---|---|
| **Ptdpma** |  | 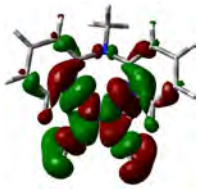 |  |
| **Ptdpea** | 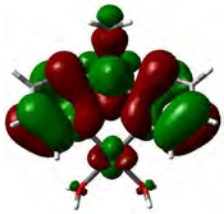 | 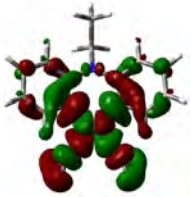 |  |
| **Ptdppa** |  | 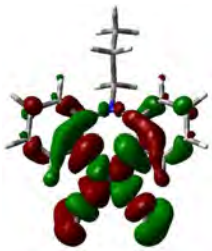 | 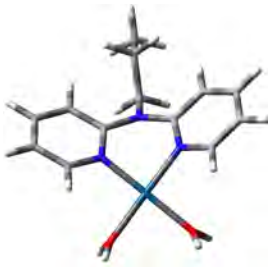 |
| **Ptdpba** | 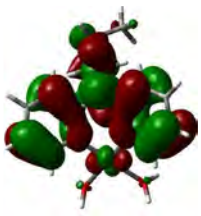 | 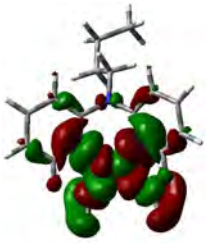 |  |
| **Ptdpha** | 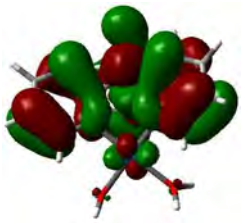 | 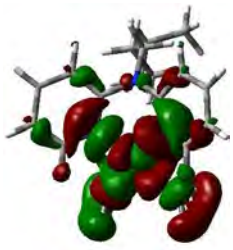 |  |

**Table 4.3:** DFT-calculated parameters for the investigated Pt(II) complexes

| 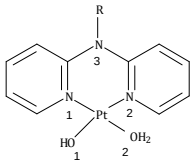 | **Ptdpma** | **Ptdpea** | **Ptdppa** | **Ptdpba** | **Ptdpha** |
|---|---|---|---|---|---|
| **HOMO-LUMO energy** | | | | | |
| LUMO /eV | -9.094 | -8.901 | -8.862 | -8.833 | -8.794 |
| HOMO/eV | -12.913 | -12.872 | -12.793 | -12.785 | -12.723 |
| ΔE /eV | 3.819 | 3.971 | 3.931 | 3.952 | 3.929 |
| **Reactivity descriptors** | | | | | |
| Electrophilicity index (ω) | 31.704 | 29.845 | 29.823 | 29.564 | 29.459 |
| **NBO Charges** | | | | | |
| Pt | 0.762 | 0.759 | 0.759 | 0.756 | 0.757 |
| $N_{1/2}$ | -0.520 | -0.523 | -0.523 | -0.525 | -0.528 |
| $N_3$ | -0.489 | -0.495 | -0.491 | -0.507 | -0.511 |
| **Dipole moment (debye)** | 2.678 | 3.648 | 4.803 | 5.209 | 6.469 |
| **Bond Length** (Å) | | | | | |
| $Pt–O_1$ | 2.125(46) | 2.128(58) | 2.128(93) | 2.126(98) | 2.125(46) |
| $Pt–O_2$ | 2.125(62) | 2.128(66) | 2.128(90) | 2.126(23) | 2.125(62) |
| **Bond Angles** (°) | | | | | |
| Dihedral | 39.94 | 38.53 | 38.13 | 41.26 | 42.10 |
| $N_2–Pt–O_1$ | 177.961 | 175.834 | 177.950 | 178.215 | 177.904 |
| $N_1–Pt–O_2$ | 177.949 | 177.812 | 177.953 | 178.514 | 178.605 |
| $N_1–Pt–N_2$ | 87.973 | 87.717 | 87.763 | 87.722 | 87.651 |
| $O_1–Pt–O_2$ | 87.506 | 86.878 | 86.835 | 87.623 | 87.396 |

R = alkyl group

### 4.3.3 Kinetic Measurements

Spectral changes resulting from mixing of the Pt(II) complex and nucleophile solutions were recorded over the wavelength range 200 to 600 nm to establish a suitable wavelength at which kinetic measurements could be performed. The selected wavelengths are summarized in **Table S1 4.1**. The substitution reactions of the aqua complexes by a series of neutral nucleophiles, *viz*. TU, DMTU, and TMTU were investigated as a function of concentration and temperature. All the reactions showed two independent substitution steps (**Scheme 4.2**). While the first step fitted on the stopped flow, the second step was too slow and was followed by conventional UV-Visible spectroscopy for only the two less sterically hindered nucleophiles TU and DMTU. The reactions with TMTU were too slow taking more than five days to go to completion.

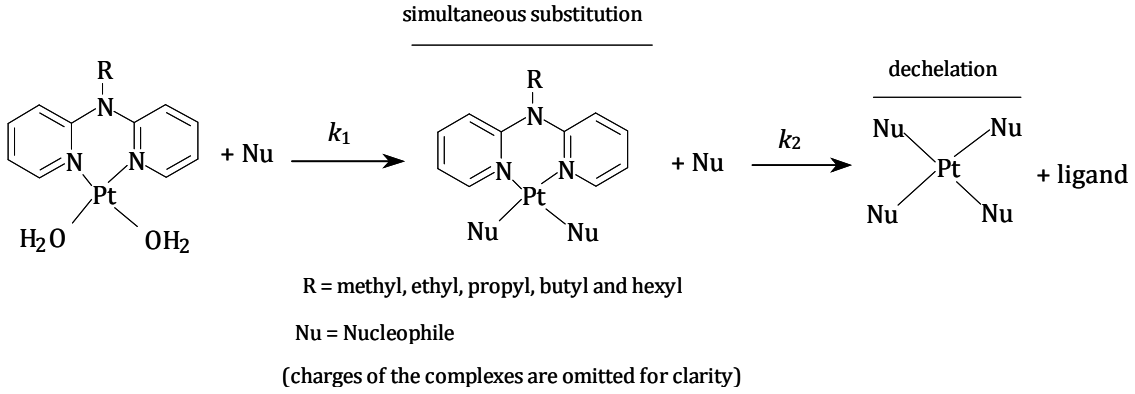


**Scheme 4.2:** Proposed mechanism of aqua substitution from the investigated Pt(II) complexes and the thiourea nucleophiles at pH 2.0**.**

The first substitution step was initiated by mixing equal volumes of a solution of the Pt(II) complex with a solution of the nucleophile directly in the stopped-flow instrument set at a

selected wavelength. An example of the kinetic trace is shown in **Figure 4.4**. Typical UV-Visible spectra obtained for the second substitution step is shown in **Figure 4.5** and inset to the **Figure** is the corresponding kinetic trace at 315 nm

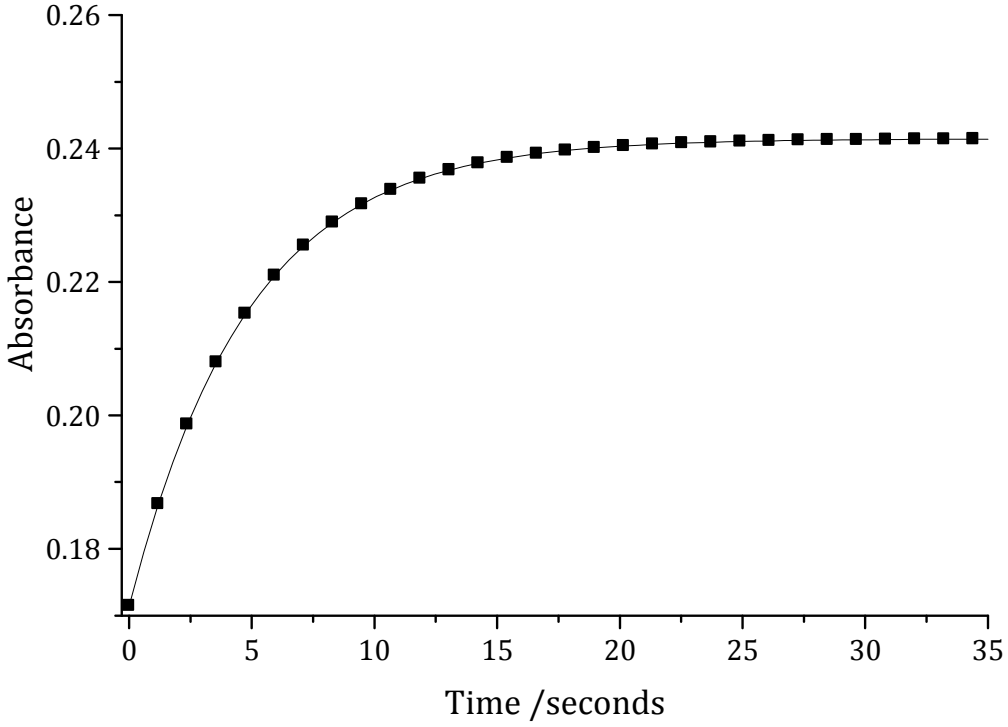


**Figure 4.4:** A typical kinetic trace for two step reaction between **Ptdppa** (0.25 mM) and TU (20 mM) recorded at 290 nm, T = 298 K, pH = 2.0, *I* = 0.1 M ($NaClO_4$) on the stopped-flow spectrophotometer.

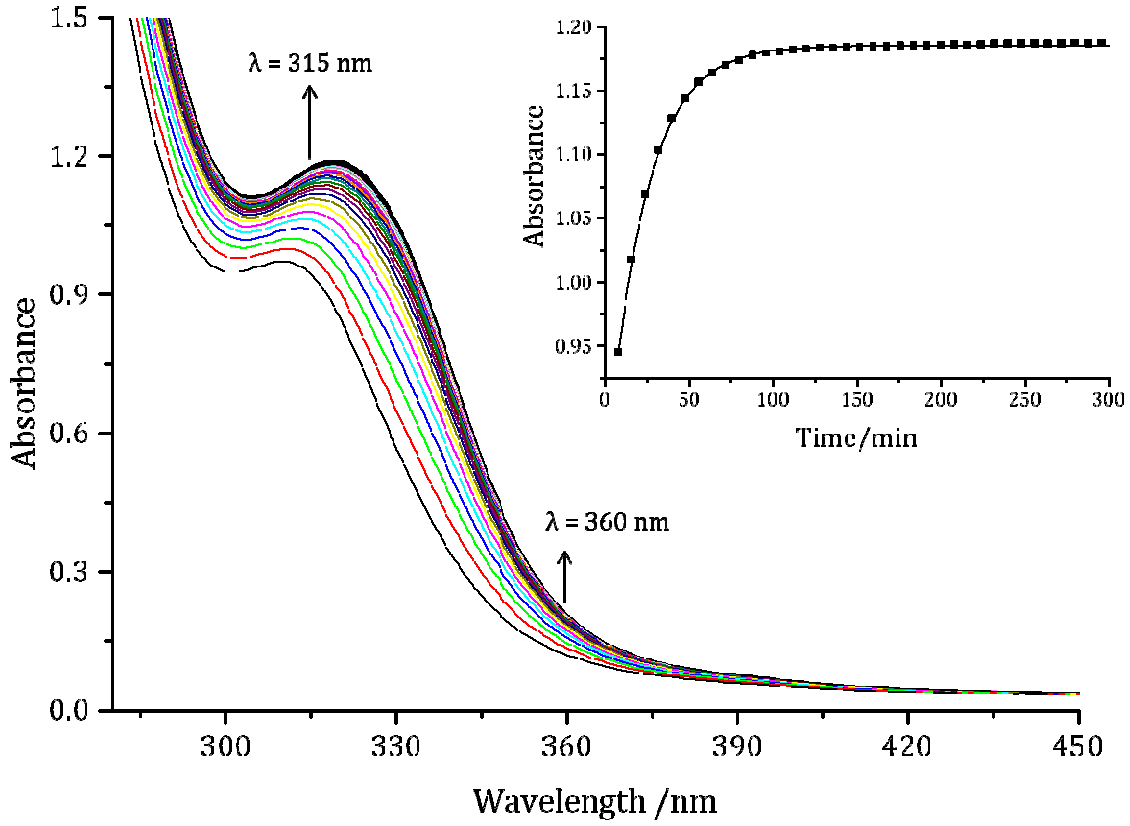


**Figure 4.5:** UV-Visible spectra recorded during the reaction of 0.25 mM **Ptdppa** with 30 mM thiourea at 25 °C and pH 2 ($I$ = 0.1 M, $NaClO_4$). *Inset*: Kinetic trace recorded at 315 nm.

In both steps, the kinetic traces for the ligand substitutions gave excellent fits to a single exponential function to generate the *pseudo* first-order rate constants, $k_{obs1or2}$ for the first and second substitution steps respectively at specific nucleophile concentrations and temperature. The second-order rate constants, $k_1$ and $k_2$ of the reactions (where $k_1$ = rate constant for the first step and $k_2$ = rate constant for the second step) were obtained from

the linear regression of the plot of $k_{\text{obs1 or 2}}$ versus nucleophile concentration using origin 7.5®.[21]

Representative plots for each of the investigated nucleophiles show a linear dependence on the concentration of the incoming nucleophile and is shown in **Figure 4.6** (also **Figures SI 4.19-4.21** and **SI 4.25**). The linear regression plots have zero intercepts which suggests that the mechanistic pathway is independent of the solvent effect.

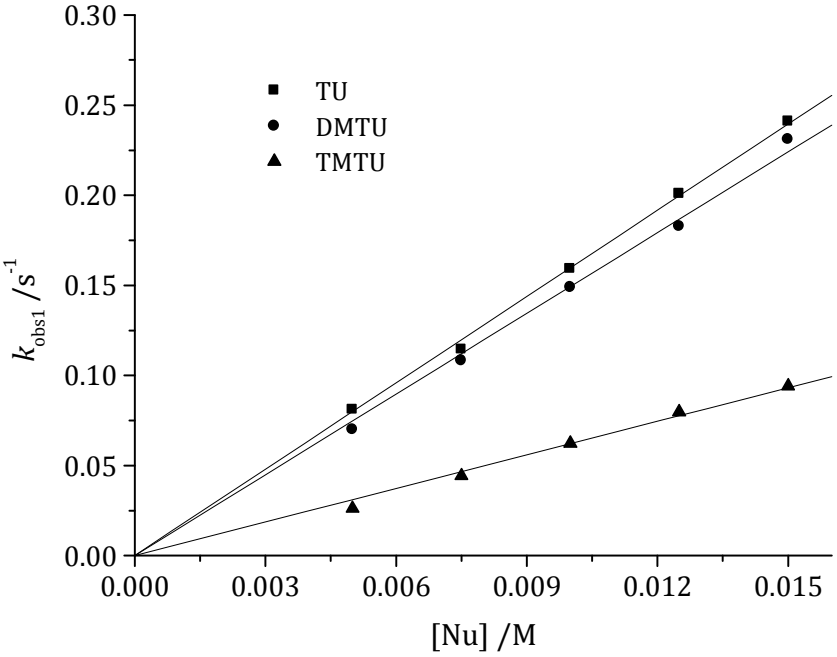


(a)

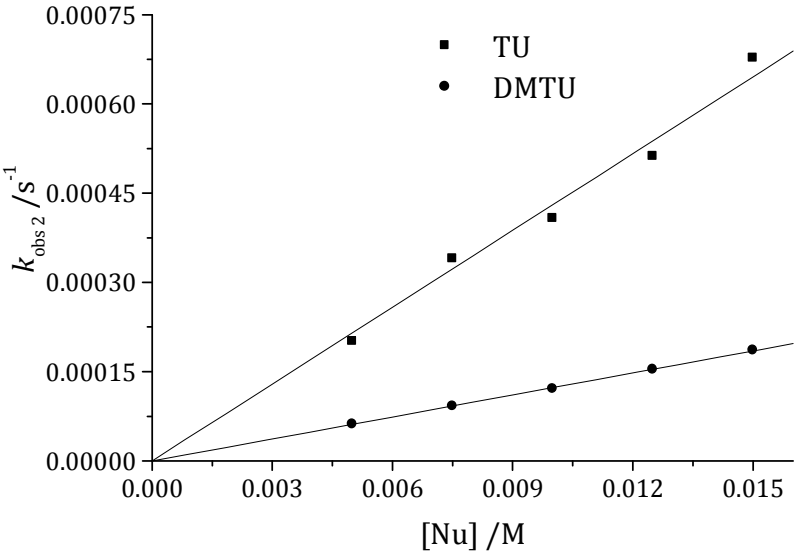


(b)

**Figure 4.6:** Concentration dependence of $k_{obs1or2}$ for the substitution of aqua from **Ptdpha** (0.25 mM) by thiourea nucleophiles for (a) the first and (b) the second substitution steps at pH 2, $I$ = 0.1 M $NaClO_4$ and 25 °C.

The proposed equations for the two substitution steps can be represented by **Equation 4.1**.

$$k_{obs1or2} = k_{1or2}[\mathrm{Nu}] \qquad (4.1)$$

The activation parameters; the enthalpy of activation, $\Delta H^{\#}$, and entropy of activation, $\Delta S^{\#}$, of each substitution step were determined by studying the temperature dependence of the rate constants, $k_1$ and $k_2$ at a fixed nucleophile concentration. Typical plots are shown in **Figure 4.7** (also **Figures SI 4.22-4.24**) and the corresponding values were calculated using the Eyring equation.[36] A summary of rate constants and activation parameters for the first and second substitution steps are shown in **Table 4.4**.

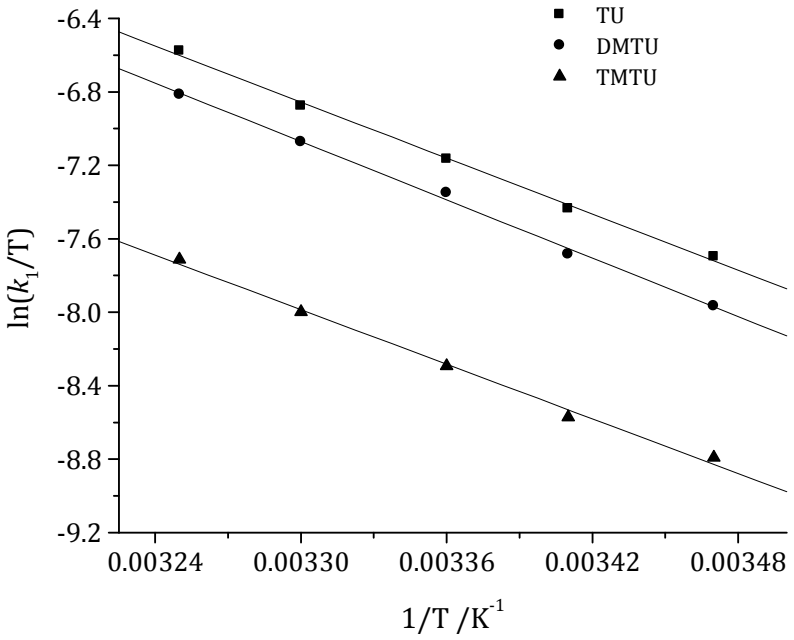


(a)

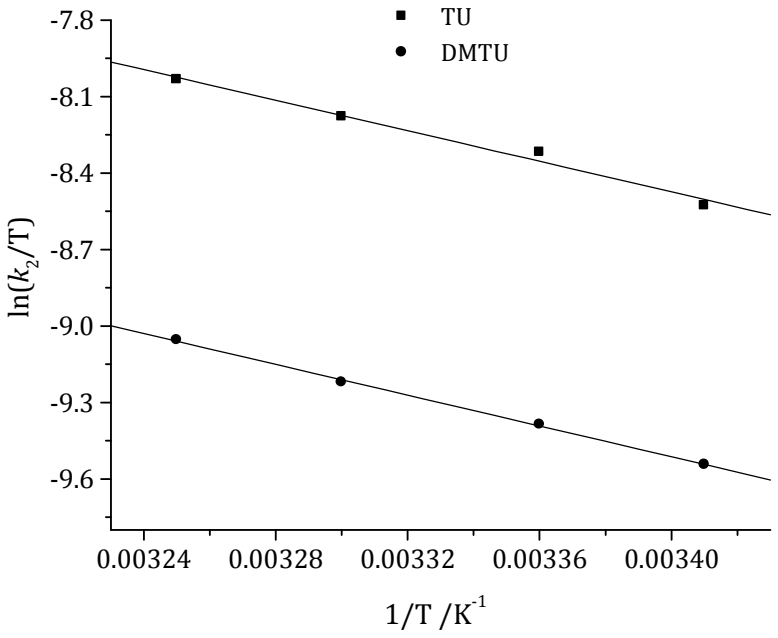


(b)

**Figure 4.7:** Eyring plots for the determination of the thermal activation parameters for (a) the first and (b) the second substitution steps of 0.25 mM **Ptdppa** for the nucleophiles studied at pH 2 ($I$ = 0.1 M $NaClO_4$)

**Table 4.4:** Summary of second order rate constants and activation parameters for the first and second substitution steps

| **Complex** | Nu | $k_1$/M$^{-1}$ s$^{-1}$ | $k_2$ /M$^{-1}$ s$^{-1}$ **x 10$^{-2}$** | $\Delta H_1^{\#}$ /kJ mol$^{-1}$ | $\Delta H_2^{\#}$ /kJ mol$^{-1}$ | $\Delta S_1^{\#}$ /J K$^{-1}$mol$^{-1}$ | $\Delta S_2^{\#}$ /J K$^{-1}$ mol$^{-1}$ |
|---|---|---|---|---|---|---|---|
| **Ptdpma** | TU | 38.7 ± 0.6 | 106 ± 3 | 41± 0.5 | 27 ± 1 | -115 ± 2 | -193 ± 3 |
| | DMTU | 48.8 ± 0.5 | 2.4 ± 0.1 | 40 ± 0.5 | 36 ± 0.5 | -115 ± 2 | -114 ± 2 |
| | TMTU | 22.8 ± 0.4 | - | 40 ± 1 | - | -122 ± 4 | - |
| **Ptdpea** | TU | 36.8 ± 0.7 | 8.6 ± 0.3 | 39 ± 2 | 37 ± 2 | -133 ± 6 | -127 ± 6 |
| | DMTU | 28.5 ± 0.6 | 2.2 ± 0.1 | 42 ± 1 | 46 ± 1 | -122 ± 3 | -121 ± 3 |
| | TMTU | 16.7 ± 0.2 | - | 38 ± 1 | | -142 ± 3 | - |
| **Ptdppa** | TU | 23.7 ± 0.3 | 7.4 ± 0.4 | 41 ± 1 | 24 ± 2 | -119 ± 3 | -185 ± 6 |
| | DMTU | 18.9 ± 0.4 | 1.4 ± 0.1 | 43 ± 1 | 25 ± 0.6 | -115 ± 3 | -191 ± 2 |
| | TMTU | 7.7 ± 0.1 | - | 40 ± 2 | - | -132 ± 6 | - |
| **Ptdpba** | TU | 20.6 ± 0.3 | 5.0 ± 0.2 | 41 ± 2 | 40 ± 2 | -121 ± 6 | -125 ± 6 |
| | DMTU | 17.0 ± 0.1 | 1.2 ± 0.05 | 44 ± 1 | 37 ± 2 | -113 ± 3 | -196 ± 6 |
| | TMTU | 7.4 ± 0.2 | - | 39 ± 2 | - | -137 ± 6 | - |
| **Ptdpha** | TU | 16.0 ± 0.1 | 4.3 ± 0.1 | 44 ± 1 | 22 ± 1 | -113 ± 3 | -157 ± 3 |
| | DMTU | 14.9 ± 0.2 | 0.7 ± 0.01 | 47 ± 0.4 | 39 ± 1 | -105 ± 1 | -169 ± 3 |
| | TMTU | 6.2 ± 0.1 | - | 79 ± 3 | - | -120 ± 9 | - |
| **Pt(bpy)**[a] | TU | 5080 ± 275 | 1119 ±22 | 45 ± 2 | 34 ± 2 | -24 ± 7 | -73 ± 5 |

[a]Data extracted from reference 15d.

To further understand the kinetics of the second and slower step of the reaction, the ligand substitutions of **Ptdppa-Cl** was followed using $^{1}H$ and $^{195}Pt$ NMR. An array of the $^{1}H$ NMR spectra (showing only the aromatic resonances) for the reaction between **Ptdppa-Cl** and excess TU (six equivalents) is shown in **Figure 4.8**. The pyridyl protons were chosen to monitor the progress of the reaction as they are in a close proximity with the N-donor atom bonded to the metal centre. The numbering scheme employed for the pyridyl protons is shown in the structure of the **Ptdppa-$Cl_2$** complex in **Scheme 4.3**.

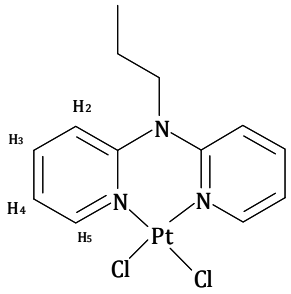


**Scheme 4.3:** The numbering scheme employed for the pyridyl protons of Ptdppa-$Cl_2$

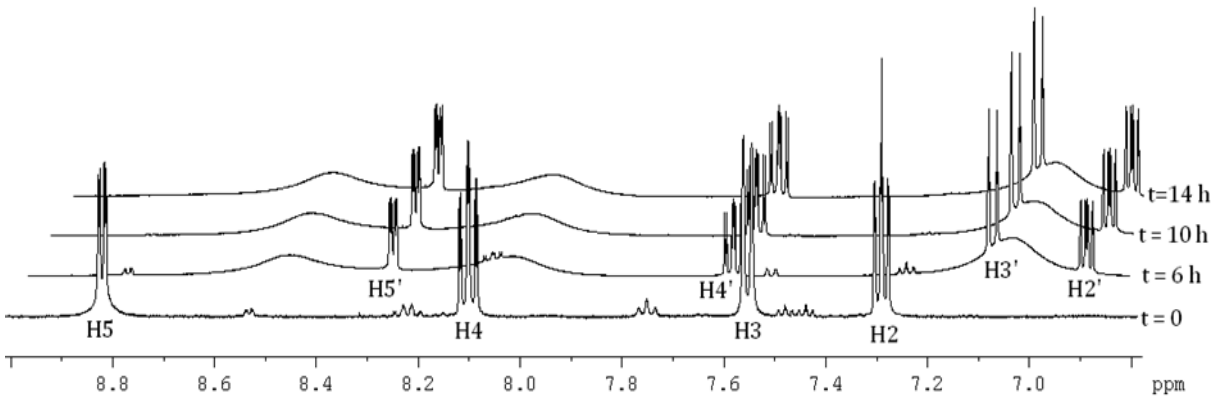


**Figure 4.8:** $^{1}H$ NMR spectra of Ptdppa-$Cl_2$ acquired during the reaction with TU 6 equiv. at the time scale shown on the spectra.

The resonances of the unreacted **Ptdppa-Cl$_2$** protons labelled $H_5$, $H_4$, $H_3$ and $H_2$ appear at δ = 8.82, 8.10, 7.55 and 7.28 ppm respectively with the $^{195}$Pt NMR peak at δ = -2178.9 ppm (**Figure 4.9**). The $^1$H and $^{195}$Pt NMR spectra show that within the time scale of the reaction only two main products had been formed. These are identified as uncoordinated **dppa** ligand with its aromatic protons appearing at δ = 8.29, 7.62, 7.11 and 6.93 ppm for $H_{5'}$, $H_{4'}$, $H_{3'}$ and $H_{2'}$ respectively and the $^{195}$Pt peak at δ = -3914.2 ppm corresponding to $Pt(TU)_4$. No intermediate peaks were observed in the $^{195}$Pt NMR spectra during the course of reaction thus, the coordinated aqua ligands are simultaneously substituted from Pt(II) centre in the first step. The disappearance of the original $^1$H and $^{195}$Pt NMR peaks of **Ptdppa-Cl$_2$** and the appearance of the $^{195}$Pt NMR peak at δ = 3914.2 ppm corresponding to $Pt(TU)_4$ all support the proposed reaction given in **Scheme 4.2**.

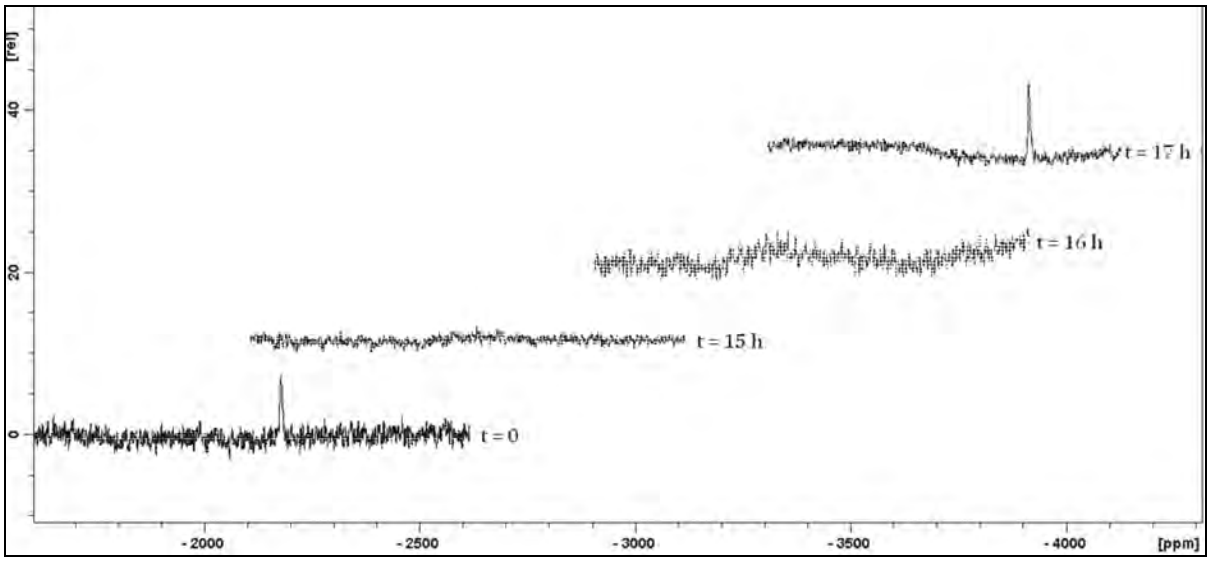


**Figure 4.9:** $^{195}$Pt NMR spectra of Ptdppa-$Cl_2$ acquired during the reaction with TU (2 and 3 equiv.) in DMSO-$d_6$, at 30 °C.

## 4.4 Discussion

As stated before all substitution reactions were characterized by two steps. The first step involves simultaneous displacement of the aqua ligands and the second step involved dechelation of the dipyridylalkylamine ligand following the coordination of further thiourea nucleophiles to the Pt(II) centre. This conclusion was arrived at after monitoring the reaction between **Ptdppa-$Cl_2$** and TU (excess) by $^{1}H$ and $^{195}Pt$ NMR spectroscopy.

It is well known from the literature that $^{195}Pt$ NMR is effective in identifying the species in the solution. The $^{195}Pt$ chemical shifts are influenced by all the ligands in the coordination sphere of the Pt atom and are highly sensitive to the nature of the binding atoms.[37,38] The σ-bond between the ligand and the metal (L→M) reduces the electron density on the ligand and increases it on the Pt atom. If there is a back-donation of π electrons (M→L), the electron density is then reduced on the Pt atom and is increased on the ligand. In lieu of most ligands, π-bonding is not very important, and a deshielding effect is observed on the ligand. For a series of Pt complexes, the resonance is shifted toward higher fields (more negative) when the donor atom varies from chlorine, nitrogen and sulfur in the following order Cl < N < S. Platinum complexes have chemical shifts of [$PtN_3Cl$] at δ = -1700 to -2369 ppm,[38,39,] [$PtN_2Cl_2$] at δ = -1900 to -2400 ppm,[38] [$PtN_3S$] at δ = -2800 to-3200 ppm,[39,40] [$PtN_2S_2$] at δ = -3100 to -3500 ppm[41] and [$PtS_4$] at δ = -3800 to -4800 ppm[38] while a value near δ = -5900 ppm is indicative of five coordinated sulfurs.[42] The peak of the unreacted **Ptdppa-$Cl_2$** at δ = -2178.9 and a new peak at δ = -3914.2 ppm are therefore, mainly due to [$PtN_2Cl_2$] and [$PtS_4$] after decoordination of dppa ligand. The assignment of these peaks in $^{195}Pt$ NMR spectra to [$PtN_2Cl_2$] and [$PtS_4$] coordination spheres is in agreement with that

reported in literature.[38,42] Furthermore, taking the solvent used into account, the chemical shifts of the aromatic protons in spectrum resulting after addition of TU (excess) to the **Ptdppa-Cl$_2$** correspond well with those of the **dppa** free ligand (**See Figure SI 4.26**).

Based on the $^{1}$H NMR spectroscopy together with $^{195}$Pt NMR results all support the proposed reaction **Scheme 4.2**. Therefore it is reasonable to conclude that the presence of strong labilizing thiourea nucleophiles at the Pt(II) centre enhances ring opening of the bidentate ligand attached to the metal centre leading to metal-ligand dissociation upon exposure to excess TU. Results on ring opening influenced by the strong labilizing effect of thiourea nucleophiles have been reported by Jaganyi *et al*.[28,43]

Taking the simultaneous substitution reaction of the aqua molecules with TU as a reference, the rate constant of the complexes (**Table 4.4**) decreases in the order of 38.7 > 36.8 > 23.7 > 20.6 > 16.0 $M^{-1}$ $s^{-1}$ for **Ptdpma**, **Ptdpea**, **ptdppa**, **ptdpba** and **Ptdpha** respectively. The difference in reactivity can be ascribed by the steric hindrance and electronic effect of the pendant alkyl chain bonded on the tertiary nitrogen joining the *cis* pyridine rings. In all the five complexes, the pendant alkyl chain on the tertiary nitrogen is sticking out of the plane blocking the approach of the nucleophile from either the top or bottom of the square planar geometry depending on its length. In **Ptdpma** and **Ptdpea**, the chain is not long enough to block the entry of the nucleophile from both sides so the nucleophile can easily attack the Pt(II) centre from either side resulting into higher rate of substitution reaction. However, for **Ptdppa**, **PtPtdpba** and **Ptdpha** the aliphatic chain is bending downwards and so blocks

the approach of the nucleophile from both sides of the square planar Pt(II) contributing to the lowering of reaction rate.

The individual HOMO and LUMO energies increase with an increase in alkyl chain length resulting into destabilization of the energies of both the HOMO and LUMO.[44] This affects electrophilicity of the complexes[45] as revealed in **Table 4.3** that the electrophilicity index decreases with an increase in σ-donicity of the aliphatic chain. The electronic effect of the alkyl chain to the tertiary nitrogen and to the pyridine nitrogen's is supported by their dipole moments and NBO charges shown in **Table 4.3**. The tertiary nitrogen becomes more negative with increase in alkyl chain length and so the pyridine nitrogen's. This causes the accumulation of the electron density into the LUMO type of the pyridyl rings making them weak π-acceptors hence less reactive Pt(II) centre towards substitution reaction. The decrease in reactivity of the complexes on moving from **Ptdpma** to **Ptdpha** in addition to the steric hindrance is also controlled by the σ-donation of electron density to the complex brought by the alkyl group through tertiary nitrogens which then destabilizes the transition state resulting into slow substitution reactions. On the other hand, slight changes in reactivity of the complexes with the increase in aliphatic chain length (from **Ptdppa** to **Ptdpha**) suggest that the bendiness of the chain reduces the sigma donation. The apparent increase in dipole moments by 1 debye with subsequent addition of -$(CH_2)_n$- fragment from **Ptdpma** to **Ptdpha** except from **Ptdppa** to **Ptdpba** where the increase is only 0.4 debye is expected given that the parameter correlate to the inductive negative charge in the complex.[46]

A comparison also reveals that dpa Pt(II) complexes are generally less reactive towards thiourea nucleophile by two orders of magnitude compared to bipyridine Pt(II) complex, **Pt(bpy)** reported preveously.[15d] This is because dpa is a less π-acceptor ligand than bipyridine (bpy).[47] In addition, dpa coordinates with six-membered chelate rings instead of five-membered rings for bpy thus **Pt(bpy)** complex is rigid and planar with both pyridine moieties situated within the plane resulting in a very efficient π-back donation of the incoming electron density from the nucleophile to the pyridine chelate.[15d] This stabilizes the five-coordinate transition state relative to the ground state, since the ground state cannot benefit much from the π-back donation given that the $6p_z$ orbital of the Pt centre is empty and hence enhancement of the reaction rate. On contrary, the bidentate chelate system in dpa Pt(II) complexes investigated in this study is more flexible adopting tilted pyridyl ring planes which then thwarts the flow of π-electrons around the ring rendering poor π-acceptor ability of the ligand and steric retardation on the metal centre towards the approach of the nucleophile.

The slower second substitution step can be ascribed to substitution of the labilised Pt-pyridinic N bonds *trans* positions to two TU molecules, as a result of the strong *trans* effect of S-donor nucleophiles following their coordination to the soft Pt(II) centre. Having a closer look on this second substitution step, it is forty times slower than the first step in all the investigated complexes. The presence of the two thiourea groups after the first substitution step makes the Pt(II) centre more crowded and sterically hindered. In addition due to the σ-donation of the thiourea towards the Pt(II) centre makes it difficult for another nucleophile to attack. This accounts for the observed slow rate of reaction in comparison to

the aqua substitution noting also that the leaving groups are different. This same reason explains why the second substitution reaction using the most sterically hindered tetramethyl thiourea (TMTU) nucleophile could not be followed.

Generally, the substitution of coordinated aqua ligands by the more sterically hindered nucleophiles DMTU and TMTU shows a clear dependence on the steric bulk of the nucleophiles.[28,43,48-49] For example, the values of the rate constants for the first substitution step of **Ptdpea** decrease in the order TU (36.8) > DMTU (28.5) > TMTU (16.7). The most sterically hindered nucleophile TMTU shows the lowest reactivity reflecting the steric effects characteristic of a mechanism involving bond making in the transition state. However, the first substitution step for **Ptdpma** shows that DMTU reacts faster than TU. This can be explained by the increase in basicity of its sulfur donor atom caused by the σ-donation of electrons by the two methyl group relative to that of TU which outweighs any steric contribution.[50]

For all investigated complexes, the enthalpies of activation, ($\Delta H^{\#}$), are small and positive whereas activation entropies, ($\Delta S^{\#}$) are large and negative. This confirms the associative mode of activation for all investigated complexes and substitution steps.[51]

## 4.5 Conclusion

The novel dpa Pt(II) complexes (**Ptdppa** and **Ptdpha**) and **Ptdpma**, **Ptdpea** and **Ptdpba** were synthesized and the kinetics of ligand substitution with thiourea nucleophiles were studied. In all complexes, two substitution steps were observed corresponding to the

simultaneous displacement of the aqua ligands and dechelation of the dpa ligand by thiourea nucleophiles. For both substitution steps, it was found that the reactivity of the metal centre decrease with the increase in length of aliphatic chain attached on the tertiary nitrogen bridging the *cis* coordinated pyridyl units. The trend in reactivity is attributed to the steric hindrance of the alkyl chain which blocks the attack of the nucleophile from either the top or bottom side of the Pt(II) centre.

In addition, the σ-donor effect of the pendant alkyl chain towards the tertiary bridging nitrogen is felt in the *cis* pyridine rings resulting into the decrease in their π-acceptor ability. The decrease in reactivity of the Pt(II) complexes with the increase in length of the alkyl chain is also supported by the dipole moments and the calculated electrophilicity indices. The decrease in enthalpy of activation, ($\Delta H^{\#}$) with an increase in the reaction rate and the more negative entropy of activation, ($\Delta S^{\#}$) is an indication of the low energy transition state compared to the reactant state. This enthalpies and entropies of activation confirm an associative mode of activation common in many Pt(II) complexes.

Furthermore, the systematic tuning of the 2,2'-dipyridylalkylamine chelate ligands as shown in this work represents the possibility of having Pt(II) complexes with different steric and electronic behaviour which might improve the cellular activity of the Pt(II) compared to cisplatin through increased cellular uptake brought by the surfactant effect of the alkyl chain. Possible concern is the likelihood of disintegration of these complexes if used as drugs based on the evidence of dechelation of the ligand.

## 4.6 References


1. Bose, D., Rahaman, S.H., Mostafa, G., Walsh, R.D.B., Zaworotko, M.J., Ghosh, B.K., *Polyhedron*., **2004**, *23*, 545.
2. Rahaman, S.H., Bose, D., Chowdhury, H., Mostafa, G., Fun, H.-K., Ghosh, B.K., *Polyhedron*., **2005**, *24*,1837.
3. Camus, A., Marsich, N., Lanfredi, A. M. M., Ugozzoli, F., Massera, C., *Inorg. Chim. Acta*., **2000**, *309*, 1.
4. Cotton, F.A., Daniels, L.M., Jordan, G.T., Murillo, C.A., *J. Am. Chem. Soc*., **1997**, *119* , 10377.
5. Yang, E.-C., Cheng, M.-C., Tsai, M.-S., Peng, S.-M., *Chem. Commun.,* **1994**, 2377.
6. Youngme, S., Chailuecha, C., van Albada, G.A., Pakawatchai, C., Chaichit, N., Reedijk, J., *Inorg. Chim. Acta.,* **2005***,* 358, 1068.
7. Sletten, J., Svardal, K., Sørensen, A., *Acta. Chem. Scand*., **1993**, *47*, 1091.
8. Paul, A. K., Mansuri-Torshizi, H., Srivastava, T. S., Chavan, S. J., Chitnis, M. P., *J. Inorg. Biochem*., **1993**, *50*, 9.
9. (a) Yodoshi, M., Okabe, N., *Chem. Pharm. Bull*., **2008**, *56*, 908; (b) Fakih, S., Tung, W. C., Eierhoff, D., Mock, C., Krebs, B., *Z. Anorg. Allg. Chem*., **2005**, *631*, 1397.
10. (a) Grehl, M., Krebs, B., *Inorg. Chem*., **1994**, *33*, 3877; (b) Puscasu, I., Mock, C., Rauterkus, M., Röndigs, A., Tallen, G., Gangopadhyay, S., Wolff, J. E. A., Krebs, B., *Z. Anorg. Allg. Chem*., **2001**, *627*, 1292; (c) Bloemink, M. J., Engelking, H., Gütschow, N., Karentzopoulos, S., Krebs, B., Reedijk, J., *J. Inorg. Biochem*., **1995**, *59*, 222; (d)

Rauterkus, M. J., Fakih, S., Mock, C., Puscasu, I., Krebs, B., *Inorg. Chim. Acta.,* **2003,** *350*, 355.

11. Mock, C., Puscasu, I., Rauterkus, M. J., Tallen, G., Wolff, J. E. A., Krebs, B., *Inorg. Chim. Acta*., **2001**, *319*, 109.

12. Bloemink, M. J., Engelking, H., Karentzopoulos, S., Krebs, B., Reedijk, J., *Inorg. Chem.,* **1996**, *35,* 619.

13. Gangopadhyay, S. B., Röndigs, A., Kangarloo, S. B., Krebs, B., Wolff, J. E. A., *Anticancer Res*., **2001**, *21*, 2039.

14. Tallen, G., Mock, C., Gangopadhyay, S. B., Kangarloo, B., Krebs, B., Wolff, J. E. A., *Anticancer Res.,* **2000**, *20*, 445.

15. (a) Bogojeski, J., Bugarčić, Ź. D., Puchta, R., and van Eldik, R.., *Eur. J. Inorg. Chem.,* **2010**, 5439; (b) Jovanović, S., Petrović, B., Čanović, D. and Bugarčić, Ž. D., *Int. J. Chem. Kinet*., **2011**, *43*,99; (c) Hochreuther, S., Nandibewoor, S. T., Puchta, R., van Eldik, R., *Dalton Trans*., **2012**, *41*(2), 512; (d) Summa, N., Schiessl, W., Puchta, R., van Eikema Hommes, N. and van Eldik, R., *Inorg. Chem*., **2006**, *45*, 2948.; (e) Soldatoví, T., Bugarčić, Ž. D, and van Eldik, R., *Dalton Trans*., **2009**, 4526.

16. Schreier, S., Malheiros, S. V. P., de Paula, E., *Biochim. Biophys. Acta-Biomembranes.*, **2000**, *1508*, 210.

17. (a) Ashby, M. T., *Comments Inorg. Chem.*, **1990**, *10*, 297;(b) Murray, S. G. and Hartley, F. R., *Chem. Rev.*, **1981**, *81*, 365; (c) Reedijk, J., *Chem. Rev.*, **1999**, *99*, 2499.

18 Schiessl, W. C., Summa, N. K., Weber, C. F., Gubo, S., Dücker-Benfer, C., Puchta, R., van Eikema Hommes, N. J. R. and van Eldik, R., *Z. Anorg. Allg. Chem*., **2005**, *631*, 2812.

19 Ashby, M. T., *Comments. Inorg. Chem*., **1990**, *10*, 297.

20 Murray, S. G and Hartley, F. R., *Chem. Rev*., **1981**, *81*, 365.

21. Origin7.5TM v7.5714 (B5714), Origin Lab Corporation, Northampton, One, Northampton, MA, 01060, USA, **2003**.

22. Frisch, M. J., Trucks, G. W., Schlegel, H. B., Scuseria, G. E., Robb, M. A., Cheeseman, J. R., Scalmani, G., Barone, V., Mennucci, B., Petersson, G. A., Nakatsuji, H., Caricato, M., Li, X., Hratchian, H. P., Izmaylov, A. F., Bloino, J., Zheng, G., Sonnenberg, J. L., Hada, M., Ehara, M., Toyota, K., Fukuda, R., Hasegawa, J., Ishida, M., Nakajima, T., Honda, Y., Kitao, O., Nakai, H., Vreven, T., Montgomery, J. A., Peralta, J. E., Ogliaro, F., Bearpark, M., Heyd, J. J., Brothers, E., Kudin, K. N., Staroverov, V. N., Kobayashi, R., Normand, J., Raghavachari, K., Rendell, A., Burant, J. C., Iyengar, S. S., Tomasi, J., Cossi, M., Rega, N., Millam, J. M., Klene, M., Knox, J. E., Cross, J. B., Bakken, V., Adamo, C., Jaramillo, J., Gomperts, R., Stratmann, R. E., Yazyev, O., Austin, A. J., Cammi, R., Pomelli, C., Ochterski, J. W., Martin, R. L., Morokuma, K., Zakrzewski, V. G., Voth, G. A., Salvador, P., Dannenberg, J. J., Dapprich, S., Daniels, A. D., Farkas, O., Foresman, J. B., Ortiz, J. V., Cioslowski, J., and Fox, D. J., *Gaussian 09, Revision A.1*, Gaussian, Inc., Wallingford CT, **2009**.

23. Becke, A. D., *J. Chem .Phys.*, **1997**, *107*, 8554.

24. Lee, C., Yang, W. Parr, G. R., *Phys. Rev., B.*, **1988**, *37*, 785.

25. Miehlich, B., Savin, A., Stoll, H., and Preuss, H., *Chem. Phys. Lett.*, **1989**, 157, 200.

26. Hay, P. J, Wadt, W. R., *J. Chem .Phys.,* **1985**, *82*, 299.

27. Soldatović, T., Jovanović, S., Bugarčić, Ž. D., van Eldik, R., *Dalton Trans*., **2012**, *41*(3), 876.

28. Mambanda, A and Jaganyi, D. *Dalton Trans.*, **2012**, *41*, 908.

29. Hofmann, A., van Eldik, R., *Dalton Trans.*, **2003**, 2979.

30. Hofmann, A., Jaganyi, D., Munro, O. Q., Liehr, G., van Eldik, R., *Inorg Chem.*, **2003**, *42*, 1688.

31. Kumar, L. and Srivastava, T.S. *Inorg. Chim. Acta.*, **1983**, *80*, 47.

32. Kidani, Y., Asano, Y. and Noji, M. *Chem. Pharm. Bull*., **1979**, *27*, 2577.

33. Dehand, J., Jordanov, J. *J. Chem. Soc., Chem. Comm*., **1976**, 598.

34. Howell, B. A., Walles, E. *Inorg. Chim. Acta*., **1988**, *142*, 185.

35. Mebi, C., A *J. Chem. Sci.,* **2011**, *123*(5), 727.

36. (a) Espenson J. H., *Chemical Kinetics and Reaction Mechanisms*, **1995**, 2nd edn McGraw-Hill, New York, Chapter 2 and 6; (b) Eyring, H., *J. Chem. Phys*., **1935**, *3*, 107.

37. Fazlur-Rahman, A. K. and Verkade, J. G., *Inorg. Chem*., **1992**, *31*, 2064.

38. Priqueler, J. R. L., Butler, I. S., Rochon, F. D., *Applied Spectroscopy Reviews.*, **2006**, *41*, 185.

39. Ma G, Min Y, Huang F, Jiang T, Liu Y. *Chem Commun (Camb*)., **2010**, *46*(37):6938.

40. (a) Crossley, E. L, Caiazza, D. and Rendina, L. M., *Dalton Trans.*, **2005**, 2825;
(b) Todd, J. A. and Rendina, L. M., *Inorg. Chem*., **2002**, *41*, 3331.

41. (a) Norman, R. E., Ranford, J. D., and Sadler, P. J., *Inorg.Chem*., **1992**,*31*, 877;

(b) Todd, J. A., Caiazza, D., Tiekink, E. R. T, Rendina, L. M. *Inorg. Chim. Acta.,* **2003**, *352,* 208.; (c) Appleton, T. G., Connor, J. W., Hall, J. R., and Prenzler, P. D., *Inorg. Chem*., **1989**, *28*, 2030.

42. Grant, G. J., Brandow, C. G., Galas, D. F., Davis, J. P., Pennington, W. T., Valente E. J., Zubkowski, J. D., *Polyhedron.*, **2001**, *20*, 3333.

43. (a) Jaganyi, D and Ongoma, P., *Dalton Trans*., **2013**, *42*, 2724; (b) Ertürk, H., Puchta, R., and van Eldik, R., *Eur. J. Inorg. Chem.,* **2009**, 1331.

44. (a) Salzner, U. and Kızıltepe, T., *J. Org. Chem.,* **1999**, *64,* 764; (b) Kistler, K. A. and Matsika, S., *J. Phys. Chem. A*., **2007**, *111,* 8708; (c) Mburu, E. and Matsika, S., *J. Phys. Chem. A*., **2008**, *112*, 12485.

45. Singh, R. K., Verma, S. K. and Sharma, P. D., *Int. J. ChemTech Res*., **2011**, *3*(3), 1571.

46. Das, M. and Livingstone, S. E., *J. Chem. Soc., Dalton Trans.*, **1975**, 452.

47. (a) Mittal, S. K., Kumar, P., Ashok Kumar S. K and Lindoy, L. F. *Int. J. Electrochem. Sci.,* **2010**, *5*, 1984; (b) Shepherd, R.E., Chen, Y., Kortes, R. A., Ward, M. S., *Inorganica Chimica Acta*., **2000**, *303*, 30.

48. Jaganyi, D. and Tiba, F., *Transition Met. Chem.*, **2003**, *28*, 803.

49. Jaganyi, D. Reddy, D., Gertenbach, J. A., Munro, O. Q. and van Eldik, R., *Dalton Trans.*, **2004**, 299.

50. Bruice, P. Y., *Organic Chemistry*, 2nd Edn, Prentice Hall, New York, **1998**, pg. 363–366.

51. Tobe, M. L. and Burgess, J., *Inorganic Reaction Mechanisms*, Addison-Wiley, Longman, Ltd., Essex, **1999**, pg. 30–33, 70–112.

## 4.7 Supporting Information (SI)

Representative NMR, mass spectra and pH titration spectra, summary of wavelengths used for kinetics, concentration dependence and Eyring plots and HOMO-LUMO energy diagram of the investigated complexes in this chapter are reported below.

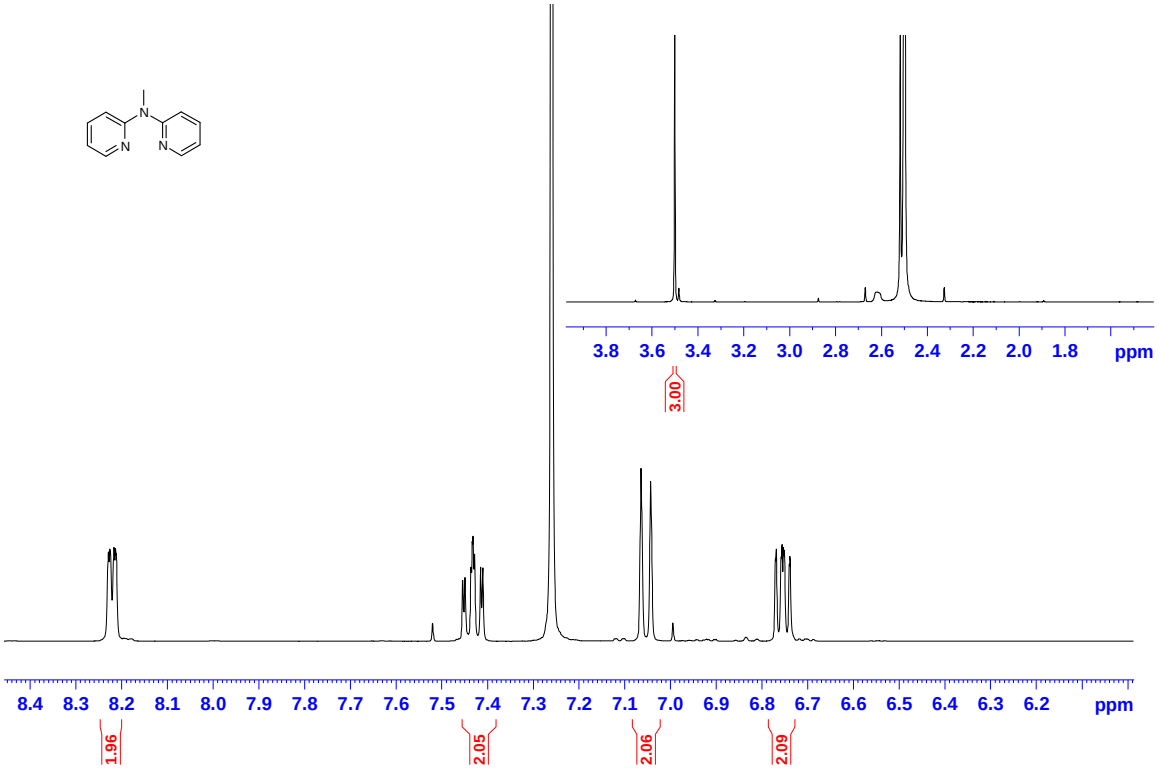


**Figure SI 4.1**: $^{1}H$ NMR spectrum for **dpma** ligand in $CHCl_3$

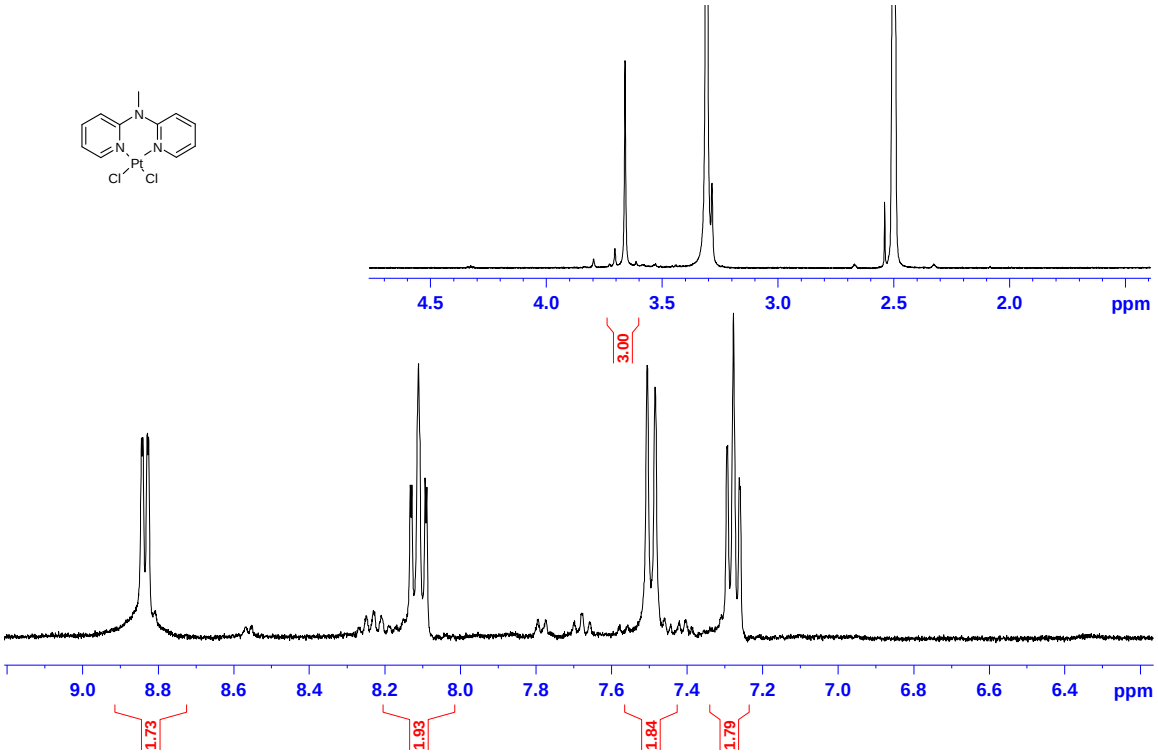


**Figure SI 4.2**: $^{1}$H NMR spectrum for **Ptdpma** in DMSO.

Monoisotopic Mass, Even Electron Ions
18 formula(e) evaluated with 1 results within limits (all results (up to 1000) for each mass)
Elements Used:
C: 10-15 H: 10-15 N: 0-5 Na: 0-1 Cl: 2-2 Pt: 0-1

Grace Kinunda
Ptdpma 2 (0.017) Cm (1:31)

TOF MS ES+
1.45e+004

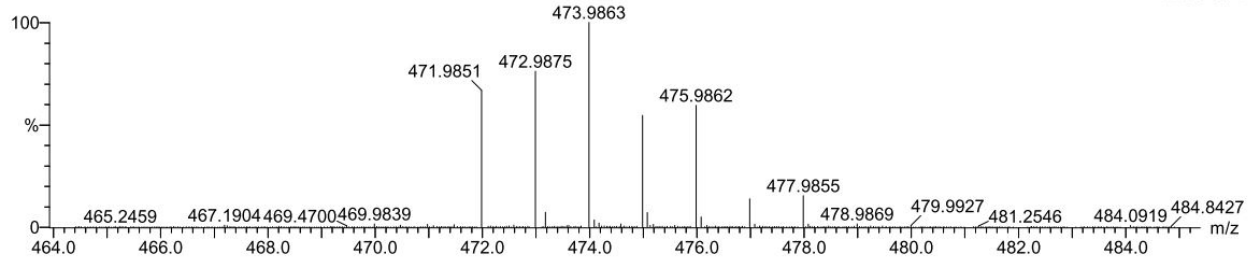


| | | | | | | | |
|---|---|---|---|---|---|---|---|
| Minimum: | | | | -1.5 | | | |
| Maximum: | | 5.0 | 5.0 | 50.0 | | | |
| Mass | Calc. Mass | mDa | PPM | DBE | i-FIT | i-FIT (Norm) | Formula |
| 472.9875 | 472.9876 | -0.1 | -0.2 | 7.5 | 459.0 | 0.0 | C11 H11 N3 Na Cl2 Pt |

**Figure SI 4.3**: Mass spectrum for **Ptdpma** in DMSO.

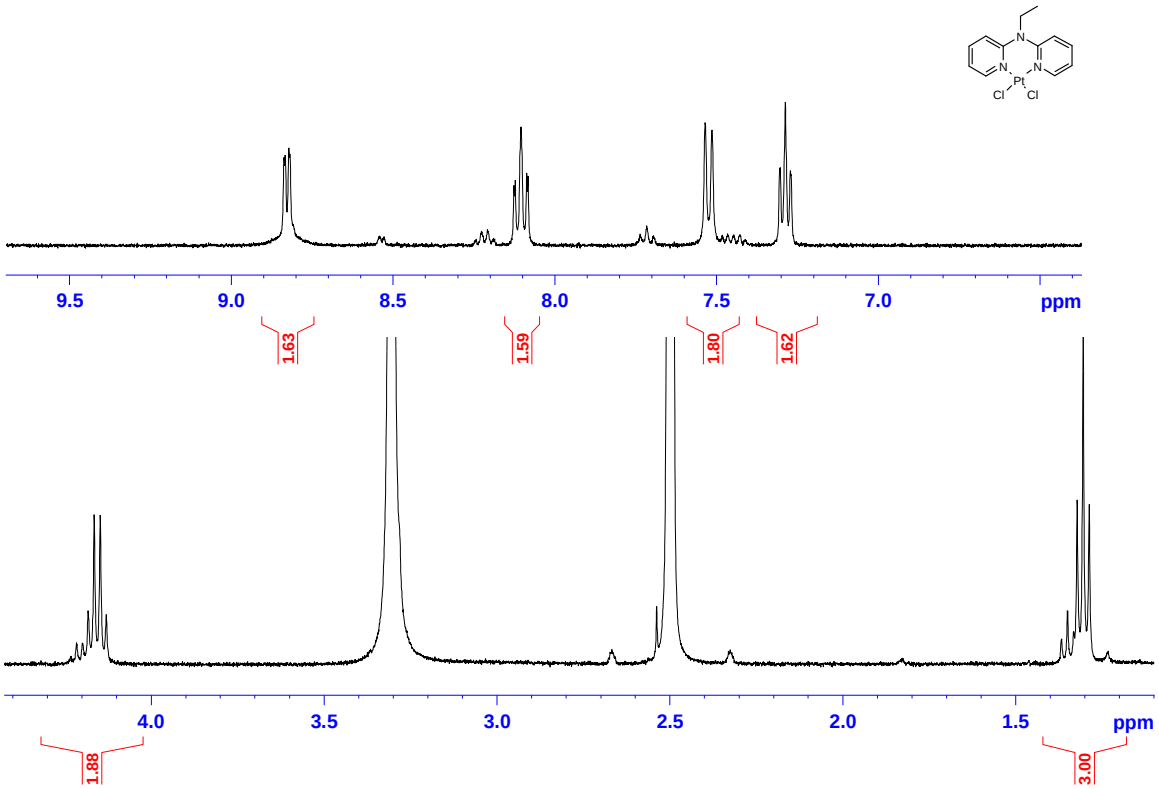


**Figure SI 4.4**: $^{1}$H NMR spectrum for **Ptdpea** in DMSO.

Monoisotopic Mass, Even Electron Ions
15 formula(e) evaluated with 1 results within limits (all results (up to 1000) for each mass)
Elements Used:
C: 10-15 H: 13-15 N: 0-5 Na: 0-1 Cl: 2-2 Pt: 0-1

Grace Kinunda
Ptdpea 25 (0.410) Cm (1:31)

TOF MS ES+
4.53e+004

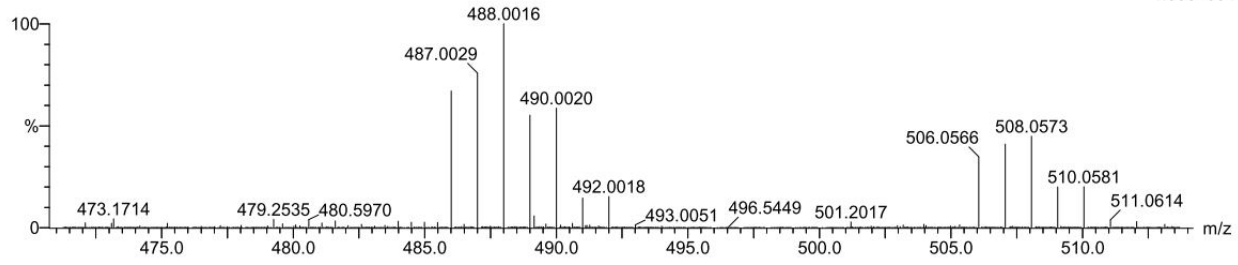


| | | | | | | | |
|---|---|---|---|---|---|---|---|
| Minimum: | | | | -1.5 | | | |
| Maximum: | | 5.0 | 50000.0 | 50.0 | | | |
| Mass | Calc. Mass | mDa | PPM | DBE | i-FIT | i-FIT (Norm) | Formula |
| 487.0029 | 487.0032 | -0.3 | -0.6 | 7.5 | 466.9 | 0.0 | C12 H13 N3 Na Cl2 Pt |

**Figure SI 4.5**: Mass spectrum for **Ptdpea** in DMSO.

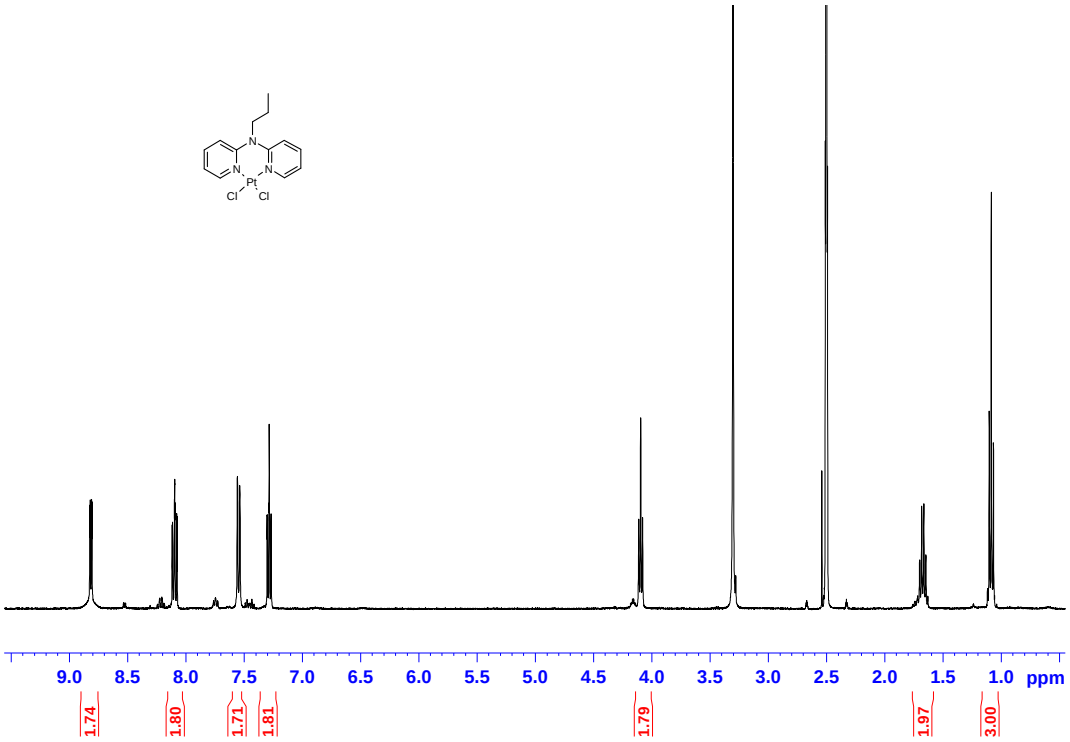


**Figure SI 4.6**: $^{1}$H NMR spectrum for **Ptdppa** in DMSO.

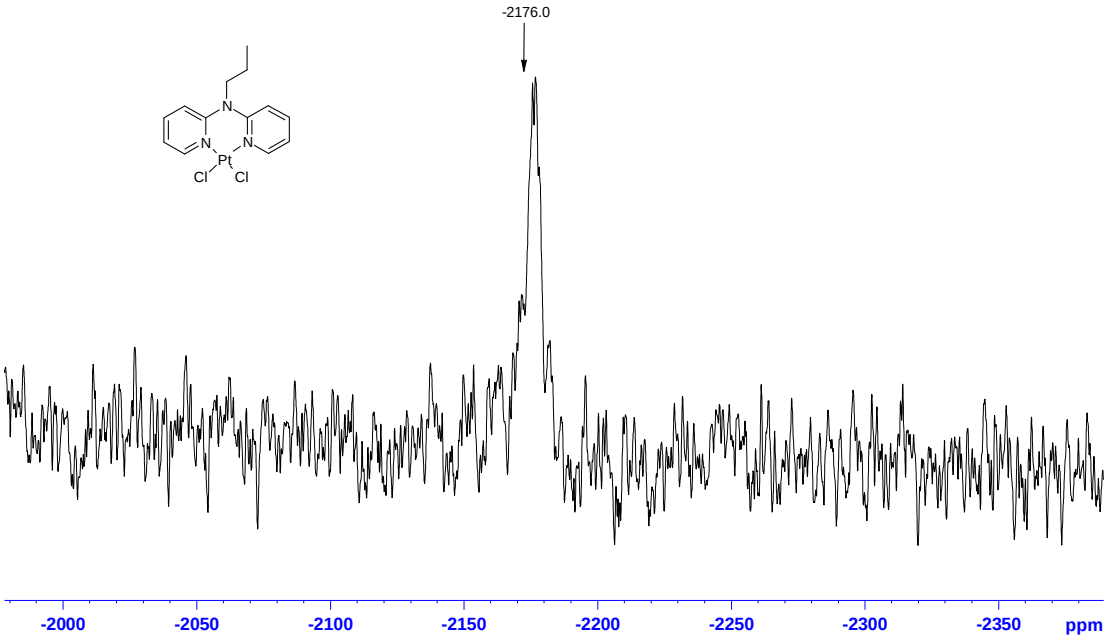


**Figure SI 4.7**: $^{195}$Pt NMR spectrum for **Ptdppa** in DMSO.

Monoisotopic Mass, Even Electron Ions
19 formula(e) evaluated with 1 results within limits (all results (up to 1000) for each mass)
Elements Used:
C: 10-15 H: 10-15 N: 0-5 Na: 0-1 Cl: 2-2 Pt: 0-1

Grace Kinunda
Ptdppa 2 (0.017) Cm (1:30)

TOF MS ES+
2.91e+004

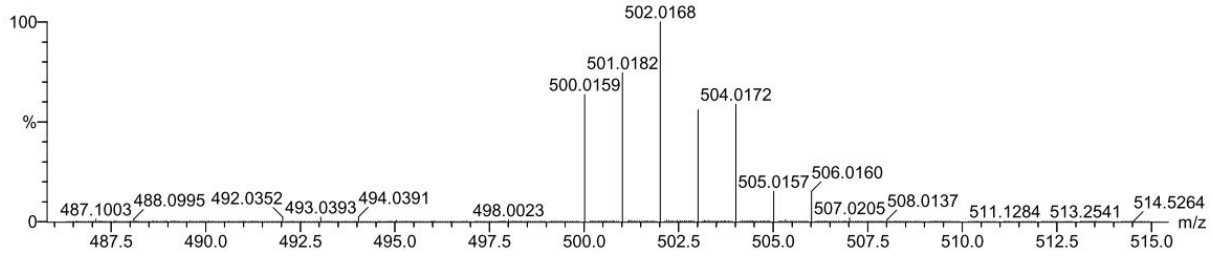


| | | | | | | | |
|---|---|---|---|---|---|---|---|
| Minimum: | | | | -1.5 | | | |
| Maximum: | | 5.0 | 5.0 | 50.0 | | | |
| Mass | Calc. Mass | mDa | PPM | DBE | i-FIT | i-FIT (Norm) | Formula |
| 501.0182 | 501.0189 | -0.7 | -1.4 | 7.5 | 453.8 | 0.0 | C13 H15 N3 Na Cl2 Pt |

**Figure SI 4.8**: Mass spectrum for **Ptdppa** in DMSO.

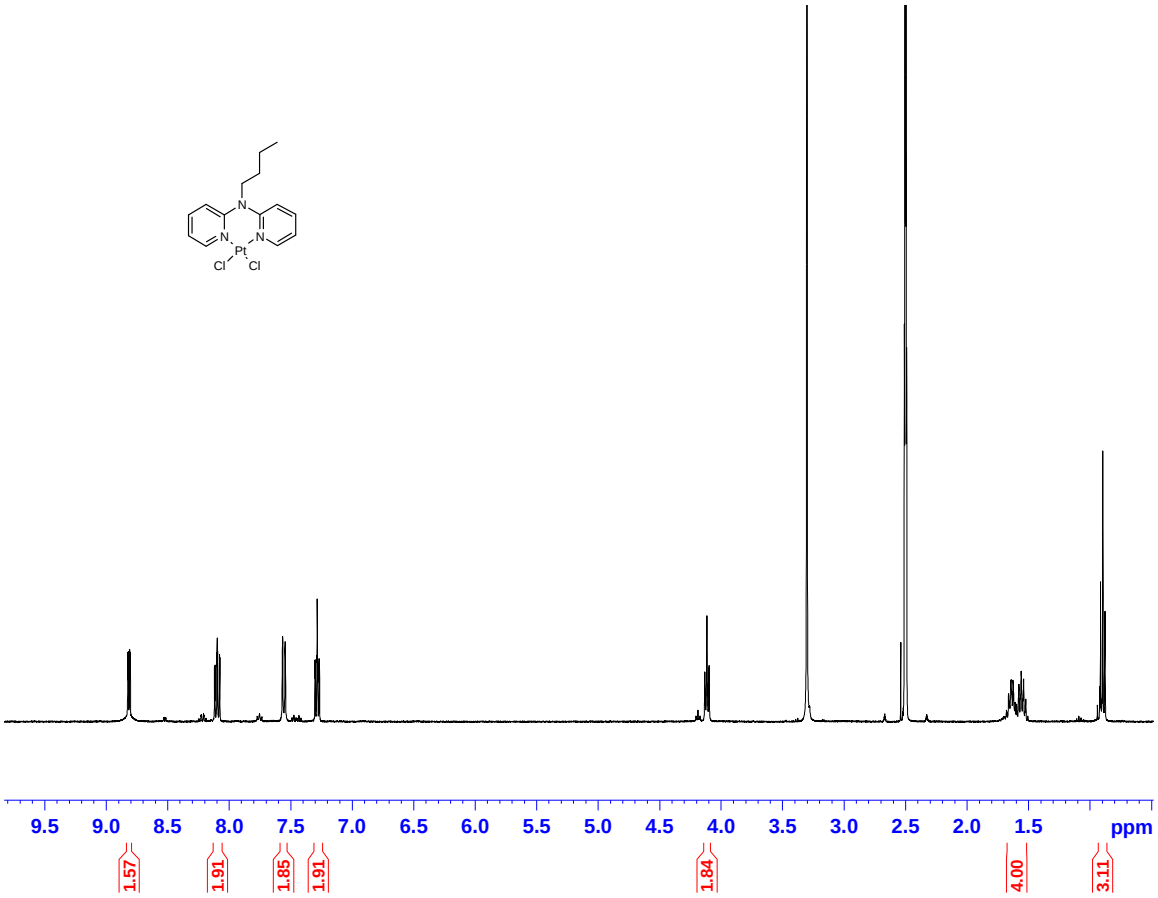


**Figure SI 4.9**: $^{1}$H NMR spectrum for **Ptdpba** in DMSO.

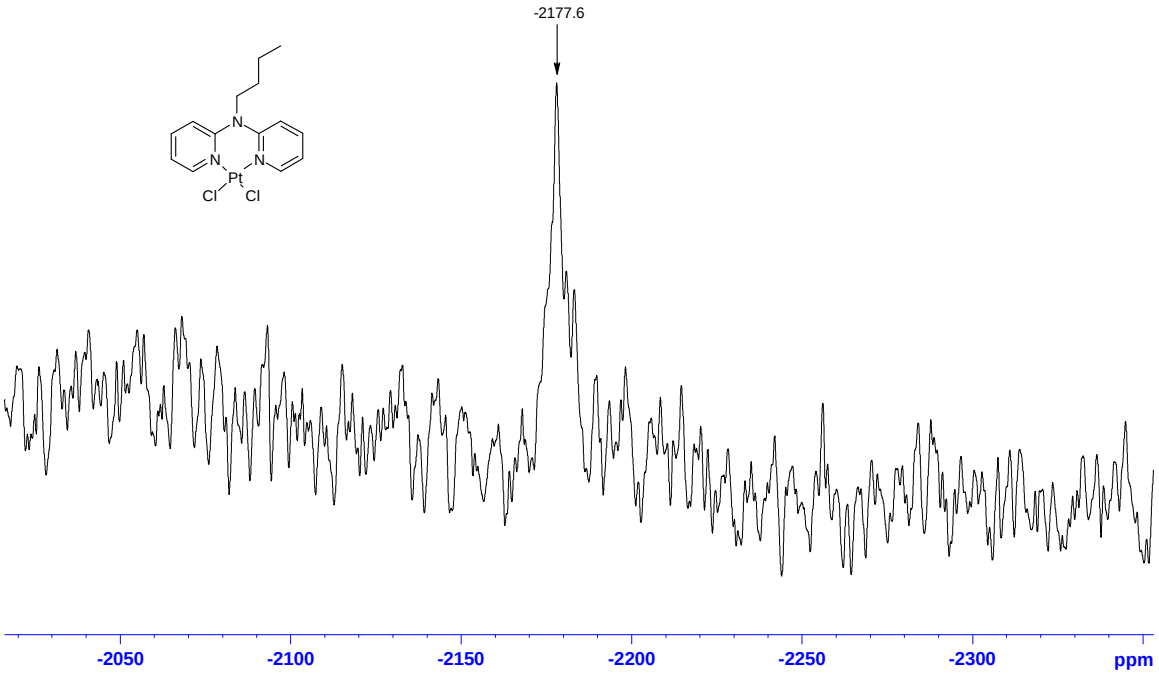


**Figure SI 4.10**: $^{195}$Pt NMR spectrum for **Ptdpba** in DMSO.

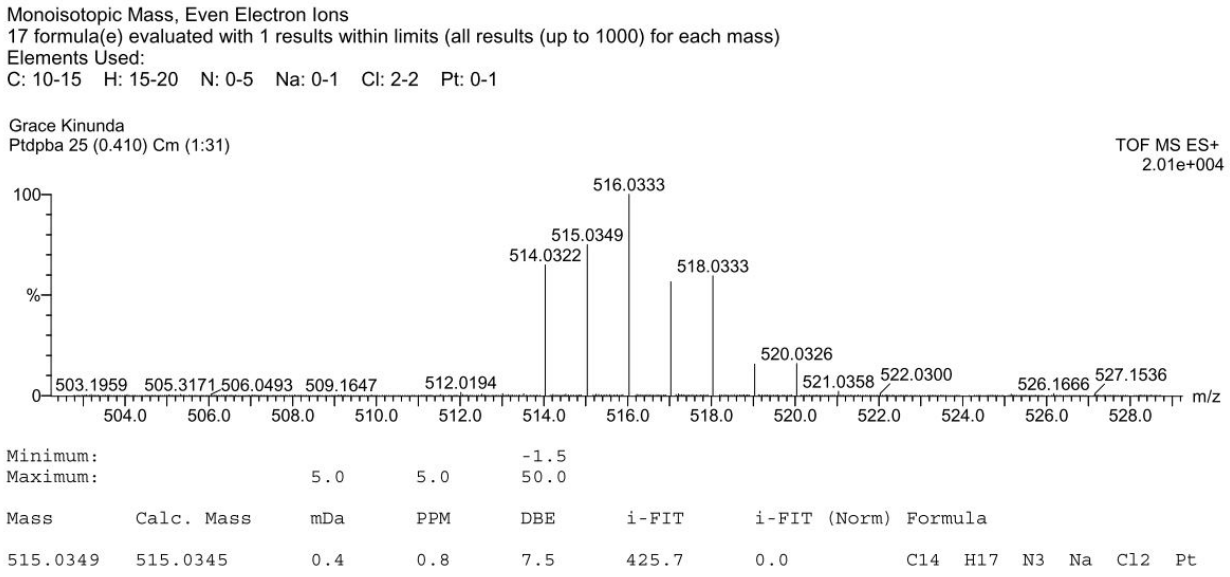


| | | | | | | | |
|---|---|---|---|---|---|---|---|
| Minimum: | | | | -1.5 | | | |
| Maximum: | | 5.0 | 5.0 | 50.0 | | | |
| Mass | Calc. Mass | mDa | PPM | DBE | i-FIT | i-FIT (Norm) | Formula |
| 515.0349 | 515.0345 | 0.4 | 0.8 | 7.5 | 425.7 | 0.0 | C14 H17 N3 Na Cl2 Pt |

**Figure SI 4.11**: Mass spectrum for **Ptdpba** in DMSO.

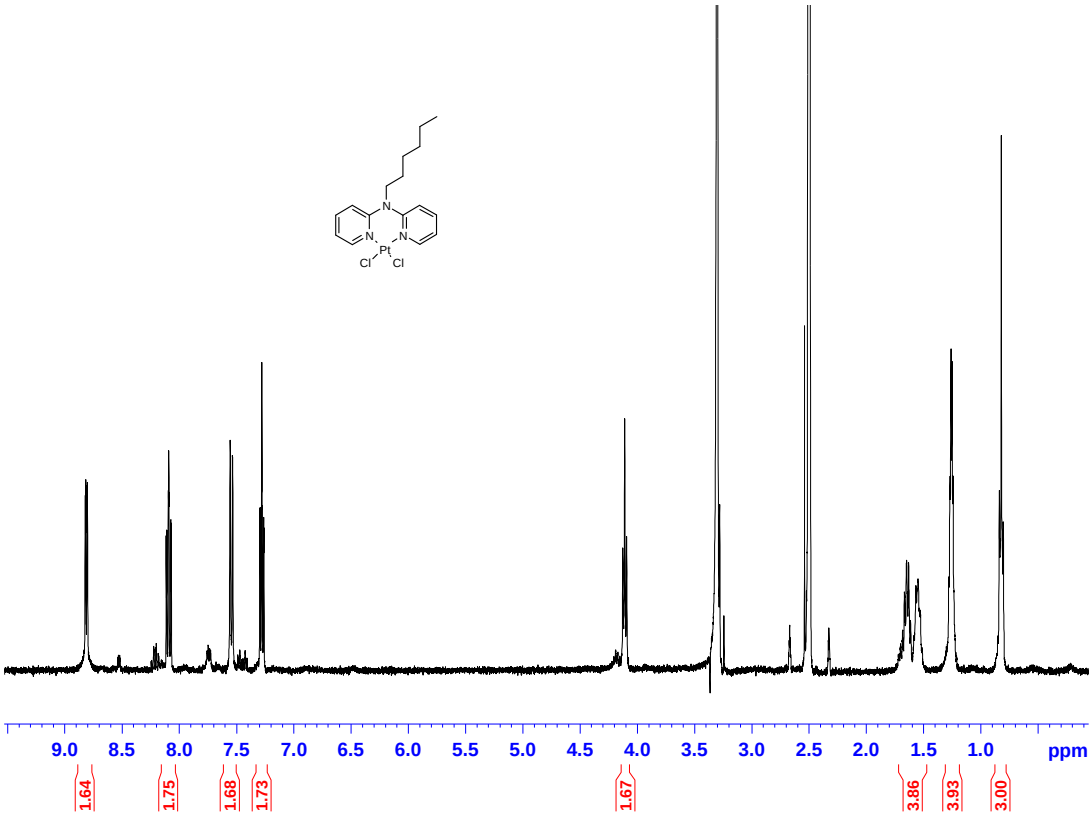


**Figure SI 4.12**: $^{1}$H NMR spectrum for **Ptdpha** in DMSO.

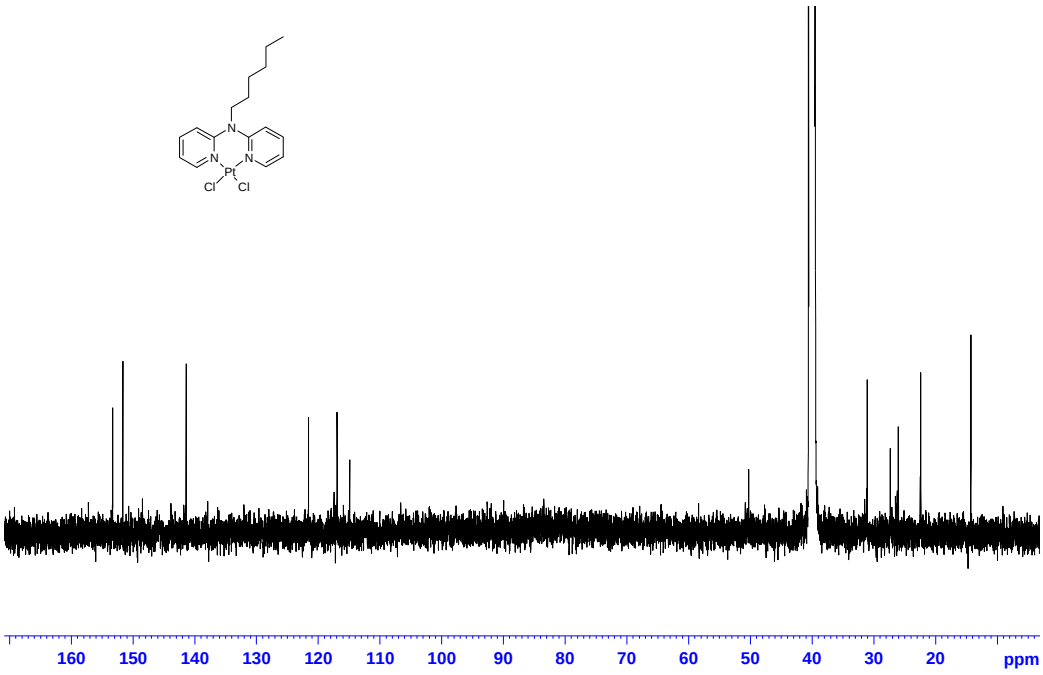


**Figure SI 4.13**: $^{13}$C spectrum for **Ptdpha** in DMSO.

Monoisotopic Mass, Even Electron Ions
15 formula(e) evaluated with 1 results within limits (all results (up to 1000) for each mass)
Elements Used:
C: 15-17 H: 20-25 N: 0-5 Na: 0-1 Cl: 2-2 Pt: 0-1

Grace Kinunda
Ptdpha 2 (0.017) Cm (1:31)

TOF MS ES+
7.90e+003

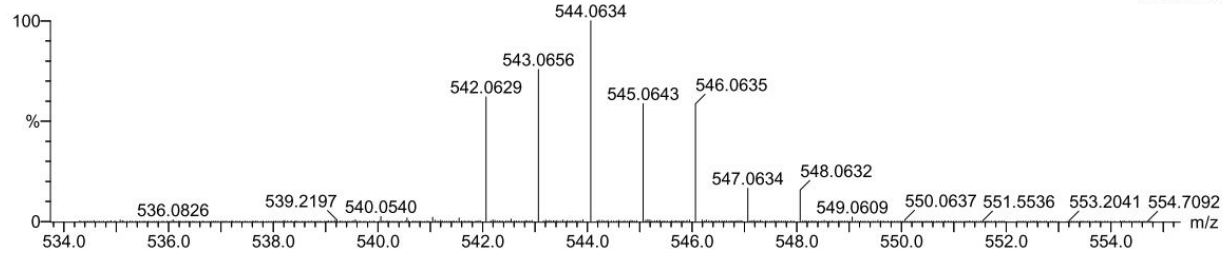


| Minimum: | | | | -1.5 | | | | | | | |
|---|---|---|---|---|---|---|---|---|---|---|---|
| Maximum: | | 5.0 | 5.0 | 50.0 | | | | | | | |
| Mass | Calc. Mass | mDa | PPM | DBE | i-FIT | i-FIT (Norm) | Formula | | | | |
| 543.0656 | 543.0658 | -0.2 | -0.4 | 7.5 | 380.1 | 0.0 | C16 | H21 | N3 | Na | Cl2 | Pt |

**Figure SI 4.14**: Mass spectrum for **Ptdpha** in DMSO.

**Table SI 4.1**. Summary of the selected wavelength used for kinetics studies for the first and second substitution steps.

| **Complex** | **Nucleophiles** | **Wavelength, (nm)** | |
|---|---|---|---|
| | | 1st step | 2nd step |
| **Ptdpma** | TU | 286 | 314 |
| | DMTU | 286 | 330 |
| | TMTU | 365 | 365 |
| **Ptdpea** | TU | 290 | 340 |
| | DMTU | 286 | 345 |
| | TMTU | 355 | 360 |
| **Ptdppa** | TU | 290 | 315 |
| | DMTU | 287 | 330 |
| | TMTU | 355 | 355 |
| **Ptdpba** | TU | 290 | 310 |
| | DMTU | 287 | 335 |
| | TMTU | 357 | 355 |
| **Ptdpha** | TU | 290 | 315 |
| | DMTU | 286 | 330 |
| | TMTU | 354 | 365 |

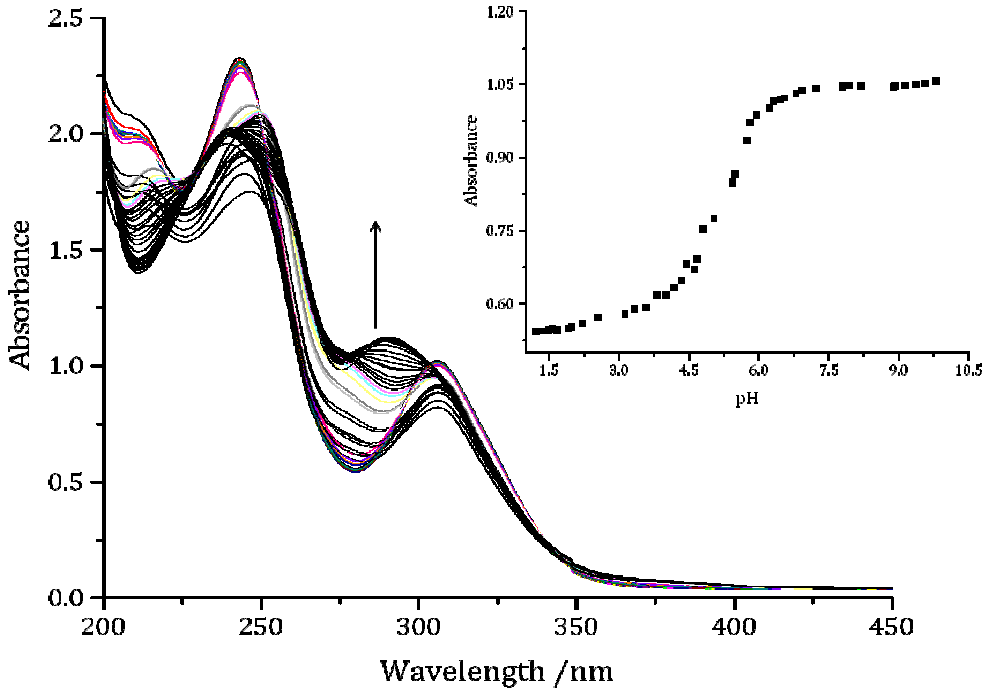


**Figure SI 4.15**: UV-Vis spectra of the **Ptdpma** diaqua complex recorded as a function of pH in the range 1 to 10. *Inset*: Plot of absorbance versus pH at 280 nm for the **Ptdpma** diaqua complex.

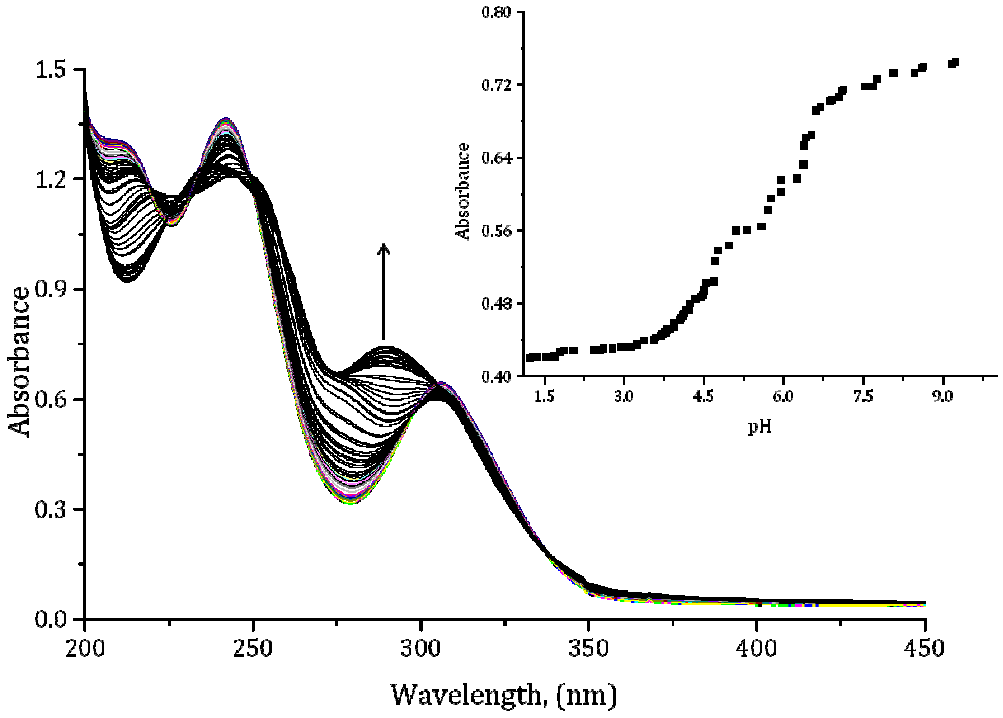


**Figure SI 4.16**: UV-Vis spectra of the **Ptdpea** diaqua complex recorded as a function of pH in the range 1 to 10. *Inset*: Plot of absorbance versus pH at 290 nm for the **Ptdpea** diaqua complex.

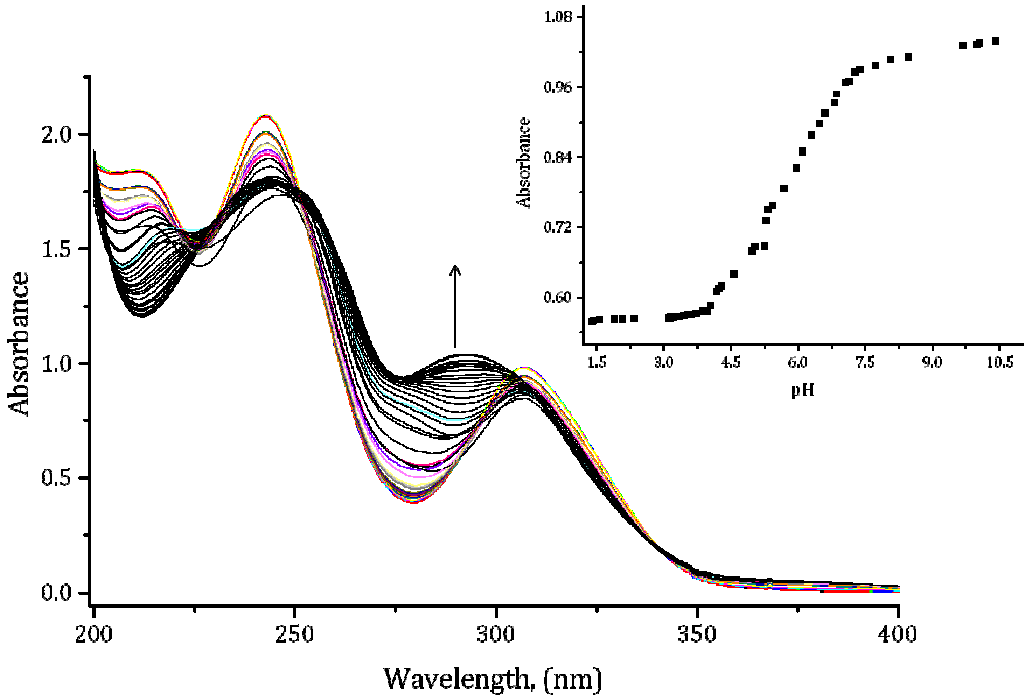


**Figure SI 4.17**: UV-Vis spectra of the **Ptdppa** diaqua complex recorded as a function of pH in the range 1 to 10. *Inset*: Plot of absorbance versus pH at 290 nm for the **Ptdppa** diaqua complex.

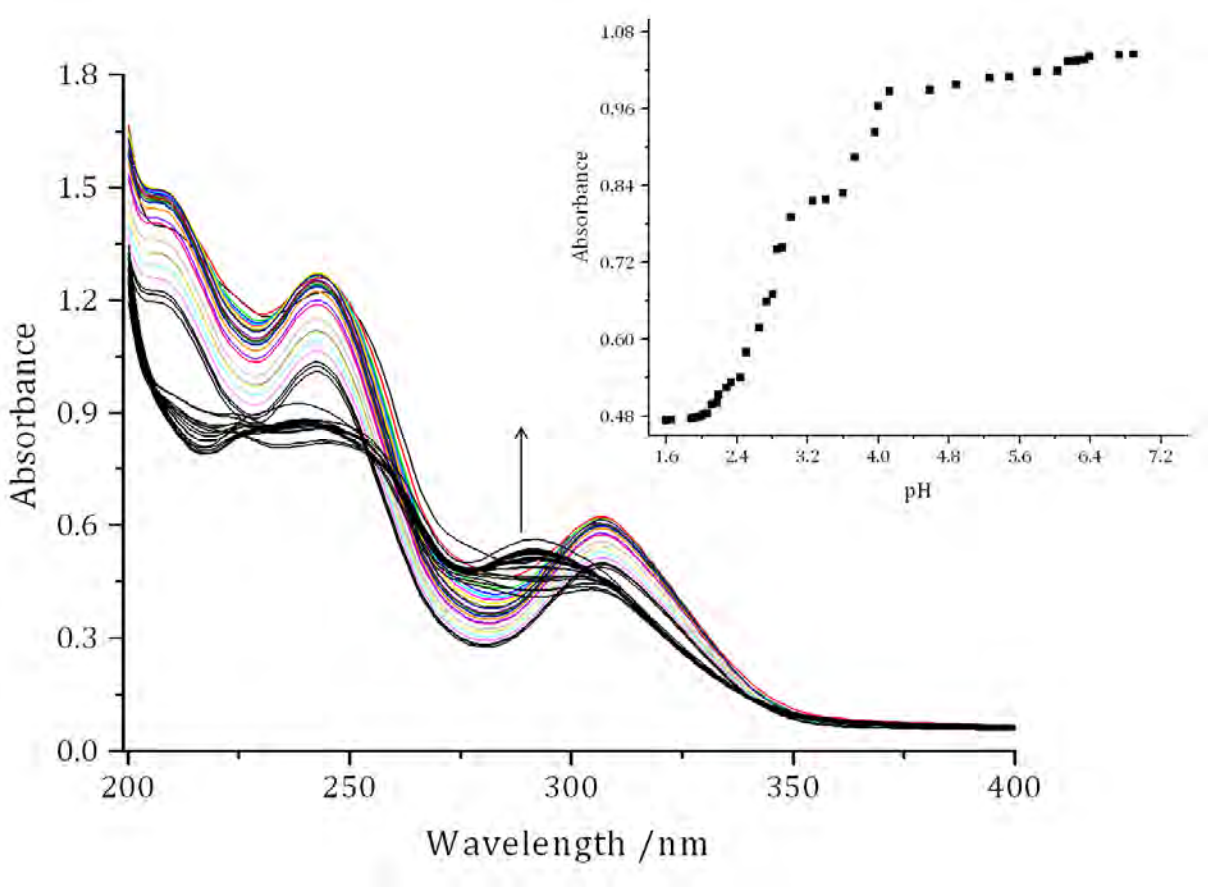


**Figure SI 4.18**: UV-Vis spectra of the **Ptdpha** diaqua complex recorded as a function of pH in the range 1 to 8. *Inset*: Plot of absorbance versus pH at 260 nm.

**Table SI 4.2**: Average observed rate constants, $k_{obs}$, $s^{-1}$, for the first displacement of the aqua ligands in **Ptdpma**, **Ptdpea**, **Ptdppa**, **Ptdpba** and **Ptdpha** by thiourea, (TU) nucleophile, T = 298 K, pH = 2, $I$ = 0.1 M $NaClO_4$

| **Ptdpma** | | **Ptdpea** | | **Ptdppa** | | **Ptdpba** | | **Ptdpha** | |
|---|---|---|---|---|---|---|---|---|---|
| **[TU] /M** | $k_{obs}$ **/$s^{-1}$** | **[TU] /M** | $k_{obs}$ **/$s^{-1}$** | **[TU] /M** | $k_{obs}$ **/$s^{-1}$** | **[TU] /M** | $k_{obs}$ **/$s^{-1}$** | **[TU] /M** | $k_{obs}$ **/$s^{-1}$** |
| 0.005 | 0.184 | 0.0018 | 0.063 | 0.005 | 0.13 | 0.005 | 0.112 | 0.005 | 0.081 |
| 0.0075 | 0.291 | 0.0027 | 0.094 | 0.0075 | 0.177 | 0.0075 | 0.151 | 0.0075 | 0.114 |
| 0.01 | 0.397 | 0.0036 | 0.134 | 0.01 | 0.230 | 0.01 | 0.205 | 0.01 | 0.159 |
| 0.0125 | 0.501 | 0.0045 | 0.159 | 0.0125 | 0.294 | 0.0125 | 0.250 | 0.0125 | 0.200 |
| 0.015 | 0.563 | 0.0054 | 0.206 | 0.015 | 0.356 | 0.015 | 0.314 | 0.015 | 0.2411 |

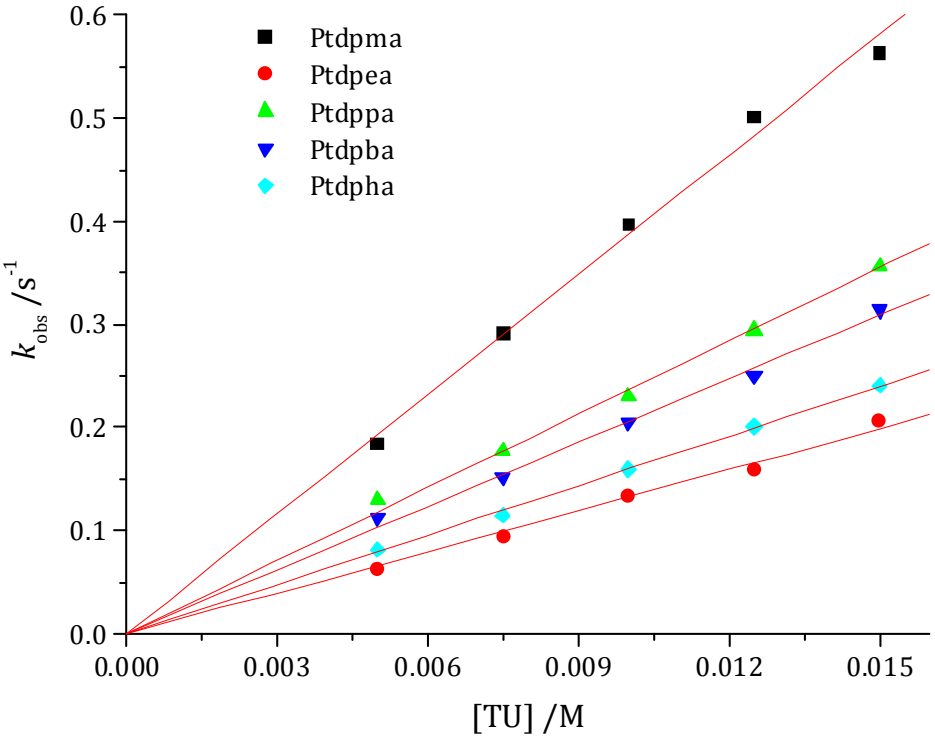


**Figure SI 4.19**: Dependence of $k_{obs}$ on the entering TU nucleophile for the first displacement of the aqua ligands in **Ptdpma**, **Ptdpea**, **Ptdppa**, **Ptdpba** and **Ptdpha** by thiourea, (TU) nucleophile, T = 298 K, pH = 2, $I$ = 0.1 M NaClO4.

**Table SI 4.3**: $k_{obs}$, $s^{-1}$, for the first displacement of the aqua ligands in **Ptdpma**, **Ptdpea**, **Ptdppa**, **Ptdpba** and **Ptdpha** by dimethylthiourea, (DMTU) nucleophile, T = 298 K, pH = 2, $I$ = 0.1 M $NaClO_4$.

| | **Ptdpma** | **Ptdpea** | **Ptdppa** | **Ptdpba** | **Ptdpha** |
|---|---|---|---|---|---|
| **[DMTU] /M** | $k_{obs}$, **$s^{-1}$** | $k_{obs}$, **$s^{-1}$** | $k_{obs}$, **$s^{-1}$** | $k_{obs}$, **$s^{-1}$** | $k_{obs}$, **$s^{-1}$** |
| 0.005 | 0.246 | 0.045 | 0.1033 | 0.09451 | 0.06997 |
| 0.0075 | 0.347 | 0.0756 | 0.13738 | 0.12352 | 0.10825 |
| 0.01 | 0.493 | 0.105 | 0.19152 | 0.17358 | 0.14894 |
| 0.0125 | 0.604 | 0.123 | 0.22413 | 0.20868 | 0.18283 |
| 0.015 | 0.744 | 0.160 | 0.2899 | 0.25669 | 0.23098 |

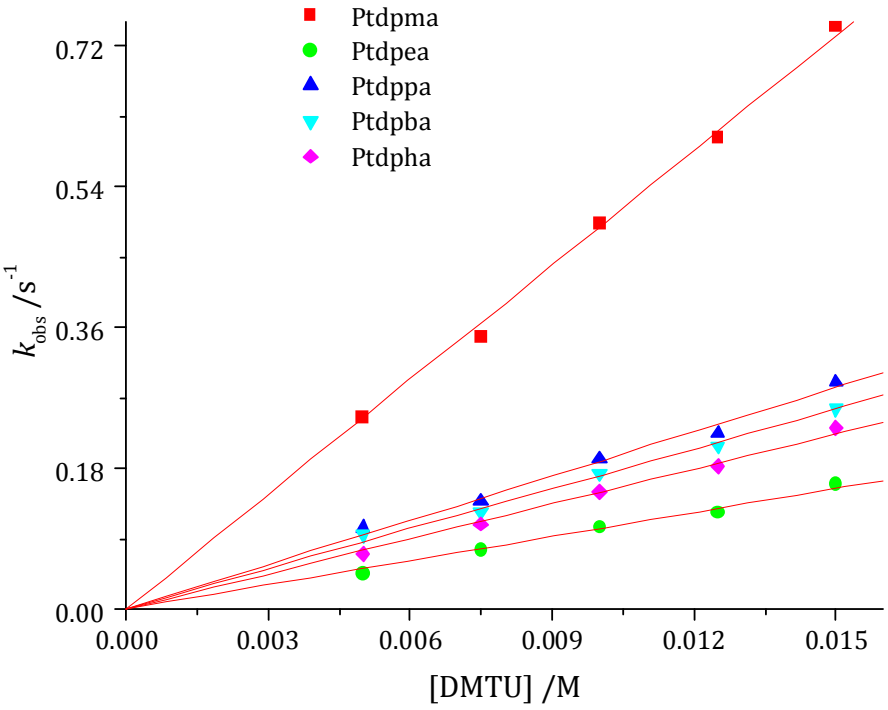


**Figure SI 4.20**: Dependence of $k_{obs}$ on the entering DMTU nucleophile for the first displacement of the aqua ligands in Ptdpma, Ptdpea, Ptdppa, Ptdpba and Ptdpha by thiourea, (DMTU) nucleophile, T = 298 K, pH = 2, $I$ = 0.1 M NaClO4.

**Table SI 4.4**: Average $k_{obs}$, $s^{-1}$, for the first displacement of the aqua ligands in **Ptdpma**, **Ptdpea**, **Ptdppa**, **Ptdpba** and **Ptdpha** by tetramethylthiourea, (TMTU) nucleophile, T = 298 K, pH = 2, $I$ = 0.1 M $NaClO_4$

| **Ptdpma** | | **Ptdpea** | | **Ptdppa** | | **Ptdpba** | | **Ptdpha** | |
|---|---|---|---|---|---|---|---|---|---|
| **[TMTU] /M** | $k_{obs}$ **/s$^{-1}$** | **[TMTU] /M** | $k_{obs}$ **/s$^{-1}$** | **[TMTU] /M** | $k_{obs}$ **/s$^{-1}$** | **[TMTU] /M** | $k_{obs}$ **/s$^{-1}$** | **[TMTU] /M** | $k_{obs}$ **/s$^{-1}$** |
| 0.005 | 0.122 | 0.0018 | 0.0323 | 0.005 | 0.038 | 0.005 | 0.043 | 0.005 | 0.026 |
| 0.0075 | 0.179 | 0.0027 | 0.044 | 0.0075 | 0.055 | 0.0075 | 0.054 | 0.0075 | 0.044 |
| 0.01 | 0.233 | 0.0036 | 0.06 | 0.01 | 0.075 | 0.01 | 0.0714 | 0.01 | 0.062 |
| 0.0125 | 0.2913 | 0.0045 | 0.078 | 0.0125 | 0.099 | 0.0125 | 0.0954 | 0.0125 | 0.08 |
| 0.015 | 0.323 | 0.0054 | 0.088 | 0.015 | 0.116 | 0.015 | 0.1084 | 0.015 | 0.094 |

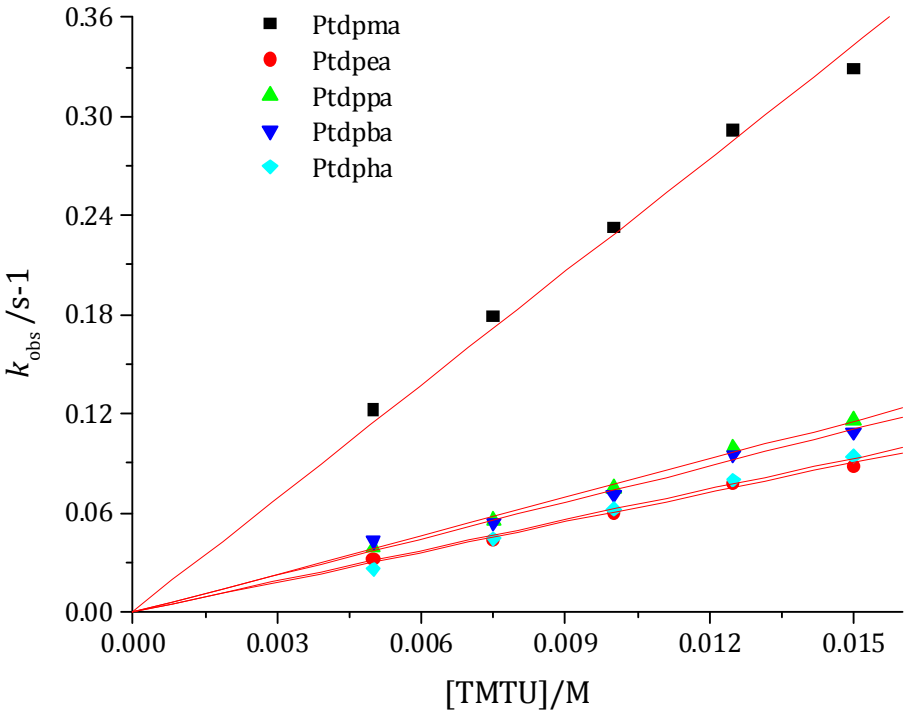


**Figure SI 4.21**: Dependence of $k_{obs}$ on the entering DMTU nucleophile for the first displacement of the aqua ligands in **Ptdpma**, **Ptdpea**, **Ptdppa**, **Ptdpba** and **Ptdpha** by tetramethylthiourea, (TMTU) nucleophile T = 298 K, pH = 2, $I$ = 0.1 M $NaClO_4$.

**Table SI 4.5**: Temperature dependence of rate constants, $k_{1}$ /M$^{-1}$ s$^{-1}$, for the first displacement of the aqua ligands in **Ptdpma**, **Ptdpea**, **Ptdppa**, **Ptdpba** and **Ptdpha** by thiourea, (TU) nucleophile, pH = 2, $I$ = 0.1 M $NaClO_4$, T = 15-35 ℃.

| | **Ptdpma** | **Ptdpea** | **Ptdppa** | **Ptdpba** | **Ptdpha** |
|---|---|---|---|---|---|
| $1/T$ /K$^{-1}$ | $ln\left(k_1/T\right)$ | $ln\left(k_1/T\right)$ | $ln\left(k_1/T\right)$ | $ln\left(k_1/T\right)$ | $ln\left(k_1/T\right)$ |
| 0.00347 | -7.18971 | -8.27378 | -7.69654 | -7.79215 | -8.10685 |
| 0.00341 | -6.9157 | -8.00189 | -7.43602 | -7.54474 | -7.80615 |
| 0.00336 | -6.62102 | -7.70772 | -7.16532 | -7.28011 | -7.53432 |
| 0.0033 | -6.35882 | -7.41791 | -6.87608 | -6.97216 | -7.22683 |
| 0.00325 | -6.07617 | -7.25979 | -6.57686 | -6.68947 | -6.90758 |

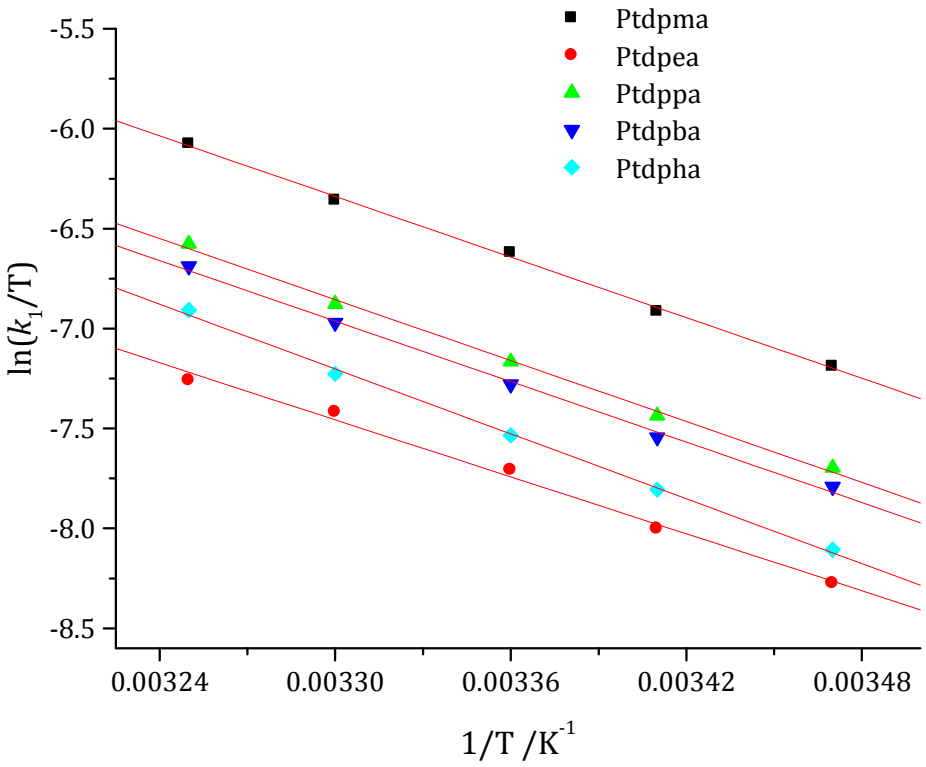


**Figure SI 4.22**: Plots of $\ln k_1/T$ *versus* $1/T$ for the first displacement of the aqua ligands in **Ptdpma**, **Ptdpea**, **Ptdppa**, **Ptdpba** and **Ptdpha** by thiourea, (TU) nucleophile, $I$ = 0.1 M $NaClO_4$, pH = 2, T = 15-35 °C.

**Table SI 4.6**: Temperature dependence of rate constants, $k_{1\,/M}$-1 s-1, for the first displacement of the aqua ligand in **Ptdpma**, **Ptdpea**, **Ptdppa**, **Ptdpba** and **Ptdpha** by dimethyl thiourea, (DMTU) nucleophile, pH = 2, *I* = 0.1 M $NaClO_4$, T = 15-35 ℃.

| | **Ptdpma** | **Ptdpea** | **Ptdppa** | **Ptdpba** | **Ptdpha** |
|---|---|---|---|---|---|
| $1/T$ /K-1 | $ln\left(k_1/T\right)$ | $ln\left(k_1/T\right)$ | $ln\left(k_1/T\right)$ | $ln\left(k_1/T\right)$ | $ln\left(k_1/T\right)$ |
| 0.00347 | -6.95353 | -8.5031 | -7.96535 | -8.03256 | -8.23998 |
| 0.00341 | -6.66519 | -8.2501 | -7.68406 | -7.74874 | -7.92468 |
| 0.00336 | -6.40437 | -7.95458 | -7.34986 | -7.44822 | -7.60128 |
| 0.0033 | -6.12586 | -7.66593 | -7.07246 | -7.1475 | -7.28631 |
| 0.00325 | -5.85214 | -7.36434 | -6.81402 | -6.84742 | -6.9805 |

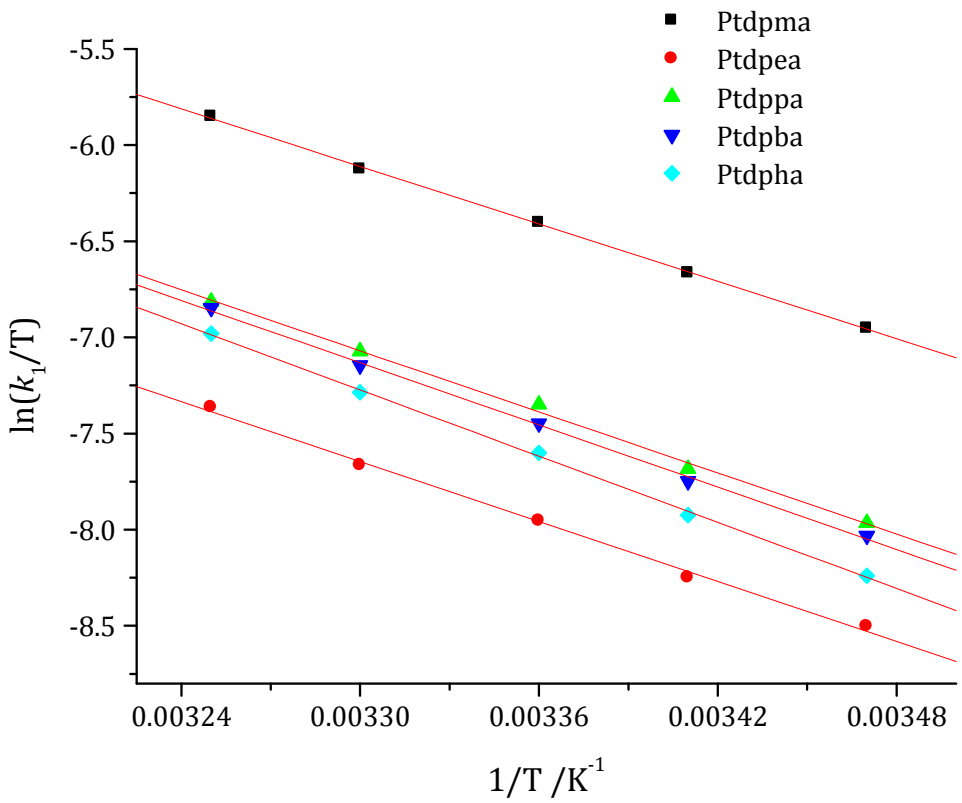


**Figure SI 4.23**: Plots of $\ln k_1/T$ *versus* $1/T$ for the first displacement of the aqua ligand in **Ptdpma**, **Ptdpea**, **Ptdppa**, **Ptdpba** and **Ptdpha** by dimethyl thiourea, (DMTU) nucleophile, pH = 2, $I$ = 0.1 M $NaClO_4$.T= 15-35 ℃.

**Table SI 4.7**: Temperature dependence of rate constants, $k_{1}$ /M$^{-1}$ s$^{-1}$, for the first displacement of the aqua ligands in **Ptdpma**, **Ptdpea**, **Ptdppa**, **Ptdpba** and **Ptdpha** by tetramethylthiourea, (TMTU) nucleophile, pH = 2, *I* = 0.1 M $NaClO_4$, T = 15-35 ℃.

| | **Ptdpma** | **Ptdpea** | **Ptdppa** | **Ptdpba** | **Ptdpha** |
|---|---|---|---|---|---|
| $1/T$ /K$^{-1}$ | $ln(k_1/T)$ | $ln(k_1/T)$ | $ln(k_1/T)$ | $ln(k_1/T)$ | $ln(k_1/T)$ |
| 0.00347 | -7.67758 | -9.1465 | -8.79057 | -8.95172 | -9.78952 |
| 0.00341 | -7.44401 | -8.83987 | -8.57136 | -8.61552 | -9.08402 |
| 0.00336 | -7.15542 | -8.58815 | -8.29271 | -8.33837 | -8.4739 |
| 0.0033 | -6.89348 | -8.3702 | -7.99826 | -8.06888 | -8.03179 |
| 0.00325 | -6.58641 | -8.0939 | -7.71251 | -7.90782 | -7.63772 |

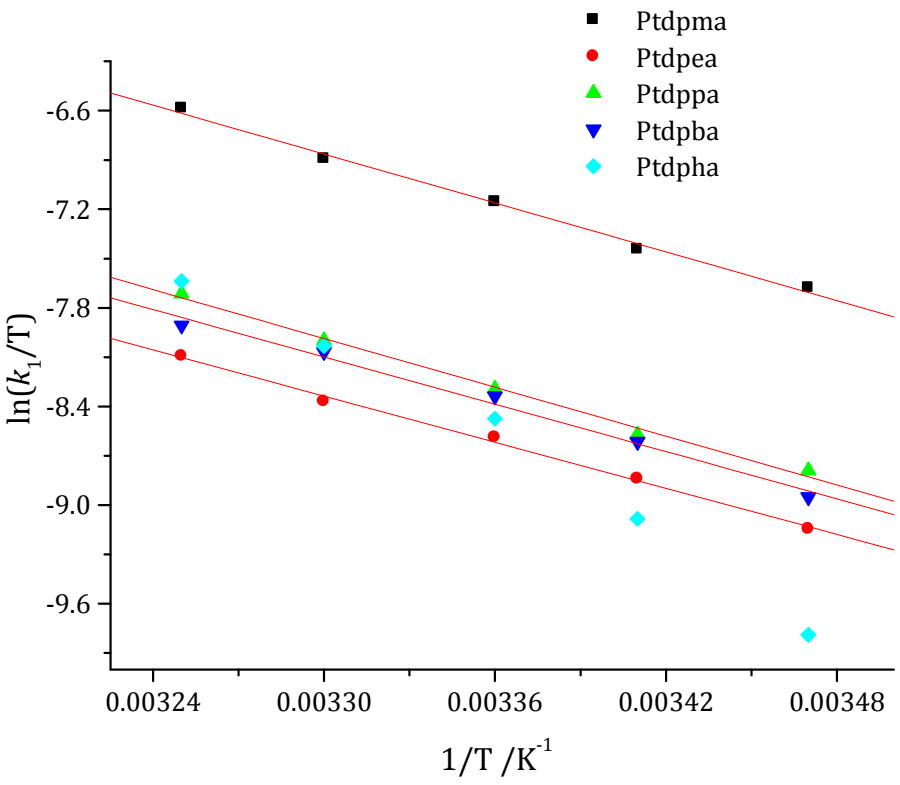


**Figure SI 4.24**: Plots of $ln\left(k_1/T\right)$ *versus* $1/T$ for the first displacement of the aqua ligands in **Ptdpma**, **Ptdpea**, **Ptdppa**, **Ptdpba** and **Ptdpha** by tetramethylthiourea, (TMTU) nucleophile, pH = 2, $I$ = 0.1 M $NaClO_4$, T = 15-35 ℃.

**Table SI 4.8**: Average $k_{obs2}/s^{-1}$, for the second displacement of the aqua ligands in **Ptdpma**, **Ptdpea**, **Ptdppa**, **Ptdpba** and **Ptdpha** by thiourea, (TU) nucleophile, T = 298 K, pH = 2, $I$ = 0.1 M $NaClO_4$.

| **Ptdpma** | | **Ptdpea** | | **Ptdppa** | **Ptdpba** | **Ptdpha** |
|---|---|---|---|---|---|---|
| **[TU] /M** | $k_{obs2}$ **/s$^{-1}$** | **[TU] /M** | $k_{obs2}$ **/s$^{-1}$** | $k_{obs2}$ **/s$^{-1}$** | $k_{obs2}$ **/s$^{-1}$** | $k_{obs2}$ **/s$^{-1}$** |
| 0.005 | 0.00485 | 0.0027 | 3.643E-5 | 9.813E-5 | 1.989E-4 | 7.987E-5 |
| 0.0075 | 0.00772 | 0.0036 | 6.139E-5 | 2.083E-4 | 3.616E-4 | 1.719E-4 |
| 0.01 | 0.01018 | 0.0045 | 9.251E-5 | 3.978E-4 | 5.396E-4 | 3.547E-4 |
| 0.0125 | 0.01378 | 0.0054 | 1.344E-4 | 5.531E-4 | 7.603E-4 | 4.895E-4 |
| 0.015 | 0.01633 | | | 7.987E-4 | | 6.832E-4 |

**Table SI 4.9**: Average $k_{obs2}$, $s^{-1}$, for the second displacement of the aqua ligands in **Ptdpma**, **Ptdpea**, **Ptdppa**, **Ptdpba** and **Ptdpha** by dimethyl thiourea, (DMTU) nucleophile, T = 298 K, pH = 2, $I$ = 0.1 M $NaClO_4$.

| **Ptdpma** | | **Ptdpea** | | **Ptdppa** | **Ptdpba** | **Ptdpha** |
|---|---|---|---|---|---|---|
| **[DMTU] /M** | $k_{obs2}$ **/s$^{-1}$** | **[DMTU] /M** | $k_{obs2}$ **/s$^{-1}$** | $k_{obs2}$ **/s$^{-1}$** | $k_{obs2}$ **/s$^{-1}$** | $k_{obs2}$ **/s$^{-1}$** |
| 0.005 | 7.136E-5 | 0.0027 | 1.903E-5 | 7.628E-5 | 7.136E-5 | 6.199E-5 |
| 0.0075 | 1.306E-4 | 0.0036 | 2.472E-5 | 1.382E-4 | 9.906E-5 | 9.228E-5 |
| 0.01 | 1.896E-4 | 0.0045 | 3.213E-5 | 1.932E-4 | 1.296E-4 | 1.214E-4 |
| 0.0125 | 2.377E-4 | 0.0054 | 3.919E-5 | 2.650E-4 | 1.777E-4 | 1.538E-4 |
| 0.015 | 3.136E-4 | | | | | 1.863E-4 |

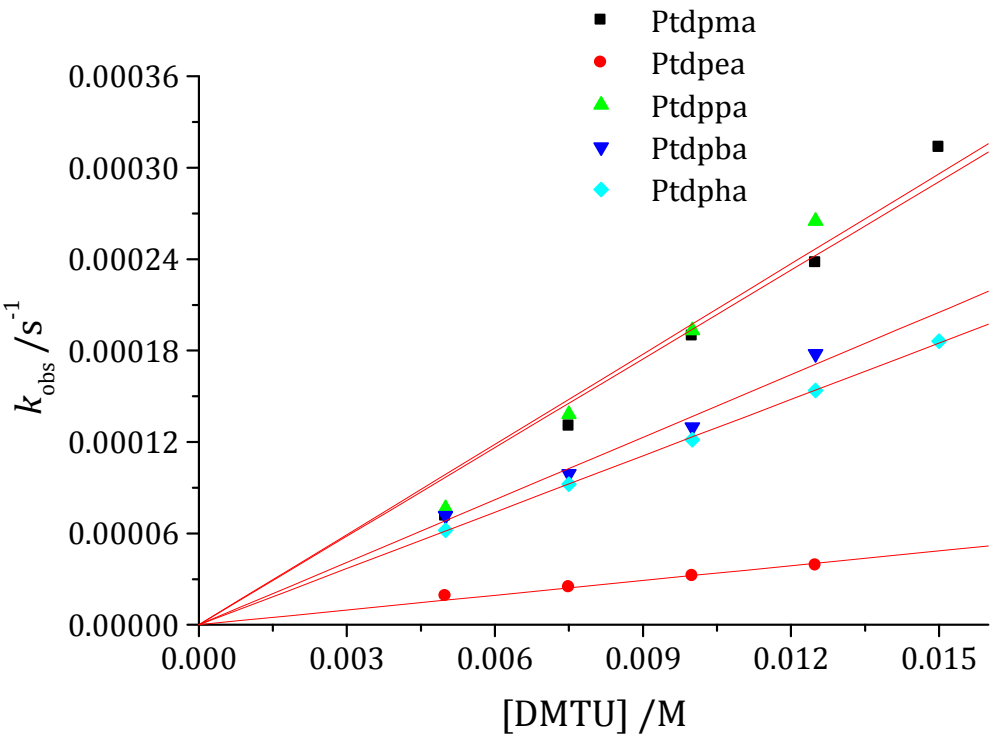


**Figure SI 4.25**: Plots of $k_{obs2}$ *versus* [DMTU] for the second displacement of the aqua ligands in **Ptdpma**, **Ptdpea**, **Ptdppa**, **Ptdpba** and **Ptdpha** by dimethylmethylthiourea, (DMTU) nucleophile, pH = 2, $I$ = 0.1 M $NaClO_4$ T = 15-35 ℃.

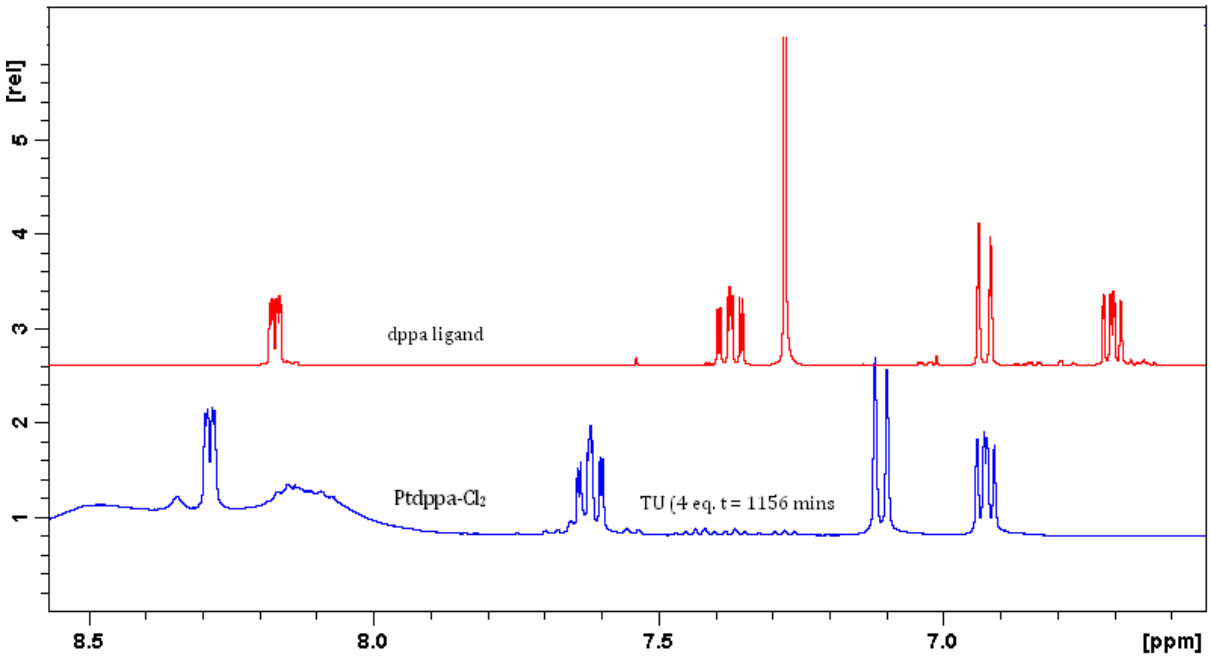


**Figure SI 4.26**: $^{1}$H NMR spectrum showing the aromatic protons of **PtdppaCl$_2$** with excess TU in DMSO and **dppa** in $CDCl_3$

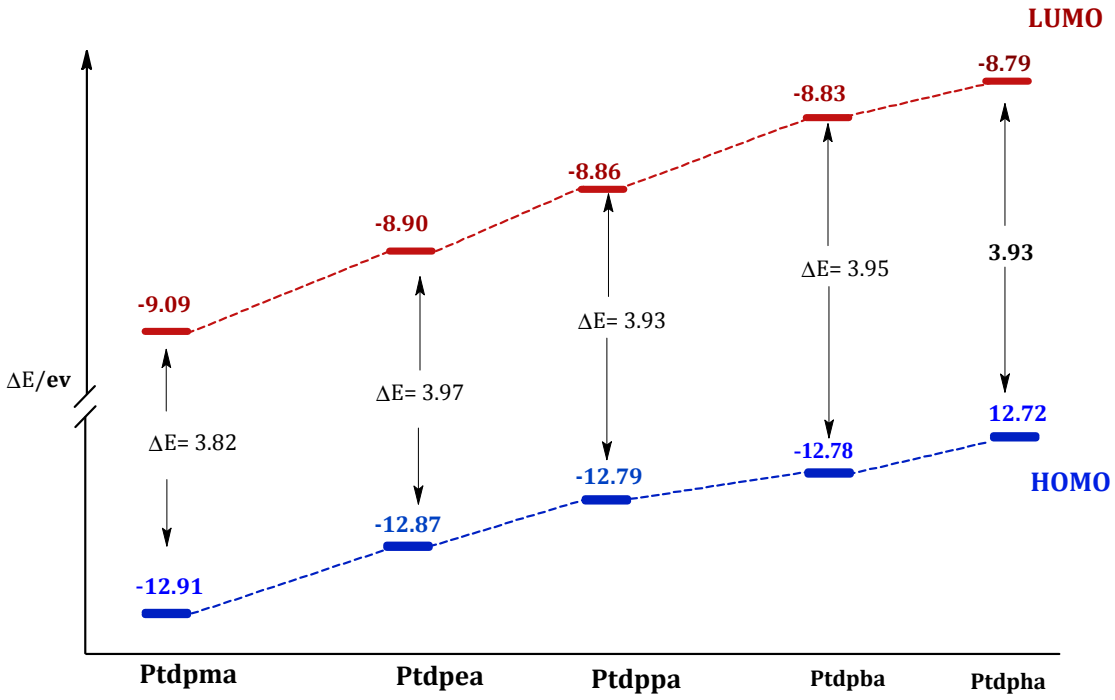


**Figure SI 4.27**: HOMO and LUMO energy gap for the platinum(II) complexes investigated.

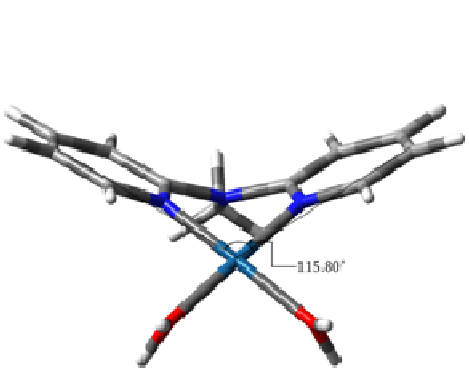


**Ptdpma**

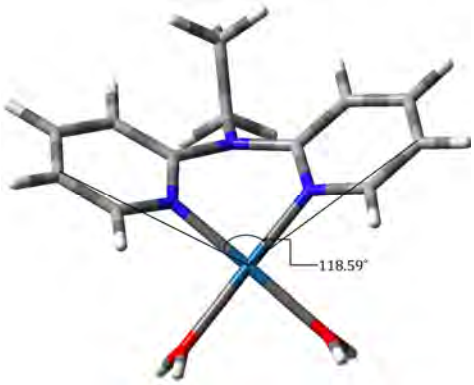


**Ptdpea**

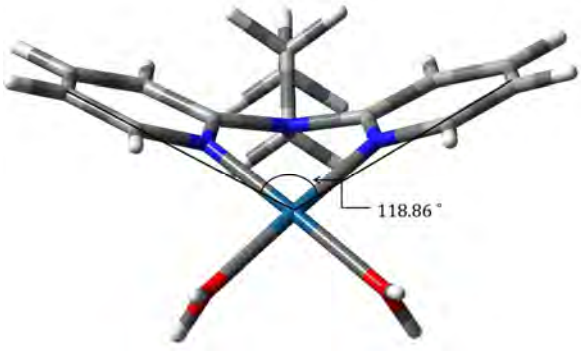


**Ptdppa**

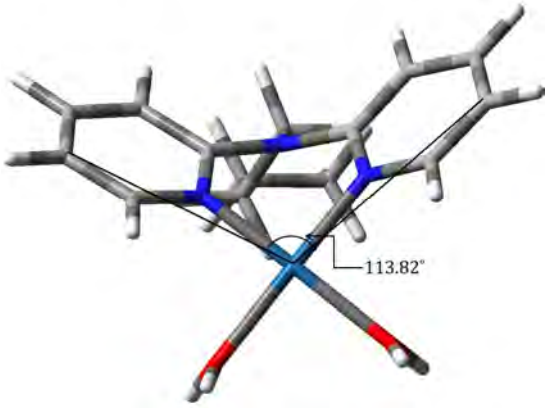


**Ptdpba**

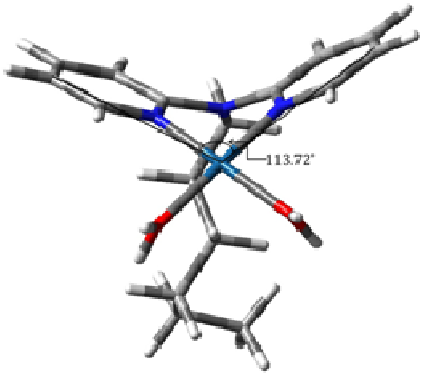


**Figure SI 4.28:** Basal angles of Pt centre with respect to *cis* pyridine rings

**Table of Contents**

**List of Figures**

**List of Tables**

# Chapter 5

## A Kinetic Study of Novel Dinuclear Pt(II) Complexes Containing Four Non-Coplanar Pyridine Ligands


### Abstract

Substitution reaction of aqua ligands of azine-bridged dinuclear platinum(II) complexes of the type [*{cis*-$Pt(py)_2(OH_2)$*}*$_2$(μ-pzn)]$(ClO4)_4$ (where pzn = pyrazine (**Pt-PZN**), 2,3-dimethylpyrazine (**Pt-2,3PZN**), 2,5-dimethylpyrazine (**Pt-2,5PZN**) and 2,6-dimethylpyrazine (**Pt-2,6PZN**) by thiourea nucleophiles was investigated under *pseudo* first-order conditions as a function of concentration and temperature using the stopped-flow technique. The experimental results are discussed in reference to structures obtained by DFT (B3LYP/LanL2Dz) calculations. The reactivity of the complexes follows the trend **Pt-PZN** > **Pt2,6PZN** > **Pt-2,5PZN** > **Pt-2,3PZN** and **Pt-PZN** > **Pt2,5PZN** > **Pt-2,3PZN** > **Pt-2,6PZN** for the first and second substitution steps respectively. The results are well supported by the p*K*a values as well as the calculated data from density functional theory (DFT). The trend in reactivity observed in this study can be explained in terms of electronic effects and steric hindrance imposed by the methyl groups introduced into the bridging ligand. Compared to [*{cis/trans*-$Pt(NH_3)_2(OH_2)$*}*$_2$(μ-pzn)]$(ClO4)_4$, the complexes in this series react faster by a factor of 10 or 23 respectively due to the presence of pyridine rings which forces the structural geometry to allow π-backbonding to take place where the electrons from the metal centres are accepted to the empty $\pi^*$-orbitals of the pyridine sub units. The reactivity of the nucleophile is steric dependent with TMTU reacting three times slower than TU. In all complexes and for both substitution steps the mode of activation remains associative in nature.

## 5.1 Introduction

In order to understand how dinuclear Pt(II) complexes interact with the biological molecules in the body, it has become increasingly important to understand the mechanism of their ligand substitution reactions using model molecules which mimic bionucleophiles such as thiol, certain groups of enzymes, peptides and protein molecules present in the body. Through suitable kinetic investigations of Pt(II) complexes results obtained may contribute to a better understanding of the precise rate of important biochemical transformations as well as the underlying mechanism for those complexes. Moreover, by monitoring the substitution reactions with sulfur-donors, more information can be gained on the possible modes of interaction of Pt(II) complexes with *in vivo* targets and their subsequent application in the study of their anti-tumour properties.

Because of this kinetics of ligand substitution of dinuclear Pt(II) complexes with flexible and rigid linkers has been reported.[1] Substitutional reactivity of the metal centres has been shown to depend on the length and nature of the bridging ligand.[1] For example, when a straight aliphatic chain is used in dinuclear complexes with monodentate ammine[1h] and bis(2-pyridylmethyl)amine[1a,i-l] carrier ligand around the Pt centres, the reactivity increases with the increase in chain length until it reaches the point where it is independent of the chain length. The increase in reactivity as the chain length increases was ascribed to the decrease in charge addition of the Pt atoms caused by a combination of increased electrostatic interactions with a concomitant increase in the σ-donor capacity towards each Pt atom.[1a,b] A similar trend in reactivity was observed by van Eldik and co-workers[1i-l] when anionic and biological relevant nucleophiles were used to study the ligand substitution

reactions in alkanediamine-bridged Pt(II) complexes with a bis(2-pyridylmethyl)amine chelate framework around each Pt atom. The trend in reactivity is the same in all cases as the one reported in the study by Jaganyi *et al*[1h] for the dinuclear complexes with monodentate amine ligands around the Pt(II) centres. In addition, the decrease in reactivity with increase in alkanediamine chain was observed for dinuclear complexes with the linker on *cis* position to the leaving group.[2] The retardation of the rate of substitution on increasing the alkanediamine chain is attributed to the strong σ-donor ability of the -$(CH_2)_n$- moiety that is in the *cis*-position with respect to the leaving group. This causes accumulation of the electron density to the metal centre making it less electrophilic.[2] On the other hand when rigid and semi rigid ligands are used to link Pt(II) centres, the reactivity of the complex depends on the ability of the linker to reduce electron from the metal centre through π-back bonding.[1e,g,3]

The substitution results obtained for dinuclear Pt(II) complexes edify that the reactivities of these complexes may be manipulated by the geometry of the complex, especially with respect to the relationship of leaving groups to diamine bridge, and the nature of the diamine bridge itself as well as the other ligands in the Pt coordination sphere. It has been reported that the DNA binding properties of Pt(II) complexes differ dramatically when the ligand coordinated to the Pt centre is varied from $NH_3$ to pyridine.[4] The current study is an expansion of an earlier study from our group on azine bridged dinuclear Pt(II) complexes with $NH_3$ ligands *cis* or *trans* to each other[1g,3] and is intended to resolve the thermodynamic and kinetic properties of the complexes as a function of pyridine ligands bonded to Pt centre. I am particularly interested to know if the pyridine rings will enter into electronic

communication with the Pt(II) orbitals through π-backbonding and how will this affect the reactivity of the complexes taking into account the steric effect imposed by the methyl groups on the pyrazine linker. For this reason, I set out to synthesize and study the kinetics of ligand substitution of novel cationic dinuclear Pt(II) complexes bearing two pyridine rings at each Pt centre (**Figure 5.1**). The choice of the pyridine ligand and azine as a linker was due to the interesting cytotoxic activity of their mononuclear and dinuclear Pt(II) complexes.[4,5]

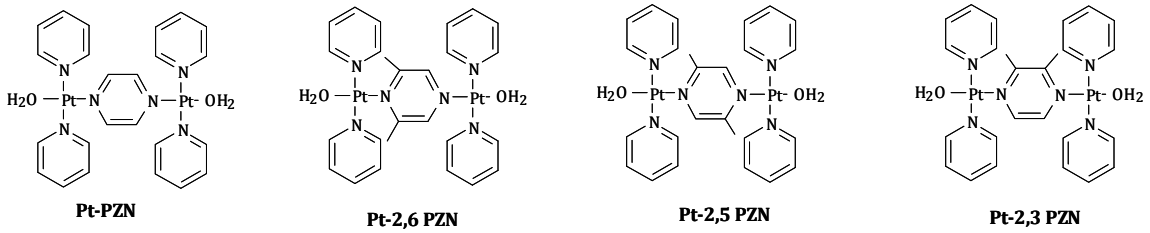


**Figure 5.1:** Structures of the complexes investigated in this study (charges omitted for clarity).

## 5.2 Experimental

### 5.2.1 Chemicals and Reagents.

Pyrazine (99%), 2,3-dimethylpyrazine (99%), 2,5-dimethylpyrazine (99%), 2,6-dimethylpyrazine (99%), $NaClO_4 \cdot H_2O$ (98%), $HClO_4$ (70%), $AgClO_4$ (99.98%) and pyridine (99%) were obtained from Aldrich and were used without further purification. Potassium tetrachloroplatinate [$K_2(PtCl_4)$] (99.99%) was purchased from Strem Chemicals. The nucleophiles; thiourea, TU (99%), 1,3-dimethyl-2-thiourea, DMTU (99%), 1,1,3,3-tetramethyl-2-thiourea, TMTU (98%) used in the kinetic measurements were obtained

from Aldrich. Ultrapure water (PureLab Systems) was used in all experiments. All other reagents used were of analytical grade quality.

### 5.2.2 Synthesis of the Complexes

Four dinuclear Pt(II) complexes with the formulae [*trans*-{$PtCl(Py)_2$}$_2$-μ-pzn] $(ClO_4)_2$ (**Pt-PZN**) (pzn = pyrazine), [*trans* -{$PtCl(Py)_2$}$_2$-μ-2,3-pzn]$(ClO_4)_2$ (**Pt-2,3PZN**) (2,3pzn = 2,3-dimethylpyrazine), [*trans* -{$PtCl(Py)_2$}$_2$-μ-2,5-pzn]$(ClO_4)_2$ (**Pt-2,5PZN**) (2,5pzn = 2,5-dimethylpyrazine) and [*trans* -{$PtCl(Py)_2$}$_2$-μ-2,6-pzn]$(ClO_4)_2$ (**Pt-2,6PZN**) (2,6pzn = 2,6-dimethylpyrazine) were prepared from [*trans*-{$PtCl(Py)_2(DMF)$}]$ClO_4$.

### 5.2.3 Synthesis of [*trans*-$PtCl_2Py_2$]

The mononuclear starting compound of the general formula [*trans*-$PtCl_2(Py)_2$] was prepared according to literature procedure.[6] To a solution of $K_2PtCl_4$ (1.62 g, 3.89 mmol) in 100 mL of water was added pyridine (1.25 mL, 15.58 mmol) and the mixture was heated at reflux temperature (115 °C) until the yellow precipitate which formed dissolved to give a clear solution. HCl (2.0 M, 100 mL) was added to the hot solution and the mixture heated at reflux until the solution turned to yellow. On reducing the volume of the solution to *ca* 10 mL, a light yellow solid precipitated. The solid was filtered off and washed with water and acetone. The crude product was recrystallized from $CHCl_3$/ether.

***trans*-[$PtCl_2Py_2$]** Light yellow powder, yield 1.44 g, (89 %). $^1$H NMR ($CDCl_3$, 400 MHz,): δ = 8.92 (d, 4H), 7.79 (t, 2H), 7.32 (t, 4H). $^{13}$C NMR ($CDCl_3$, 400 MHz,): 153.7, 138.3 and 125.2.

Anal. Calcd. for $C_{10}H_{10}N_2PtCl_2$: C 28.30, H 2.36, N 6.60. Found C 28.27, H 2.36, N 6.54. TOF MS $ES^+$: m/z, $[M+Na]^+$ = 446.97.

### 5.2.4 Synthesis of [*trans*-{$PtCl(Py)_2(DMF)$}]$ClO_4$

The title compound was prepared following the literature method.[7,8] To a solution of known amount of *trans*-$[PtCl_2(Py)_2]$ in 10 mL of DMF was added one equivalent of $AgClO_4$. The solution was stirred in the dark overnight at room temperature. After cooling to 5 ˚C the precipitated AgCl was filtered off and a yellow filtrate retained.

### 5.2.5 Synthesis of Dinuclear Pt(II) Complexes

The synthesis of the new tetra pyridyl coordinated dinuclear compounds was adopted from a previously published method[8] starting with [*trans*-{$PtCl(Py)_2(DMF)$}]$ClO_4$ and pyrazine derivatives as the bridging ligand with some minor modifications. To a filtrate of [*trans*-{$PtCl(Py)_2(DMF)$}]$ClO_4$ was added dropwise a solution of the pyrazine derivatives (half equivalent that of the metal complex) in 2 mL of DMF. The mixture was stirred overnight at 30-40 °C in the dark. The solution was then cooled and concentrated on a rotary evaporator at a reduced pressure to a volume of approximately 2 mL. The off-yellow compounds which precipitated out after addition of methanol (20 mL) was filtered and repeatedly recrystallized in minimal $H_2O$/ethanol. All complexes were prepared as perchlorate salts and were characterized by $^1H$ NMR and elemental analysis. Characterization data were in complete agreement with the proposed structures.

**Pt-PZN** Light yellow powder, yield 76.60 mg, (35 %). $^1$H NMR (DMSO-$d_6$, 400 MHz,): δ = 8.95 (d, 2H), 8.79 (d, 8H), 8.02 (t, 4H), 7.73 (d, 2H), 7.53 (dd, 8H). *Anal. Calcd*. for $C_{24}H_{24}N_6O_8Pt_2Cl_4$: C 27.27, H 2.65, N 7.95. *Found* C 27.57, H 2.46, N 7.64.

**Pt-2,3PZN** Light yellow powder, yield 74.40 mg, (33 %). $^1$H NMR (DMSO-$d_6$, 400 MHz,): δ = 8.97 (d, 8H), 8.94 (d, 2H), 8.22 (t, 4H), 7.76 (dd, 8H), 2.35 (s, 6H). *Anal. Calcd*. for $C_{26}H_{28}N_6O_8Pt_2Cl_4$: C 28.78, H 2.58, N 7.75. *Found* C 28.21, H 2.76, N 7.53.

**Pt-2,5 PZN** Light yellow powder, yield 67.64 mg, (30 %). $^1$H NMR (DMSO-$d_6$, 400 MHz,): δ = 8.95 (d, 8H), 8.39 (s, 2H), 8.19 (t, 4H), 7.74 (dd, 8H), 2.43 (s, 6H). *Anal. Calcd*. for $C_{26}H_{28}N_6O_8Pt_2Cl_4$: C 28.78 H 2.58, N 7.75. *Found* C 28.66, H 2.49, N 7.56.

**Pt-2,6 PZN** Light yellow powder, yield 67.64 mg, (30 %). $^1$H NMR (DMSO-$d_6$, 400 MHz,): δ = 8.74 (s, 2H), 8.96 (d, 8H), 7.81 (t, 4H), 7.32 (dd, 8H), 2.61 (s, 6H). *Anal. Calcd*. for $C_{26}H_{28}N_6O_8Pt_2Cl_4$: C 28.78, H 2.58, N 7.75. *Found* C 29.07, H 2.61, N 7.67.

### 5.2.6 Preparation of Aqueous Complex Solutions

The desired solutions of the diaqua complexes were prepared by reacting a known amount of chloro Pt(II) complex with $AgClO_4$ in a ratio of 1:1.98 molar ratio of the chloro complexes to silver perchlorate in 0.1 M $HClO_4$ acid. The mixture was vigorously stirred in the dark at 50 °C for 24 h. After cooling in ice cold water, the precipitated AgCl was filtered off through a 0.45-μm nylon membrane filter using a Millipore filtration apparatus. The resulting aqueous solution was brought to a final complex concentration of, 3.4 x $10^{-4}$, 2.15 x $10^{-4}$,

4.37 x $10^{-4}$ and 5.78 x $10^{-4}$ M for **Pt-PZN**, **Pt-2,3PZN**, **Pt-2,5PZN** and **Pt-2,6PZN**, using 0.1M $HClO_4$ acid respectively.

### 5.2.7 Instrumentation and Measurements

NMR spectra were recorded on a Bruker Avance III 500 at frequencies of 500 MHz using either a 5 mm BBOZ probe or a 5 mm TBIZ probe. All proton chemical shifts are quoted relative to the relevant solvent signals at 30 °C unless stated otherwise. Elemental compositions of the complexes were determined from a Carlo Erba Elemental Analyzer 1106. The pH of the aqueous solutions of the complexes were measured using a Jenway 4330 Conductivity/pH meter equipped with a Micro 4.5 diameter glass electrode. The electrode was calibrated at 25 °C using standard buffer solutions of pH 4.0, 7.0 and 10.0 (Merck). The pH electrode was filled with 3.0 M NaCl and not KCl to prevent precipitation of $KClO_4$. An Applied photophysics SX 20 stopped-flow spectrophotometer thermostated to within ± 0.1 °C was used for the kinetic measurements. p$K_a$ and kinetic traces were graphically analysed using the software package, Origin 7.5®.[9]

### 5.2.8 Computational Methods

The geometry optimizations of the complexes **Pt-PZN**, **Pt-2,3PZN**, **Pt-2,5PZN** and **Pt-2,6PZN** were carried out in the gas phase at the level of DFT-B3LYP[10] with LanL2DZ basis sets[11] using a Gaussian 09 program suite.[12] B3LYP relates to the hybrid functional Becke's three-parameter formulation, which has been proven to be superior to traditional functionals. LANL2DZ is double-zeta basis set containing effective core potential (ECP)

representations of electrons near the nuclei for transition metal complexes.[13] The complexes were optimized in their diaqua form as cations of total charge of +4.

### 5.2.9 p$K_a$ Titrations of the Diaqua Complexes.

Spectrophotometric pH titrations of the aqua complex solutions were performed using NaOH as the base in the pH range of 1–10 at 25 ˚C. In order to avoid absorbance corrections due to dilution, a large volume (150 mL) of the metal complex solution was used during the titration. Adjustments in pH were made by stepwise additions of crushed solid NaOH pellets in the pH range 1-3 while micropipette dropwise additions of NaOH solutions of different concentrations (1.0, 0.5, 0.1 and 0.01 M) or conc. HClO4 (for reversibility of the pH) were added to the solution in the pH range of 4-10 until the desired pH was attained prior to withdrawal of 1.0 mL aliquot from the solution for pH measurement and 2 mL aliquots for monitoring the absorbance spectrophotometrically. The 1 mL aliquot after each pH measurement was discarded to avoid *in situ* contamination of the complex solution by chloride ions leaching from the pH electrode.

### 5.2.10 Kinetic Measurements

The kinetics of the substitution of coordinated aqua ligands of the complexes **Pt-PZN**, **Pt-2,3PZN**, **Pt-2,5PZN** and **Pt-2,6PZN** were monitored under *pseudo* first-order conditions with at least a 20-fold excess of the nucleophile concentration over the dinuclear complex at pH 2 in order to force the reactions to go to completion The reactions were initiated by mixing of equal volumes of a solution of the Pt(II) complex with a solution of the nucleophile directly in the stopped-flow instrument at suitable wavelengths predetermined

from UV-Vis spectrophotometer (**Table SI 5.1**). Observed rate constants, $k_{obs1}$ and $k_{obs2}$ were calculated by a double exponential fit to the kinetic traces. The reported $k_{obs1}$ and $k_{obs2}$ are mean values of at least five independent kinetic runs on the stopped-flow spectrophotometer. The second-order rate constants, $k_1$ and $k_2$ were obtained by a fit of a straight line to the plot of $k_{obs1}$ and $k_{obs2}$ versus concentration of nucleophile, [Nu] using a standard least-squares minimizing procedure by Origin 7.5® software package.[9] The temperature dependencies of the rate constants in the range of 15-35 °C at a 5 °C interval allowed for the calculation of the enthalpies and entropies of activation, $\Delta H^{\neq}$ and $\Delta S^{\neq}$, with the nucleophile concentration held constant at 60 times the concentration of the metal complex. The respective values were obtained by a linear fit of the natural logarithm of the second-order rate constant, $\ln\left(\frac{k_{1or2}}{T}\right)$ versus $\frac{1}{T}$ using Eyring equation.[14]

## 5.3 Results

### 5.3.1 Computational Analysis

In this study, one of the most important structural parameter is the presence of two pyridine moieties *trans* to each other and *cis* to leaving group at each Pt(II) centre. Computational calculations were performed in order to gain an in-depth understanding of the structural as well as the electronic differences that exist in the complexes compared to those reported in previous studies.[1g,3] Geometry optimized structures and the HOMO/LUMO maps are shown in **Table 5.1**, while the selected metric data are presented in **Table 5.2**.

It is important to mention that the complexes were synthesized and drawn as *trans* but at the end of the calculation the pyridine rings had twisted to the equatorial plane adopting the *cis* geometry in relation to the second pyridine ring. The calculations also show that the square planarity around the Pt centres is maintained and the pyrazine ligand plus the twisted pyridine rings all lie on the same plane with the Pt(II) centres creating an environment for electronic communication through π-backbonding between them to take place.

For all complexes investigated, the HOMO orbitals are concentrated on the horizontal pyridyl π-acceptor carrier ligands and the LUMO is centred primarily on the pyrazine bridging ligand and partly on the $d_{xy}$ orbital of the Pt centre. A general increase in the energy gap, ΔE (HOMO–LUMO), of the frontier orbitals and decrease in NBO charges dependent on the position of the methyl group is observed upon introducing electron-donating methyl group to the pyrazine moiety. This is linked with the increase in electron density at the metal centre which results in destabilization and minimum interactions of the molecular orbitals. Because of the outcome of twisting the pyridine rings to the equatorial plane as revealed in **Table 5.1**, the thermodynamic and kinetic data in this paper are discussed in line with the geometry optimized structures. Included in the **Table 5.2** are DFT-based reactivity descriptors such as chemical hardness and electrophilicity index which were calculated from their energies of HOMO and LUMO[15] to elucidate the observed reactivity trend of the complexes. From **Table 5.2**, the chemical hardness decreases in the order **Pt-2,3PZN > Pt-2,5PZN > Pt-2,6PZN > Pt-PZN** and tallies well with the reactivity trend observed where **Pt-PZN** is more reactive than **Pt-2,3PZN**. It is worth noting that the

values of chemical potential (**Table 5.2**) which describes the escaping tendency of electrons from an equilibrium system are all of the same magnitude and negative because the electron acceptance by the complexes is accompanied by a decrease in energy. The electrophilicity trend which measures the capacity of a complex as a whole to accept electrons (**Table 5.2**) is **Pt-2,3PZN < Pt-2,5PZN < Pt-2,6PZN < Pt-PZN**. A good electrophile is characterized by a high value of electrophilicity index, therefore, **Pt-PZN** is the most reactive complex in the series and **Pt-2,3PZN** is the least reactive.

**Table 5.1:** Geometry optimized structures and DFT-calculated (B3LYP/LACVP+**) HOMO and LUMO for the investigated complexes.

| Complex | HOMO | LUMO | Planarity |
|---|---|---|---|
| **Pt-PZN** | 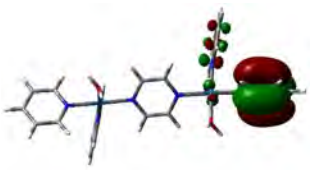 | 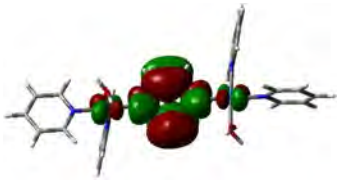 | 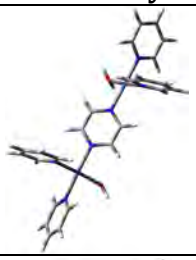 |
| **Pt-2,3PZN** | 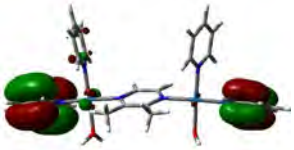 | 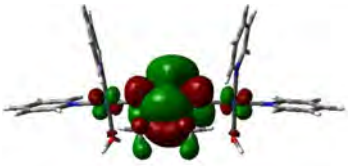 | 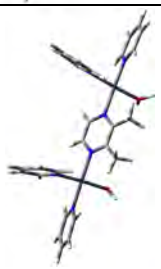 |
| **Pt-2,5PZN** | 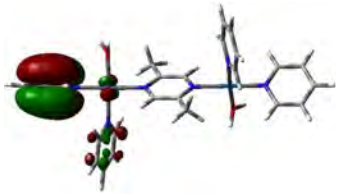 | 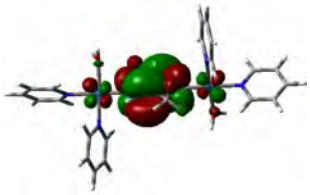 | 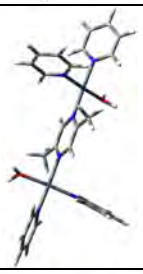 |
| **Pt-2,6PZN** | 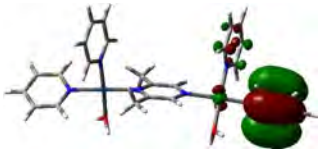 | 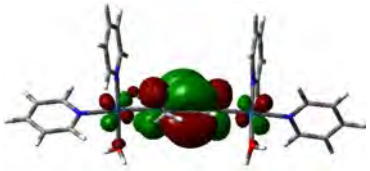 |  |

**Table 5.2:** DFT-calculated parameters for the investigated Pt(II) complexes.

| 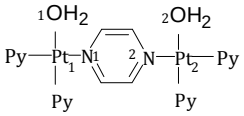 | **Pt-PZN** | **Pt-2,6PZN** | **Pt-2,5PZN** | **Pt-2,3PZN** |
|---|---|---|---|---|
| **HOMO-LUMO energy** | | | | |
| LUMO /eV | -14.10 | -13.83 | -13.64 | -13.54 |
| HOMO/eV | -17.26 | -17.30 | -17.16 | -17.16 |
| ΔE /eV | 3.16 | 3.47 | 3.52 | 3.62 |
| **NBO Charges** | | | | |
| $Pt_1$ | 0.756 | 0.719 | 0.702 | 0.694 |
| $Pt_2$ | 0.756 | 0.690 | 0.702 | 0.694 |
| **Chemical hardness** (eV) | 1.58 | 1.73 | 1.76 | 1.81 |
| **Chemical potential** (eV) | -15.68 | -15.56 | -15.40 | -15.35 |
| **Electrophilicity index** (ω) | 77.80 | 69.77 | 67.40 | 65.09 |
| **Bond Length** (Å) | | | | |
| $Pt_1$–$Pt_2$ | 7.033 | 7.045 | 7.039 | 7.027 |
| $Pt_1$–$N_1$ | 2.105 | 2.128 | 2.114 | 2.119 |
| $Pt_2$–$N_2$ | 2.105 | 2.105 | 2.116 | 2.119 |
| $Pt_1$–$OH_1$ | 2.139 | 2.139 | 2.137 | 2.136 |
| $Pt_2$–$OH_2$ | 2.139 | 2.134 | 2.136 | 2.136 |
| **Bond Angles** (°) | | | | |
| $N_1$–$Pt_1$–$O_1$ | 89.01 | 88.89 | 89.75 | 89.16 |
| $N_2$–$Pt_2$–$O_2$ | 89.01 | 88.95 | 88.54 | 89.12 |
| **Point group symmetry** | $C_2$ | $C_1$ | $C_1$ | $C_s$ |

### 5.3.2 Acidity of the Aqua Complexes

**Figure 5.2 (also Figures SI 5.8-5.10)** shows an example of the spectral changes observed during the pH titration of **Pt-2,6PZN** with NaOH. The p$K_a$ values of the coordinated aqua ligands were calculated from the pH profiles and an example of which is shown as an inset in **Figure 5.2**. When the data were fitted to separate single sigmoidal functions using Origin 7.5® software[9], p$K_a$ values for the deprotonation of the protons of the coordinated aqua ligands were obtained. Their values are summarised in **Table 5.3**. Included for comparison purposes in **Table 5.3** are the p$K_a$ values of the analogous dinuclear Pt(II) complexes having *cis* $NH_3$ ligands at each metal centre. The overall titration process can be presented by following the reactions stepwise as given in **Scheme 5.1**.

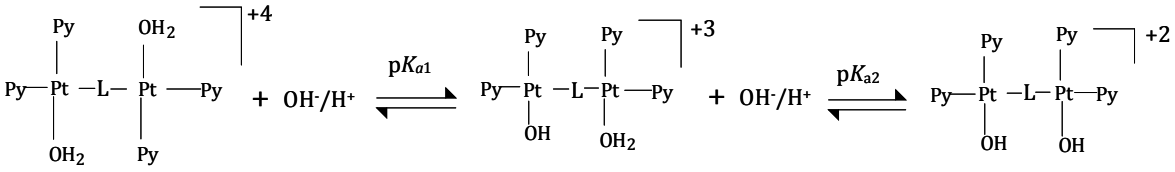


where, L = bridge = pzn, 2,3-pzn, 2,5-pzn, and 2,6-pzn
Py = pyridine

**Scheme 5.1**: Stepwise deprotonation steps for the investigated complexes in an aqueous medium

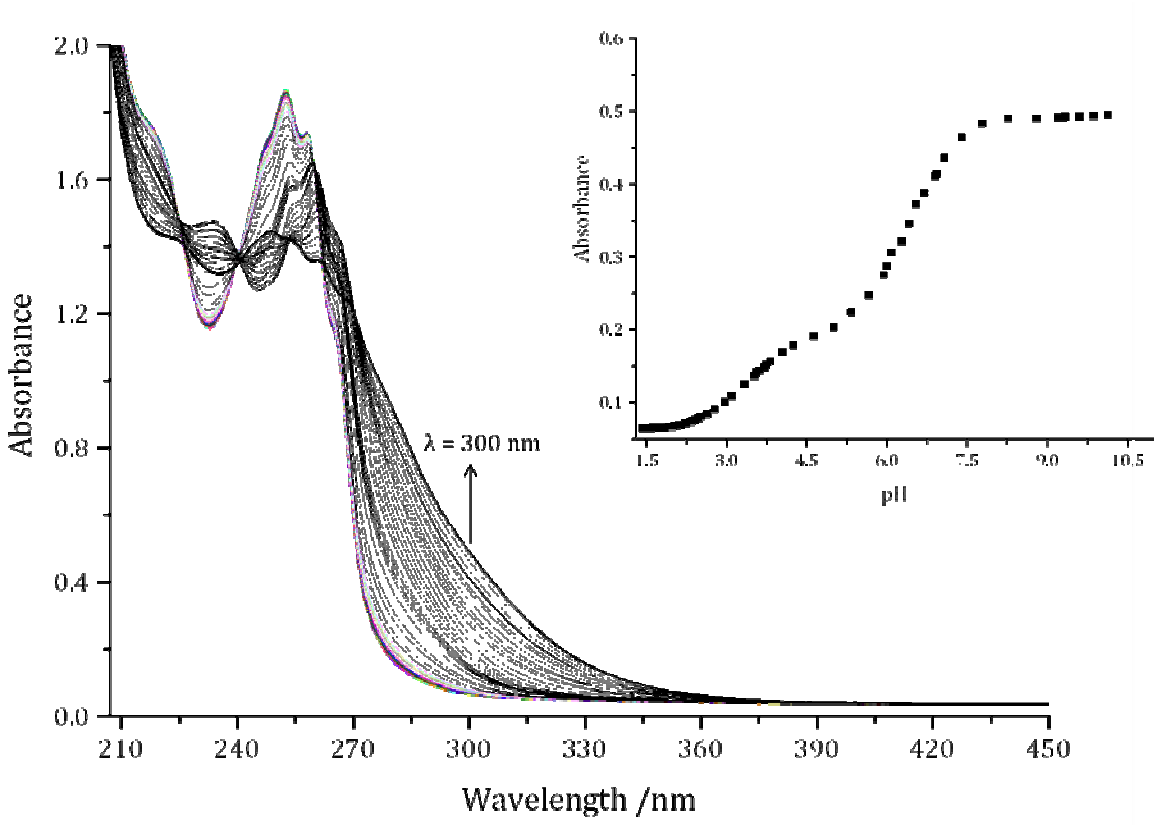


**Figure 5.2:** UV-Vis spectra of the Pt-2,6PZN diaqua complex recorded as a function of pH in the range 1-10 at 25 °C. *Inset*: Plot of absorbance versus pH at 300 nm.

Results in **Table 5.3** clearly show a correlation between the p$K_a$ values and electronic as well as steric demands of the pyrazine ligand linking the two Pt(II) centres. The p$K_{a1}$ values of the deprotonation of the first coordinated aqua ligand increase in the order of 3.14 < 3.35 ≈ 3.37< 3.59 for **Pt-PZN, Pt-2,3PZN, Pt-2,5PZN** and **Pt-2,6PZN** respectively. The trend in p$K_a$ values is associated with the electronic effect of methyl substituents on the pyrazine moiety which through inductive effect results in the Pt–$OH_2$ bond being longer and consequently high p$K_a$ values of the resultant complex. The second deprotonation step (**Table 5.3**) in all complexes occurs at higher pH values than the first one and this is

attributed to the decrease in overall charge from +4 to +3 of the complexes upon formation of the hydroxo species. Interestingly, the p$K_a$ values for the first deprotonation step obtained in this study are slightly lower than those obtained for the analogous dinulear complexes with $sp^3$-hybridized ammine unit ($NH_3$) on *trans* and *cis* position to the leaving group.[1g,3] This may be attributed to the effect of the introduced pyridine rings which help to stabilize the electron density on the Pt(II) centre and the hydroxo ligand as the pyridine is a better π-acceptor compared to $NH_3$.[16]

**Table 5.3:** The p$K_a$ values for the deprotonation of Pt-bound aqua ligands in the dinuclear Pt(II) complexes.

| Complex | **Pt-PZN** | **Pt-2,6PZN** | **Pt-2,5PZN** | **Pt-2,3PZN** |
|---|---|---|---|---|
| p$K_{a1}$ | 3.14 ± 0.03 | 3.59 ± 0.03 | 3.37 ± 0.01 | 3.35 ± 0.01 |
| | 3.32 ± 0.06[a] | 3.48 ± 0.51[a] | 3.96 ± 0.12[a] | 3.98 ± 0.11[a] |
| p$K_{a2}$ | 5.93 ± 0.04 | 6.12 ± 0.05 | 6.15 ± 0.02 | 6.43 ± 0.03 |
| | 5.64 ± 0.09[a] | 6.88 ± 0.04[a] | 6.13 ± 0.05[a] | 6.01 ± 0.18[a] |
| Δp$K_a$ | 2.79 | 2.84 | 2.78 | 2.77 |

[a]p$K_a$ values extracted from reference 3.

### 5.3.3 Kinetics Measurements

As already mentioned, all the kinetic measurements were done under *pseudo* first-order conditions with respect to the nucleophile in order to force the reactions to go to completion. The substitution reactions of the complexes with thiourea nucleophiles (TU,

DMTU, TMTU) were carried out at pH 2 and they were characterized by two reaction steps (**Scheme 5.2**).

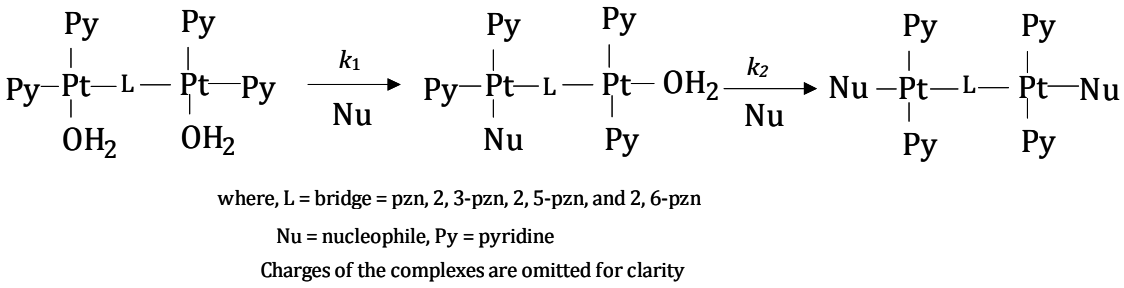


**Scheme 5.2:** The general reaction scheme for the reactions between the Pt(II) complexes and the thiourea nucleophiles at pH 2.

Both substitution steps are irreversible and the overall reaction can be summarized by the rate law given by **Equation 5.1**.

$$k_{\text{obs}1/2} = k_{1/2}[\text{Nu}] \qquad (5.1)$$

The kinetic traces of the ligand substitution reaction for all complexes investigated gave excellent fits to a double exponential decay to generate the *pseudo* first-order rate constants, $k_{\text{obs}1}$ and $k_{\text{obs}2}$ at specific nucleophile concentration and temperature for the first and second substitution step respectively. An example of the kinetic trace obtained for the reaction of **Pt-2,3PZN** with TU is shown in **Figure 5.3**.

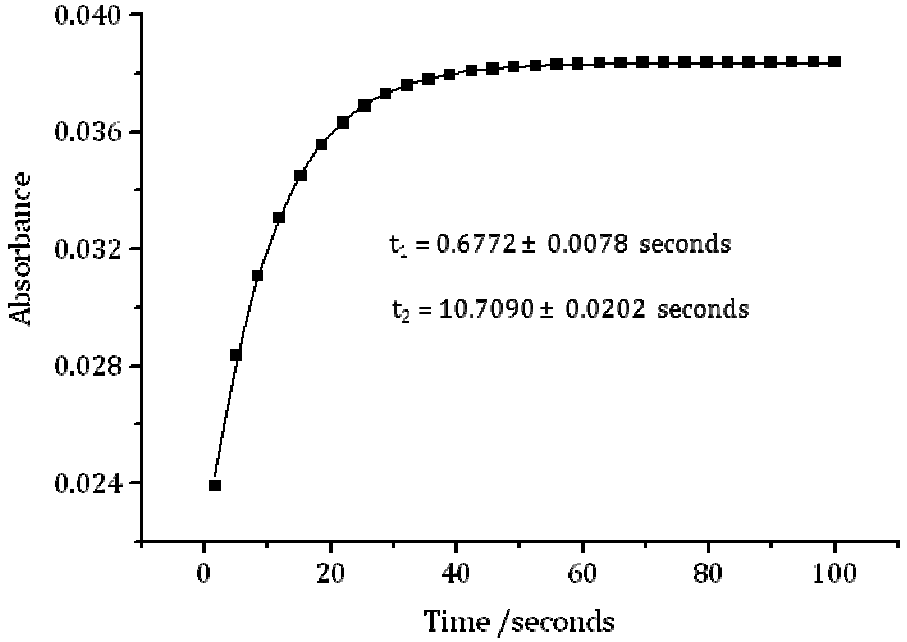


**Figure 5.3:** Typical double exponential fit for a two step reaction between Pt-2,3PZN (0.2 mM) and TU (1.2 mM) recorded at 295 nm, T = 298 K, pH = 2.0, $I$ = 0.1 M ($NaClO_4$) on the stopped-flow spectrophotometer. $t_1$ and $t_2$ are time values from which $k_{obs1}$ and $k_{obs2}$ are obtained.

The rate constants, $k_1$ and $k_2$ were obtained from the slope of the plot of $k_{obs1}$ or $k_{obs2}$ against nucleophile concentrations at 25 °C and are summarized in **Table 5.4**. Representative plots for the first and second substitution step for **Pt-PZN** with the three investigated nucleophiles are shown in **Figure 5.4** (also **Figures SI 6.13, 6.15** and **6.17**). The dependence of rate constant on temperature was studied at a temperature range 15-35 ˚C. Typical Eyring plots are shown in **Figure 5.5** (also **Figures SI 6.14, 6.16** and **6.18**) and the activation parameters, $\Delta H^{\neq}$ and $\Delta S^{\neq}$, obtained are presented in **Table 5.4**.

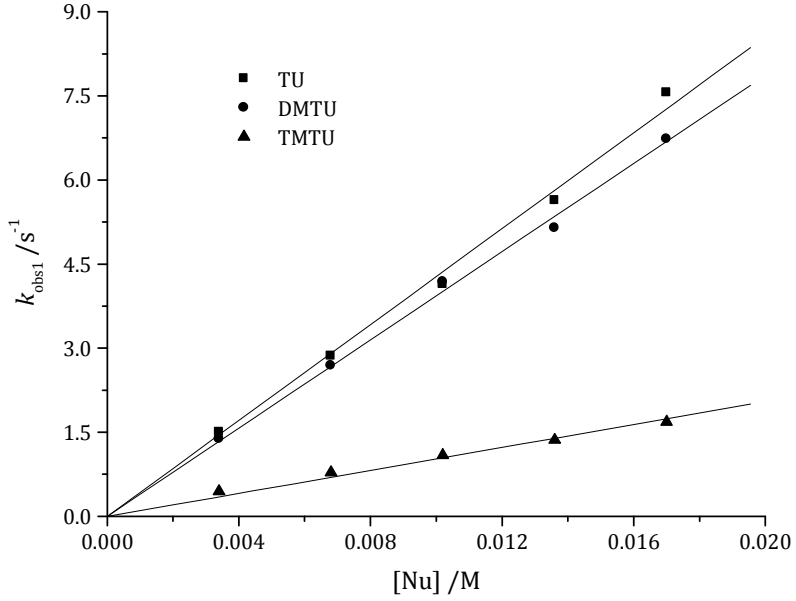


(a)

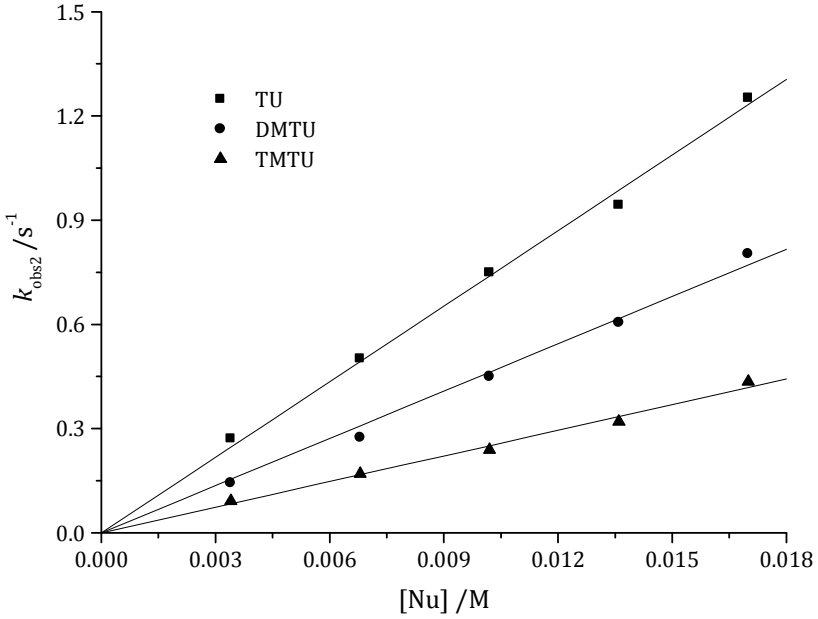


(b)

**Figure 5.4:** Plots of $k_{obs1/2}$ versus nucleophile concentration for the (a) first and (b) second substitution steps of the reaction of 0.25 mM Pt-PZN at pH 2 and 25 ˚C, ($I$ = 0.1 M, $NaClO_4$).

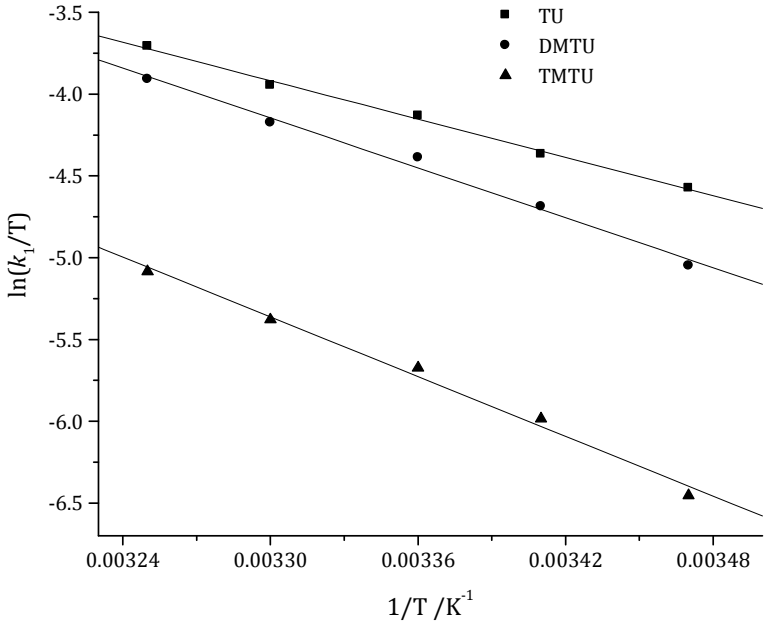


(a)

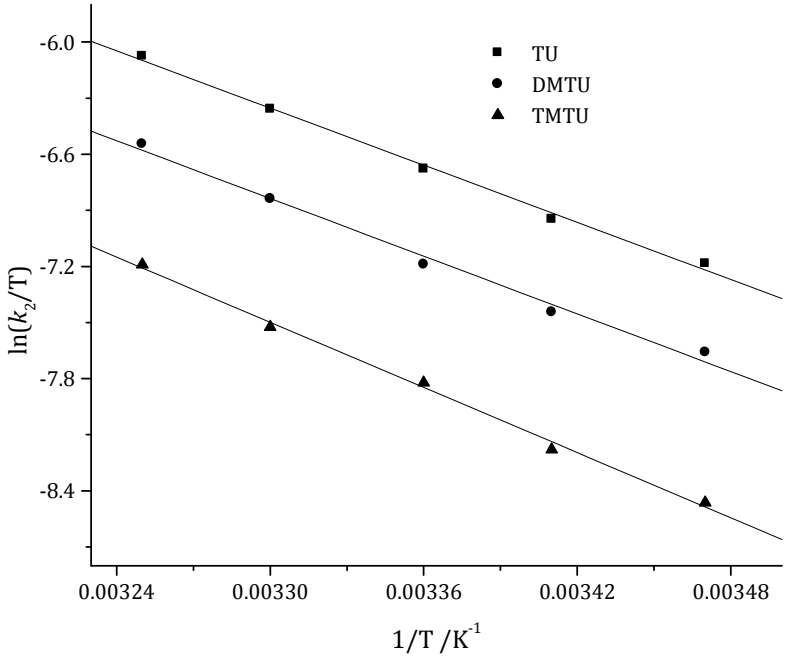


(b)

**Figure 5.5:** Eyring plots for the determination of the thermal activation parameters for the (a) first and (b) second substitution steps of 0.22 mM Pt-PZN for all three nucleophiles studied at pH 2 ($I$ = 0.1 M $NaClO_4$).

**Table 5.4:** Summary of rate constants and activation parameters of the investigated complexes for the first and second substitution steps.

| Complex | Nu | $k_1$/M$^{-1}$ s$^{-1}$ | $k_2$ /M$^{-1}$ s$^{-1}$ | $\Delta H^{\neq}_1$ /kJ mol$^{-1}$ | $\Delta H^{\neq}_2$ /kJ mol$^{-1}$ | $\Delta S^{\neq}_1$/ J K$^{-1}$ mol$^{-1}$ | $\Delta S^{\neq}_2$/ J K$^{-1}$ mol$^{-1}$ |
|---|---|---|---|---|---|---|---|
| 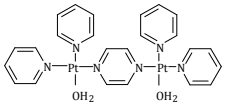 **Pt-PZN** | TU | 427.7 ± 8.2 | 72.5 ± 1.1 | 27 ± 1 | 41 ± 1 | -142 ± 4 | -114 ± 3 |
| | DMTU | 393.3 ± 5.5 | 45.4 ± 1.0 | 41 ± 2 | 42 ± 2 | -96 ± 6 | -177 ± 7 |
| | TMTU | 102.4 ± 3.1 | 24.6 ± 0.5 | 49 ± 2 | 47 ± 1 | -79 ± 6 | -104 ± 3 |
| 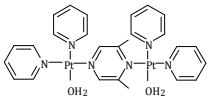 **Pt-2,6PZN** | TU | 338.7 ± 6.5 | 16.2 ± 0.3 | 40 ± 1 | 38 ± 2 | -122 ± 3 | -132 ± 6 |
| | DMTU | 200.6 ± 4.1 | 5.6 ± 0.1 | 43 ± 2 | 46 ± 2 | -108 ± 6 | -104 ± 6 |
| | TMTU | 146.1 ± 3.3 | 3.3 ± 0.05 | 48 ± 1 | 47 ± 2 | -100 ± 4 | -104 ± 5 |
| 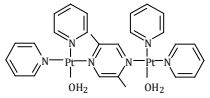 **Pt-2,5PZN** | TU | 314.0 ± 1.4 | 43.4 ± 0.6 | 27 ± 1 | 37 ± 2 | -151 ± 3 | -139 ± 6 |
| | DMTU | 304.7 ± 6.1 | 38.4 ± 0.6 | 26 ± 1 | 37 ± 2 | -154 ± 3 | -139 ± 6 |
| | TMTU | 102.2 ± 0.9 | 27.3 ± 0.3 | 39 ± 1 | 43 ± 2 | -119 ± 3 | -122 ± 6 |
| 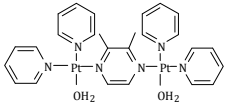 **Pt-2,3PZN** | TU | 247.8 ± 6.1 | 29.7 ± 0.7 | 31 ± 1 | 30 ± 1 | -102 ± 3 | -166 ± 3 |
| | DMTU | 185.5 ± 4.6 | 24.1 ± 0.7 | 30 ± 2 | 47 ± 3 | -124 ± 6 | -120 ± 9 |
| | TMTU | 136.1 ± 2.7 | 18.6 ± 0.6 | 43 ± 1 | 33 ± 2 | -118 ± 3 | -160 ± 6 |

## 5.4 Discussion

Previous studies have shown that there is relationship between p$K_a$ values and electrophilicity of the metal centre.[1i,k,17,18] It has also been reported that, electron-withdrawing $\pi$-acceptor effect tends to stabilize the electron-rich hydroxo species in comparison to the aqua species resulting in lower p$K_a$ values.[1k,17,18] Alternatively, if the $\sigma$-donor capacity of the ligand *trans* to the aqua moiety is enhanced, then a higher p$K_a$ value is obtained.[19] In this study the p$K_a$ results obtained show that the introduction of methyl groups to the pyrazine moiety as in **Pt-2,3PZN**, **Pt-2,5PZN** and **Pt-2,6PZN** decreases the electrophilicity of the metal centre through electron donation via the pyrazine ring. This result into a moderate increase in p$K_a$ values for these complexes compared to **Pt-PZN**. One can see that the position of the methyl groups in the pyrazine moiety of **Pt-2,3PZN** and **Pt-2,5PZN** gave equal distribution of the charges at each Pt(II) centre explaining why these two complexes have p$K_a$ values that are approximately the same. However, donation of charge from methyl groups of **Pt-2,6PZN** is not symmetrical resulting into $Pt_1$ being more electrophilic compared to $Pt_2$. This is in line with the huge difference in p$K_a$ values observed for this complex when compared with other complexes in this study. The trend in the pKa values are well supported by the DFT NBO calculated charges and the reactivity descriptors (**Table 5.3**) where the second Pt centre is less positive compared to other Pt centres in the complexes investigated.

Comparing the current p$K_a$ findings with those of related *cis*-complexes[3] [*cis*-$\{Pt(NH_3)_2(OH_2)\}_2$-μ-pzn]$^{4+}$(**Table 5.3**), p$K_a$ values obtained in this study were slightly lower. This can only mean that by addition of pyridine units as monodentate ligands the electron

density on the Pt(II) centre and the hydroxo ligand is slightly stabilized by the poor σ-donor pyridine rings[16] compared to $NH_3$ which is a strong σ-donor and increases the electron density on the metal centre. Moreover, the mapping of the frontier orbitals confirmed enhancement of electronic communication between the metal and ligand as Pt(II) centre is free in electrons. Further observation also shows that deprotonation of the second coordinated aqua molecule to the dihydroxo species occurs at higher pH values than in the first step in all the four complexes. This is ascribed to reduction of the overall charge from +4 to +3 following deprotonation of the first coordinated aqua molecule in all the dinuclear complexes causing a decrease in acidity and electrophilicity of the second Pt(II) centre. This increase in p$K_a$ value due to the change in overall charge of the complex has also been observed and reported in previous studies.[1,2,3]

Substitution reactions of the series of dinuclear Pt(II) complexes with thiourea nucleophiles was monitored at pH 2 where all the complexes exists in their diaqua form and protonation of thiourea can be ruled out.[20] Two substitution steps were observed for all dinuclear Pt(II) complexes studied indicating that there is electronic communication between the two Pt centres resulting in each having different kinetic properties. The smallness and rigidness of the azine linker enhances metal-metal electronic communication by electrostatic charge transfer from the metal centre to the lowest unoccupied molecular orbitals of the bridging ligand, making the Pt(II) centre more electrophilic.[21] It is worth mentioning that as previously reported,[1g,3] the reactivity of the complexes reported is also dependent on the electronic and steric effect of the pyrazine linker.

The first substitution step is assigned to the replacement of one aqua ligand with the thiourea nucleophiles (TU, DMTU, TMTU) whilst the second step is the substitution of the second aqua ligand. Since other dinuclear Pt(II) complexes studied in our group[3] were involving dechelation or dissociation of the linker, ligand substitutions of **Pt-2,5PZN-Cl$_2$** was followed using $^1$H NMR to evaluate the possibility of dechelation. An array of the $^1$HNMR spectra (showing only the aromatic resonances) for the reaction between **Pt-2,5PZN-Cl$_2$** and excess thiourea (6 equivalents) is shown in **Figure 5.6**. The pyridyl protons were chosen to monitor the progress of the reaction as they are in close vicinity with the N-donor atom bonded to the metal centre and hence to the incoming TU. The numbering scheme employed for the pyridyl protons is shown in the structure of the **Pt-2,5PZN-Cl$_2$** complex in **Scheme 5.3**. From **Figure 5.6**, the $H_2$ and $H_{2'}$ resonances of the pyridine in **Pt-2,5PZN-Cl$_2$** complex which appear at $\delta$ = 8.89 ppm are shifted downfield to $\delta$ = 9.07 ppm upon coordination of TU-six equivalent while the electronic environments of the other pyridyl and the pyrazine protons are not affected to a great extent by the coordination of thiourea. It is worth mentioning that no extra sets of resonances in support of a dechelation process were observed during the progression of the reactions with TU for up to 19 hours.

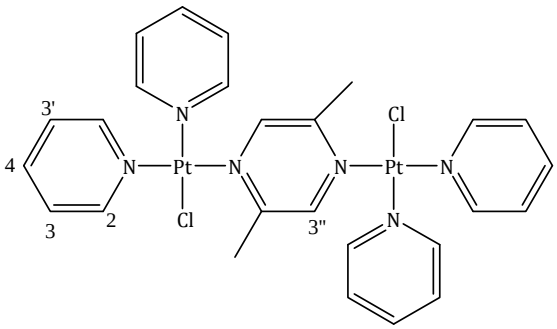


**Scheme 5.3**: The numbering scheme employed for the pyridyl protons of **Pt-2,5PZN-Cl$_2$**.

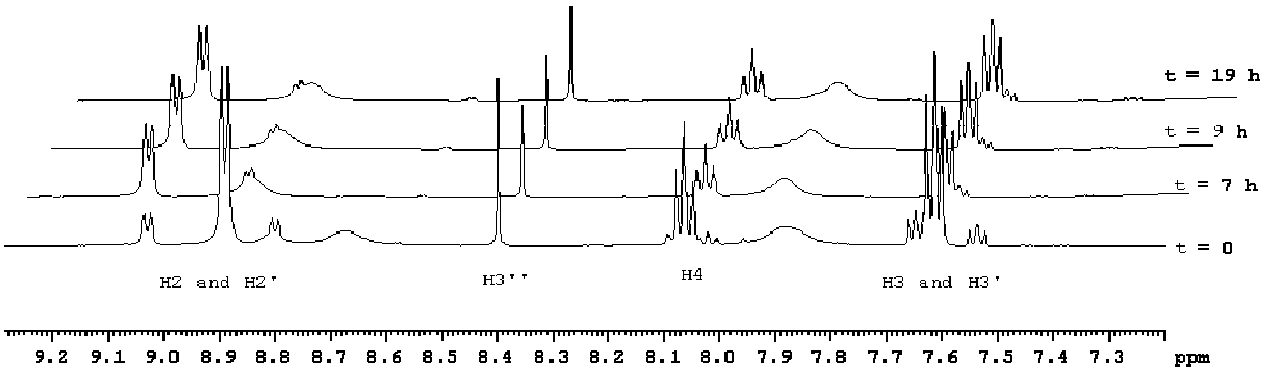


**Figure 5.6:** $^{1}$H NMR spectra of **Pt-2,5PZN-Cl$_2$** acquired during the reaction with 6 equivalent TU at 30 °C. The first spectrum labelled t = 0 is for the unreacted Pt(II) chloro complex and the rest are after the reaction with 6 equivalent TU at a specified time.

Taking the first substitution with thiourea as a reference, the reactivity of the dinuclear Pt(II) complexes decreases in the order 427.7 > 338.6 ≃ 314.0 > 247.8 $M^{-1}$ $s^{-1}$ for **Pt-PZN**, **Pt2,6PZN**, **Pt-2,3PZN** and **Pt-2,5PZN**, respectively. The trend in reactivity observed in this study can be explained in terms of electronic effect and steric hindrance imposed by the methyl groups introduced into the bridging ligand as reported in previous studies.[1g,3] The higher lability of the **Pt-PZN** complex is ascribed to less steric hindrance and the decrease in electron density on the platinum centre caused by the π-acceptor ability of the pyrazine ligand and the twisted pyridine rings. This makes the metal centres in **Pt-PZN** more electrophilic and favour the rapid binding of the entering nucleophile. The high reactivity of **Pt-PZN** is supported by the observed lower p$K_a$ values, narrow HOMO-LUMO gap, small value of chemical hardness and large values of electrophilicity index and NBO charges. The decrease in reactivity of the **Pt-2,6PZN**, **Pt-2,3PZN** and **Pt-2,5PZN** compared to **Pt-PZN** can

be ascribed to the increased $\sigma$-inductive effect due to the additional methyl groups on the bridging pyrazine ligand. Previous studies have shown that methyl groups and other electron-donating groups collectively lead to a reduction in the rate of ligand substitution, by reducing the positive charge density on the platinum atom, thus lowering the electrophilicity of the metal centre.[1g,2,3,22-24] The introduced methyl groups also impose the steric hindrance which restrict the path of the incoming nucleophile to one or both sides of the square planar of the platinum(II) centres.

The second-order rate constant of **Pt-PZN** is greater than that of **Pt-2,6PZN** by a factor of *ca*. 1.3. These two complexes differ from each other due to the fact that one of the platinum centre in **Pt-2,6PZN** is crowded with methyl groups making it less electrophilic compared to the second metal centre as supported by DFT calculated NBO charges. From the NBO charges in **Table 5.2**, the electrophilicity of the unshielded metal centre of **Pt-2,6PZN** is of the same magnitude with that of **Pt-PZN**. This explains why the reactivity of the first substitution step in **Pt-2,6PZN** is close to that of **Pt-PZN** and higher than that of **Pt-2,5PZN** and **Pt-2,3PZN**. In addition, the determined p$K_a$ values and the observed HOMO-LUMO gap for **Pt-2,6PZN** confirms the difference in electrophilicity between the two Pt(II) centres.

In the case of **Pt-2,3PZN** and **Pt-2,5PZN**, the positioning of the methyl groups in *ortho* and *para* position of the pyrazine makes the two complexes symmetrical as the charges are equally distributed between the two Pt(II) centres. Due to this fact one expects the reactivity of these two complexes to be similar in magnitude. Surprisingly, this was not the case showing that the position of the methyl groups influences the twisting of the pyridine

rings which in turn influences the extend of π-backbonding. The steric effect brought by the methyl groups in **Pt-2,3PZN** causes the twisting of the complex to the extent that the two Pt centres lie on a different plane by 9.1° (**Figure SI 5.20**) which interferes with the electronic communication and slowing down of the reactivity.

The second substitution step was significantly slower than the first in all the investigated complexes. This is possibly due to change in the electronic communication between the two platinum atoms. The order of reactivity for the second substitution step with TU is **Pt-PZN** > **Pt-2,5PZN** > **Pt-2,3PZN** > **Pt-2,6PZN**. The same trend in reactivity is also observed for other nucleophiles, DMTU and TMTU. As for the first substitution step, this is caused by the increased *σ*-inductive effect of methyl groups on the bridging pyrazine ligand which in turn increases its σ-donation to the metal centre (reducing its π-acceptability) resulting into a less positive metal centre. With this effect, the incoming nucleophile is repelled by the increased amount of electron density around the metal centre, leading to a less stable five-coordinate transition-state and reduced rate of substitution. In case of **Pt-2,6PZN** there is additional steric effect which blocks entry of the incoming nucleophile on both sides of the hindered Pt(II) centre as supported by the reduced NBO charges of the second metal centre.

When the reactivity of the **Pt-pzn** derivatives for both substitution steps is compared with [*cis*-{$Pt(NH_3)_2(OH_2)$}$_2$-μ-pzn]$^{4+}$ and then to [*trans*-{$Pt(NH_3)_2(OH_2)$}$_2$-μ-pzn]$^{4+}$, its second-order rate constants are higher by a factor of 10 and 23 respectively.[1g,3] This indicates that the structure containing pyridyl units labilizes the aqua ligands more than their *cis* and *trans*-counterparts with $NH_3$ as the ligand. The introduction of pyridine groups into the

$[\{Pt(NH_3)_2(OH_2)\}_2$-μ-pzn$]^{4+}$ complex changes the structural geometry of the complex in such a way that a significant increase in $\pi$-acceptor abilities of the ligands is induced. The net outcome is a significant increase in the electrophilicity of the complex as a whole and the metal centre as reflected by a more positive charge on the Pt(II) centres, high electrophilicity indices and lower p$K_a$ values for the deprotonation of the aqua ligands. This increases the rate of substitution of the coordinated aqua ligands. In addition, from **Table 5.1**, the HOMO in all dinuclear complexes is distributed on the pyridine ligand and the LUMO is highly populated on the pyrazine bridging ligand. The HOMO orbital of the previously studied pyrazine bridged dinuclear Pt(II) complexes[1g,3] was located at the metal centres as the $NH_3$ is a more of σ-donor than pyridine making the Pt(II) centres less electrophilic compared to the current Pt(II) complexes investigated.

The dependence on the rate of substitution of the aqua on the steric hindrance of the incoming nucleophiles is clearly evident from results shown in **Table 5.4**. Substitutions involving TMTU gave the slowest rates, whereas those with TU reacted significantly faster. This reactivity trend is in line with the steric size of TMTU nucleophile relative to the other two, TU and DMTU.[18b,25-26] The activation parameters in **Table 5.4** show that the entropies of activation are large and negative. This indicates that the transition state is highly ordered and more compact than either the reactant or product species. In addition, the enthalpies of activation are relatively low, showing the ease with which the new bond can form due to the electrophilicity of the metal centre. These activation parameter results are consistent with substitution reactions for square-planar Pt(II) complexes which are known to proceed via associative mechanism.[27]

## 5.5 Conclusion

Novel dinuclear Pt(II) complexes were synthesized and their kinetic substitution reactions undertaken. It was found that the use of pyridine ligands instead of $NH_3$ on $Pt(NH_3)_2(OH_2)\}_2$-μ-pzn]$^{4+}$ complexes increases the substitution rates of diaqua complexes by a factor of 10 and 23 for the *trans* and *cis* complexes respectively during which an associative mode of substitution is retained. This is because pyridine enhances the π-backbonding by accepting the electrons from the metal centres to the empty $\pi^*$-orbitals of the pyridine sub units. This is made possible due to the geometry configuration that results in pyridine rings, pyrazine and Pt centre being on the same plane. This situation results in lower p$K_a$ values, increase in electrophilicity of the Pt(II) centre and an increase in reactivity of the metal centre as supported by DFT calculations. The trend in these azine bridged Pt(II) complexes remain the same as those reported containing $NH_3$ ligands.[1g,3] Electron-donating groups such as methyl as used in this study donate electrons in the pyrazine bridge and impart steric hindrance to the approach of nucleophile on the metal ions.

## 5.6 References


1. (a) Mambanda, A., Jaganyi, D., Hochreuther, S. and van Eldik, R., *Dalton Trans.*, **2010**, *39*, 3595; (b) Mambanda, A and Jaganyi, D. *Dalton Trans.*, **2012**, *41*, 908; (c) Hochreuther, S. and van Eldik, R., *Inorg. Chem*., **2012**, *51*, 3025; (d) Hochreuther, S., Puchta, R., and van Eldik, R., *Inorg. Chem*., **2011**, *50*, 8984; (e) Soldatović, T, Jovanović, S, Bugarčić, Ž.D, van Eldik R., *Dalton Trans.*, **2012**, *41*, 876; (f) Hochreuther, S., Puchta, R., and van Eldik, R., *Inorg. Chem*., **2011**, *50*, 12747; (g)

Reddy, D and Jaganyi, D. *Int. J. Chem. Kinet*., **2011**, *43*, 161; (h) Jaganyi, D., Munisamy, V. M. and Reddy, D., *Int. J. Chem. Kinet*., **2006**, *38*(3), 202; (i) Ertürk, H., Hofmann, A., Puchta, R. and van Eldik, R. *Dalton Trans.*, **2007**, 2295; (j) Ertürk, H., Maigut, J., Puchta, R. and van Eldik, R., *Dalton Trans.*, **2008**, 2759; (k) Hofmann, A. and van Eldik, R., *Dalton Trans.*, **2003**, 2979; (l) Ertürk, H., Puchta, R., and van Eldik, R., *Eur. J. Inorg. Chem.*, **2009**, 1334.

2. Jaganyi, D., Ongoma P., manuscript in preparation.

3. Jaganyi, D and Ongoma, P., *Dalton Trans*., **2013**, *42*, 2724.

4. Zou, Y., Van Houten, B and Farrell, N., *Biochemistry.*, **1993**, *32*, 9632.

5. (a) Farrell, N., Appleton, T. G., Qu, Y., Roberts, J. D., Soares Fontes, A. P., Skov, K. A., Wu, P., and Zou, Y., *Biochemistry*., **1995**, *34,* 15480; (b) Kasparková, J. Novaková, O., Marini, V., Najajreh, Y., Gibson, D., Perez, J.-M., and Brabec, V., *J. Biol. Chem*., **2003**, *278*(48), 47516; (c) Kalinowska-Lis, U., Ochocki, J., Matlawska-Wasowska, K., *Coordination Chemistry Reviews.*, **2008**, *252*,1328.

6. Farrer, N. J., Woods, J. A., Salassa, L., Zhao, Y., Robinson, K. S., Clarkson, G., Mackay, F. S. and Sadler, P. J., *Angew. Chem. Int. Ed*., **2010**, *49*, 8905.

7. (a) Hollis, L. S., Amundsen, A. R., Stern, E. W., *J. Med. Chem*., **1989**, *32*, 128; (b) Y. Qu, N. Farrell,. *Inorg. Chem*., **1992**, *31*, 930.

8. Jansen, B. A. J., van der Zwan, J., den Dulk, H., Brouwer, J., and Reedijk, J., *J. Med. Chem.,* **2001**, *44,* 245.

9. Origin$^{7.5TM}$ SRO, v7.5714 (B5714), Origin Lab Corporation, Northampton, One, Northampton, MA, 01060, USA, **2003**.

10. Becke, A. D. *J. Chem. Phys*., **1993**, *98*, 5648.

11. Wadt, W. R.; Hay, P. J. *J. Chem. Phys.,* **1985**, *82*, 284.

12. Frisch, M. J., Trucks, G. W., Schlegel, H. B., Scuseria, G. E., Robb, M. A., Cheeseman, J. R., Scalmani, G., Barone, V., Mennucci, B., Petersson, G. A., Nakatsuji, H., Caricato, M., Li, X., Hratchian, H. P., Izmaylov, A. F., Bloino, J., Zheng, G., Sonnenberg, J. L., Hada, M., Ehara, M., Toyota, K., Fukuda, R., Hasegawa, J., Ishida, M., Nakajima, T., Honda, Y., Kitao, O., Nakai, H., Vreven, T., Montgomery, J. A., Peralta, J. E., Ogliaro, F., Bearpark, M., Heyd, J. J., Brothers, E., Kudin, K. N., Staroverov, V. N., Kobayashi, R., Normand, J., Raghavachari, K., Rendell, A., Burant, J. C., Iyengar, S. S., Tomasi, J., Cossi, M., Rega, N., Millam, J. M., Klene, M., Knox, J. E., Cross, J. B., Bakken, V., Adamo, C., Jaramillo, J., Gomperts, R., Stratmann, R. E., Yazyev, O., Austin, A. J., Cammi, R., Pomelli, C., Ochterski, J. W., Martin, R. L., Morokuma, K., Zakrzewski, V. G., Voth, G. A., Salvador, P., Dannenberg, J. J., Dapprich, S., Daniels, A. D., Farkas, O., Foresman, J. B., Ortiz, J. V., Cioslowski, J., and Fox, D. J., *Gaussian 09, Revision A.1*, Gaussian, Inc., Wallingford CT, **2009**.

13. G.-Y. Lee and M.-S. Jun*, Bull. Korean Chem. Soc.,* **2001**, *22*(1), 11.

14. Eyring, H., *J. Chem. Phys*., **1935**, *3*, 107.

15. (a) Mebi, C. A. *J. Chem. Sci.*, **2011**, *123*(5), 727; (b) Jaramillo, P.,. Domingo, L. R, Pérez, P., *www.captura.uchile.cl/jspui/bitstream/2250/5781/1/Jaramillo_P.pdf,* **2006**; (c) Cedillo, A. and Contreras, R., *J. Mex. Chem. Soc.*, **2012**, *56(3),* 257; (d) (Parr, R. G.; Szentpály, L. V.; Liu, S. *J. Am. Chem. Soc.*, **1999**, *121*, 1922; (e) Parthasarathi, R., Subramanian, V., Roy, D. R. and Chattaraj, P. K., *Bioorg. Med. Chem*., **2004**, *12*, 5533.

16. Katritzky, A. R. and Pozharski, A. F. "*Handbook of Heterocyclic Chemistry*", Pergamon/Elsevier 2nd, Edition, **2000**, pg 177-178.

17. Hofmann, A, D. Jaganyi, O. Q. Munro, G. Leihr and R. van Eldik, *Inorg. Chem.*, **2003**, *42*, 1688.

18. (a) Jaganyi, D., Hofmann, A., van Eldik, R., *Angew Chem. Int., Ed*., **2001**,*40*, 1680; (b) Jaganyi, D., Reddy,D., Gertenbach, J-A., Hofmann, A and van Eldik, R., *Dalton Trans*., **2004**, 299.

19. Schmülling, M., Grove, D.M., van Koten, G., van Eldik, R., Veldman, N., Spek, A. L., *Organometallics.*, **1996**, *15*, 1384.

20. Schiessl, W. C., Summa, N. K., Weber, C. F., Gubo, S., Dücker-Benfer, C., Puchta, R., van Eikem Hommes, N. J. R and van Eldik, R., *Z. Anorg. Allg. Chem.,* **2005**, *631*, 2812.

21. Field, J. S., Gertenbach, J-A., Haines, R. J., Munro, O. Q and McMillin, D. R., *Z. Naturforsch.*, **2007**, *62b*, 447.

22. Jaganyi, D., Pantoja, E., Gallipoli, A., van Zutphen, S., Komeda, S., Reddy, D., Lutz, M., Tooke, D. M., Spek, A. L., Navarro-Ranninger, C and Reedijk, J., *J. Inorg. Biochem*., **2006**, *100*, 1955.

23. Hofmann, A., Dahlernburg, L and van Eldik, R., *Inorg. Chem.*, **2003**, *42*, 6528.

24. Pasini, A., Rigamonti, L., Forni, A., Manassero, M., Manassero, C*., Inorg. Chem.,* **2010**, *49*, 123.

25. Jaganyi, D. and Tiba, F., *Transition Met. Chem.*, **2003**, *28*, 803.

26. Reddy, D. and Jaganyi, D., *Transition Met. Chem.*, **2006**, *31*, 792.

27. Tobe, M. L. and Burgess, J., *Inorganic Reaction Mechanisms*, Addison Wiley, Longman, Ltd., Essex, **1999**, pp. 30–33, 70–112.

## 5.7 Supporting Information (SI)

The available SI includes a number of NMR and mass spectra, wavelengths for kinetic measurements, pH titration spectra, concentration dependence and Eyring plots for determination of second order rate constants and activation parameters respectively, HOMO-LUMO energy diagrams and planarity of the investigated complexes.

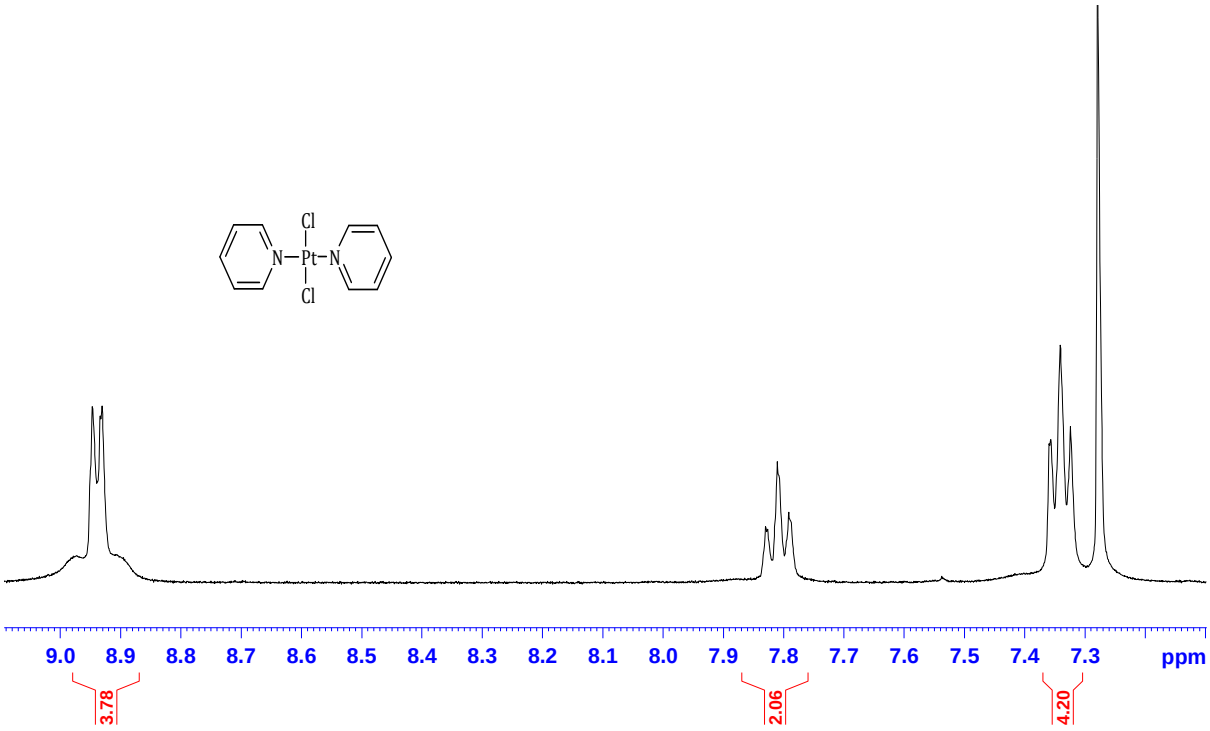


**Figure SI 5.1**: $^{1}$H NMR spectrum of ***trans*-[$PtCl_2Py_2$]**

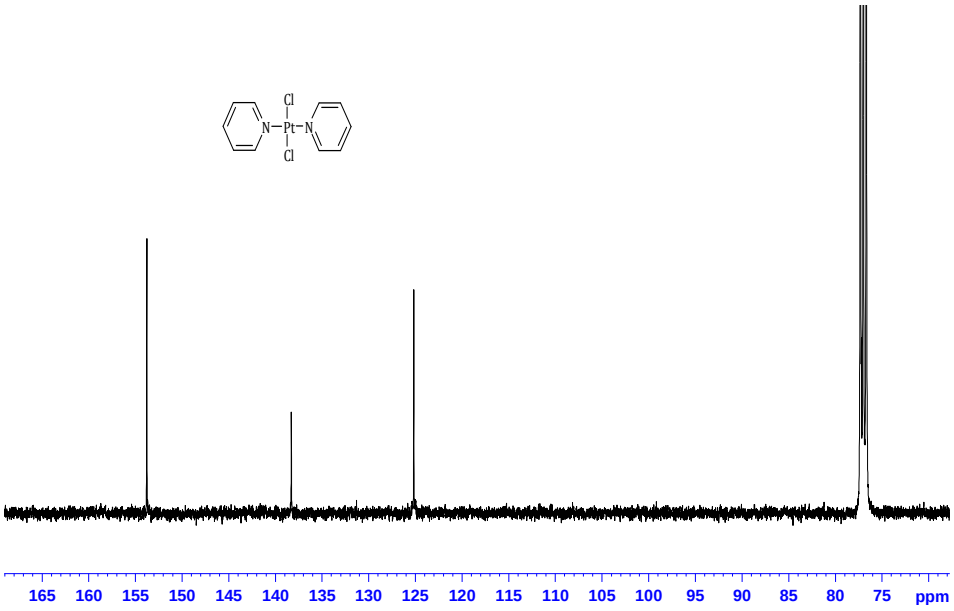


**Figure SI 5.2**: $^{13}$C NMR spectrum of ***trans*-[PtCl$_2$Py$_2$]**

**Elemental Composition Report** Page 1

**Single Mass Analysis**
Tolerance = 4.0 PPM / DBE: min = -1.5, max = 50.0
Element prediction: Off
Number of isotope peaks used for i-FIT = 3

Monoisotopic Mass, Even Electron Ions
63 formula(e) evaluated with 1 results within limits (all results (up to 1000) for each mass)
Elements Used:
C: 5-15 H: 5-15 N: 0-5 Na: 0-1 Cl: 0-2 Pt: 0-1

Grace Kinunda
trans py 38 (0.632) Cm (1:59)

TOF MS ES+
1.62e+005

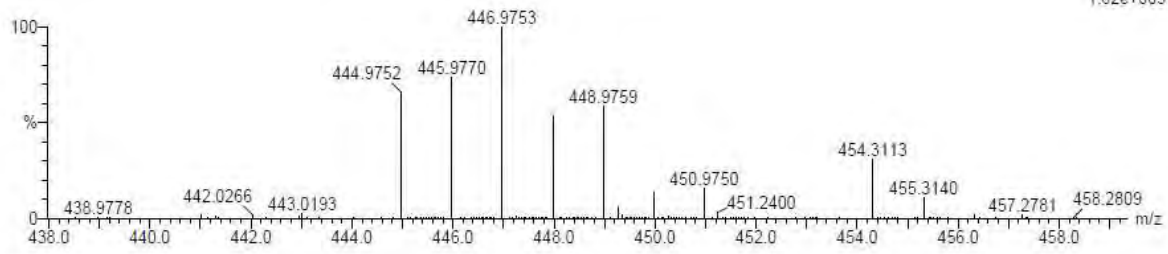


| | | | | | | | |
|---|---|---|---|---|---|---|---|
| Minimum: | | | | -1.5 | | | |
| Maximum: | | 5.0 | 4.0 | 50.0 | | | |
| Mass | Calc. Mass | mDa | PPM | DBE | i-FIT | i-FIT (Norm) | Formula |
| 445.9770 | 445.9767 | 0.3 | 0.7 | 6.5 | 583.5 | 0.0 | C10 H10 N2 Na Cl2 Pt |

**Figure SI 5.3**: Mass spectrum of ***trans*-[PtCl$_2$Py$_2$]**

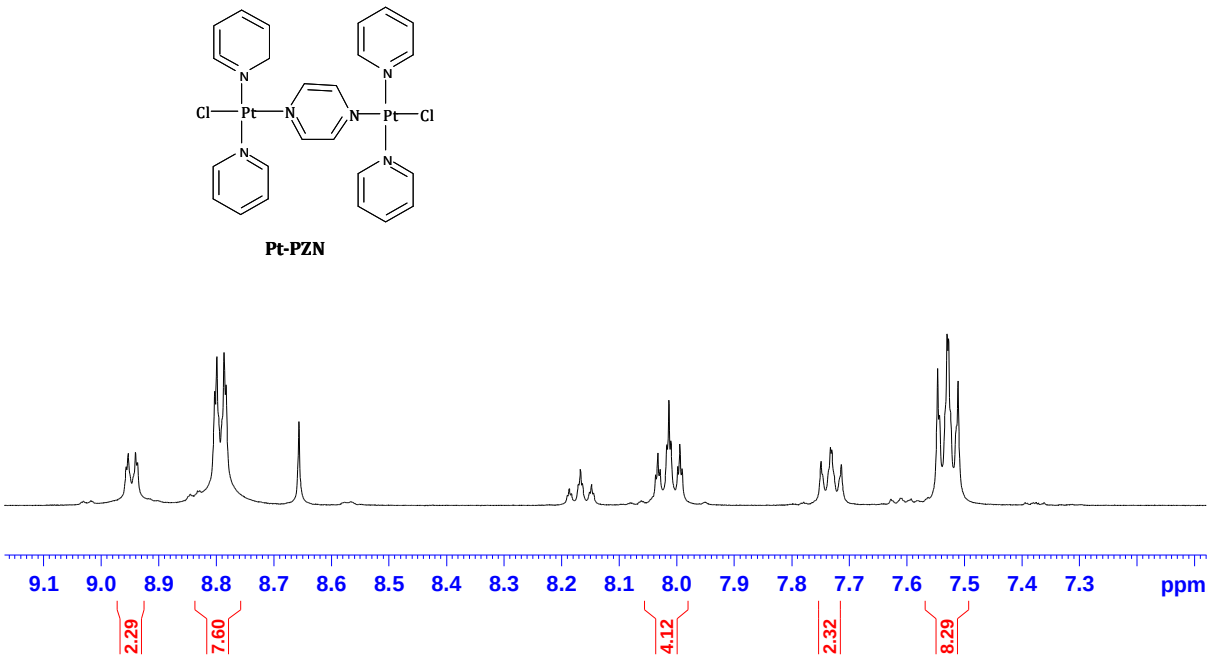


**Figure SI 5.4**: $^{1}$H NMR spectrum of **Pt-PZN**

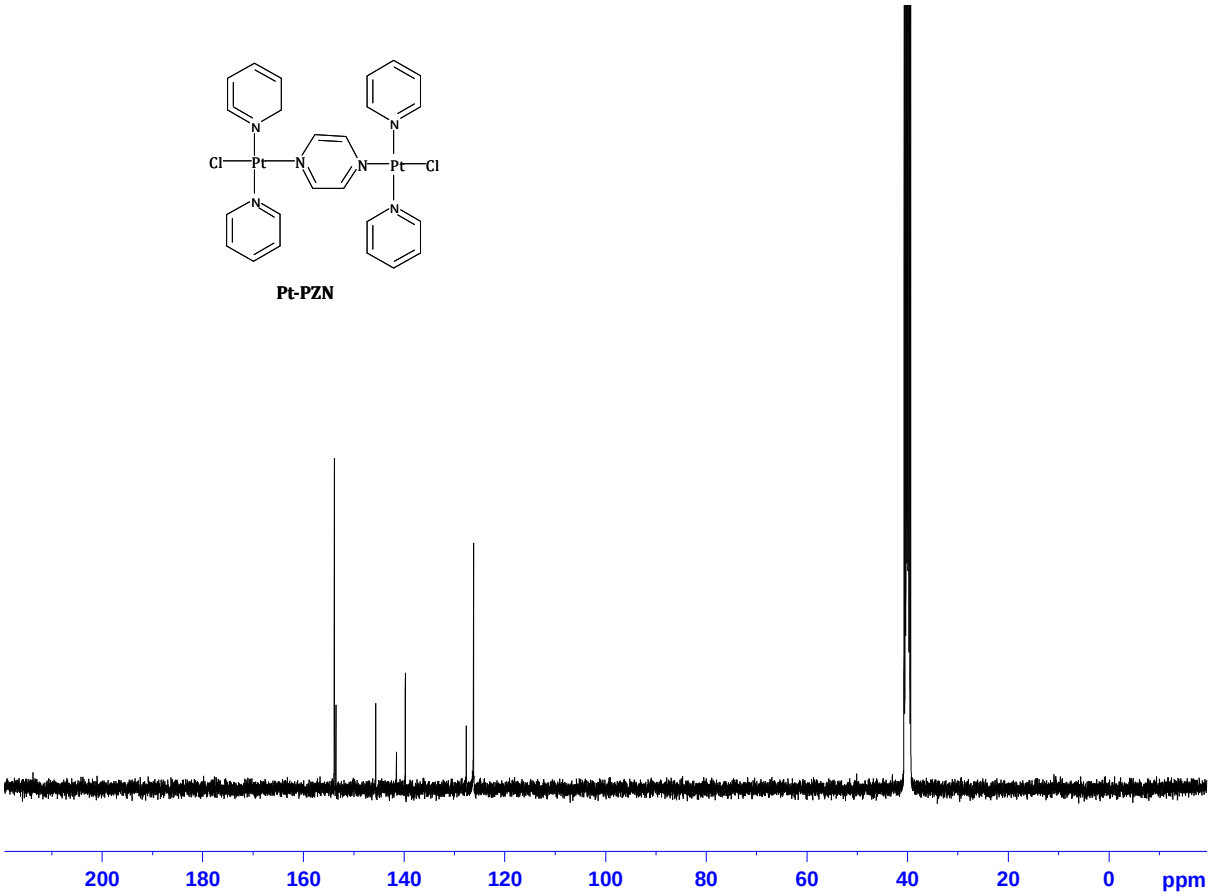


**Figure SI 5.5**: $^{13}$C NMR spectrum of **Pt-PZN**

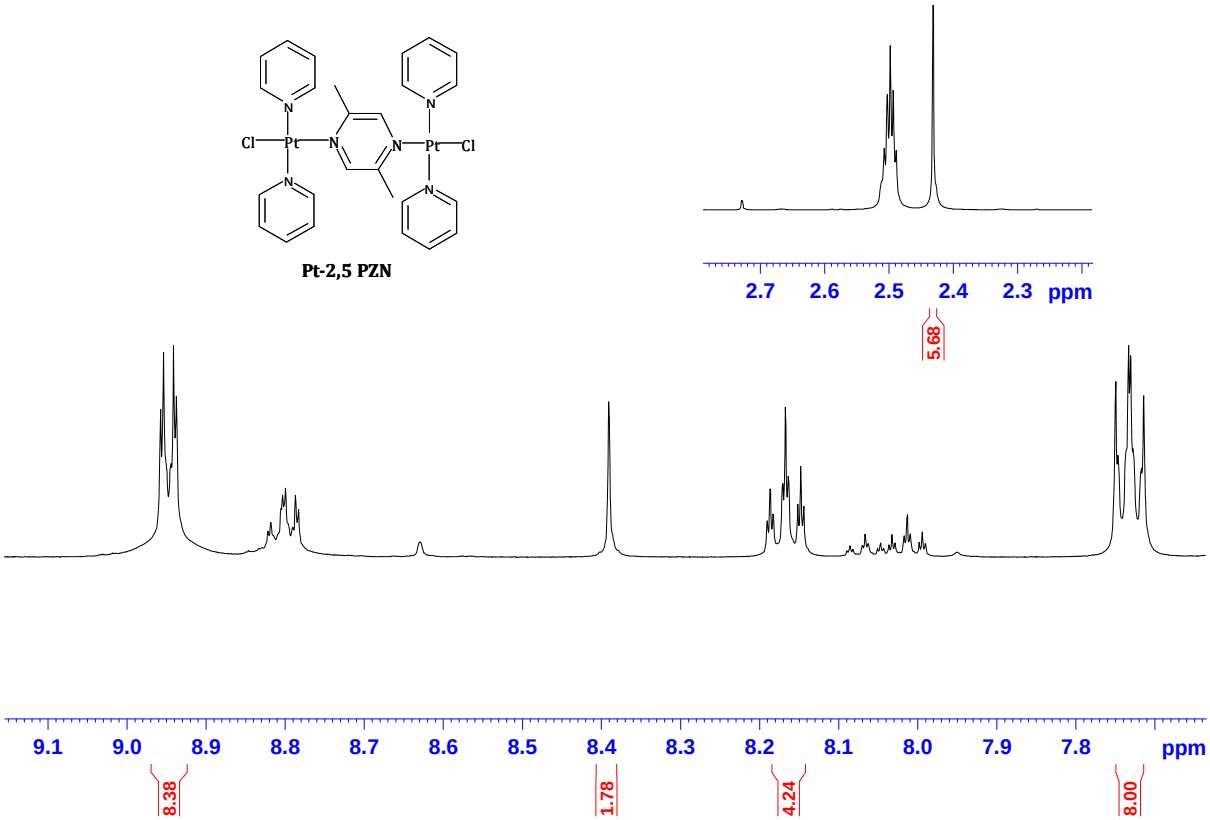


**Figure SI 5.6**: $^{1}$H NMR spectrum of **Pt-2,5PZN**

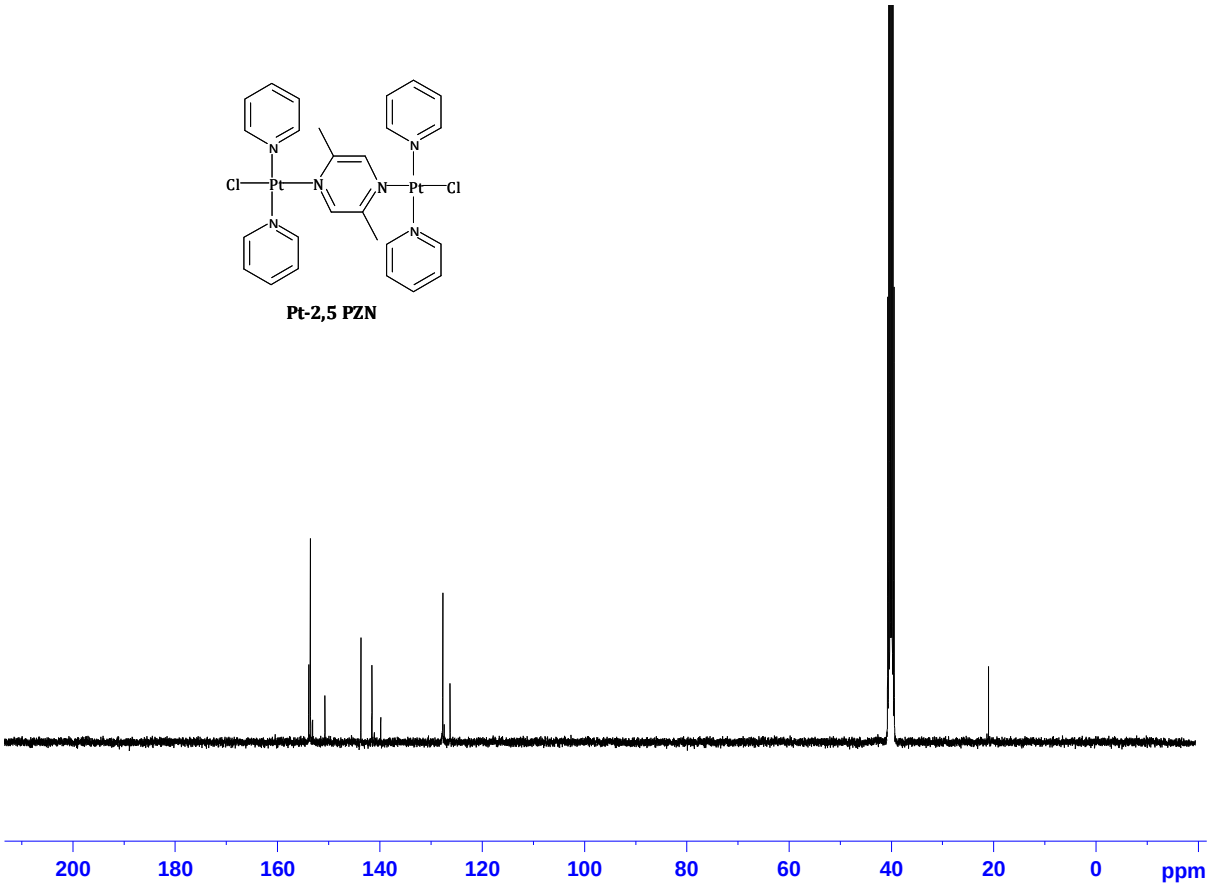


**Figure SI 5.7**: $^{13}$C NMR spectrum of **Pt-2,5PZN**

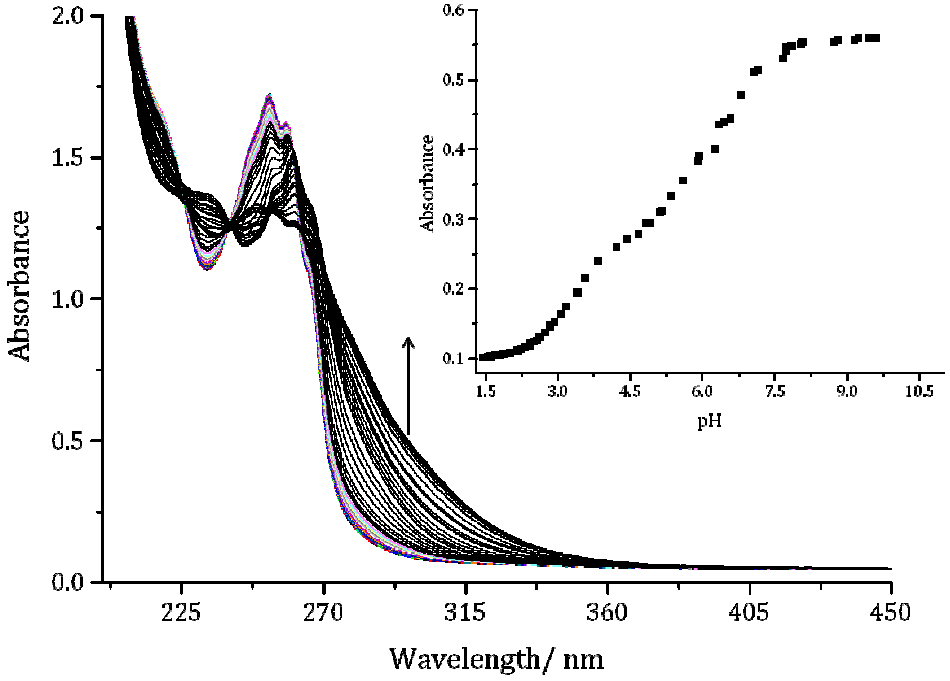


**Figure SI 5.8**: UV-Vis spectra of the **Pt-2,3PZN** diaqua complex recorded as a function of pH in the range of 1 to 10 at 25 °C. *Inset*: Plot of absorbance versus pH at 293 nm.

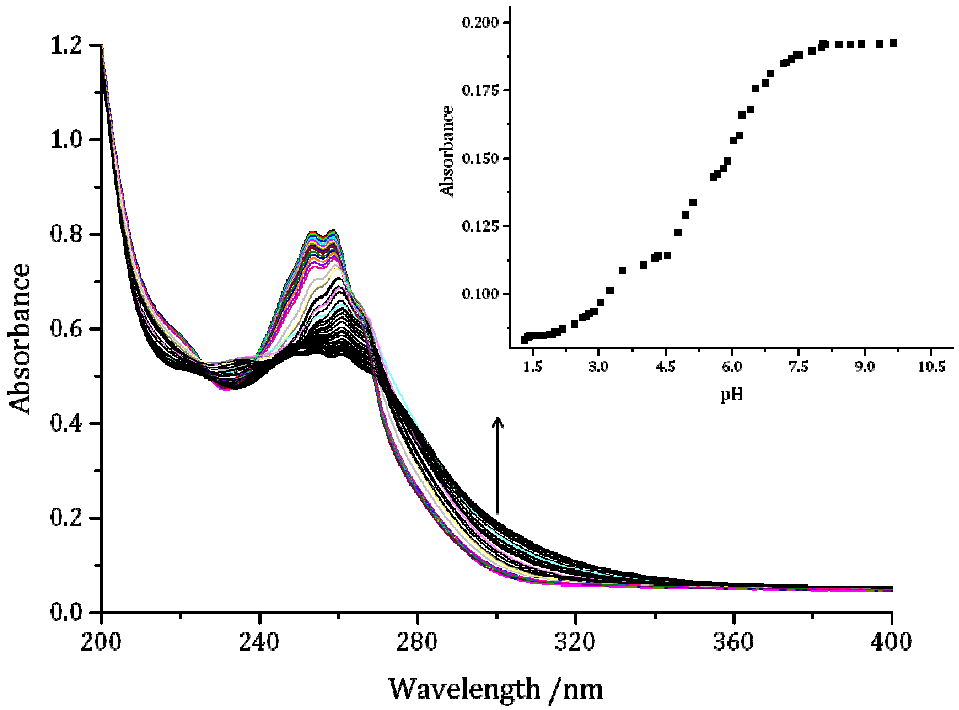


**Figure SI 5.9:** UV-Vis spectra of the **Pt-2,5PZN** diaqua complex recorded as a function of pH in the range of 1 to 10 at 25 °C. *Inset*: Plot of absorbance versus pH at 300 nm.

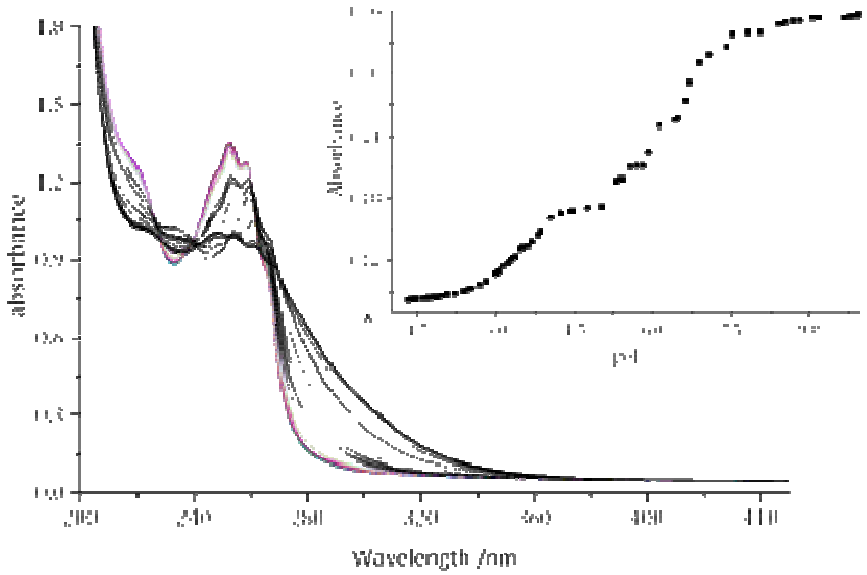


**Figure SI 5.10:** UV-Vis spectra of the **Pt-PZN** diaqua complex recorded as a function of pH in the range of 1 to 10 at 25 °C. *Inset*: Plot of absorbance versus pH at 300 nm.

**Table S1 5.1:** Summary of the wavelengths (nm) used for monitoring the kinetic reactions between a series of Pt(II) complexes and thiourea nucleophiles.

| Complex | Nucleophiles | Wavelength, λ (nm) |
|---|---|---|
| **Pt-PZN** | TU<br>DMTU<br>TMTU | 295<br>296<br>315 |
| **Pt-2,3PZN** | TU<br>DMTU<br>TMTU | 295<br>296<br>315 |
| **Pt-2,5PZN** | TU<br>DMTU<br>TMTU | 294<br>300<br>320 |
| **Pt-2,6PZN** | TU<br>DMTU<br>TMTU | 295<br>300<br>317 |

**Table SI 5.2**: Average observed rate constants, $k_{obs1/2}$ ($s^{-1}$), for the first and second displacement of the aqua ligands in **Pt-PZN**, by thiourea nucleophiles, T = 298 K, pH = 2, $I$ = 0.1 M $NaClO_4$

| $k_{obs1}$ ($s^{-1}$) | | | | $k_{obs2}$ ($s^{-1}$) | | |
|---|---|---|---|---|---|---|
| [NU] /M | TU | DMTU | TMTU | TU | DMTU | TMTU |
| 0.0034 | 1.50331 | 1.38221 | 0.44642 | 0.27128 | 0.14384 | 0.0917 |
| 0.0068 | 2.86203 | 2.6906 | 0.78597 | 0.50164 | 0.27428 | 0.16978 |
| 0.0102 | 4.1375 | 4.18243 | 1.09161 | 0.74936 | 0.45012 | 0.23902 |
| 0.0136 | 5.63436 | 5.14312 | 1.361 | 0.94356 | 0.60564 | 0.3198 |
| 0.017 | 7.55946 | 6.73364 | 1.68249 | 1.25218 | 0.8032 | 0.43498 |

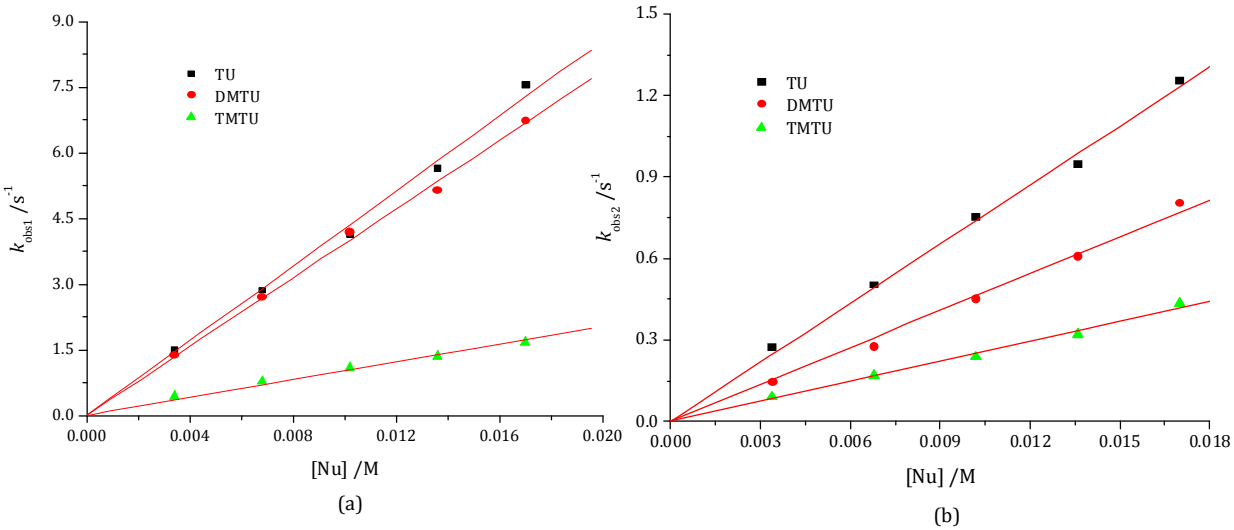


**Figure SI 5.11**: Dependence of the $k_{obs1/2}$ on the entering nucleophile concentration for the (a) first and (b) second displacement of the aqua ligands in **Pt-PZN** by thiourea nucleophiles, T = 25 °C, pH = 2, $I$ = 0.1 M $NaClO_4$.

**Table SI 5.3**: Temperature dependence of $k_{obs1/2}$ ($s^{-1}$) for the displacement of aqua ligands in **Pt-PZN** by thiourea nucleophiles at 60-fold excess over [Pt], pH = 2, $I$ = 0.1 M $NaClO_4$.

| **Parameter** | $\ln(k_1/T)$ | | | $\ln(k_2/T)$ | | |
|---|---|---|---|---|---|---|
| | **Nucleophile** | | | **Nucleophile** | | |
| $1/T$, ($K^{-1}$) | TU | DMTU | TMTU | TU | DMTU | TMTU |
| 0.00347 | -4.57338 | -5.04894 | -6.45389 | -7.18388 | -8.46313 | -8.46313 |
| 0.00341 | -4.36579 | -4.68733 | -5.98511 | -6.94618 | -8.17877 | -8.17877 |
| 0.00336 | -4.13094 | -4.38711 | -5.67243 | -6.67878 | -7.82144 | -7.82144 |
| 0.0033 | -3.9465 | -4.17314 | -5.37874 | -6.35838 | -7.52332 | -7.52332 |
| 0.00325 | -3.70683 | -3.90795 | -5.08522 | -6.07485 | -7.1903 | -7.1903 |

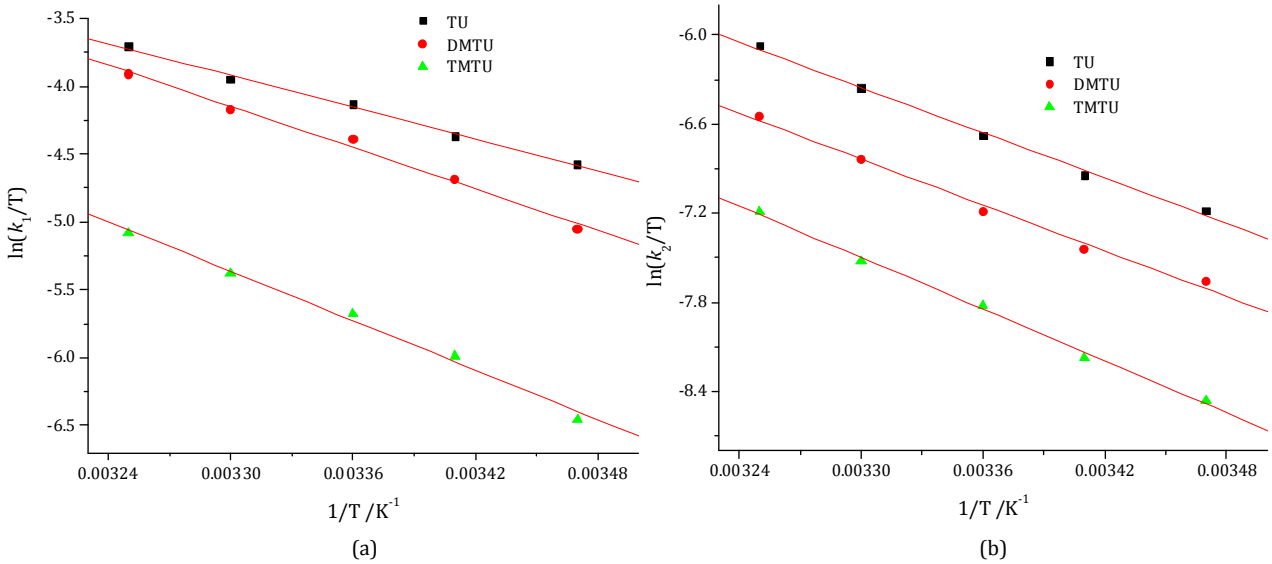


**Figure SI 5.12**: Eyring plots of the reaction between **Pt-PZN** and thiourea nucleophiles at various temperatures in the range of 15-35 °C.

**Table SI 5.4**: Average $k_{obs1/2}$ ($s^{-1}$), for the first and second displacement of the aqua ligands in **Pt-2,3PZN**, by thiourea nucleophiles, T = 298 K, pH = 2, $I$ = 0.1 M $NaClO_4$.

| $k_{obs1}$ ($s^{-1}$) | | | | $k_{obs2}$ ($s^{-1}$) | | |
|---|---|---|---|---|---|---|
| [NU] /M | TU | DMTU | TMTU | TU | DMTU | TMTU |
| 0.002 | 0.534 | 0.43624 | 0.28936 | 0.064 | 0.05277 | 0.03462 |
| 0.004 | 1.14128 | 0.8248 | 0.58784 | 0.12941 | 0.11324 | 0.08709 |
| 0.006 | 1.5562 | 1.192 | 0.8546 | 0.19044 | 0.15588 | 0.1237 |
| 0.009 | 2.1312 | 1.61432 | 1.245 | 0.25355 | 0.2115 | 0.1657 |
| 0.011 | 2.708 | 1.99956 | 1.43976 | 0.32963 | 0.25562 | 0.19445 |

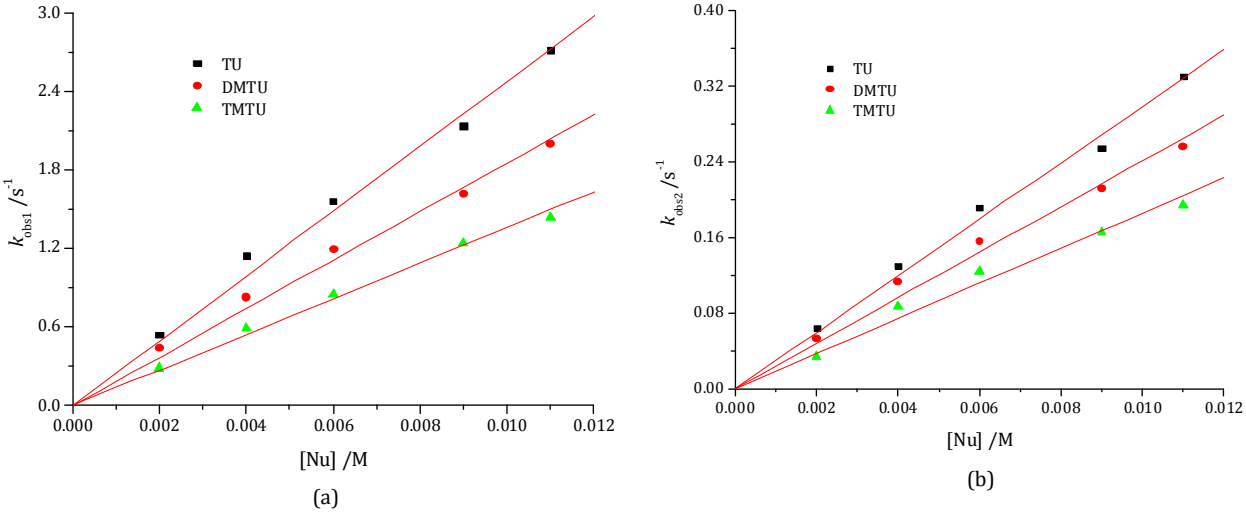


**Figure SI 5.13**: Dependence of the $k_{obs1/2}$ on the entering nucleophile concentration for the (a) first and (b) second displacement of the aqua ligands in **Pt-2,3PZN** by thiourea nucleophiles, T = 25 °C, pH = 2, $I$ = 0.1 M $NaClO_4$.

**Table SI 5.5**: Temperature dependence of $k_{obs1/2}$ ($s^{-1}$) for the displacement of aqua ligands in **Pt-2,3PZN** by thiourea nucleophiles at 60-fold excess over [Pt], pH = 2, *I* = 0.1 M $NaClO_4$.

| **Parameter** | $\ln(k_1/T)$ | | | $\ln(k_2/T)$ | | |
|---|---|---|---|---|---|---|
| | **Nucleophile** | | | **Nucleophile** | | |
| $1/T$ ($K^{-1}$) | TU | DMTU | TMTU | TU | DMTU | TMTU |
| 0.00347 | -7.61912 | -7.57256 | -8.45298 | -8.84238 | -10.32132 | -9.36736 |
| 0.00341 | -7.02853 | -7.25174 | -7.92795 | -8.61572 | -9.99911 | -9.04516 |
| 0.00336 | -6.64114 | -6.90776 | -7.45387 | -8.38622 | -9.557 | -8.81915 |
| 0.0033 | -6.18179 | -6.54041 | -7.19258 | -8.21865 | -9.3372 | -8.64181 |
| 0.00325 | -5.92066 | -6.23796 | -6.81955 | -8.04097 | -9.05819 | -8.47234 |

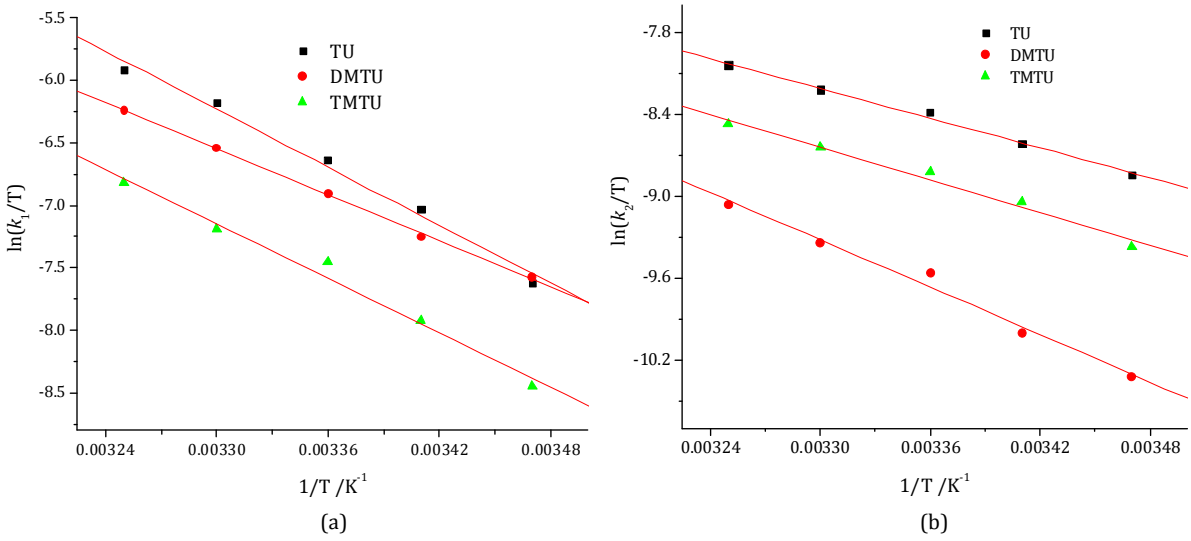


**Figure SI 5.14:** Plots of $\ln\frac{k_{1/2}}{T}$ *versus* $1/T$ for the reaction of **Pt-2,3PZN** with thiourea nucleophiles at various temperatures in the range of 15-35 °C.

**Table SI 5.6**: Average $k_{obs1/2}$ ($s^{-1}$), for the first and second displacement of the aqua ligands in **Pt-2,5PZN**, by thiourea nucleophiles, T = 298 K, pH = 2, $I$ = 0.1 M $NaClO_4$.

| $k_{obs1}$ ($s^{-1}$) | | | | $k_{obs2}$ ($s^{-1}$) | | |
|---|---|---|---|---|---|---|
| [NU] /M | TU | DMTU | TMTU | TU | DMTU | TMTU |
| 0.002 | 0.64354 | 0.58385 | 0.19757 | 0.09622 | 0.07088 | 0.04984 |
| 0.004 | 1.28572 | 1.08063 | 0.40691 | 0.17146 | 0.1388 | 0.10452 |
| 0.006 | 1.8644 | 1.84714 | 0.61593 | 0.247 | 0.22508 | 0.16206 |
| 0.008 | 2.51818 | 2.37915 | 0.79863 | 0.35234 | 0.3073 | 0.21748 |
| 0.01 | 3.1318 | 3.14346 | 1.03766 | 0.43636 | 0.3932 | 0.27744 |

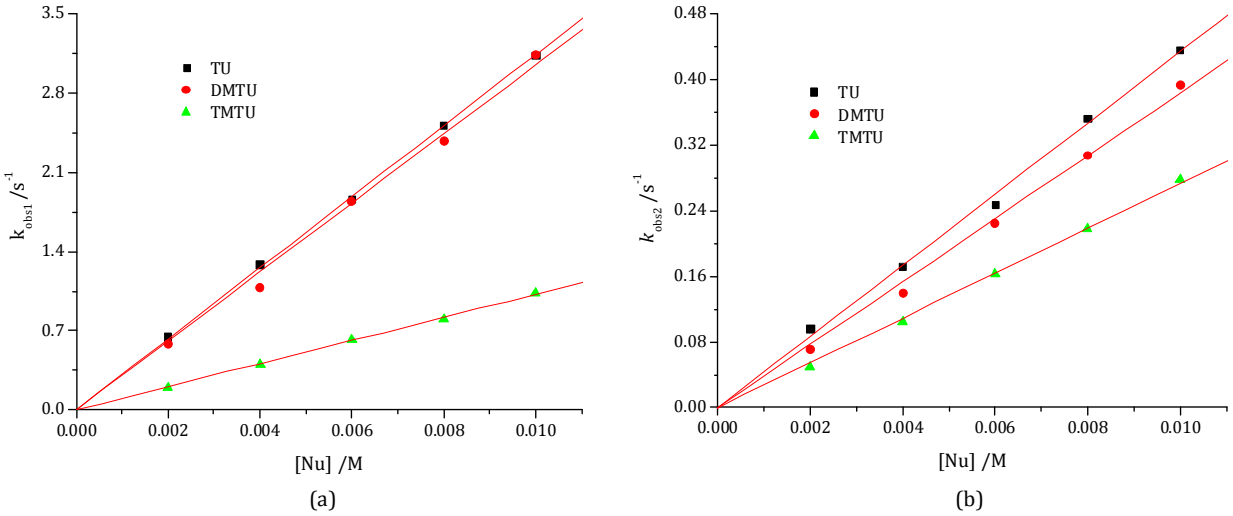


**Figure SI 5.15**: Dependence of the $k_{obs1/2}$ on the entering nucleophile concentration for the (a) first and (b) second displacement of the aqua ligands in **Pt-2,5PZN** by thiourea nucleophiles, T = 25 °C, pH = 2, $I$ = 0.1 M.

**Table SI 5.7**: Temperature dependence of $k_{obs1/2}$ ($s^{-1}$), for the displacement of aqua ligands in **Pt-2,5PZN** by thiourea nucleophiles at 60-fold excess over [Pt], pH = 2, $I$ = 0.1 M $NaClO_4$.

| **Parameter** | $\ln(k_1/T)$ | | | $\ln(k_2/T)$ | | |
|---|---|---|---|---|---|---|
| | **Nucleophile** | | | **Nucleophile** | | |
| $1/T$, ($K^{-1}$) | TU | DMTU | TMTU | TU | DMTU | TMTU |
| 0.00347 | -5.5960 | -5.4479 | -6.7586 | -8.2572 | -8.3290 | -8.7514 |
| 0.00341 | -5.4105 | -5.2236 | -6.4810 | -8.0808 | -8.1343 | -8.5320 |
| 0.00336 | -5.2197 | -5.0834 | -6.1817 | -7.7886 | -7.8815 | -8.2100 |
| 0.0033 | -5.0285 | -4.9448 | -5.9610 | -7.5534 | -7.6216 | -7.9317 |
| 0.00325 | -4.8970 | -4.7157 | -5.7001 | -7.2747 | -7.3279 | -7.5965 |

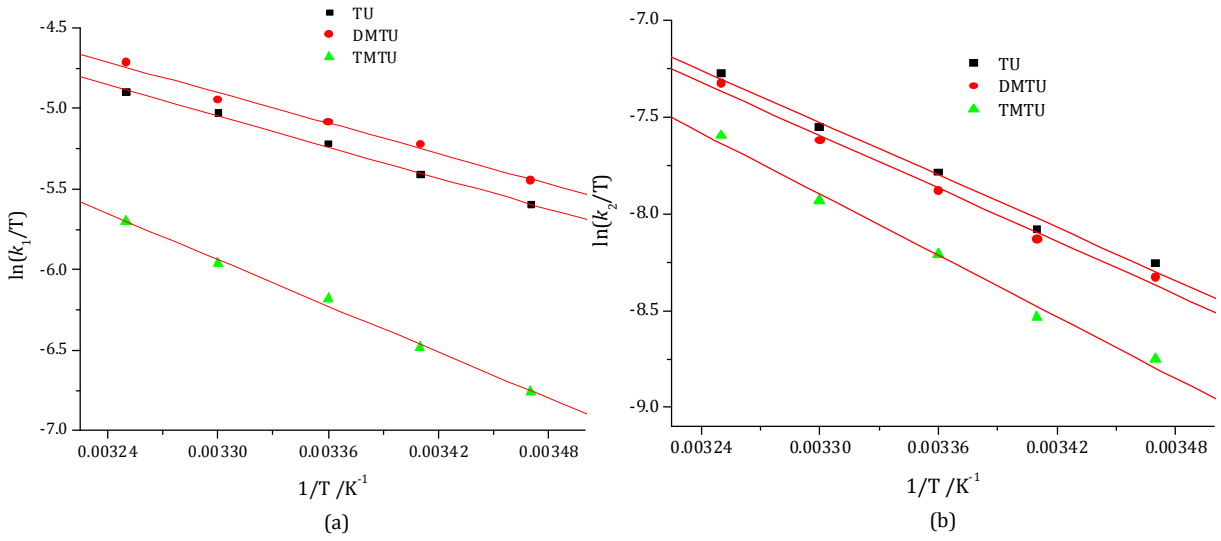


**Figure SI 5.16:** Plots of $\ln\frac{k_{1/2}}{T}$ *versus* $1/T$ for the reaction of **Pt-2,5PZN** with thiourea nucleophiles at various temperatures in the range of 15-35 °C.

**Table SI 6.8**: Average $k_{obs1/2}$ ($s^{-1}$), for the first and second displacement of the aqua ligands in **Pt-2,6PZN**, by thiourea nucleophiles, T = 298 K, pH = 2, $I$ = 0.1 M $NaClO_4$.

| $k_{obs1}$ /$s^{-1}$ | | | | $k_{obs2}$ /$s^{-1}$ | | |
|---|---|---|---|---|---|---|
| [NU] /M | TU | DMTU | TMTU | TU | DMTU | TMTU |
| 0.003 | 0.99156 | 0.50126 | 0.38488 | 0.05028 | 0.01632 | 0.01016 |
| 0.006 | 2.18952 | 1.14952 | 0.85088 | 0.09132 | 0.03202 | 0.0191 |
| 0.009 | 2.92896 | 1.7234 | 1.3008 | 0.13588 | 0.04758 | 0.02814 |
| 0.012 | 3.9162 | 2.39263 | 1.72008 | 0.19504 | 0.06738 | 0.03974 |
| 0.0144 | 5.0136 | 2.99495 | 2.2432 | 0.24286 | 0.08272 | 0.04862 |

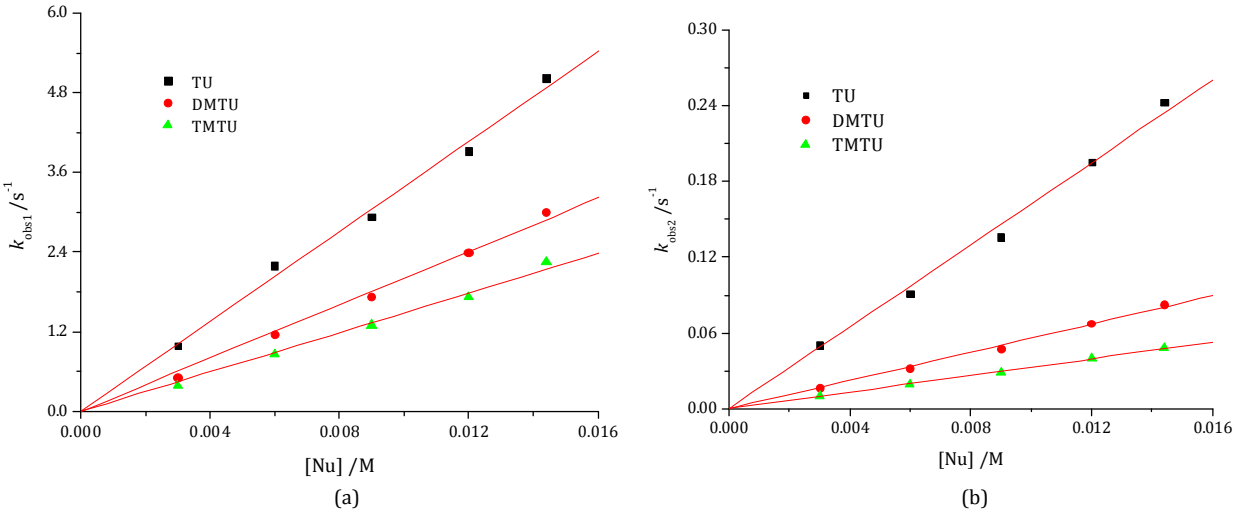


**Figure SI 5.17**: Dependence of the $k_{obs1/2}$ on the entering nucleophile concentration for the (a) 1st and (b) 2nd displacement of the aqua ligands in **Pt-2,6PZN** by thiourea nucleophiles, T = 25 °C, pH = 2, $I$ = 0.1 M.

**Table SI 5.9**: Temperature dependence of $k_{obs1/2}$ ($s^{-1}$) for the displacement of aqua ligands in **Pt-2,6PZN** by thiourea nucleophiles at 60-fold excess over [Pt], pH = 2, $I$ = 0.1 M.

| **Parameter** | $\ln(k_1/T)$ | | | $\ln(k_2/T)$ | | |
|---|---|---|---|---|---|---|
| | **Nucleophile** | | | **Nucleophile** | | |
| $1/T$, ($K^{-1}$) | TU | DMTU | TMTU | TU | DMTU | TMTU |
| 0.00347 | -7.63835 | -7.37212 | -8.19924 | -7.96047 | -7.78156 | -8.58619 |
| 0.00341 | -7.34248 | -7.07611 | -7.87146 | -7.65959 | -7.39392 | -8.22419 |
| 0.00336 | -7.10733 | -6.8604 | -7.53935 | -7.48387 | -7.1659 | -7.94875 |
| 0.0033 | -6.82076 | -6.45565 | -7.258 | -7.21563 | -6.76576 | -7.63979 |
| 0.00325 | -6.53864 | -6.20499 | -6.88528 | -6.92478 | -6.54994 | -7.26609 |

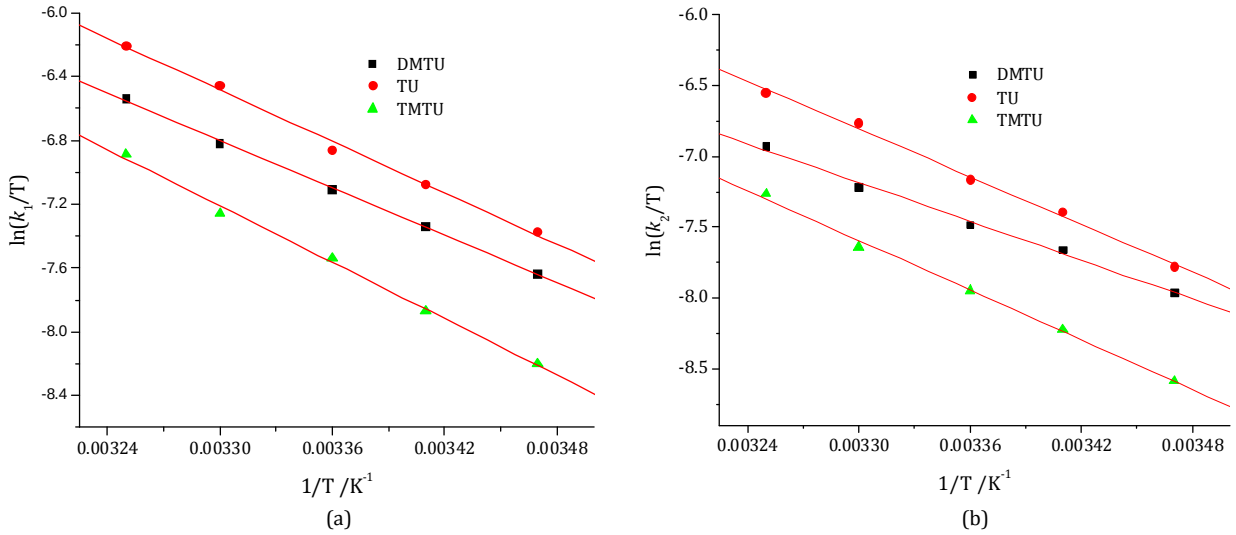


**Figure SI 5.18:** Plots of $\ln\frac{k_{1/2}}{T}$ *versus* $1/T$ for the reaction of **Pt-2,6PZN** with thiourea nucleophiles at various temperatures in the range of 15-35 °C.

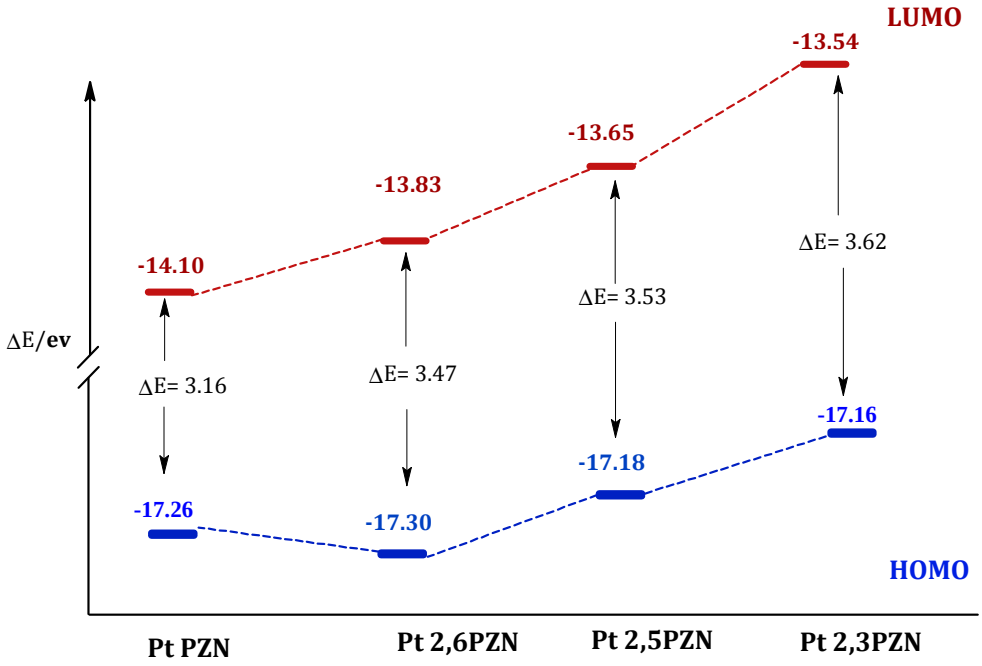


**Figure SI 5.19**: HOMO and LUMO energy gap for the investigated Pt(II) complexes.

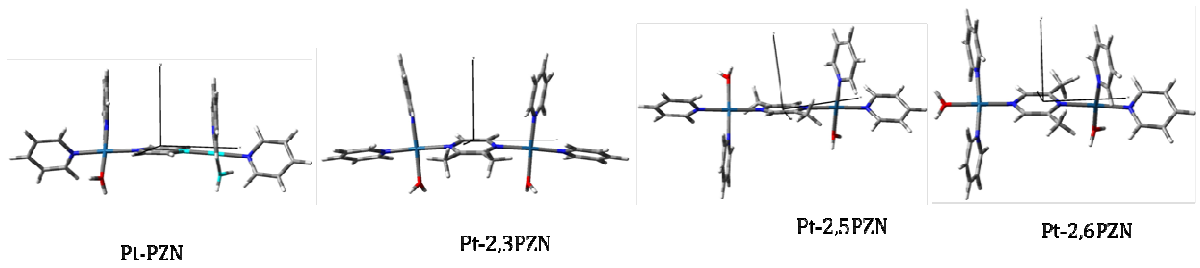


**Figure SI 5.20:** Cartesian coordinate axis of the complexes

## Table of Contents

**List of Tables**



**List of Figures**

# Chapter 6

## A Study on *Trans* Influence and π-conjugation Effects on Ligand Substitution Reactions of Pt(II) Complexes with Tridentate N/S-Donor Ligands


### Abstract

The rate of displacement of the chloride ligands by three neutral nucleophiles (Nu) of different steric demands, namely thiourea (TU), N,N'-dimethylthiourea (DMTU) and N,N,N,'N-tetramethylthiourea (TMTU) in the complexes *viz*; [{bis(2-pyridylmethyl)amine} platinum(II) chloride]$ClO_4$, (**Pt1**), [{N-(2-pyridinylmethyl)-8-Quinolinamine} platinum(II) chloride]Cl, (**Pt2**), {di-(2-picolyl) sulfide} platinum(II) chloride ]Cl, (**Pt3**) and [{8-((2-pyridylmethyl)thiol)Quinoline} platinum(II) chloride]Cl, (**Pt4**) was studied under *pseudo* first-order conditions as a function of concentration and temperature using a stopped-flow technique and UV-Visible spectrophotometry. The observed *pseudo* first-order rate constants for substitution reactions obeyed the simple rate law $k_{obs} = k_2[\mathrm{Nu}]$. The results showed that two substitution steps were observed for **Pt(N^S^N)** complexes with their chloro ligand being more labile by a factor of ten than **Pt(N^N^N)** complexes due to the high *trans* labilizing effect brought about by the S-donor atom. Quinoline based Pt(II) complexes (**Pt2** and **Pt4**) are found to react slower than their pyridine counterparts **Pt1** and **Pt3** due to poor π-acceptor ability of quinoline. The low values of activation enthalpy and large negative entropies of activation support an associative mode of activation.

## 6.1 Introduction

The substitution kinetics of different platinum(II) complexes towards biomolecules with sulfur donor atoms is very important from a biological and bioinorganic point of view.[1] Over the last few decades, there has been great interest in studying of the substitution reactions of monofunctional Pt(II) complexes, especially those with tridentate ligands, such as diethylenetriamine (dien), bis(2-pyridylmethyl)amine (bpma) or 2,2':6',2-terpyridine (terpy) as non-leaving groups.[2-4] It has been shown that small structural modifications in the non-labile chelate ligand can produce significant changes in the substitutional reactivity of the Pt(II) complexes. Most importantly, the reactivity of these Pt(II) complexes is significantly increased when π-back donation of electron density from the metal centre into the non-leaving ligand is involved. For example, chloride substitution in $[Pt(terpy)Cl]^+$ in methanol is $10^2$ to $10^4$ times faster than for the cationic $[Pt(dien)Cl]^+$.[2-4] This difference is attributed to stabilization of the five-coordinate transition state relative to the ground state brought about by the delocalization of the π-electron density which is back-donated from platinum *d*π-orbitals into the π*-molecular orbitals of the terpy ligand.[4]

Addition of electron-donating groups on the ancillary positions of the terpy ligand has been shown to weaken this stabilization resulting in retarded rates of substitution of the chloride.[4f] The opposite is true for electron-withdrawing groups.[4g] On the other hand, increasing the number and varying the position (*cis*/*trans*) of π-acceptor groups such as pyridine affects the electronic communication in the system hence affecting the reactivity of the Pt(II) centre.[5] The study by Hofmann *et al.*[6] showed that *cis* π-back donation of electron density is stronger than the *trans* π-back donation. While the *cis* σ-donor effect slows down

the reactivity of the Pt(II) complex, the *trans* σ-donor accelerates the rate of substitution reaction.[7]

Pitteri *et al.*[8] studied substitution reactions of Pt(II) complexes containing neutral tridentate chelating ligands with sulfur and nitrogen donors of the type N^S^N and N^N^N (where N^S^N = bis(2-pyridylmethyl)sulphide and N^N^N = bis(2-pyridylmethyl)amine) using ionic, neutral and pyridine nucleophiles. The reactivity data of the Pt(II) complexes indicated that apart from the π-interaction of the pyridine rings, the lability of the leaving group also depends on the nature or number of the donor atoms *trans* and/or *cis* to the replaceable chloride ligand.[8] For example, Pt(N^S^N) complexes were found to be more reactive than their Pt(N^N^N) counterparts. The high reactivity of Pt(N^S^N) complexes was attributed to the strong *trans*-labilization effect of the coordinated sulfur which results into elongation of the Pt–Cl bond at the ground state.[8] Such labilization has also been illustrated by an earlier study of Hofmann *et al* when *trans* donor atoms of the tridentate chelate were varied from N to C. The reactivity of Pt(N^C^N) complexes was accelerated by a factor of three compared with Pt(N^N^N) owing to strong *trans*-labilizing effect of Pt–C that induces high intrinsic reactivity.[6] This is due to the ability of the Pt–C bond to labilize the leaving group in square-planar metal complexes through the kinetic *trans*-effect.

Recent work in our laboratories showed that introduction of isoquinoline and quinoline ligand in the non-labile chelated framework can decrease the substitution rate of the Pt(II) complex in the range of 3-5 orders of magnitude owing to the fact that isoquinoline and quinoline are net σ-donors and poor π-acceptors.[9-11] A search in the literature domain

shows limited information on the factors which influence the reactivity of Pt(II) complexes bearing ligands with extended π-conjugation and different *trans* donor atoms.

This has led me to investigate the competing roles of π-backbonding through the extended chelate and the strong σ-donor *trans* effect of sulfur atom on the reactivity of Pt(II) metal complex within the chelate framework. To achieve this, I systematically replaced the *cis* positioned pyridyl groups with quinoline groups, and in *trans* position with N and S donor atoms. Therefore, chloride substitution of platinum(II) complexes with the general formulae [Pt(N^N^N)Cl] and [Pt(N^S^N)Cl namely: [{bis(2-pyridylmethyl)amine} Platinum(II) chloride]$ClO_4$, (**Pt1**), [{N-(2-pyridinylmethyl)-8-Quinolinamine} Platinum(II) chloride]Cl, (**Pt2**), {di-(2-picolyl) sulfide} Platinum(II) chloride ]Cl, (**Pt3**) and [{8-((2-pyridylmethyl)thiol)Quinoline} Platinum(II) chloride]Cl, (**Pt4**) (**Figure 6.1**) were studied using thiourea nucleophiles of different steric demand; thiourea (TU), 1,3-dimethyl-2-thiourea (DMTU), and 1,1,3,3,-tetramethyl-2-thiourea (TMTU). The thiourea nucleophiles were chosen because of their good solubility, neutral character, different nucleophilicity, steric hindrance, binding properties, and biological relevance.[12] Thiourea is a very useful nucleophile since it combines the ligand of thiolates (σ-donor) and thioethers (σ-donor and π-acceptor).[13-15] In addition, it is used as a protecting agent to minimize nephrotoxicity following cisplatin treatment.[16] NMR kinetics study was done to account for the dechelation of the N^S^N ligand framework.

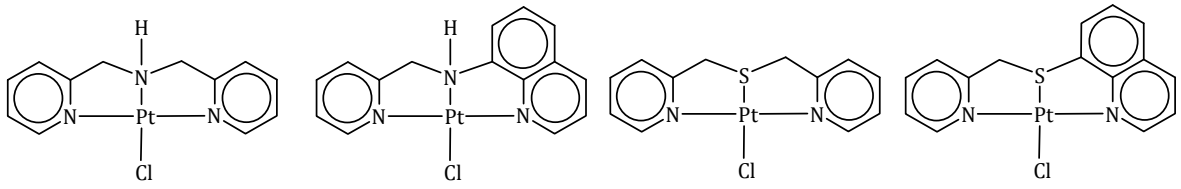


**Figure 6.1:** Structures of the complexes investigated

## 6.2 Experimental

### 6.2.1 Materials

All synthetic work was performed under nitrogen atmosphere using standard Schlenk techniques and vacuum-line systems. Solvents were dried by standard methods[17] and distilled prior to use. Thiosemicarbazide (99.0%), 8-bromoquinoline (98%), 8-aminoquinoline (98%), 2-picolyl chloride hydrochloride (98%), 8-mercaptoquinoline hydrochloride (98%), $NaO^tBu$ (97%), pyridine-2-carboxaldehyde (99%), lithium perchlorate (98%) and sodium borohydride (98%) were obtained from Aldrich. Potassium tetrachloroplatinate ($K_2PtCl_4$, 99.99%) was procured from Strem. All other chemicals were of the highest purity commercially available and were used without further purification.

### 6.2.2 Synthesis of the Ligands

Ligands di-(2-picolyl)sulfide (**dps**),[18] 8-((2-pyridylmethyl)thiol)quinoline (**NSNQ**)[19] and N-(2-pyridinylmethyl)-8-quinolinamine (**NNNQ**)[10] were synthesized following literature methods. Character identification data of the ligands were in agreement with the proposed structures.

**dps**: Yield: brown oil, 712.8 mg, 66%. $^{1}$H NMR ($CDCl_3$, 400 MHz): δ/ppm = 8.52 (br-d, 2H), 7.61 (td, 2H), 7.35 (d, 2H), 7.13 (ddd, 2H), 3.81 (s, 4H). $^{13}$C NMR ($CDCl_3$, 400 MHz): δ/ppm = 158.5, 149.5, 136.6, 123.3, 121.9 and 37.6. *Anal. calcd*. for $C_{12}H_{12}N_2S$: C 66.67, H 5.55, N 12.96. *Found*: C 66.16, H 5.36, N 13.01. TOF MS ES$^+$: $m/z$, $[M+Na]^+$ = 239.06.

**NSNQ**: Yield yellow powder, 572.3 mg, 90%. $^{1}$H NMR ($CDCl_3$, 400 MHz,): δ/ppm = 8.94(br-d, 1H), 8.54 (d, 1H), 8.11(dd, 1H), 7.63-7.52 (m, 4H), 7.45-7.35 (m, 2H), 7.14 (t, 1H), 4.47 (s, 2H). $^{13}$C NMR ($CDCl_3$, 400 MHz): δ/ppm = 157.7, 149.3, 149.0, 145.6, 137.7, 136.9, 136.4, 128.3, 126.7, 125.3, 124.4, 123.0, 122.1, 121.7, 37.7. *Anal. Calcd*. for $C_{15}H_{12}N_2S$: C 71.43, H 4.76, N 11.11, S 12.70. *Found* C 71.41, H 4.70, N 11.19, S 12.72. TOF MS ES$^+$: $m/z$, $[M+Na]^+$ = 275.06.

**NNNQ**: Yield yellow oil, 686.7 mg, 63%. $^{1}$H NMR ($CDCl_3$, 400 MHz): δ/ppm = 8.76(td, 1H), 8.62 (d, 1H), 8.05(ddd, 1H), 7.60 (td, 1H), 7.42-7.29 (m, 3H), 7.14 (dd, 1H), 7.09(dd, 1H), 6.92(dd, 1H), 6.63(d, 1H), 4.71 (s, 2H). $^{13}$C NMR ($CDCl_3$, 400 MHz): δ/ppm = 159.3, 149.3, 147.6, 136.7, 136.3, 127.7, 127.4, 122.0, 121.4, 121.3, 116.3, 114.5, 110.2, 105.6, 49.3. TOF MS ES$^+$: $m/z$, $[M + 23]^+$ = 258.10.

### 6.2.3 Synthesis of Pt(II) Complexes

Complexes **Pt1**[20], **Pt2**[10,] **Pt3**[21] and **Pt4**[21] were synthesized according to the published procedures. Platinum precursor *cis*/*trans*-$PtCl_2(SMe_2)_2$ was synthesized as described in literature.[22] The purity of all the Pt(II) complexes were confirmed by NMR, elemental analysis and LC-MS.

**Pt1**: Yield: 242.3 mg, yellow powder (95%). $^{1}$H NMR (DMSO-d$_6$, 400 MHz,): δ/ppm = 8.82(dd, 2H), 8.60 (br s, 1H), 8.23(ddd, 2H), 7.76 (d, 2H), 7.63 (t, 2H), 4.92(m, 2H), 4.51 (dd, 2H). $^{13}$C NMR (DMSO, 400 MHz): δ/ppm = 167.4, 149.4, 141.4, 125.7, 123.4, 59.4. $^{195}$Pt NMR (DMSO-$d_6$, 400 MHz): δ/ppm = 2344.8. *Anal. Calcd*. for $C_{12}H_{13}N_3PtCl_2O_4$: C 27.22, H 2.46, N 7.94. *Found* C 26.72, H 2.45, N 7.62. TOF MS ES$^+$: *m*/*z*, $[M + H]^+$ = 430.05.

**Pt2**: Yield: 15.1 mg, (57%). $^{1}$H NMR (DMSO-d$_6$, 400 MHz,): δ/ppm =8.91 (d, 1H), 8.78(dd, 1H), 8.64 (dd, 1H), 8.54 (dd, 1H), 8.40 (td, 1H), 8.29 (ddd, 1H), 8.17-8.09 (m, 1H), 7.93 (m, 1H), 7.76 (m, 2H), 7.64 (m, 1H), 7.57 (s, 2H). $^{13}$C NMR (DMSO, 400 MHz,): δ/ppm = 159.8, 148.7, 147.6, 135.7, 135.3, 128.7, 128.4, 125.0, 122.4, 121.7, 115.3, 113.5, 109.2, 106.6, 51.1. $^{195}$Pt NMR (DMSO-$d_6$, 400 MHz): δ/ppm = 2314.8. *Anal. Calcd*. for $C_{15}H_{13}N_3PtCl_2$: C 35.93, H 2.59, N 8.38. *Found* C 35.44, H 2.39, N 7.91. TOF MS ES$^+$: *m*/*z*, $[M+H]^+$ = 466.04.

**Pt3**: Yield yellowish brown powder, 56.3 mg, 63%. $^{1}$H NMR (DMSO-$d_6$, 400 MHz): δ/ppm = 8.98 (dd, 2H), 8.27 (td, 2H), 7.90 (d, 2H), 7.67 (t, 2H), 4.85 (m, 4H). $^{13}$C NMR (DMSO-$d_6$, 400 MHz): δ/ppm = 166.6, 156.6, 150.1, 142.0, 137.5 and 17.7. $^{195}$Pt NMR (DMSO-$d_6$, 400 MHz): δ/ppm = 2960.7. *Anal. calcd*. for $C_{12}H_{12}N_2SPtCl_2$: C 29.87, H 2.49, N 5.81, S 6.64. *Found*: C 29.35, H 2.29, N 5.90, S 6.48. TOF MS ES$^+$: *m*/*z*, $[M+H]^+$ = 447.01.

**Pt4**: Yield orange powder, 138.3 mg, 61%. $^{1}$H NMR (DMSO-d$_6$, 400 MHz,): δ/ppm = 9.44(dd, 1H), 8.93 (dd, 1H), 8.65(dd, 1H), 8.46-7.89 (m, 4H), 7.31-7.14 (m, 2H), 6.63 (d, 1H), 4.86 (d, 2H). $^{13}$C NMR (DMSO, 400 MHz,): δ/ppm = 157.7, 149.3, 149.0, 145.6, 137.7, 136.9, 136.4, 128.3, 126.7, 125.3, 124.4, 123.0, 122.1, 121.7, 37.7. $^{195}$Pt NMR (DMSO-$d_6$, 400 MHz): δ/ppm

= 2149.3. *Anal. Calcd*. for $C_{15}H_{12}N_2SPtCl_2$: C 34.75, H 2.32, N 5.40, S 6.18. *Found* C 34.21, H 2.06, N 4.96, S 6.32. TOF MS ES$^+$: $m/z$, $[M+H]^+$ = 483.01.

### 6.2.4 Preparation of Complex and Nucleophile Solutions for Kinetic Analysis

Stock solutions of the complexes were prepared by dissolving the known amounts in 2% DMF to improve the solubility and topped up with 98% of methanolic solution of constant ionic strength of 0.1 M. The ionic strength of the solution was maintained using sodium perchlorate ($NaClO_4$, 0.09 M) and lithium chloride (LiCl, 0.01 M) because perchlorate anion is non-coordinating.[23] 10 mM LiCl was added to the solvent system to prevent any possibility of solvolysis of the chloro ligand. The resulting complex concentrations were approximately 0.2 mM for **Pt1**, **Pt3** and **Pt4** and 0.26 mM for **Pt2** before mixing with nucleophile solutions. A total of three neutral nucleophiles, *viz*. TU, DMTU and TMTU with different steric hindrance were used as entering nucleophiles. Solutions of these nucleophiles were prepared fresh before use by dissolving in a 0.1 M $NaClO_4$/LiCl methanolic solution. Nucleophiles concentrations of approximately 40, 30, 20 and 10-fold in excess over that of the metal complex were prepared by diluting the stock solution which was 50-fold in excess over that of Pt complex. These concentrations were chosen to maintain the *pseudo* first-order conditions and to push the reaction to completion.

### 6.2.5 Physical Measurements and Instrumentation

$^{1}H$, $^{13}C$ and $^{195}Pt$ NMR spectra were recorded on a Bruker Avance III 500 or Bruker Avance III 400 at frequencies of 500 MHz or 400 MHz and 125 MHz/100 MHz using either a 5 mm BBOZ probe or a 5 mm TBIZ probe. All chemical shifts are quoted relative to the relevant solvent signal at 30 ˚C unless stated otherwise. Elemental (CHNS) analysis of the ligands and complexes were performed on Carlo Erba Elemental Analyzer 1106. Low resolution electron-spray ionization ($ESI^{+}$) mass spectra of the samples were recorded on a Waters Micromass LCT Premier spectrometer operated in positive ion mode. UV-Visible spectra and kinetic measurements of slow reactions were recorded on a Cary 100 Bio UV-Visible spectrophotometer with a cell compartment thermostated by a Varian Peltier temperature controller having an accuracy of ± 0.05 ℃. Kinetic measurements of fast reactions were monitored using an Applied Photophysics SX 20 stopped-flow reaction analyser coupled to an online data acquisition system. The temperature of the instrument was controlled to within ± 0.1 °C.

### 6.2.6 Computational Calculations

In order to gain an in-depth understanding of the structural as well as the electronic differences that exist in the complexes under study, Density Functional Theoretical (DFT) calculations were performed using a well-established approach for the third row transition metal complexes, to identify the energy-minimized structures based on B3LYP/LANL2DZ[24,25] (Los Alamos National Laboratory 2 double ζ) level theory, with inner core electrons of Pt replaced by relativistic effective core potential (ECP). The singlet states were used due to low electronic spin of Pt(II) complexes. The frontier molecular orbitals of

these complexes were generated in Gauss view 5.0 using the same level of theory. The influence of the methanol solvent was evaluated via single-point computations using the CPCM[26] formalism. Gaussian09 suite of programs was used for all DFT computations.[27]

### 6.2.7 Kinetic Measurements

The working wavelengths (**Table SI 6.1**) were determined by recording spectra of the reaction mixture over the wavelength range of 200 to 650 nm using Cary 100 Bio UV-visible spectrophotometer. All kinetic experiments were performed under *pseudo* first-order conditions for which the concentration of the nucleophile was always at least a 10-fold excess. Kinetic data were graphically analysed using the software package, Origin 7.5®.[28] The activation parameters, $\Delta H^{\#}$ and $\Delta S^{\#}$, were obtained by studying temperature dependence of the rate constant in the range of 15-35 °C at an interval of 5 °C with the nucleophile concentration held constant at 30 times the concentration of the metal complex.

## 6.3 Results

### 6.3.1 Computational Analysis

In order to understand the role of the structural and electronic differences that exist in the complexes on the observed kinetic results, computational studies were carried out at the DFT (B3LYP(CPCM)/LANL2DZp//B3LYP/-LANL2DZp) level of theory. Geometry-optimized structures as well as the key data are presented in **Tables 6.1** and **6.2** respectively. For all investigated complexes, the HOMO is located on the d$z^2$ orbital of the metal and the LUMO is

populated on the aromatic region of the ligand. Complexes **Pt1**, **Pt3** and **Pt4** show maximum overlap of the *d*π-orbitals of the metal with the π*-orbitals of the ligand. This is expected to enhance the π-back bonding character which will result into increase in reactivity of the metal centre. Generally, the electrophilicity indices show that quinoline based complexes (ω = 6.067 for **Pt2** and ω = 6.155 for **Pt4**) are less electrophilic compared to pyridine based complexes (ω = 7.518 for **Pt1** and ω = 7.608 for **Pt3**) with **Pt(N^S^N)** being superior in electrophilicity. **Pt2** and **Pt4** are characterized by the rise in LUMO energy level making them inaccessible for π-back donation. The HOMO-LUMO energy gap decreases with increasing π-conjugation in the order of 3.65 ≳ 3.57 < 3.51 < 3.41 for **Pt3**, **Pt1**, **Pt2** and **Pt4** respectively. The NBO charges are more positive by 0.17 units for **Pt(N^N^N)** complexes than **Pt(N^S^N)** indicating that the reactivity of the complexes towards substitution does not sorely depends on the NBO charges on the Platinum metal but rather on electrons distributed within the whole complex.

**Table 6.1:** Geometry optimized structures and DFT-calculated (B3LYP(CPCM)/LANL2DZp//B3LYP/-LANL2DZp) HOMOs and LUMOs for the investigated complexes.

| Complex Structure | HOMO | LUMO | Planarity |
|---|---|---|---|
|  **Pt1** |  | 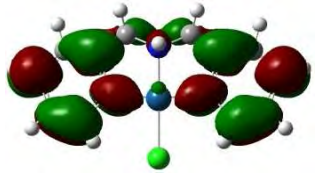 |  |
|  **Pt2** | 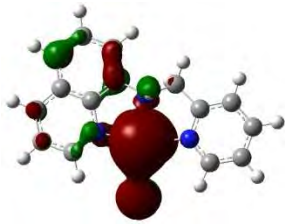 |  |  |
|  **Pt3** | 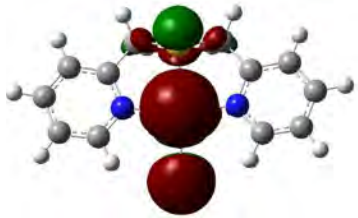 |  |  |
|  **Pt4** |  | 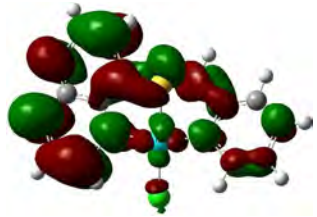 | 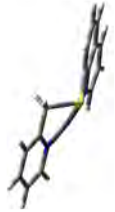 |

**Table 6.2:** Summary of DFT calculated parameters for complexes studied

| Property | Pt1 | Pt2 | Pt3 | Pt4 |
|---|---|---|---|---|
| **HOMO-LUMO energy** | | | | |
| LUMO /eV | -3.396 | -2.860 | -3.445 | -2.974 |
| HOMO/eV | -6.967 | -6.371 | -7.097 | -6.388 |
| ΔE /eV | 3.571 | 3.511 | 3.652 | 3.414 |
| **NBO charges** | | | | |
| Pt | 0.540 | 0.550 | 0.365 | 0.380 |
| $N/S_{trans}$ | -0.637 | -0.651 | 0.409 | 0.443 |
| $N_{q/py}$ | -0.510 | -0.495 | -0.507 | -0.499 |
| $N_{py}$ | -0.510 | -0.509 | -0.507 | -0.506 |
| **Dipole moment** (Debye) | 14.005 | 12.071 | 11.125 | 10.738 |
| **Electrophilicity index** (ω) | 7.518 | 6.067 | 7.608 | 6.418 |
| **Bond Length** (Å) | | | | |
| $Pt–N/S_{trans}$ | 2.051 | 2.062 | 2.392 | 2.396 |
| Pt–Cl | 2.440 | 2.437 | 2.444 | 2.442 |
| **Bond Angles** (°) | | | | |
| $N/s_{trans}$–Pt–Cl | 179.43 | 178.35 | 175.15 | 176.25 |
| $N_{q/py}$–Pt–$N_{py}$ | 165.94. | 165.12 | 168.56 | 166.19 |

q and py are quinoline and pyridine respectively

### 6.3.2 Kinetic Measurements

The kinetics of the substitution of coordinated chloride by thiourea nucleophiles was investigated under *pseudo* first-order conditions in order to drive the reactions to completion. Conventional UV-Visible spectrophotometry and Stopped-Flow technique were used for kinetic measurements by following the change in absorbance at suitable wavelengths as a function of time. The selected wavelengths are recorded in **Table SI 6.1**. The substitution of the chloro ligand from Pt(N^S^N) complexes involves two reaction

steps. The first substitution step by TU and its derivatives for both **Pt3** and **Pt4** complexes was too fast to be monitored on the UV-Visible or NMR time-scale and was followed by the stopped-flow technique. The reactions for the second step were significantly slower by at least three orders of magnitude than the first step and were followed on UV-Vis for only two less sterically hindered nucleophiles, TU and DMTU.

The kinetic traces obtained at suitable wavelengths gave excellent fits to first-order exponential decay to generate the observed *pseudo* first-order rate constants, $k_{obs}$ at the specific concentration of the nucleophile and temperature. A typical Stopped-Flow kinetic trace at 375 nm recorded by mixing methanol solutions of **Pt3** (0.2 mM) and 6 mM of TU at ionic strength of 0.1 M ($NaClO_4$) is shown in **Figure 6.2**.

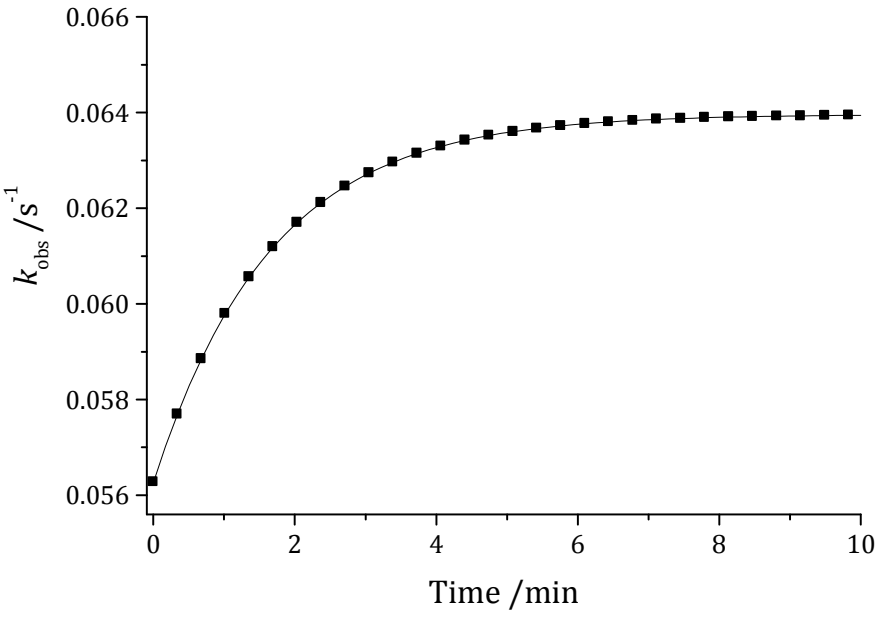


**Figure 6.2:** Stopped-Flow kinetic trace of **Pt3** and TU at 298 K.

An example of the UV-Visible spectra obtained from the reaction between **Pt3** and TU is shown in **Figure 6.3**. Inset to Figure 6.3 is the corresponding kinetic trace recorded at 460 nm.

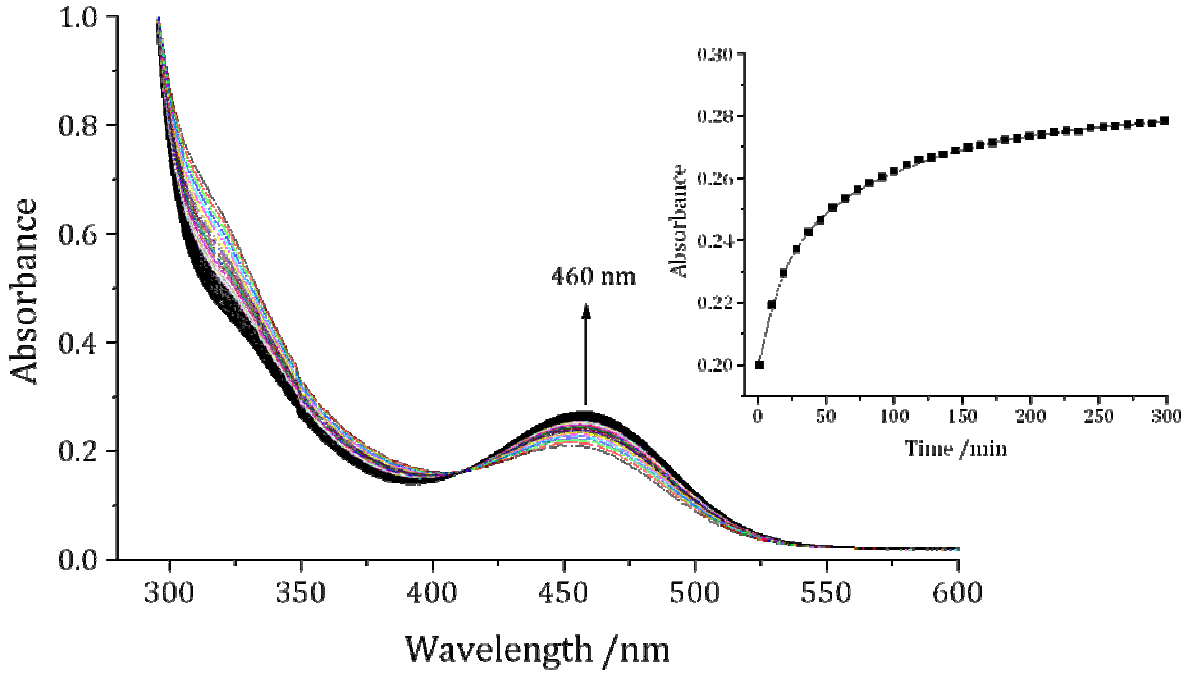


**Figure 6.3:** UV-Vis spectra recorded as a function of time for the reaction between **Pt3** and 6 mM of thiourea at 35 ˚C in methanol. *Inset*: Kinetic trace obtained at 460 nm.

When the obtained $k_{obs}$ values were plotted against the concentration of the entering nucleophile, a linear dependence on the nucleophile concentration with zero intercepts was observed for all complexes. The absence of a noticeable intercept is ascribed to the stronger binding of the soft thiourea nucleophiles to the metal centre.[29,30] Representative plots are shown in **Figure 6.4** (also **Figures SI 6.10 and 6.12**) and the observed rate constants obeys

the rate law $k_{obs} = k_2[\mathrm{Nu}]$, typical of nucleophilic substitution at planar tetra-coordinate $d^8$ metal complexes in which $k_2$ is the second-order rate constant for the direct attack of the nucleophile (Nu) at the metal centre.

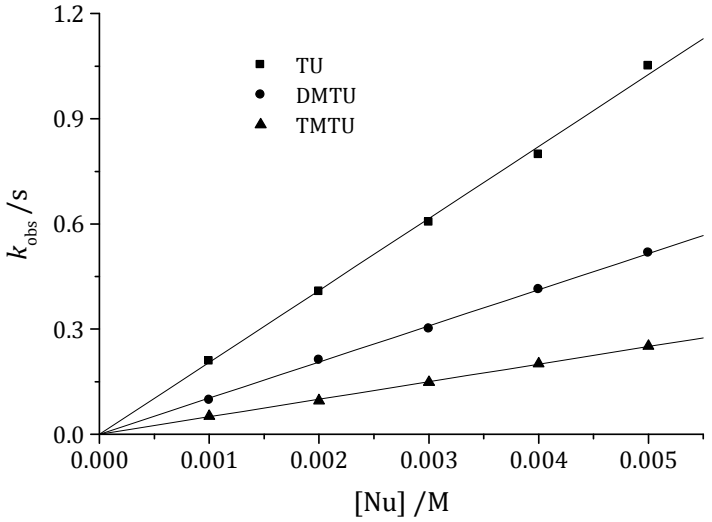


(a)

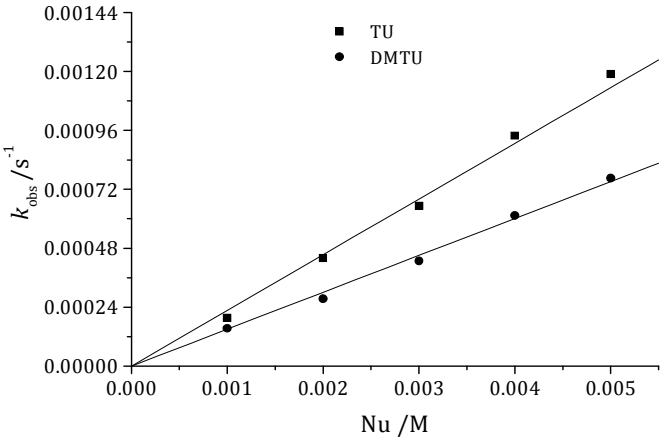


(b)

**Figure 6.4**: Dependence of $k_{obs}$ on the concentration of entering nucleophile for the (a) first and (b) second substitution steps of **Pt3** (0.2 mM) in methanol, *I* = 0.1 M ($NaClO_4$/LiCl), T= 25 ˚C.

The values of the second-order rate constants, $k_2$, were obtained from the slope of individual plot at 25 ˚C and are summarised in **Table 6.3**. The temperature dependence of the second-order rate constants was investigated over a temperature range of 15-35 ˚C. Typical Eyring plots are shown in **Figure 6.5** (also **Figures SI 6.11 and 6.13**). The enthalpy of activation, ($\Delta H^{\#}$) and entropy of activation, ($\Delta S^{\#}$) were determined using the Eyring equation.[31] These activation parameters are summarized in **Table 6.3**.

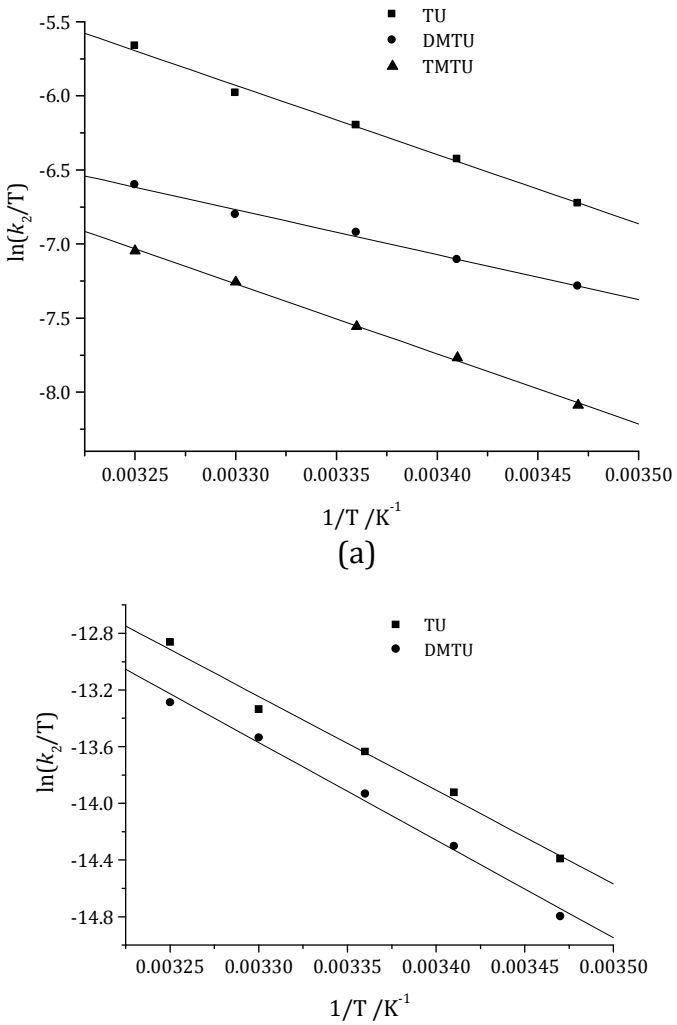


**Figure 6.5:** Eyring plots for the reaction of **Pt3** with a series of neutral nucleophiles for the (a) first and (b) second substitution steps at various temperatures in the range of 15-35 ˚C.

**Table 6.3:** Summary of $k_2$ values and activation parameters, $\Delta H^{\#}$ and $\Delta S^{\#}$.

| Complex | Nu | $k_2$ / M$^{-1}$ s$^{-1}$ | $\Delta H^{\#}$ /kJ mol$^{-1}$ | $\Delta S^{\#}$ /J K$^{-1}$ mol$^{-1}$ |
|---|---|---|---|---|
| 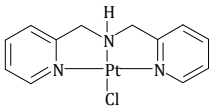 | TU | 0.50 ± 0.01 | 50 ± 2 | -130 ± 6 |
| | DMTU | 0.16 ± 0.004 | 75 ± 3 | -58 ± 10 |
| **Pt1** | TMTU | 0.03 ± 0.001 | 77 ± 1 | -109 ± 4 |
| 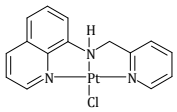 | TU | 0.29 ± 0.003 | 59 ± 3 | -104 ± 10 |
| | DMTU | 0.13 ± 0.001 | 51 ± 1 | -138 ± 3 |
| **Pt2** | TMTU | 0.05 ± 0.001 | 59 ± 2 | -150 ± 5 |
| 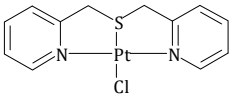 | TU | 205.19 ± 2.40 | 25 ± 2 | -132 ± 5 |
| | | 0.22 ± 0.01[a] | 52 ± 6[a] | -136 ± 18[a] |
| | DMTU | 103.07 ± 0.79 | 28 ± 1 | -173 ± 3 |
| **Pt3** | | 0.154 ± 0.004[a] | 57 ± 5[a] | -121 ± 16[a] |
| | TMTU | 49.99 ± 0.35 | 38 ± 1 | -122 ± 4 |
| 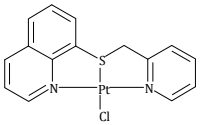 | TU | 21.03 ± 0.49 | 35 ± 1 | -170 ± 3 |
| | | 0.029 ± 0.04[a] | 54 ± 4[a] | -143 ± 14 |
| | DMTU | 11.07 ± 0.19 | 38 ± 1 | -158 ± 3 |
| **Pt4** | | 0.013 ± 0.0002[a] | 51 ± 4[a] | -157 ± 14[a] |
| | TMTU | 2.07 ± 0.03 | 48 ± 5 | -125 ± 16 |

[a] values obtained for the second substitution step

### 6.3.3 Kinetics with NMR

As stated earlier, **Pt3** and **Pt4** gave two substitution steps despite the presence of only one leaving group. Therefore, in the first step the nucleophile substitutes the chloride ion, and the second step involves the displacement of the coordinated pyridyl/quinolyl units (**Scheme 6.1**) in the chelate framework as reported previously for the complex with similar ligand framework.[7] To further confirm this, the substitution reaction of **Pt3** with TU (2 equiv.), was studied by $^{1}H$ and $^{195}Pt$ NMR spectroscopy. The $^{1}H$ and $^{195}Pt$ NMR kinetics spectra of the complex are presented in **Figure 6.6** and **Figure 6.7** respectively**.**

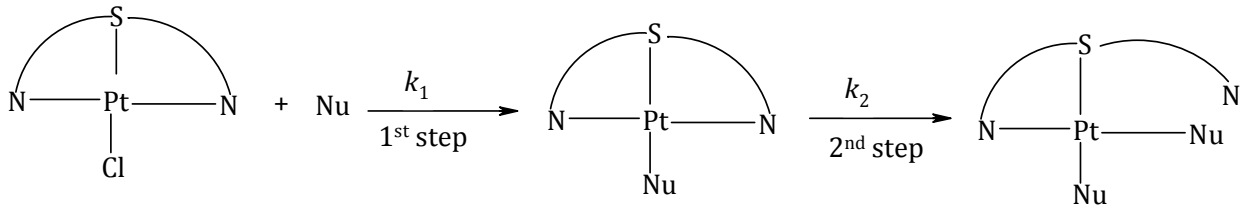


Scheme 6.1: The general reaction scheme for the reactions between Pt(N^S^N) complexes and the thiourea nucleophiles.

From **Figure 6.6**, the resonances of the aromatic protons of unreacted complex shifted upfield upon mixing the complex with two equivalents of TU. During the reaction, the proton resonances of the product formed (for example H5' and H3') further grew while their original protons decreased and disappeared accordingly. The chemical environment of the new peaks formed after t = > 20 h corresponds well with that of the **dps** ligand ran in deuterated chloroform. Furthermore $^{195}Pt$ NMR spectra of the complex (**Figure 6.7**) shows the original $^{195}Pt$ peak labelled A at δ = -2694.2ppm and after 24 h of the reaction a new peak labelled B at δ =3938.1 ppm was observed. These $^{195}Pt$ NMR signals (at δ = -2694.2

and 3938.1 ppm) are typical of $PtN_2SCl$ (before substitution) and $PtS_4$ (after dislodgment of the *cis* pyridine ligands) coordinating sphere respectively.[32] Based on NMR kinetic results, it can be concluded that the second slow substitution process is due to a complete detachment of the N^S^N ligand framework of the Pt centre which is enhanced by the presence of a strong labilising thiourea. This is different from a previous study where the thiourea nucleophile partially labilized the N^N^N bis(2pyridylmethyl)amine chelate system resulting into the dechelation of one of the *cis*-coordinated pyridyl units.[7] No dechelation step was observed for Pt(N^N^N) complexes indicating that they are of more biological importance as potential anticancer Pt drugs than their Pt(N^S^N) counterparts which are found to be unstable.

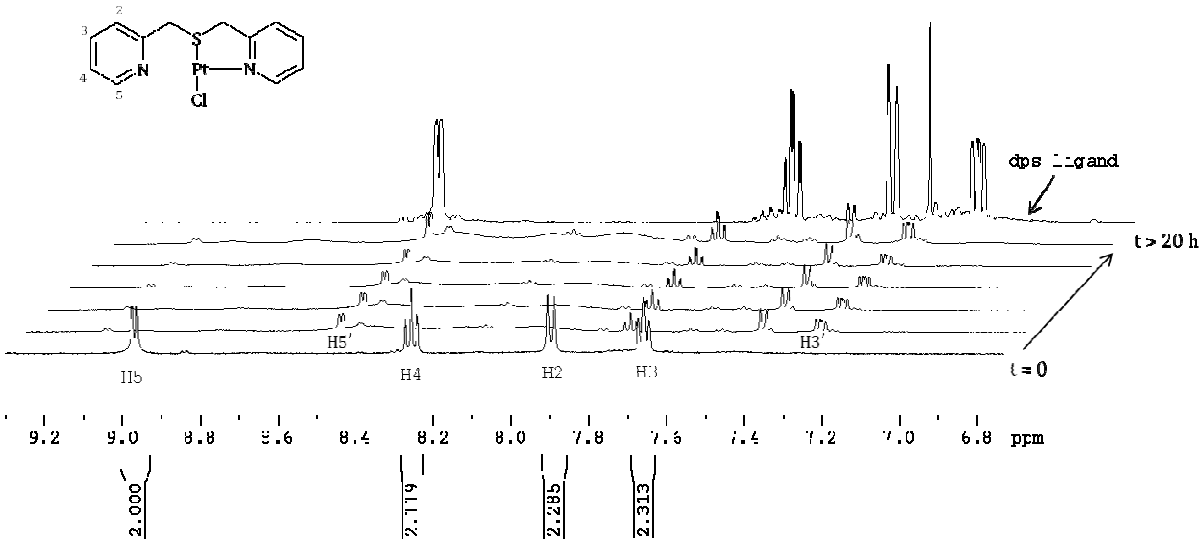


**Figure 6.6:** $^1H$ NMR spectra array of **Pt3** (the aromatic region) acquired during its reaction with two equivalents of thiourea. The numbering scheme for the pyridyl protons is shown in the structure of **Pt3** shown as an inset to this figure.

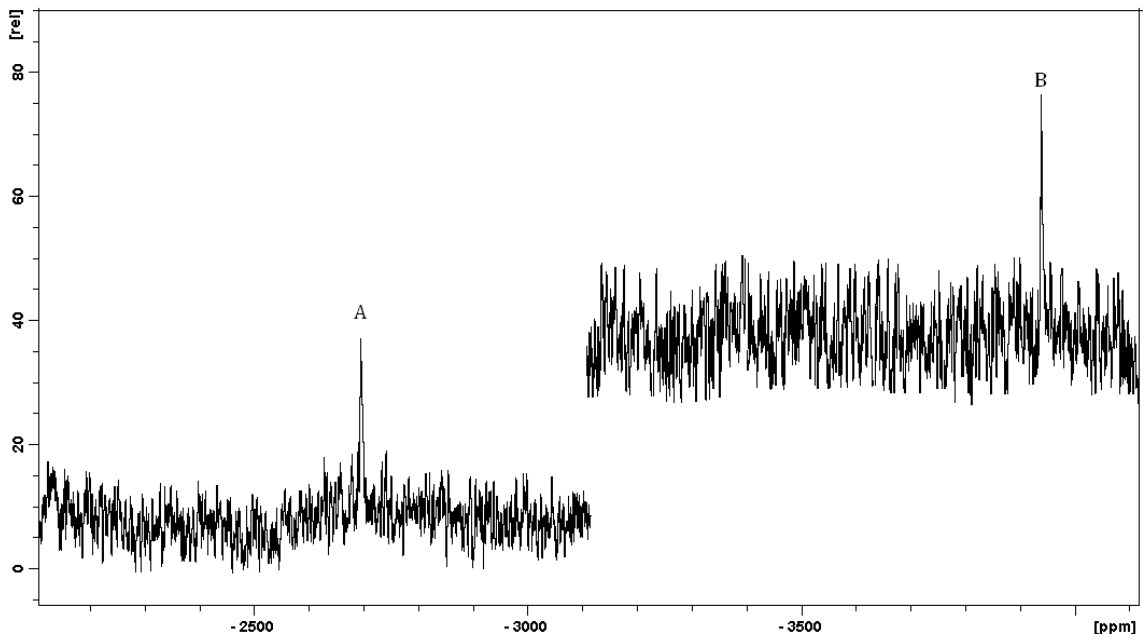


**Figure 6.7:** $^{195}$Pt NMR spectra of the reaction mixture of **Pt3** with two mole equivalents TU, showing pure Pt(II) complex, **Pt3** (A, δ = -2694.2 ppm) before the reaction and the final product (B, δ = -3938.1 ppm) corresponding to $[Pt(TU)_4]^{+2}$ 24 h after the reaction.

## 6.4 Discussion

In this chapter, the substitution behaviour of mono-functional Pt(II) complexes with thiourea-based nucleophiles is described. Thiourea nucleophiles have been chosen due to their good solubility, neutral character and high nucleophilicity. In general, thiourea coordinates through sulfur to typical electrophilic reaction partners such as Pt(II), Pd(II) and Co(III) metal. This is because sulfur-donor atoms have a high affinity for Pt(II) complexes.[2c,33]

The reactivity of the complexes towards substitution of chloride by all the nucleophiles investigated follows the trend **Pt3** > **Pt4** > **Pt1** > **Pt2** (**Table 6.3**). This can be explained by the *trans*-labilizing effect and π-interactions between the filled *d*π-orbitals of the metal with the empty π*-orbitals of the ligand. Looking at the structures of the investigated Pt(II) complexes, the donor atom *trans* to leaving group is either N or S, and the *cis*-coplanar ligands in **Pt2** and **Pt4** is quinoline and pyridine moieties whereas in **Pt1** and **Pt3** the *cis* ligands comprise of two pyridine rings.

The high reactivity of **Pt3** and **Pt4** complexes which is two orders of magnitude higher than **Pt1** and **Pt2** complexes is attributed to the sulfur atom which is known to be a strong σ-donor atom and is positioned *trans* to the leaving group. It is known that a group with strong σ-donor properties will weaken the bond *trans* to it in the ground state (σ-*trans* effect and *trans* influence). This is because the bonding character shares a greater amount of metal *p*-orbitals in the transition state than in the ground state (transitional state σ-effect).[34] On the other hand, strong π-acceptor groups accelerate the substitution reaction by accommodating the excess electron charge induced on the metal through a bimolecular attack of the entering group resulting into stabilization of the penta-coordinate transition state.[34,35] Comparing the σ-donicity of the *trans* atoms, N and S in these two sets of complexes investigated, sulfur is superior owing to the fact that it is less electronegative compared to nitrogen.[36] The *trans* effect of sulfur causes electrostatic destabilization of the ligand in the *trans* position. Thus, the higher reactivity of **Pt3** and **Pt4** complexes compared to **Pt1** and **Pt2** complexes is mainly due to the stronger *trans*-labilizing effect of the Pt–S bond which induces a high intrinsic reactivity. Also by being bigger in size, the greater

polarizability of the sulfur allows some charge transfer to move away from the metal through the σ-framework as the incoming group becomes bound.[8d] Such labilization and polarizability has clearly been demonstrated in a number of studies.[8,37]

In addition, the HOMO-LUMO maps shows that there is a metal to ligand π-interactions through the sulfur bridge in **Pt3** and **Pt4**, whose strength helps to stabilize the five coordinate transition state by making the complexes more reactive towards substitution reaction. This is facilitated by the lone pair of electrons in the *p*-orbitals of sulfur which forms π-bonds with platinum *d*π-orbitals to such an extent that the metal centre achieves an 18-electron configuration.

Complexes **Pt1** and **Pt3** react faster than their respective counterpart **Pt2** and **Pt4**. The difference in reactivity between these two sets of complexes can be explained by the degree of π-backbonding character of pyridine compared to quinoline ligand. The two pyridine rings in the chelate framework of **Pt1** and **Pt3** increase the lability of the leaving group due to their electron-withdrawing effect from the metal centre through π-back bonding. The π-back bonding decreases electron density in the *xz* plane hence facilitates a nucleophilic attack and stabilizes corresponding penta-coordinated transition state. The decrease in reactivity of **Pt2** and **Pt4** is due to the poor π-acceptor property of quinoline ligand.[9-11] The high reactivity of **Pt1** and **Pt3** when compared to **Pt2** and **Pt4** is supported by the electrophilicity values and the high values of dipole moment due to its π-withdrawing character of two pyridine rings compared to quinoline moiety.

Having a close look on DFT data, the Pt NBO charges show that **Pt1** and **Pt2** complexes are more positive than **Pt3** and **Pt4**. The low NBO charges observed for **Pt3** and **Pt4** is attributed to the strong σ-donor effect of the *trans* sulfur atom. This reduces the total (positive) NBO charge of the Pt(II) atom by an increase of electron density in the *xy* plane leaving the metal centre less positive. For **Pt1** and **Pt2** complexes, the electronegativity of *trans* nitrogen helped to quench the electron density on the metal centre rendering high NBO charges.

In a situation where competing parameters such as σ-donor, π-acceptor and *trans* effect all play a role in influencing the reactivity of a complex, it is worth using electrophilicity index, (ω) to explain the intrinsic electronic properties of Pt(II) complexes. This is because electrophilicity index possesses adequate information regarding structure, stability, reactivity, toxicity, bonding interactions and dynamics.[38] The quantification of the electrophilicity concept is based on the maximum energetic stabilization of a species that arises from accepting charge. The electrophilicity indices in **Table 6.2** show that generally quinoline based complexes, **Pt2** and **Pt4** are less electrophilic therefore should be less reactive than their **Pt1** and **Pt3** counterparts with two pyridine rings. Also **Pt(N^S^N)** complexes have high values of electrophilicity indices which is in harmony with the observed rate constants.

In addition, the slowness in reactivity of **Pt2** compared to **Pt1** and that of **Pt4** compared to **Pt3** despite their high positive NBO charges observed can be explained by the *trans* labilizing effect through σ-donation of electrons by carbon atom through t*rans* N/S-donor

atom. **Pt1** and **Pt3** have one extra $sp^3$ carbon which can further donate electron density into the N/S leading to a high *trans* labilizing effect than **Pt2** and **Pt4**. This is evidenced by the increase in NBO charges of the N/S atoms *trans* to the leaving group and a net increase in positive charge of the Pt(II) centre upon substitution of the $sp^3$ carbon in **Pt1**(0.540) and **Pt3**(0.365) with an $sp^2$ carbon as for **Pt2**(0.550) and **Pt4**(0.380). The reactivity trend is well supported by the calculated electrophilicity indices which takes into account all these parameters.

The substitution of coordinated chloride by the most sterically hindered nucleophiles TMTU shows a clear dependence on the steric bulk of the nucleophile. The values of the rate constants for the substitution reaction of **Pt3** decrease in the order TU (205 $M^{-1}$ $s^{-1}$) > DMTU (103 $M^{-1}$ $s^{-1}$) > TMTU (50 $M^{-1}$ $s^{-1}$). It was observed that the most sterically hindered nucleophile TMTU shows by far the lowest reactivity. The trend in the reactivity of the investigated complexes for the different nucleophiles can also be seen in the activation enthalpies for the investigated reactions. Generally, as the reaction becomes slower, the process is less favoured resulting in high activation enthalpy due to destabilization of the transition state. This general comment is valid in our results the exception is in the case of **Pt2**. The activation enthalpy and entropy show that the mode of activation is associative in nature in line with the substitution mechanisms for square planar systems.[39]

## 6.5 Conclusion

The general reactivity trend for the complexes is **Pt3 > Pt4 > Pt1 > Pt2**. The difference in the rate of substitution of all the complexes is purely electronic in origin. The rate constants

for the substitution of chloro ligand with TU in **Pt3** ($k_2$ = 205.19 $M^{-1}$ $s^{-1}$) and **Pt4** ($k_2$ = 21.03 $M^{-1}$ $s^{-1}$) complexes decrease to $k_2$ = 0.50 $M^{-1}$ $s^{-1}$ for **Pt1** and $k_2$ = 0.29 $M^{-1}$ $s^{-1}$ for **Pt2** complexes due to the high *trans* labilizing effect brought by the S-donor atom *trans* to the leaving group. Moreover, complexes with two pyridine rings (**Pt1** and **Pt3**) are superior in reactivity by a factor of ten or two than those with quinoline moiety in a ligand framework (**Pt2** and **Pt4**). The dominance in reactivity is explained by a better ability of the pyridine ring to delocalize negative charge away from the reaction centre which eventually leads to an increase in the electrophilicity of the Pt centre. The net weak π-accepting and σ-donor effect of quinoline moiety in **Pt4** is overpowered by the *trans* effect of sulfur atom leading to high substitution reactions relative to **Pt2**. On the other hand, **Pt3** and **Pt4** complexes were found to be unstable in the presence of thiourea nucleophiles as they showed a second substitution process which is due to the dechelation of the ligand framework from the metal complex. The substitution of chloride in **Pt1**, **Pt2**, **Pt3** and **Pt4** complexes by thiourea nucleophiles has been characterized by sensitivity to the steric of the incoming ligand. The large negative entropies and small activation enthalpies suggest that formation of the transition is accompanied by a net increase in bonding supporting the well-known substitution mechanism for Pt(II) complexes which is associative.

## 6.6 Supporting Information (SI)

The available SI includes a number of NMR and mass spectra, wavelengths for kinetic measurements, concentration dependence and Eyring plots for determination of second order rate constant and activation parameters and HOMO-LUMO energy diagram of the investigated complexes.

## 6.7 References


1. Banerjee, P., *CoordinationChemistry Reviews.*, **1999**, *190–192*, 19.

2. (a) Soldatović, T. Bugarčić, Ž.D., *J. Inorg. Biochem*., **2005**, *99*, 1472; (b) Summa, N., W. Schiessl, R. Puchta, N. van Eikema Hommes, R. van Eldik, *Inorg. Chem*., **2006**, *45*, 2948; (c) Bugarčić, Ž.D., Rosić, J., Petrović, B., Summa, N., Puchta, R., van Eldik, R., *J. Biol. Inorg. Chem*., **2007**, *12*, 1141; (d) Hofmann, A., Jaganyi, D., Munro, O.Q., Liehr, G., Van Eldik, R., *Inorg. Chem*., **2003**, *42*, 1688. (e) Bugarc̆ic´, Z̆.D, Heinemann, F. W., van Eldik, R., *Dalton Trans*., **2004**, 279; (f) Petrović, D., Stojimirović, B., Petrović, B., Bugarčić, Ž.D., *Bioorg. Med. Chem*., **2007**, *15*, 4203.

3. (a) Jaganyi D. and Tiba F., *Transition Met. Chem.*, **2003**, *28*, 803. (b) Jaganyi, D., Tiba, F., Munro, O. Q., Petrovi´c, B. and Bugarčić, Z. D., *J. Chem. Soc., Dalton Trans.*, **2006**, 2943. (c) Bugarčić, Ž. D., Liehr G. and van Eldik, R. *J. Chem. Soc., Dalton Trans.*, **2002**, 951.; (d) Pitteri, B., Annibale, G., Marangoni, G., Cattalini, L., Visentin, F., Bertilasi, V. and Gilli, P., *Polyhedron.*, **2001**, *20*, 869; (e) Annibale, G., Brandolisio, M. and Pitteri, B., *Polyhedron.*, **1995**, *14*, 451; (f) Mambanda, A., Jaganyi, D., Hochreuther, S., van Eldik, R., Dalton Trans **2010**, *39*, 3595; (g) Mambanda, A., Jaganyi, D., *Dalton Trans*., **2012**, *41*, 908.

4. (a) Annibale, G., Brandolisio, M., Bugarčić, Ž. D and Cattalini, L., *Transition Met. Chem*., **1998**, *23*, 715. (b) Pitteri, B., Marangoni, G., Cattalini, L., Viseulim F. V. and Bobbo, T., *Polyhedron.*, **1998**, *17*, 475. (c) Petrović, B. V., Djuran M. I. and Bugarčić, Ž. D.,, Z. D., *Met.-Based Drugs.*, **1999**, *6*, 355. (d) Pitteri, B., Annibale, G., Marangoni, G., Bertilasi V. and Ferretti, V., *Polyhedron.*, **2002**, *21*, 2283. (e) Bugarčić, Ž. D., Heinmann F. W. and

van Eldik, R., *J. Chem. Soc., Dalton Trans*., **2004**, 279; (f) Reddy, D. and Jaganyi, D., Dalton Trans., **2008**, 6724; (g) Jaganyi, D., de Boer, K., Gertenbach, J. and Perils, J., *Int. J. Chem. Kinetics.*, **2008**,809.

5. Jaganyi, D., Hofmann, A., van Eldik, R., *Angew Chem. Int., Ed*., **2001**,*40*, 1680.
6. Hofmann, A and van Eldik, R., *Dalton Trans.,* **2003**,2979.
7. Mambanda, A., Jaganyi, D., *Dalton Trans*., **2011**, *40*, 79.
8. (a) Pitteri, B., Marangoni, G., and Cattalini, L., *Polyhedron.*, **1995**, *14*, 2331; (b) Pitteri, B., Marangoni, G., Cattalini, L. and Bobbo, T., *J. Chem. Soc. Dalton Trans*., **1995**, 3853; (c) Pitteri, B., Marangoni, G., and Cattalini, L., *J. Chem. Soc. Dalton Trans*., **1994**, 35539; (d) Pitteri, B., Bortoluzzi, M. and Marangoni G., *Transition Metal Chemistry*., **2005**, *30*, 1008;
9. Jaganyi, D., Ongoma, P. O., *Dalton Trans.*, **2012**, *41*, 10724.
10. Jaganyi, D., Kinunda, G., (manuscript in preparation)
11. Jaganyi, D., Wekesa, I., (submitted)
12. (a) Ashby, M. T., *Comments Inorg. Chem.*, **1990**, *10*, 297;(b) Murray, S. G. and Hartley, F. R., *Chem. Rev.*, **1981**, *81*, 365; (c) Reedijk, J., *Chem. Rev.*, **1999**, *99*, 2499.
13 Schiessl, W. C., Summa, N. K., Weber, C. F., Gubo, S., Dücker-Benfer, C., Puchta, R., van Eikema Hommes, N. J. R. and van Eldik, R., *Z. Anorg. Allg. Chem*., **2005**, *631*, 2812.
14 Ashby, M. T., *Comments. Inorg. Chem*., **1990**, *10*, 297.
15 Murray, S. G and Hartley, F. R., *Chem. Rev*., **1981**, *81*, 365.
16. Reedijk, J., *Chem. Rev*., **1999**, *99*, 2499.
17. Carlsen, L., Egsgaard, H., Anderson, J.R., *Anal Chem.*, **1979**, *51*, 1593.

18. Sung, N-D, Choi, K-Y., Lee, H-H., Lee, K-C., Kim, M-J., *Transition Metal Chemistry.*, **2005**, *30*, 273.

19. Canovese, L., Visentin, F., Chessa, G., Uguagliati, P., Levi, C., Dolmella, A.,Bandoli, G., *Organometallics.*, **2006**, *25*, 5355.

20. Weber, C.F and van Eldik, R., *Eur*. *J*. *Inorg*. *Chem.*, **2005**, 4755.

21. Annibale, G., Bortoluzzi, M., Marangoni, G. and Pitteri, B., *Transition Metal Chemistry.*, **2005**, *30*(6), 748.

22. Darensbourg, M.Y., Hill, G. S., Irwin, M. J., Levy, C. J., Rendina, L. M., Puddephatt, R. J., Andersen, R. A., Mclean, L., *Inorganic Syntheses.*, **2007**, *32*, 149

23 Appleton, T.G., Hall, J. R., Ralph, S. F. and Thomson, C. S. M., *Inorg. Chem*., **1984**, *23*, 3521.

24 (a) Becke, A. D., *Chem. Phys*., **1993**, *98*, 5648. (b) Lee, C. T., Yang, W. T. and Parr, R. G., *Phys. Rev*. B., **1988**, *37*, 785.

25 Hay, P. J. and Wadt, W. R., *Chem. Phys*., **1985**, *82*, 270.

[26]. (a) Barone, V.; Cossi, M. *J. Phys. Chem. A.,* **1998**, *102*, 1995; (b) Cossi, M.; Scalmani, G.; Rega, N.; Barone, V. J. *Comput. Chem.*, **2003**, *24*, 669.

27 Gaussian 09, Revision *A.1*, M. J. Frisch, G. W. Trucks, H. B. Schlegel, G. E. Scuseria, M. A. Robb, J. R. Cheeseman, G. Scalmani, V. Barone, B. Mennucci, G. A. Petersson, H. Nakatsuji, M. Caricato, X. Li, H. P. Hratchian, A. F. Izmaylov, J. Bloino, G. Zheng, J. L. Sonnenberg, M. Hada, M. Ehara, K. Toyota, R. Fukuda, J. Hasegawa, M. Ishida, T. Nakajima, Y. Honda, O. Kitao, H. Nakai, T. Vreven, J. A. Montgomery, Jr., J. E. Peralta, F. Ogliaro, M. Bearpark, J. J. Heyd, E. Brothers, K. N. Kudin, V. N. Staroverov, R.

Kobayashi, J. Normand, K. Raghavachari, A. Rendell, J. C. Burant, S. S. Iyengar, J. Tomasi, M. Cossi, N. Rega, J. M. Millam, M. Klene, J. E. Knox, J. B. Cross, V. Bakken, C. Adamo, J. Jaramillo, R. Gomperts, R. E. Stratmann, O. Yazyev, A. J. Austin, R. Cammi, C. Pomelli, J. W. Ochterski, R. L. Martin, K. Morokuma, V. G. Zakrzewski, G. A. Voth, P. Salvador, J. J. Dannenberg, S. Dapprich, A. D. Daniels, O. Farkas, J. B. Foresman, J. V. Ortiz, J. Cioslowski, and D. J. Fox, Gaussian, Inc., Wallingford CT, **2009**.

28. Origin7.5TM SRO, v7.5714 (B5714), Origin Lab Corporation, Northampton, One, Northampton, M. A, 01060, USA, **2003**.

29. Schmülling, M., Ryabov, A. D and van Eldik, R., *J. Chem. Soc. Chem. Commun*., **1992**, 1609.

30. Hofmann, A., L. Dahlenburg, R. van Eldik,. *Inorg. Chem*., **2003**, *42*, 6528.

31. Eyring, H., *J. Chem. Phys*., **1935**, *3*, 107.

32. Priqueler, J. R. L., Butler, I. S., Rochon, F. D., *Applied Spectroscopy Reviews.*, **2006**, *41*, 185.

33. Reedijk, J., Teuben, J. M. In *Cisplatin: Chemistry and Biochemistry of a Leading Anticancer Drug.*, Lippert, B. Ed., Wiley-VCH:Weinheim, Germany, **1999**, pp. 339-362.; Guo, Z. J., Sadler, P. J. *Adv. Inorg. Chem.,* **2000**, *49*, 183.

34. (a) Chval, Z., Sip, M., Burda, J. V., *J. Comput. Chem*., 2008, 29, 2370; (b) Langford, C. H and Gray, H. B., *Ligand Substitution Processes*, Benjamin, New York, N. Y., **1965**

35. Orgel, L. E. *J. Inorg. Nucl. Chem*., **1956**, *2*, 137.

36. Allen, L. C and Huyee, J. E., *ibid*., **1980**, *42*, 1523.

37. (a) Hochreuther, S., Nandibewoor, S. T., Puchta, R. and van Eldik, R., *Dalton Trans.*, **2012**, *41*, 512; (b) Bogojeski, J., Bugarčić, Ž . D., Puchta, R., van Eldik, R., *Eur. J. Inorg. Chem.,* **2010**, 5439; (c) Bugarčić, Ž . D., Soldatović, T., Jelić, R., Alguero, B., Grandas, A., *Dalton Trans.,* **2004**, *22*, 3869.

38. (a) Chattaraj, P. K., Giri, S., and Duley, S., *Chem. Rev.,* **2011,** *111*(2), 43; (b) Parthasarathi, R., Subramanian, V., Roy, D. R. and Chattaraj, P. K., *Bioorg. Med. Chem.*, **2004**, *12*, 5533; (c) Mebi, C. A., *J. Chem. Sci.*, **2011**, 123( 5), 727; (d) Parthasarathi, R., Padmanabhan, J., Subramanian, V., Maiti, B., Chattaraj, P. K., *J. Phys. Chem.*, **2003**, *A107*, 10346; (e) Domingo, L. R., Perez, P., Contreras, R., *J. Org. Chem.*, **2003**, *68*, 6060; (f) Cedillo, A., Contreras, R., *J. Mex. Chem. Soc.,* **2012**, *56*(3), 257.

39. Tobe, M. L. and Burgess, J., *Inorganic Reaction Mechanisms*, Addison Wiley, Longman, Ltd., Essex, **1999**, pp. 30–33, 70–112.

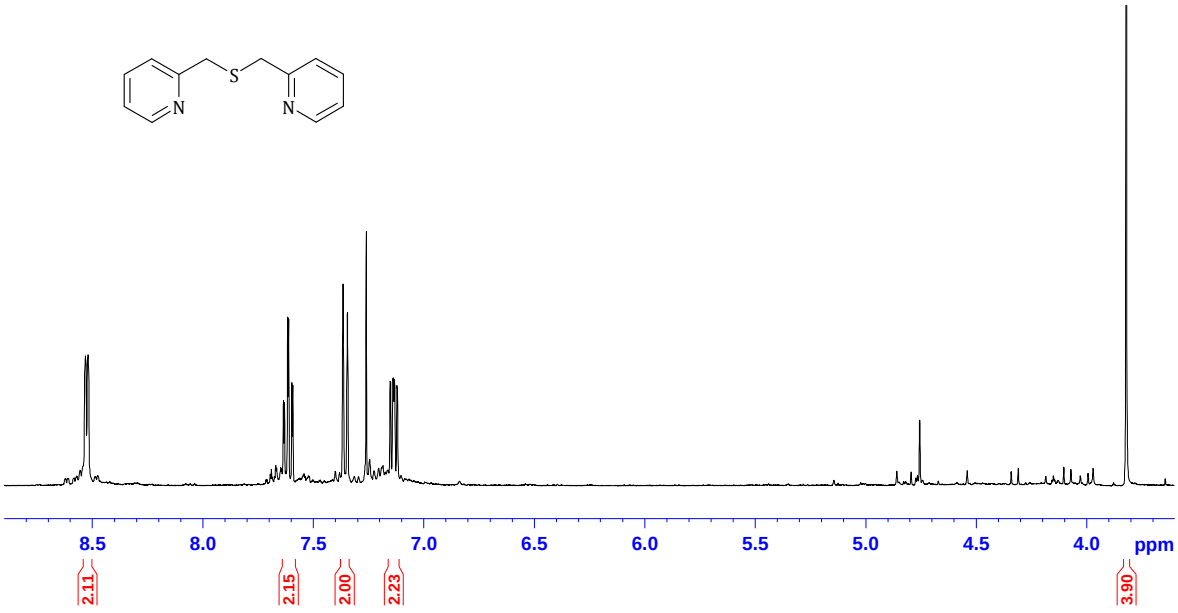


**Figure SI 6.1**: $^{1}$H NMR spectrum of **dps**

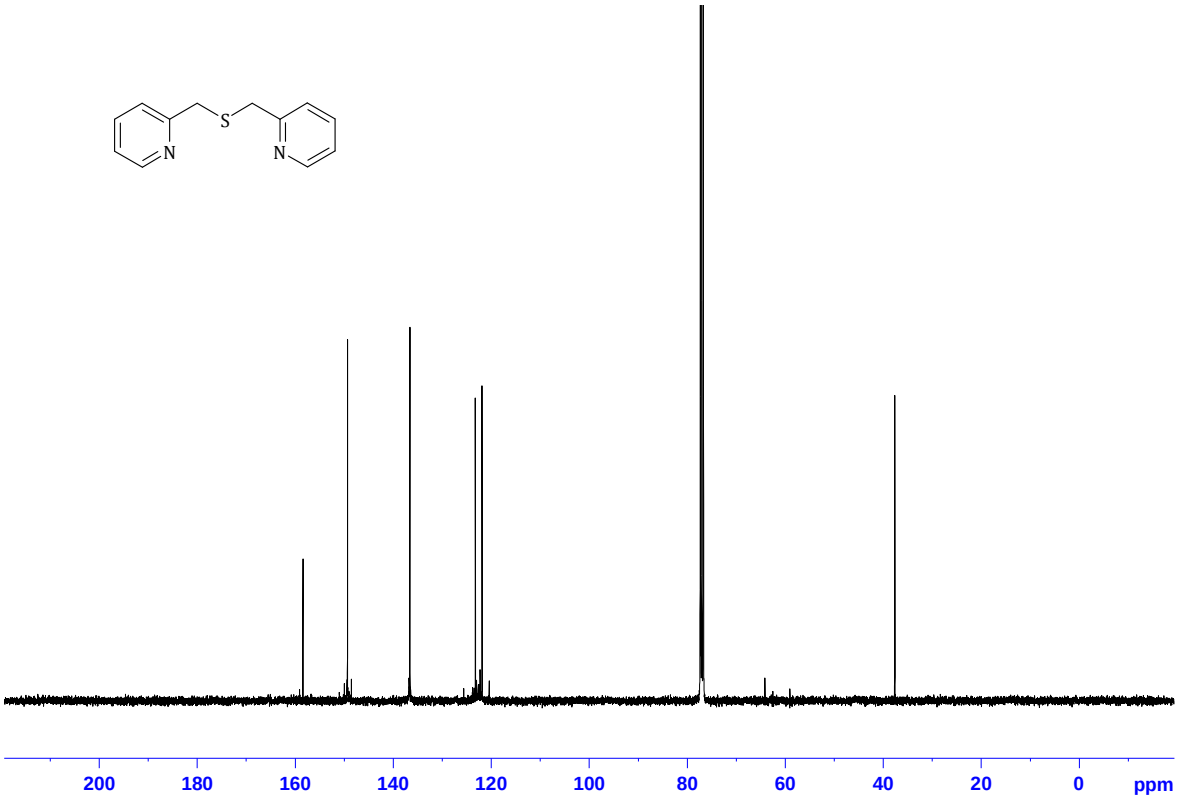


**Figure SI 6.2**: $^{13}$C NMR spectrum of **dps**

**Elemental Composition Report** **Page 1**

**Single Mass Analysis**
Tolerance = 5.0 PPM / DBE: min = -1.5, max = 50.0
Element prediction: Off
Number of isotope peaks used for i-FIT = 3

Monoisotopic Mass, Even Electron Ions
15 formula(e) evaluated with 1 results within limits (all results (up to 1000) for each mass)
Elements Used:
C: 10-15 H: 10-15 N: 0-5 Na: 0-1 S: 0-2
Grace Kinunda
dps 2 (0.017) Cm (1:60)

TOF MS ES+
1.96e+005

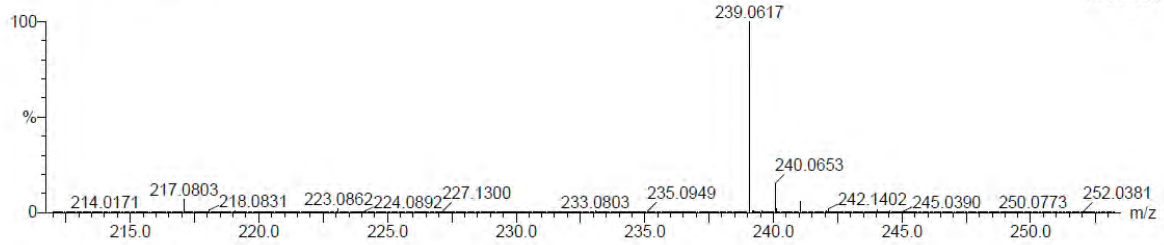


| | | | | | | | |
|---|---|---|---|---|---|---|---|
| Minimum: | | | | -1.5 | | | |
| Maximum: | | 5.0 | 5.0 | 50.0 | | | |
| Mass | Calc. Mass | mDa | PPM | DBE | i-FIT | i-FIT (Norm) | Formula |
| 239.0617 | 239.0619 | -0.2 | -0.8 | 7.5 | 636.0 | 0.0 | C12 H12 N2 Na S |

**Figure 6.3: Mass spectrum of dps**

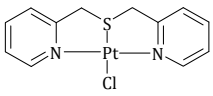


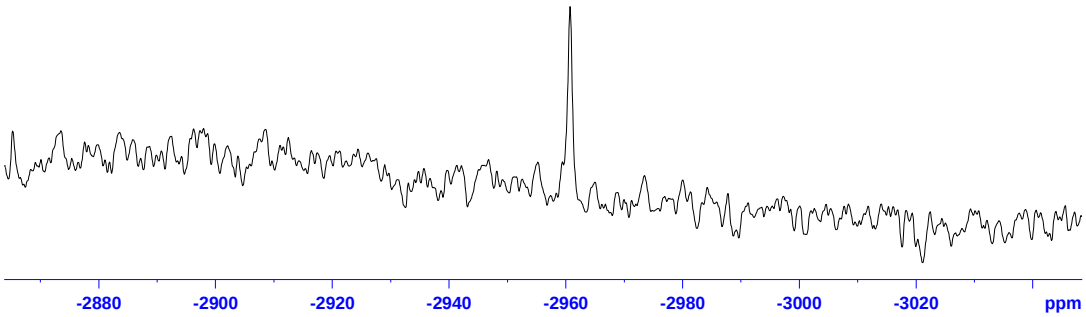


**Figure SI 6.4**: $^{195}$Pt NMR spectrum of **Pt3**

**Elemental Composition Report** **Page 1**

**Single Mass Analysis**
Tolerance = 5.0 PPM / DBE: min = -1.5, max = 50.0
Element prediction: Off
Number of isotope peaks used for i-FIT = 3

Monoisotopic Mass, Odd and Even Electron Ions
33 formula(e) evaluated with 1 results within limits (all results (up to 1000) for each mass)
Elements Used:
C: 10-15 H: 10-15 N: 0-5 S: 0-1 Cl: 0-1 Pt: 0-1

Grace Kinunda
dpsPt 2 (0.017) Cm (1:31)

TOF MS ES+
1.42e+005

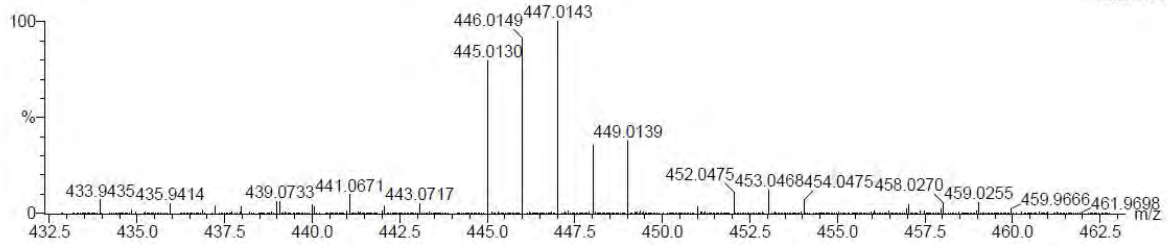


| | | | | | | | |
|---|---|---|---|---|---|---|---|
| Minimum: | | | | -1.5 | | | |
| Maximum: | | 5.0 | 5.0 | 50.0 | | | |
| Mass | Calc. Mass | mDa | PPM | DBE | i-FIT | i-FIT (Norm) | Formula |
| 447.0143 | 447.0136 | 0.7 | 1.6 | 8.0 | 575.2 | 0.0 | C12 H13 N2 S Cl Pt |

**Figure SI 6.5**: Mass spectrum of **Pt3**

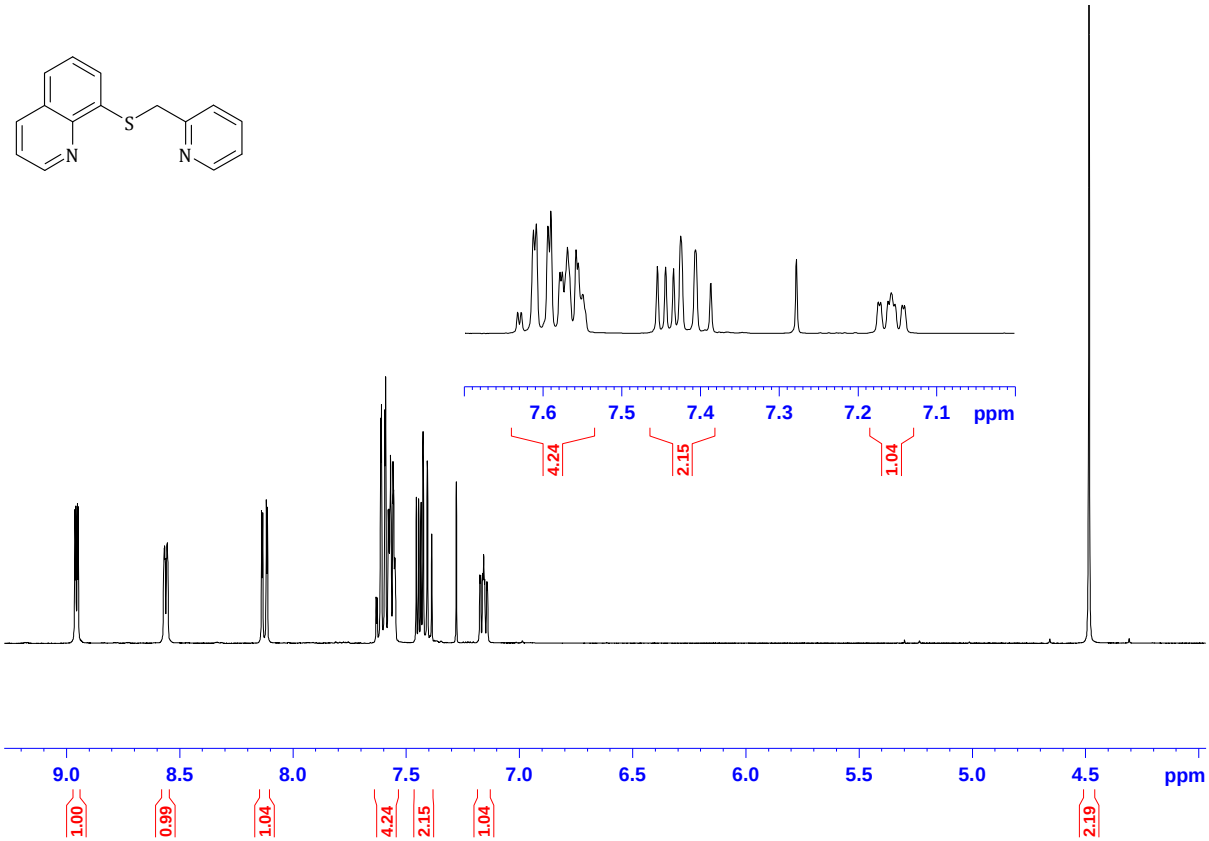


**Figure SI 6.6**: $^{1}$H NMR spectrum of **NSNQui**

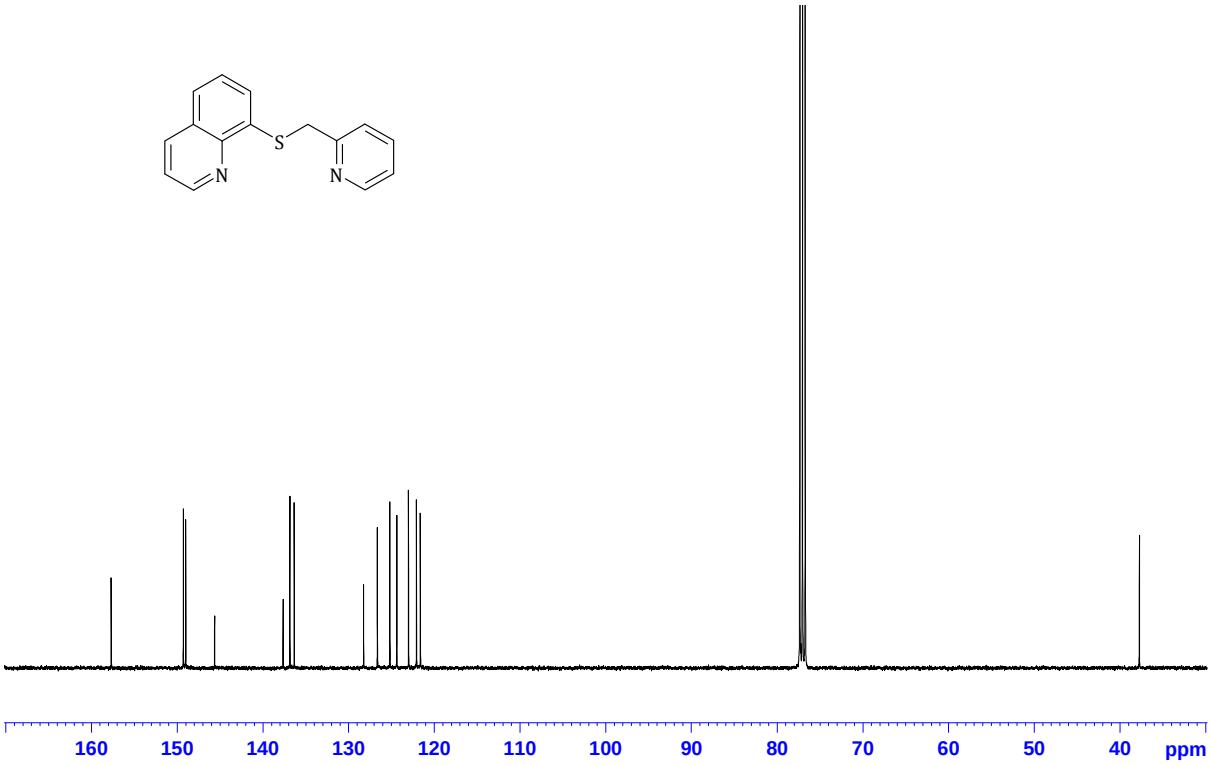


**Figure SI 6.7**: $^{13}$C NMR spectrum of **NSNQui**

**Elemental Composition Report** Page 1

**Single Mass Analysis**
Tolerance = 50.0 PPM / DBE: min = -1.5, max = 50.0
Element prediction: Off
Number of isotope peaks used for i-FIT = 3

Monoisotopic Mass, Even Electron Ions
11 formula(e) evaluated with 1 results within limits (all results (up to 1000) for each mass)
Elements Used:
C: 10-15 H: 10-15 N: 0-5 Na: 0-1 S: 0-1

Grace Kinunda
NSN Qui 6 (0.085)

TOF MS ES+
1.09e+003

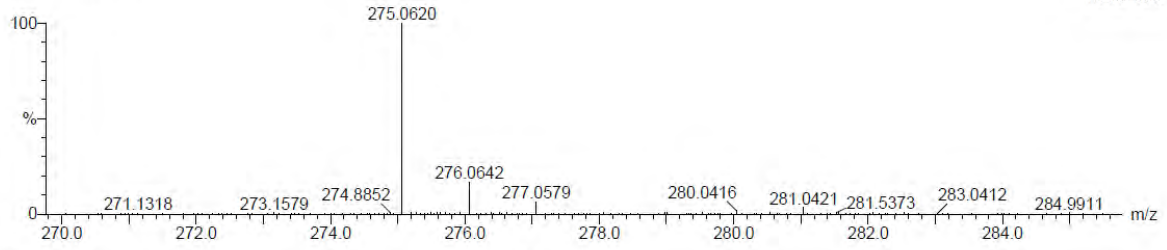


| | | | | | | | |
|---|---|---|---|---|---|---|---|
| Minimum: | | | | -1.5 | | | |
| Maximum: | | 5.0 | 50.0 | 50.0 | | | |
| Mass | Calc. Mass | mDa | PPM | DBE | i-FIT | i-FIT (Norm) | Formula |
| 275.0620 | 275.0619 | 0.1 | 0.4 | 10.5 | 99.7 | 0.0 | C15 H12 N2 Na S |

**Figure SI 6.8:** Mass spectrum of **NSNQui**

**Elemental Composition Report** Page 1

**Single Mass Analysis**
Tolerance = 5.0 PPM / DBE: min = -1.5, max = 50.0
Element prediction: Off
Number of isotope peaks used for i-FIT = 3

Monoisotopic Mass, Odd and Even Electron Ions
34 formula(e) evaluated with 1 results within limits (all results (up to 1000) for each mass)
Elements Used:
C: 15-20 H: 10-15 N: 0-5 S: 0-1 Cl: 0-1 Pt: 0-1

Grace Kinunda
NSN Qui Pt 25 (0.426)

TOF MS ES+
5.17e+002

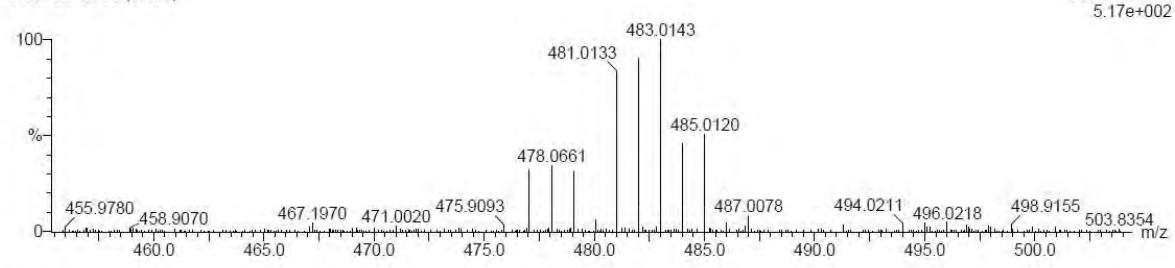


| | | | | | | | |
|---|---|---|---|---|---|---|---|
| Minimum: | | | | -1.5 | | | |
| Maximum: | | 5.0 | 5.0 | 50.0 | | | |
| Mass | Calc. Mass | mDa | PPM | DBE | i-FIT | i-FIT (Norm) | Formula |
| 483.0143 | 483.0136 | 0.7 | 1.4 | 11.0 | 97.1 | 0.0 | C15 H13 N2 S Cl Pt |

**Figure SI 6.9:** Mass spectrum of **Pt4**

**Table SI 6.1**: Summary of wavelength (nm) used for monitoring the kinetic reactions between a series of Pt(II) complexes and thiourea nucleophiles.

| **Complex** | **Nucleophiles** | **Wavelength, λ (nm)** | |
|---|---|---|---|
| | | 1st step | 2nd step |
| **Pt4** | TU | 450 | 450 |
| | DMTU | 455 | 455 |
| | TMTU | 427 | |
| **Pt3** | TU | 375 | 460 |
| | DMTU | 445 | 465 |
| | TMTU | 443 | |
| **Pt2** | TU | 375 | |
| | DMTU | 368 | |
| | TMTU | 363 | |
| **Pt1** | TU | 302 | |
| | DMTU | 300 | |
| | TMTU | 363 | |

**Table SI 6.2:** Average observed rate constants, $k_{obs}$ / $s^{-1}$, for the displacement of the chloro ligand in **Pt3** by thiourea nucleophiles, T = 298 K, $I$ = 0.1 M (0.09 M $NaClO_4$ + 0.01 LiCl).

| [TU] /M | $k_{obs}$ /$s^{-1}$ | [DMTU] /M | $k_{obs}$ /$s^{-1}$ | [TMTU] /M | $k_{obs}$ /$s^{-1}$ |
|---|---|---|---|---|---|
| 1E-3 | 0.20903 | 0.0013 | 0.09787 | 0.001 | 0.0518 |
| 0.002 | 0.40726 | 0.0026 | 0.21202 | 0.002 | 0.09589 |
| 0.003 | 0.60524 | 0.0039 | 0.30104 | 0.003 | 0.14816 |
| 0.004 | 0.79802 | 0.0052 | 0.41351 | 0.004 | 0.20168 |
| 0.005 | 1.05086 | 0.0065 | 0.51795 | 0.005 | 0.25101 |

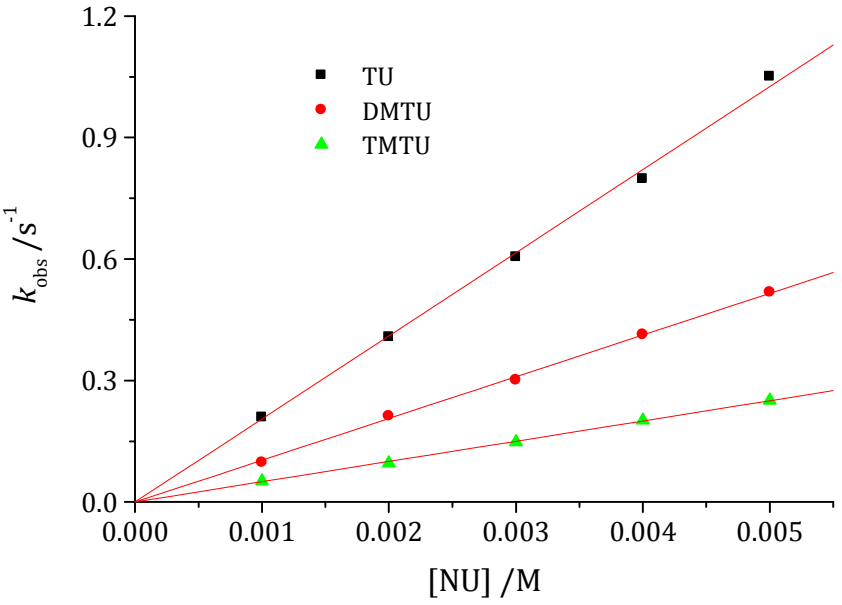


**Figure SI 6.10**: Dependence of $k_{obs}$ on the concentration of entering thiourea nucleophiles for the substitution of chloride on **Pt3** in methanol, $I$ = 0.1 M ($NaClO_4$/LiCl), T = 25 °C.

**Table SI 6.3:** Temperature dependence of $k_2$ / $M^{-1}$ $s^{-1}$ for the displacement of chloro ligands in **Pt3** by thiourea nucleophiles at 30-fold excess over [Pt], $I$ = 0.1 M $NaClO_4$/LiCl.

| TU | | DMTU | | TMTU | |
|---|---|---|---|---|---|
| $\frac{1}{T}$ /K$^{-1}$ | $\ln\left(\frac{k_2}{T}\right)$ | $\frac{1}{T}$ /K$^{-1}$ | $\ln\left(\frac{k_2}{T}\right)$ | $\frac{1}{T}$ /K$^{-1}$ | $\ln\left(\frac{k_2}{T}\right)$ |
| 0.003472 | -6.7263 | 0.003472 | -7.2864 | 0.003472 | -8.088 |
| 0.003413 | -6.42904 | 0.003413 | -7.10796 | 0.003413 | -7.76832 |
| 0.003356 | -6.19922 | 0.003356 | -6.92318 | 0.003356 | -7.55692 |
| 0.003300 | -5.9818 | 0.003300 | -6.80204 | 0.003300 | -7.25674 |
| 0.003247 | -5.66353 | 0.003247 | -6.6024 | 0.003247 | -7.0462 |

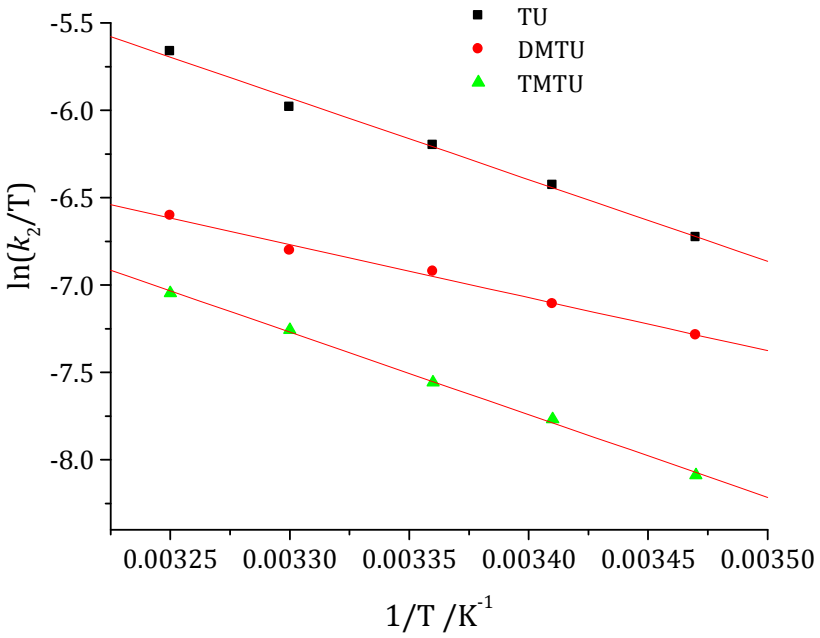


**Figure SI 6.11**: Eyring plots for the reaction of **Pt3** with thiourea nucleophiles at various temperatures in the range of 15-35℃.

**Table SI 6.4:** Average observed rate constants, $k_{obs}$, $s^{-1}$, for the displacement of the chloro ligand in **Pt4** by thiourea nucleophiles, T = 298 K, $I$ = 0.1 M (0.09 M $NaClO_4$ + 0.01 LiCl).

| [TU] /M | $k_{obs}$ /$s^{-1}$ | [DMTU] /M | $k_{obs}$ /$s^{-1}$ | [TMTU] /M | $k_{obs}$ /$s^{-1}$ |
|---|---|---|---|---|---|
| 1E-3 | 0.20903 | 0.0013 | 0.09787 | 0.001 | 0.0518 |
| 0.002 | 0.40726 | 0.0026 | 0.21202 | 0.002 | 0.09589 |
| 0.003 | 0.60524 | 0.0039 | 0.30104 | 0.003 | 0.14816 |
| 0.004 | 0.79802 | 0.0052 | 0.41351 | 0.004 | 0.20168 |
| 0.005 | 1.05086 | 0.0065 | 0.51795 | 0.005 | 0.25101 |

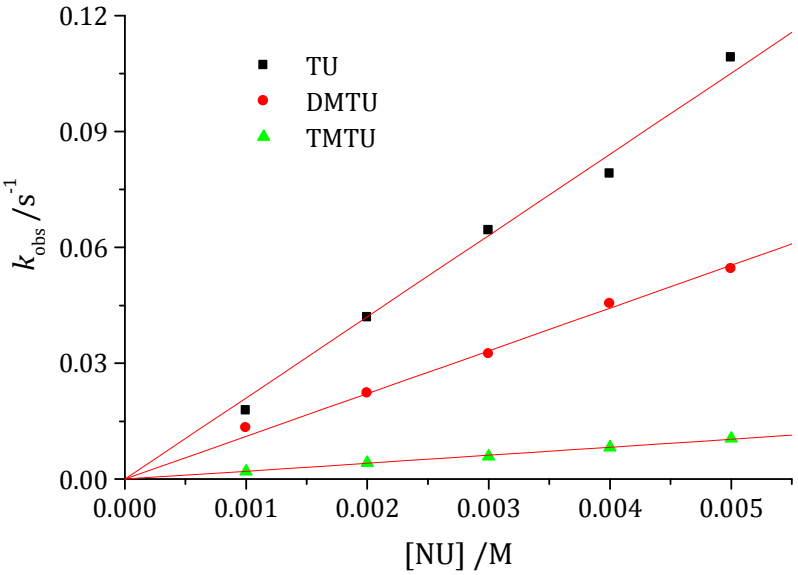


**Figure SI 6.12**: Dependence of $k_{obs}$ on the concentration of entering thiourea nucleophiles for the substitution of chloride on **Pt4** in methanol, $I$ = 0.1 M ($NaClO_4$/LiCl), T = 25 °C.

**Table SI 6.5:** Average observed rate constants, $k_{obs}$, $s^{-1}$, for the dechelation of the tridentate ligand in **Pt4** by thiourea nucleophiles, T = 298 K, $I$ = 0.1 M (0.09 M $NaClO_4$ + 0.01 LiCl).

| [TU] /M | $k_{obs}$ /s$^{-1}$ | [DMTU] /M | $k_{obs}$ /s$^{-1}$ |
|---|---|---|---|
| 1E-3 | 3.4000E-5 | 1E-3 | 1.59563E-5 |
| 0.002 | 6.2204E-5 | 0.002 | 2.86605E-5 |
| 0.003 | 8.6052E-5 | 0.003 | 4.04129E-5 |
| 0.004 | 1.1759E-4 | 0.004 | 5.23138E-5 |
| 0.005 | 1.4358E-4 | 0.005 | 6.59465E-5 |

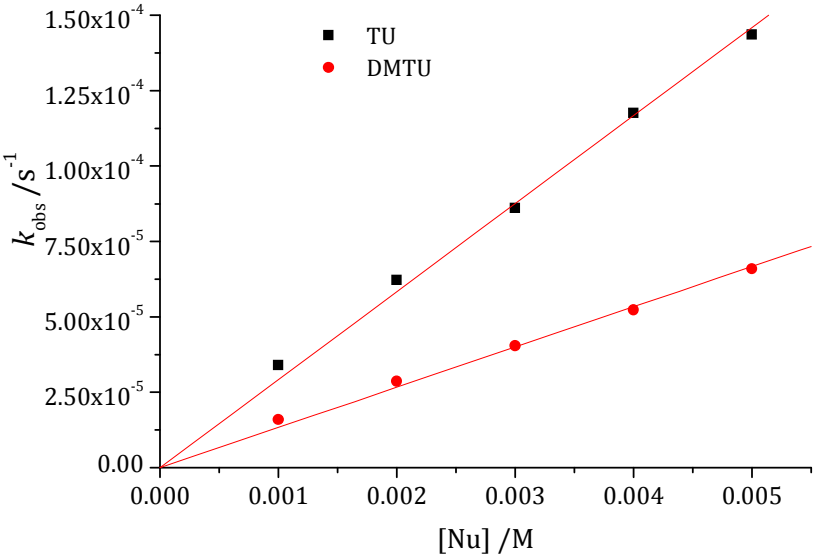


**Figure SI 6.13:** Dependence of $k_{obs}$ on the concentration of entering thiourea nucleophiles for the second substitution step on **Pt4** in methanol, $I$ = 0.1 M ($NaClO_4$/LiCl), T = 25 °C.

**Table SI 6.6:** Temperature dependence of $k_2$ / $M^{-1}$ $s^{-1}$ for the displacement of chloro ligands in **Pt4** by thiourea nucleophiles at 30-fold excess over [Pt], $I$ = 0.1 M $NaClO_4$/LiCl.

| TU | | DMTU | | TMTU | |
|---|---|---|---|---|---|
| $\frac{1}{T}$ /$K^{-1}$ | $\ln\left(\frac{k_2}{T}\right)$ | $\frac{1}{T}$ /$K^{-1}$ | $\ln\left(\frac{k_2}{T}\right)$ | $\frac{1}{T}$ /$K^{-1}$ | $\ln\left(\frac{k_2}{T}\right)$ |
| 0.003472 | -8.96057 | 0.003472 | -9.72109 | 0.003472 | -11.29775 |
| 0.003413 | -8.77168 | 0.003413 | -9.43315 | 0.003413 | -11.02786 |
| 0.003356 | -8.61586 | 0.003356 | -9.19237 | 0.003356 | -10.69383 |
| 0.003300 | -8.37585 | 0.003300 | -8.99183 | 0.003300 | -10.36077 |
| 0.003247 | -8.18514 | 0.003247 | -8.7692 | 0.003247 | -10.05263 |

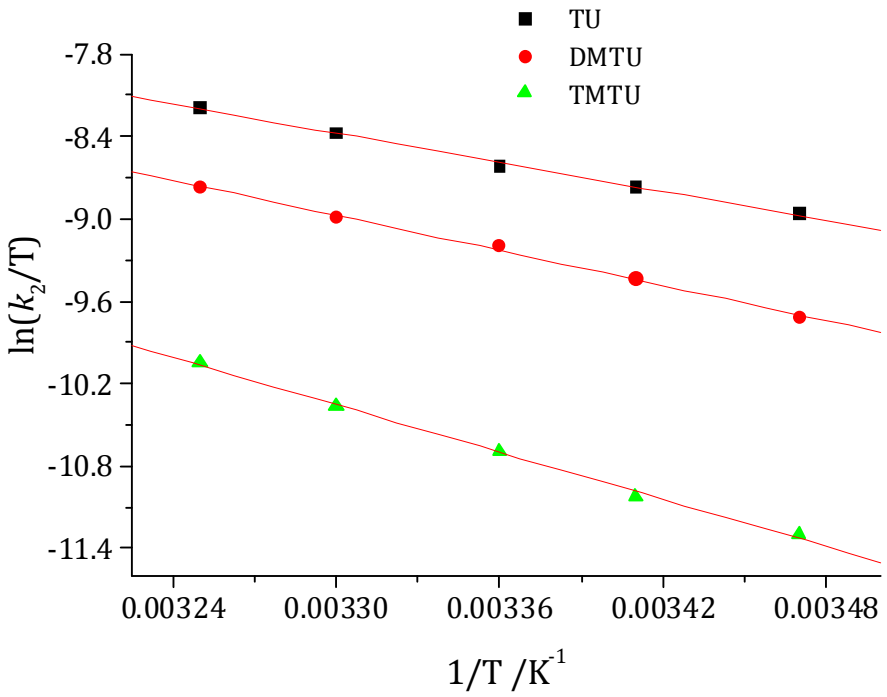


**Figure SI 6.14:** Eyring plots for the reaction of **Pt4** with thiourea nucleophiles at various temperatures in the range of 15-35 ˚C.

**Table SI 6.7:** Temperature dependence of $k_2$ / $M^{-1}$ $s^{-1}$ for the dechelation of the tridentate ligand in **Pt4** by thiourea nucleophiles at 30-fold excess over [Pt], $I$ = 0.1 M $NaClO_4$/LiCl.

| TU | | DMTU | |
|---|---|---|---|
| $\frac{1}{T}$ /$K^{-1}$ | $\ln\left(\frac{k_2}{T}\right)$ | $\frac{1}{T}$ /$K^{-1}$ | $\ln\left(\frac{k_2}{T}\right)$ |
| 0.003472 | -15.8597 | 0.003472 | -16.6480 |
| 0.003413 | -15.6283 | 0.003413 | -16.2269 |
| 0.003356 | -15.0576 | 0.003356 | -15.8135 |
| 0.003300 | -14.8212 | 0.003300 | -15.6716 |
| 0.003247 | -14.4364 | 0.003247 | -15.1843 |

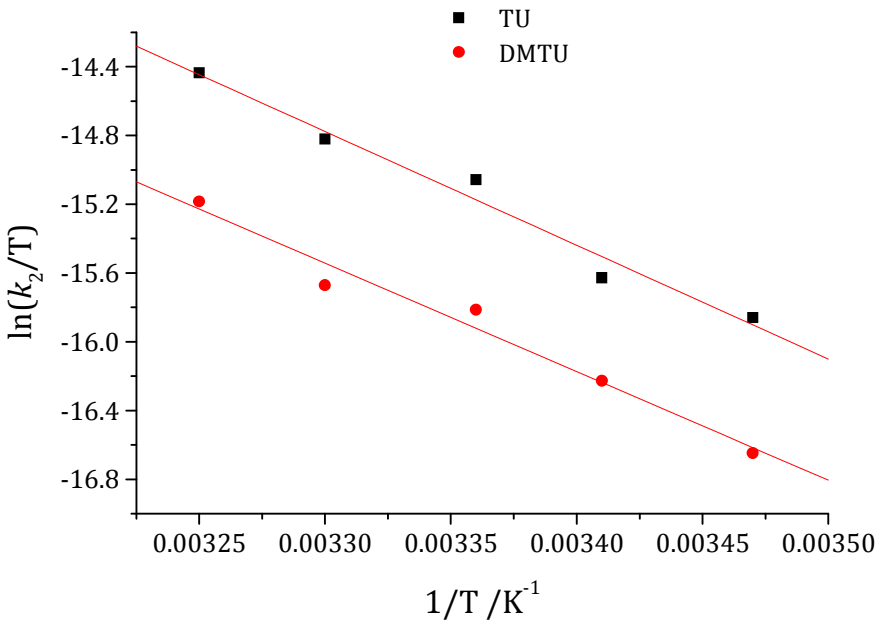


**Figure SI 6.15:** Eyring plots for the second substitution step of **Pt4** with thiourea nucleophiles at various temperatures in the range of 15-35 ˚C.

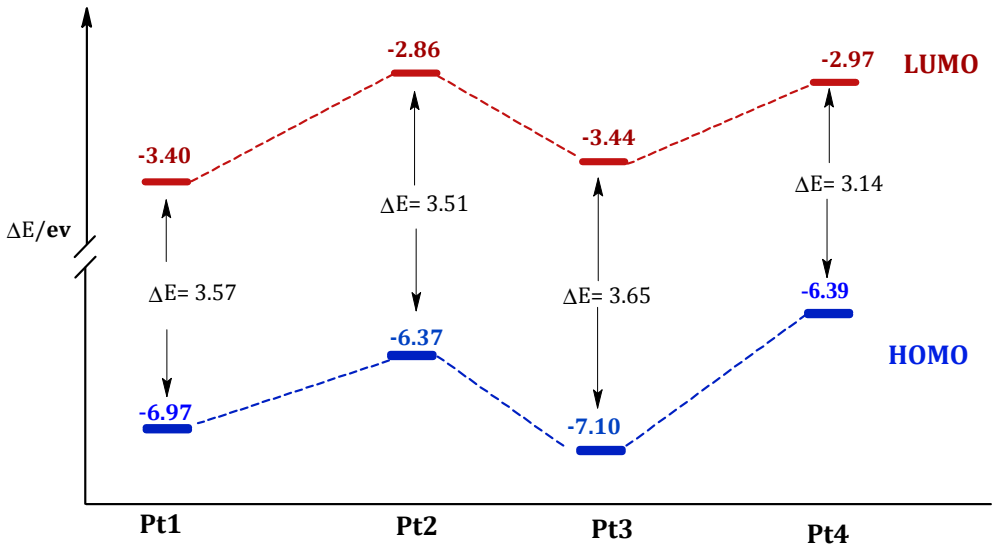


**Figure SI 6.16**: HOMO-LUMO energy diagram of the investigated complexes

# Chapter 7

## 7.1 Summary

This thesis reports the kinetic and mechanistic study of mono and dinuclear Pt(II) complexes with chloro and aqua leaving groups. The results are reported in chapter three to six.

**Chapter Three** reports the kinetics of monofunctional Pt(II) complexes whose π-conjugation was varied by introducing quinoline ligand or imine bond on the non-labile ligand framework. Quinoline and imine moieties were used because of their chemical stability and biological importance. The decrease in the rate of substitution reactions with the increase in π-conjugation is not feasible in this study whereby highly conjugated complex was found to be the least reactive in the series despite its greater number of aromatic rings joined together. It was generally found that the π-backbonding in these systems is weaker than the dominant σ-donation from the quinoline moiety as supported by DFT-calculated electrophilicity indices.

**Chapter Four** reports the substitution reactions of bifunctional Pt(II) complexes bearing 2,2'-dipyridylalkylamine (dpa) ligand. The aliphatic chain of different length was introduced in the tertiary nitrogen bridging the *cis* pyridine rings which form the bidentate chelate to induce the surfactant effect which improves the permeability of the complexes into the cell when used as drug. The kinetic and mechanistic study of the aqua complexes

was studied to investigate the influence of the alkyl chain bonded to the tertiary nitrogen atom joining the two pyridine rings on the reactivity of the chosen complexes.

In all investigated Pt(II) complexes, two substitution steps were observed corresponding to the simultaneous displacement of the aqua ligands and the dechelation of the dipyridylalkylamine ligand as confirmed by the NMR kinetics. Generally, the reactivity of the complexes decreases with increase in aliphatic chain bonded to the tertiary nitrogen joining the two *cis* pyridine ligands due to electronic and steric effect. DFT calculations show that due to the flexibility of the amine bridge joining the *cis* pyridine rings, the complexes adopted the boat conformation which brings in the steric effect resulting into decrease in reactivity of the complexes. The study also found that the σ-donor effect of the alkyl chain reduces the π-acceptor properties of the *cis* pyridine rings resulting into a less reactive metal centre. This was supported by slight decrease in electrophilicity index and an increase in p$K_a$ values upon addition of the $(CH_2)_n$ fragment.

In order to extend this knowledge on the interactions of Pt(II) complexes with thiourea nucleophiles, a set of dinuclear Pt(II) complexes was synthesized and the kinetics on ligand substitution reactions carried out. This is reported in **Chapter Five** of this thesis and is an expansion of an earlier study from our group on azine bridged dinuclear Pt(II) complexes with $NH_3$ ligands *cis* or *trans* to each other and is intended to resolve the thermodynamic and kinetic properties of the complexes as a function of pyridine ligands bonded to Pt centre.

Trend in the reactivity supported by geometry-optimized structures of the complexes indicates that the pyridine rings communicate electronically with the Pt(II) orbitals through π-backbonding hence enhancing the lability of the leaving group of the studied complexes by a factor of between 10 to 23 compared to the reported *cis/trans*-$Pt(NH_3)_2(OH_2)\}_2(\mu$-pzn)]$(ClO4)_4$ analogous. Within the time scale of the ligand substitution reactions, no dechelation step was observed. The two substitution steps observed correspond to the step-wise substitution of the aqua ligands by the thiourea nucleophiles. p$K_a$ values and DFT-calculated electrophilicity index were in agreement with the reactivity trend observed. The effect of the methyl substituents on the pyrazine linker as for **Pt-2,6PZN**, **Pt-2,5PZN** and **Pt-2,3PZN** remains the same as the one reported previously where by the methyl groups donate electrons in the pyrazine bridge and impart steric hindrance to the approach of nucleophile.

**Chapter Six** reported the kinetic and mechanistic studies of Pt(II) complexes with σ-donor quinoline ligand moiety and the σ-donor atom located on the *trans* position to the leaving group. Two substitution steps, one followed on Stopped flow and the second on UV-Vis were observed for **Pt(N^S^N)** complexes. Based on the NMR kinetics, the second step was ascribed to the ring opening up of the tridentate chelate following coordination of thiourea to the Pt(II) centre. Only one UV-Vis substitution step was observed for **Pt(N^N^N)** complexes corresponding to the substitution of the chloro ligand. In both sets of complexes, the kinetic and thermodynamic results obtained show that σ-*trans* effect is stronger in increasing the lability of the leaving group and most importantly, quinoline based Pt(II) complexes were found to be slow than their pyridine counterparts due to poor π-acceptor

ability of quinoline. The calculated electrophilicity indices are in agreement with the reactivity observed for the complexes. Negative values of activation entropies throughout the studied systems confirm an associative mode of activation.

## 7.2 Contribution to Other Paper(s)

- Enthused by the fact that dinuclear Pt(II) complexes with bidentate ligands are more cytostatic than dinuclear with only one coordination site, mononuclear Pt(II) complexes studied in **chapter four** were further investigated by linking the two Pt centres with an alkyl chain of variable length. Therefore, five dinuclear Pt(II) complexes with 2,2'-Dipyridylamine ligands featuring a cisplatin analogous structure motif and $(CH_2)_n$ as a linker where n = 2,3,4,5 and 6 were synthesized (**Scheme 7.1**). p$K_a$ studies and ligand substitution reactions of the aqua complexes with thiourea nucleophiles were attempted and were found to include the dechelation step which was too slow. For this reason, a complete kinetic investigation of all five complexes is not included in this thesis as the kinetic and mechanistic study is currently under study in our lab. X-ray crystal structure obtained for one of the ligand will be published together with the kinetics data.

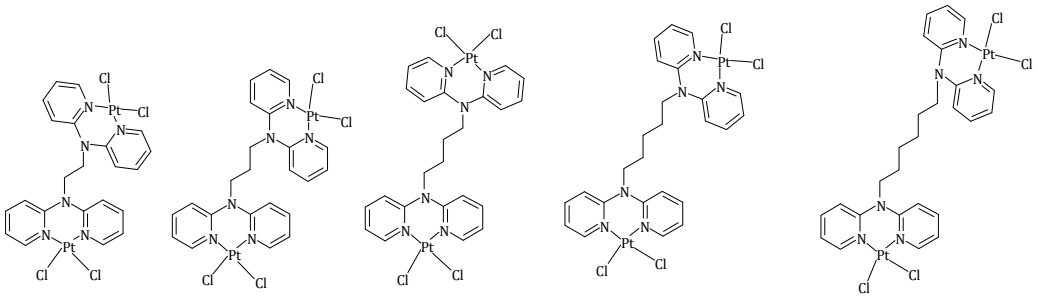

**Scheme 7.1**: Structures of Pt(II) complexes whose kinetic investigation is in progress.

## 7.2 Recommendations

Generally, since the kinetic and the mechanistic information obtained from these studies of ligand substitution reactions are intended to contribute to the design and development of effective platinum(II) antitumour drugs, this study can be extended by looking at:

i. Ligand substitution reactions carried out at the physiological conditions, *i.e* at pH 7 and at 37 ˚C.

ii. Kinetics of water soluble or aquated Pt(II) complexes. This is because it is already known that most Pt anticancer drugs should aquate before they are able to exert a cytotoxic effect.

iii. DNA titration to quantify the binding interactions of the Pt(II) complexes and the DNA.

iv. Extending ligand substitution reactions to test the antitumour activity of the complexes especially novel (**Chapter Five**) and those Pt(II) complexes with peculiar kinetic behaviour as for quinoline based complexes reported in **Chapter Three** and **Six**.